Skull Evolution
in the
Australian
Dragon Lizards

A dissertation in

Biological Science

by

Jaimi Ann Gray

Submitted in fulfilment of the requirements for the degree of

Doctor of Philosophy

At the University of Adelaide

School of Biological Sciences

Department of Ecology and Evolutionary Biology

August 2018

"Whilst this planet has gone cycling on according to the fixed law of gravity, from so simple a beginning endless forms most beautiful and most wonderful have been, and are being, evolved."

- Charles Darwin, *On the Origin of Species*

Contents

List of figures

List of tables

List of supplementary material

Figures

Tables

Electronic files

File ES2.1 – Iguanian specimen numbers and information with proportional measurements (CSV).

File ES3.1 – Amphibolurine tooth counts and tooth row length data (CSV).

File ES4.1 – Zipped file containing crania images used for 2D landmarking (ZIP).

File ES4.2 – Specimen numbers and information used to examine ontogenetic patterns (CSV).

File ES4.3 – 2D landmark coordinates used to characterise crania in this study (TPS).

File ES4.4 – Nexus tree of 18 agamid species, used to build phylomorphospace (NEX).

File ES5.1 – Folder containing 3D ply models of cranial surfaces used for landmarking (file folder).

File ES5.2 – 3D landmark coordinates used in analyses (DTA).

File ES5.3 – Nexus tree of 52 agamid species, used to build phylomorphospace (NEX).

File ES6.1 – Folder containing ply surface files used for landmarking (file folder).

File ES6.2 – 3D landmark coordinates used to characterise jacky lizard crania (DTA).

File ES6.3 – 3D landmark coordinates used to characterise comparison species crania (DTA).

File ES6.4 – Wireframe links used to build skull shape diagrams (CSV).

File ES7.1 – Specimen numbers with tooth row length and snout-vent length data (CSV).

File ES8.1 – Folder containing ply surface models of all specimens used in the analyses (file folder).

File ES8.2 – Folder containing separate DTA files of 3D landmark coordinates from maxillae models (file folder).

Summary

Today, lizards of the family Agamidae are widespread across the continent of Australia, where they are commonly referred to as dragon lizards. Since their arrival from Southeast Asia approximately 30 million years ago, they have radiated to occupy every environment that the continent has to offer, and have been particularly successful in the arid habitats as they arose 7-15 million years ago. The monophyly of the Australian agamids is well established, and they are currently regarded as a subfamily, Amphibolurinae, with relatively well understood taxonomy and phylogeny. By contrast, the morphological diversity among the group is yet to be quantitatively and systematically explored. Here, I use quantitative approaches to explore the morphological variation in the skulls of Australia's agamid lizard radiation. I used a combination of linear measurements, tooth counts, and two-dimensional and three-dimensional geometric morphometrics to characterise and explore patterns of morphological variation in the Australian dragon lizards.

The cranial morphology of the 67 Australian agamid species used in this dissertation is more morphologically diverse than all other members of the agamid family combined. This disparity is achieved by modification of growth patterns, size, and dental characters. All Australian dragons tend to have a similar juvenile phenotype but become more disparate in shape as they approach adulthood. Despite their relatively recent invasion of Australia, the amphibolurine lineage of lizards has evolved a wide variety of different skull shapes, and provides examples of divergence and convergence, as well as the evolution of some extreme skull shapes (e.g. *Gowidon*, *Moloch*) that are associated with particular ecological life habits. A phylogenetically informed comparison of skull shapes seen in adult amphibolurines reveals that life habit accounts for differences to a greater degree than phylogenetic constraint. The extent to which this is true for other members of the Australian herpetofauna (e.g. snakes, geckos and skinks) is unclear and requires further work, but this thesis provides a foundation to do so. As well as revealing macroevolutionary patterns among the extant species, all chapters of this thesis advance our knowledge of their skull anatomy, enhance the resources available for interpretation of fossil agamid material, and unlock the potential for deep-time studies of palaeoecological changes.

Declaration

I certify that this work contains no material which has been accepted for the award of any other degree or diploma in my name, in any university or other tertiary institution and, to the best of my knowledge and belief, contains no material previously published or written by another person, except where due reference has been made in the text. In addition, I certify that no part of this work will, in the future, be used in a submission in my name, for any other degree or diploma in any university or other tertiary institution without the prior approval of the University of Adelaide and where applicable, any partner institution responsible for the joint-award of this degree.

I acknowledge that copyright of published works contained within this thesis resides with the copyright holder(s) of those works.

I also give permission for the digital version of my thesis to be made available on the web, via the University's digital research repository, the Library Search and also through web search engines, unless permission has been granted by the University to restrict access for a period of time.

Jaimi Ann Gray

Acknowledgements

This PhD grew from a third-year undergraduate project that I picked from a list of many possible choices. I could never have known the significance of the choice I made that day. It was just my luck that this project was with Dr Mark Hutchinson, the human encyclopedia of herpetology, who became one of my gallant PhD advisors, and was the person who introduced me to the beauty of CT scans. I am thankful for his assistance with pretty much everything. Enormous thanks must go to Dr Marc Jones, another who I feel lucky to have had as an advisor, for guidance, for always taking the time to discuss my work and life in general, and for enduring, listening to, and responding to my extensive rambling about projects on a regular basis. I am grateful to both Mark and Marc for their guidance, support, and encouragement throughout the last five years as I grew, from a bitty baby undergraduate into (almost) Dr Gray.

Thanks go to Dr Kate Sanders for her continued guidance and support. Thanks to Dr Emma Sherratt, for advice concerning both geometric morphometrics, and the maintenance of my own mental health, especially in the final throws. Thanks to Carolyn Kovach at South Australian Museum, for letting me have free run of the herpetology collection and always lending a kind ear. For advice and support, thanks also go to Dr Liz Reed, Dr Alessandro Palci, Dr Mike Lee, Dr Matthew McDowell, and Dr Michelle Guzik.

For technical support with CT scanning, I thank Amy Watson for showing me tips and tricks for more efficient scanning and data storage, Ruth Williams for training me on the scanner, and Izzy Douvartzis for having me sit in on those very first CT scanning sessions, back when I was an undergraduate student.

For their hospitality on my trips around Australia and the world, I thank Dr Chris Bell and his lab group from the University of Texas at Austin, Alan Resetar from the Field Museum in Chicago, Dr Jane Melville from Melbourne Museum, and Dr Scott Hocknull and Dr Andrew Amey from Queensland Museum in Brisbane. Thanks to the Jackson School of Geosciences at the University of Texas at Austin, for awarding me a travel grant to go to my very first international conference: SVP in Dallas. Thanks to the Royal Society of South Australia, for awarding me a travel grant to visit the wonderful Queensland Museum for my data collection.

I was somewhat of a floater with no specific lab group, but I am grateful to have had a hodgepodge network of various fellow PhD students from both the University of Adelaide and Flinders University, and to have been adopted into various palaeontological, herpetological, and entomological lab groups, which I am very thankful for. Thanks Ray, Jessie, Jenna, Ayla, Ben, Josie, Erinn, Lucy, Bonnie, and Kailah for being part of my odd network.

I'm forever grateful to my best bud Kari, for being my one-person cheerleading squad even when I was at my most anti-social. Thanks to my supportive partner Joel, for being my rock every single day and putting up with the good and the not-so-cheerful moods over the last four years. Thanks to the staff at North Adelaide Fitness Centre, I don't think you know just how important the place was for me as a sanctuary. At the end of each day I had a place to go where not only was I pretty much guaranteed to not have to talk about my thesis for a little while, but I also was able to vent the days frustrations by kicking and punching a bag or lifting heavy objects.

Most importantly, I send thanks back home to a small town in country South Australia: props to my family, who helped this country bumpkin progress to city and university life. Thanks to my Dad, Steven, for supporting me even without understanding exactly what it is that I was doing. Thanks to my Mum, Penelope, because apparently "that's where you get your brains from". Thanks to my brother and sister, Zac and Lara. You can't pick your family, but I ended up getting a pretty good deal. Without them I wouldn't be standing here today, holding a big stack of paper that I am very proud of.

13

Contributions

CHAPTER 2 - Exceptional disparity of Australian agamid lizards is a possible result of arrival into vacant niche
Authors: Gray JA, Hutchinson MN, Jones MEH
Status: Submitted to The Anatomical Record on 30.07.2018. Previously submitted to other journals, and revised based on feedback from reviewers.

CHAPTER 3 – Patterns in tooth number among Australian agamids
Authors: Gray JA, Jones MEH, Hutchinson MN
Status: Prepared for submission to Journal of Anatomy.

CHAPTER 4 - Changes in ontogenetic patterns facilitate diversification in skull shape of Australian agamid lizards
Authors: Gray JA, Sherratt E, Hutchinson MN, Jones MEH
Status: Submitted to BMC Evolutionary Biology on 22.05.2018. Reviews received 08.08.2018, this chapter is revised and ready for resubmission.

CHAPTER 5 - Evolution of cranial shape in a continental-scale adaptive radiation of Australian lizards
Authors: Gray JA, Sherratt E, Hutchinson MN, Jones MEH
Status: Prepared for submission to Evolution.

CHAPTER 6 - The implications of using captive-bred specimens in intra-specific morphological analyses
Authors: Gray JA, Hutchinson MN, Jones MEH
Status: Prepared for submission to Biodiversity and Conservation.

CHAPTER 7 – Estimating body size of fossil agamids from jaw bones
Authors: Gray JA, Hutchinson MN, Jones MEH
Status: Prepared for submission to Journal of Vertebrate Paleontology.

CHAPTER 8 - Geometric morphometrics provides an alternative approach for interpreting the affinity of fossil lizard jaws
Authors: Gray JA, McDowell MM, Hutchinson MN, Jones MEH
Status: Published on 28.07.2017 in Journal of Herpetology, 51(3), pages 372-382.

Co-author affiliations

Marc E. H. Jones
Department of Earth Sciences
The Natural History Museum
London, United Kingdom

Mark N. Hutchinson
Herpetology Department
South Australian Museum
Adelaide, South Australia, Australia

Emma Sherratt
School of Biological Sciences
University of Adelaide
Adelaide, South Australia, Australia

Matthew C. McDowell
Biological Sciences
University of Tasmania
Hobart, Tasmania, Australia

CHAPTER 1

Introduction

CHAPTER 1 – Introduction

The skull

The skull. It houses the brain, the major sensory organs, and the feeding apparatus. It is an intriguing element because it represents the epicentre of the anatomy where sensory responses, feeding, locomotion, and various other factors interplay. There is no doubt that the resulting complex structure serves a vital functional role in vertebrates. For evolutionary biologists, it offers a means of addressing important evolutionary questions. It provides a suite of homologous and quantifiable traits that frequently show significant variation, even among closely related taxa, and thus a platform to examine hypotheses relating to mechanisms, modes, and constraints concerning adaptation (Hanken and Hall, 1993). Furthermore, skull elements are well represented in the fossil record. Studies that compare morphology across different skulls of both extinct and extant animals are often motivated by an overarching interest in the reconstruction of past evolutionary history. Understanding the evolutionary consequences of morphological form at various taxonomic levels enhances interpretations of morphology, and ultimately reveals important pieces in the puzzle of vertebrate evolution.

Today, researchers have an extensive toolkit of techniques to use for characterising morphology (Adams et al., 2004). This toolkit is the result of many years of continued development of geometric morphometric techniques that have improved and advanced the ways we characterise morphological form (see Bookstein, 1991; Dryden and Mardia, 1998; Adams, 1999; Mittroecker and Bookstein, 2011; Klingenberg and Marugán-Lobón, 2013). These developments include software for collecting landmarks in three-dimensional space and increasingly sophisticated ways to view shape differences and depict morphological variation in a multivariate shape space (Bookstein, 1989; Adams and Collyer, 2009). But researchers do not stop at just characterising shape: they can also explore and statistically describe morphospace occupation through the lens of phylogenetic, ecological, or functional hypotheses (Friedman, 2010; Klingenberg, 2010; Klingenberg and Marugán-Lobón, 2013; Adams, 2014). Morphological comparisons placed in the context of phylogeny provide a framework for reconstructing evolutionary history and understanding how a diversity of a particular clade has been assembled.

Recurring evolutionary themes

Allometry

Organisms will change shape when they change in size, either ontogenetically or evolutionarily. This is expected purely on biomechanical grounds. If organisms were to increase their size without changing shape, geometric scaling and physical properties dictate that this would decrease their ability to perform functions vital to their survival, including respiration, locomotion, and feeding (Schmidt-Nielsen, 1984). One of the most important approaches for assessing variation in skull shape is allometry: the study of changes in shape that are associated with changes in size (Klingenberg, 2016).

There are three different kinds of allometry (see Fig. 1.1). *Static* allometry concerns patterns of variation among individuals of the same population within a particular ontogenetic stage. *Ontogenetic* allometry concerns variation among individuals from the same population, at different ontogenetic stages. *Evolutionary* allometry concerns variation among individuals within a single ontogenetic stage, from multiple evolutionary lineages that share a common ancestor (Cock, 1966). Although we recognise three different levels of allometric variation, they are all closely interconnected (e.g. Rieppel, 1990). Any changes in evolutionary allometry are
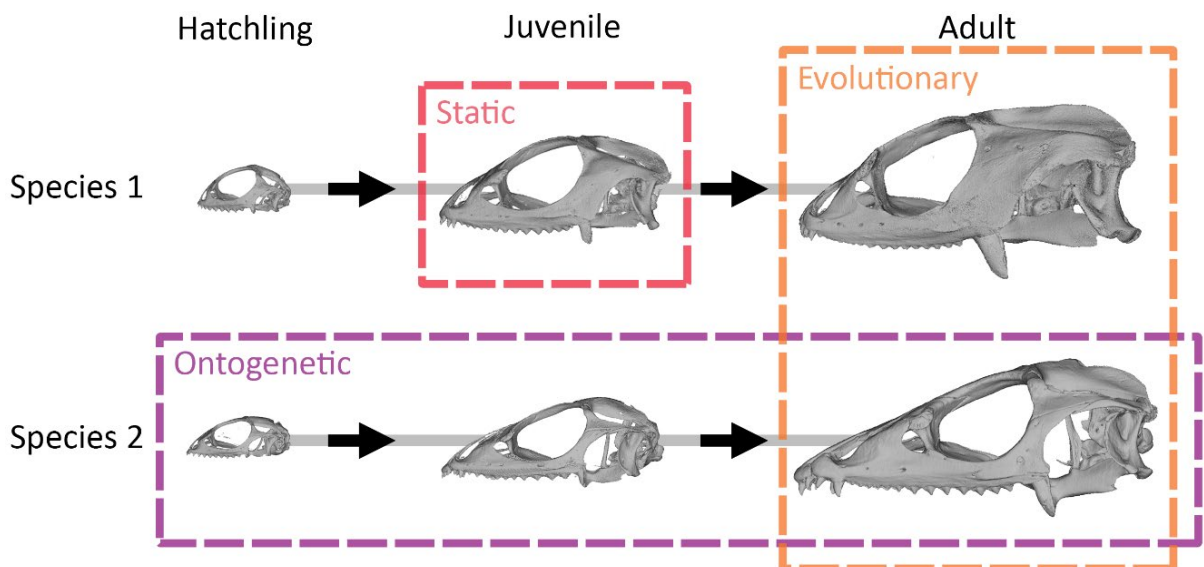
Figure 1.1 – Illustration of the scheme used to characterise the three kinds of allometry. Skulls representing three successive instars are aligned from left to right, and two species are depicted, one beneath the other. Boxes indicate how species and instars are pooled to obtain estimates of each allometric pattern.

accompanied by corresponding changes in ontogenetic allometry, and heritable static variation of morphological traits dictates the possibilities for evolutionary change. Shape changes that are associated with size are an important, and often complex, concept in evolutionary biology and related disciplines. Our ability to measure and interpret them has advanced greatly in the last 50 years, thanks to the developments in multivariate methods for characterising shape, as well as advancements in quantitative concepts and methods for analysing allometric variation (Huxley and Teissier, 1936; Gould, 1966; Klingenberg, 1998; Collyer et al., 2015; Klingenberg, 2016).

Disparity

"Disparity" is the measure of morphological spread among individuals in a given sample (Runnegar, 1987; Gould, 1989; Foote, 1991). The introduction of the concept of disparity clarified a distinction between two notions of diversity that were often confounded: phenotypic variety (disparity), and taxonomic richness (diversity) (Foote, 1990, 1993a, 1993b). Although diversity and disparity are often correlated, the fossil record tells us that evolutionary change is not always evenly distributed over time (Foote, 1991). Measures of taxonomic diversity help us grasp the number of biological units present in a given place at a given time. However, if we want to understand the nature of these units and how they evolved, then measurement of phenotypic disparity is also necessary. Although there is no accepted standard for measuring disparity, questions regarding it are best tackled using a morphospace framework, which places all individuals in the same context. This allows disparity, variability between and within clades, and convergence to be quantified (Foote, 1997). Documenting and comparing temporal patterns of disparity and investigating the dispersion of this disparity among clades and at different taxonomic levels can yield valuable information about morphological diversification throughout evolutionary history.

The study group: Australian agamid lizards

It is worth noting, although numbers of species stated here are based on the current state of iguanian phylogeny (from http://reptile-database.reptarium.cz/ on the 14th of July, 2018), the number of recognised species continually rises as researchers continue to improve the resolution of our understanding of phylogenetic relationships.

Iguanian lizards (see Fig. 1.2) make up an astonishing 18% of all extant reptile species. They are a remarkably successful lizard radiation that is distributed worldwide and exhibits a surprising amount of morphological and ecological diversity. The clade Iguania is made up of 1889 extant species of lizards from 14 families (Townsend et al., 2011). Extant iguanians are split into two major clades, the Pleurodonta and the Acrodonta (Frost et al., 2001). These clades are characterised by their tooth implantation, with Pleurodonta exhibiting pleurodont tooth implantation, and Acrodonta exhibiting acrodont tooth implantation (Cooper et al., 1970; Frost and Etheridge, 1989; Zaher and Rieppel, 1999). The Acrodonta is comprised of two families: the Agamidae, made up of 489 extant species; and the Chamaeleonidae, made up of 210 extant species. The family Agamidae, also known as "dragon lizards", are diurnal omnivores with well-developed limbs, and they commonly have keeled scales, crests, throat flaps, and frills. This charismatic family has independent radiations in Africa, Asia, and Australia, and several monophyletic clades of dragons are currently recognised (Honda et al., 2000; Hugall et al., 2008).

The focus of this thesis is on the agamid clade containing the Australian and New Guinean agamids, the Amphibolurinae. With 108 currently recognised extant species, they make up approximately 18% of the agamid family. The amphibolurines occupy a separated Gondwanan continental plate, and are likely to be the result of a single dispersal event from Southeast Asia, around 30 million years ago (Ma) (Oliver and Hugall, 2017). This dispersal just preceded global climate change during the Miocene, when Australia's increasing aridity led to shifts in vegetation distributions and dramatic changes in habitat (Fujioka and Chappell, 2010). Mesic rainforest environments were widespread up until approximately 20 Ma, but beginning from around 15 Ma, aridification resulted in their contraction (McGowran et al., 2004). Open woodlands expanded, large parts of Australia had become desert by 10–7 Ma, and intensive desertification continued until about 4–2 Ma (Fujioka et al., 2005; Martin, 2006). Today, habitats vary dramatically across the Australian continent, from wet rainforests, to open woodlands, arid deserts, and temperate scrublands (Mackey et al., 2008). The marked changes in climate experienced by the continent, and the resulting new habitats, probably played a major role in the evolutionary success of the Australian agamids.
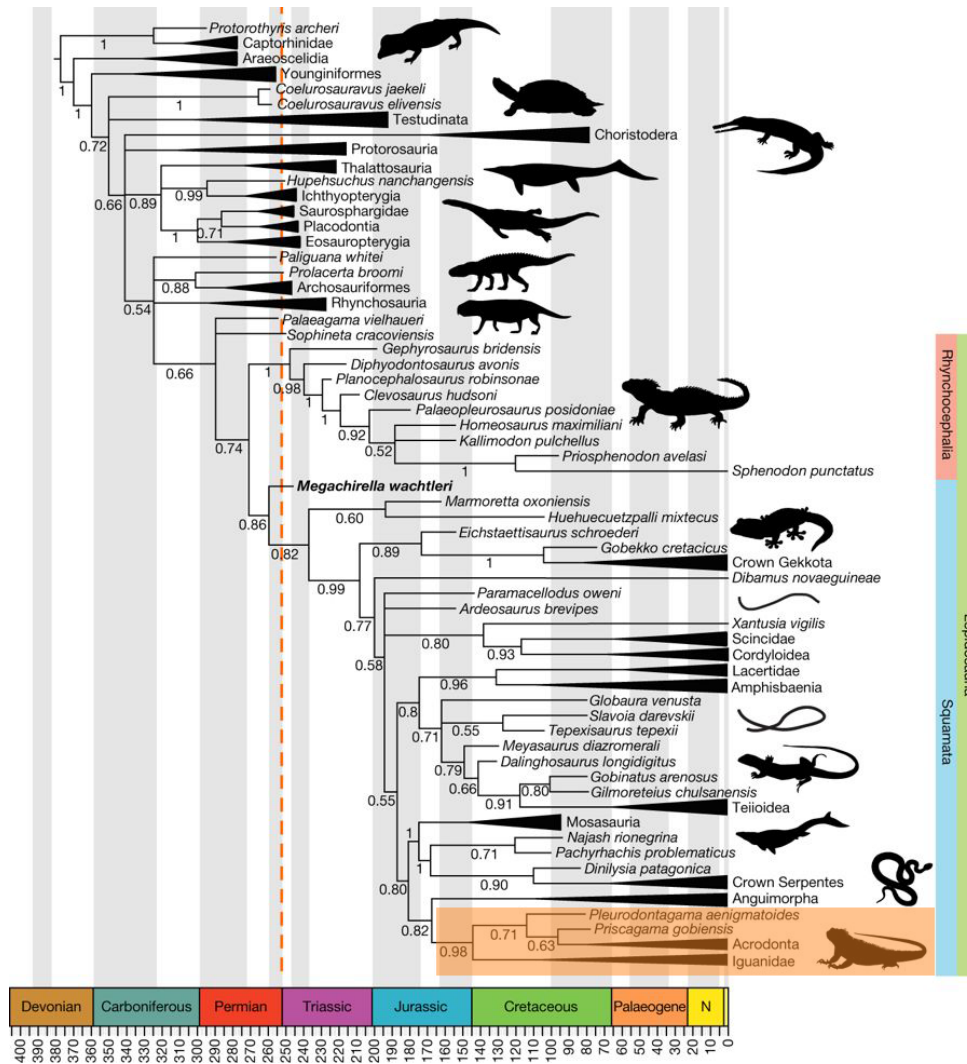
Figure 1.2 – Evolutionary tree of Squamata from Simões et al., (2018), edited to highlight the position of Iguania (in orange).

The most recent phylogeny of the Australian agamids (Hugall et al., 2008, see Fig. 1.3) indicates that the Asian water dragon, *Physignathus cocincinus,* is the sister group to all Australian and New Guinean taxa (see also Macey et al., 2000; Schulte et al., 2003). Within the Amphibolurinae, *Chelosania, Lophosaurus, Hypsilurus,* and *Moloch* form the least nested monophyletic group (herein referred to as the "LN group", cf. Sereno, 1999). Within the LN group, the rainforest dragon clade is made up of *Lophosaurus* and *Hypsilurus* (Manthey and Denzer, 2006). *Chelosania* lives in tropical woodlands, rather than rainforests, and has been suggested to be a possible remnant of early diversification out of mesic rainforest habitats (Hugall et al., 2008). *Moloch* represents the only arid adapted species in the LN group, and is an extremely isolated lineage, estimated to have split from its nearest living relative around 18 Ma. The Australian water dragon, *Intellagama lesueurii,* is the sister taxa to the core Australian radiation, and together they make up an exclusively endemic Australian radiation (Hugall et al., 2008).

The core of the Australian radiation is made up of two large and diverse clades, the *Amphibolurus* group and the *Ctenophorus* group, which are estimated to have diverged from one another around 19 Ma (Hugall et al., 2008). The *Ctenophorus* group is made up of a single genus, comprised of 29 species. They are mostly arid adapted and largely small, ground dwelling lizards, with convergent ecomorphs (Melville et al., 2001). The *Amphibolurus* group is made up of 10 genera of varying numbers of species, and are diverse in body form, size, and ecology. Several ecologically and morphologically similar forms in the core of the Australian radiation are estimated to be distantly related in phylogenetic analyses (Melville et al., 2006), implying that substantial homoplasy exists in their morphological characters.

Today, amphibolurines exhibit a variety of life history strategies (Griffiths and Christian, 1996; Stuart-Smith et al., 2005; Radder et al., 2007; Pianka and Goodyear, 2012). There are dragons that dwell in tropical forests, woodlands, terrestrial environments, and deserts (Pianka, 1971, 2013b, 2014a). They also vary greatly in their structural habitat use. Some are restricted to arboreal or rock-dwelling lifestyles, while others dig burrows, some semiaquatic forms use water as a refuge, and many species make use of different types of habitats as they see fit (e.g. semi-arboreal species) (Pianka, 2013c, 2013a, 2014b). There are some very specialised dragons, such as the Lake Eyre dragon (*Ctenophorus maculosus*), a small dragon that lives on the edge of a salt lake, and the thorny devil (*Moloch horridus*), a spiny desert-dweller with a very striking appearance and a diet consisting entirely of ants (Pianka and Pianka, 1970). They also vary greatly in body size, from the very small Shark Bay heath dragon (*Ctenophorus butleri*), with a snout-vent length of 43 mm, to the large frill-neck lizard (*Chlamydosaurus kingii*), with a snout-vent length of up to 258 mm (Wilson and Swan, 2013). Many members of the Amphibolurinae exhibit examples of extreme morphological elaboration, such as the throat of the bearded dragon (*Pogona vitticeps*), the frill of the frill necked lizard (*Chlamydosaurus kingii*), the spines of the thorny devil (*Moloch horridus*), and the impressive crest of Boyd's forest dragon (*Lophosaurus boydii*).

Ecological and taxonomic diversification has certainly occurred in amphibolurine lineages, but we do not have many insights about the morphological features and variation that might accompany this diversification. We now have a relatively sound understanding of the phylogenetic relationships among the Australian agamids. This understanding, along with their extensive ecological diversity, and the broad range of forms and functions observed in this clade, make them an ideal model group with which to explore morphological diversity.
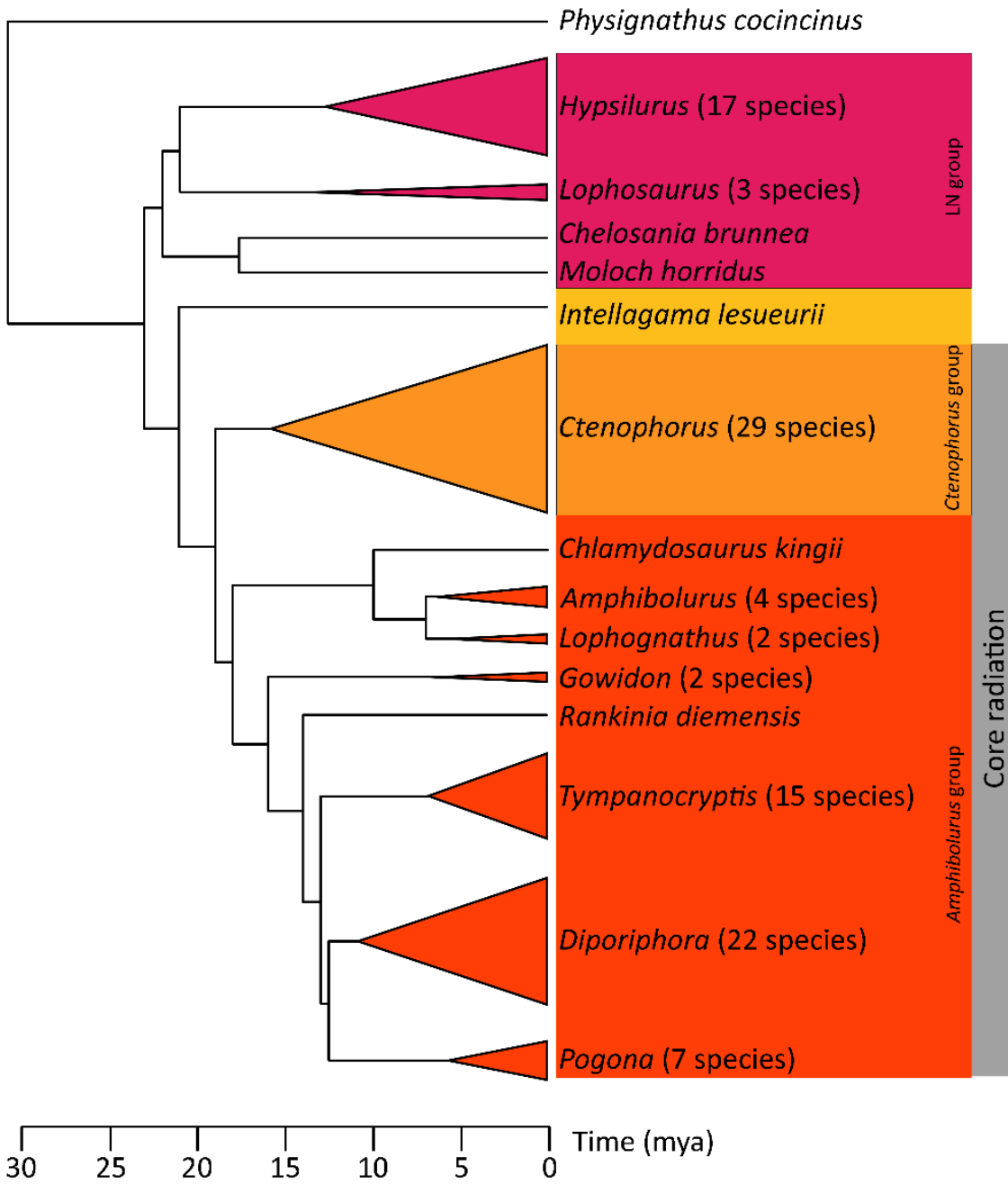
Figure 1.3 – Evolutionary tree of Amphibolurinae genera and monophyletic clades. Dates and branches are based on those in Hugall et al., (2008), and numbers of species are based on current taxonomy (on 14th July 2018) at http://reptile-database.reptarium.cz/.

Australian agamid skeletal morphology: what we know

When it comes to skeletal morphology of major lizard families, Agamidae is one of the most poorly understood. Much of the work on the osteology of agamids has been carried out as part of broader systematic analysis of Squamata, the clade containing all lizards and snakes (Estes et al., 1988; Caldwell, 1999; Conrad, 2008; Evans, 2008; Smith, 2011; Gauthier et al., 2012). Some of the first systematic studies of the skeletons of the agamid family as a single entity remain the most detailed available compilations of their morphological characteristics (Siebenrock, 1895; Moody, 1980; Evans, 2008). There have been some subsequent reviews and observations of agamid skulls (Camp, 1923; El Toubi, 1945; Jollie, 1960; Herrel et al., 1999; Evans, 2008), and the whole skeleton (Badham, 1976; Greer, 1989; Smirina and Ananjeva, 2007). In some cases, skeletons of particular species have been described in some detail (Harris, 1963; Badham, 1976; Pethiyagoda and Manamendra-Arachchi, 1998; Smirina and Ananjeva, 2007; Bell et al., 2009). Some representatives of the agamid family, including some Australian species, have been included in morphometric analyses as part of broader explorations of lizard skull shape (Metzger and Herrel, 2005; Stayton, 2005, 2006). For the Australian taxa, there has been some work comparing particular components of osteology (Greer, 1989; Hocknull, 2000, 2002), and the osteology of particular taxa (Cooper et al., 1970; Bell et al., 2009; Stilson et al., 2017). Most of the previous work describes the skeletons of species or groups based on small numbers of adult specimens, and information regarding inter- and intraspecific variation is scarce. This deficit in knowledge of osteological variation within and among extant Australian agamid species has hampered our understanding of fossil agamids recovered from Australian deposits.

The dentition of agamids has been described in some works, and this information has been used in the interpretation of fossil material (Cooper et al., 1970; Cooper and Poole, 1973; Robinson, 1976; Hocknull, 2002; Berkovitz, 2007). From published descriptions, we know that the agamid family has unique dentition: they are heterodonts, exhibiting pleurodont tooth implantation in their anterior teeth, and acrodont implantation in their posterior teeth. The anterior pleurodont teeth undergo replacement and are typically caniniform (Hocknull, 2002), although there are some exceptions (Cooper and Poole, 1973; Bell et al., 2009). The acrodont teeth are not replaced, are typically triangular in lateral view (sometimes with cusps, see Evans, 2008), and increase in size at more posterior tooth positions (Cooper et al., 1970). Throughout growth, new teeth are added to the posterior of the acrodont tooth row. This distinctive dentition is unique among vertebrates and fossil jaw bones belonging to agamids are therefore readily identified to family level (Moriarty et al., 2000).

Jaw bones of agamids are commonly recovered from fossil deposits, but their identification beyond family level is difficult. Some studies state the resemblance of a fossil compared with extant species, without details about characters or criteria used to achieve affiliations (Smith, 1976; Archer et al., 2006; Hocknull et al., 2007). The relative prevalence of agamid jaw bones in deposits compared to other bones has led to some comparative work on these elements. There have been two documented systematic attempts to identify useful characters for the identification of agamid fossils (both teeth and jaw bones), one documenting characters in extant comparative material (Hocknull, 2002), and one documenting the characters observed in Riversleigh fossil agamids (Covacevich et al., 1990). The latter names the first and only new fossil agamid species from Australian fossil deposits, *Sulcatidens quadratus*.

It is evident from preliminary observations (see Fig. 1.4) and previous works on skeletal morphology, that extensive variation exists both among and within agamid species. Furthermore, dramatic morphological changes accompany increases in size throughout a dragon's life. Quantitatively and systematically investigating this variation will contribute to an overall greater understanding of the evolutionary history of Australian agamids. It will also enhance the resolution of information used in agamid fossil identification, contributing to analyses of the faunal components in Australian fossil deposits.
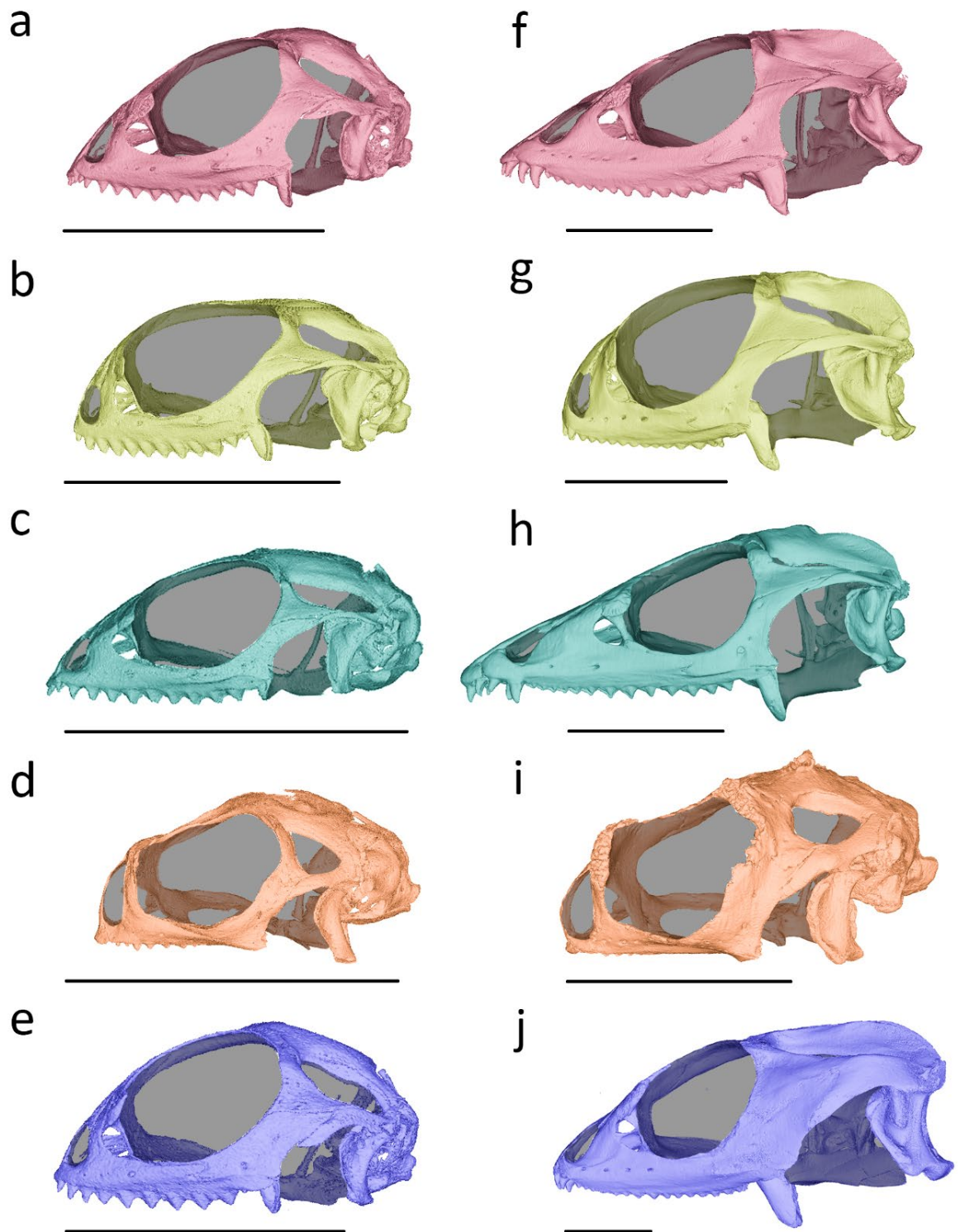
Figure 1.4 – Lateral views of computed tomography reconstructions showing examples of the range of morphology in Australian agamid skulls. Includes hatchlings (a – e) and adults (d – j) of *Amphibolurus muricatus* **(a: AMS R152446 and f: AMS R154972),** *Ctenophorus nuchalis* **(b: SAMA R57174 and g: SAMA R7296),** *Gowidon longirostris* **(c: SAMA R60498 and h: SAMA R18053),** *Moloch horridus* **(d: SAMA R10703 and i: SAMA R63565), and** *Pogona vitticeps* **(e: SAMA R58978 and j: SAMA R18545). Scale bars are 10 mm in length.**

Main aims and overview

It was through a year-long honours project involving Australian agamids in the fossil record that I came to a realisation: the skulls of this clade of lizards remained underexplored, so much so, that it greatly hindered their interpretation in the fossil record. Hence, the Australian agamids are an ideal group with which to explore skull shape in an evolutionary context. This dissertation investigates the evolutionary patterns in the skull and teeth of this ecologically and taxonomically diverse lizard radiation. I intend to address the knowledge gap in morphological variation of skull shape among and within amphibolurine clades and species, and investigate the factors that determine it. To achieve this goal, I address four main aims.

AIM 1: Explore disparity

To grasp the dynamics of morphological disparity of the amphibolurines, I draw comparisons between Amphibolurinae and other agamid subfamilies, and also with other iguanian families. I also probe further into amphibolurine disparity, by investigating how the disparity is distributed among amphibolurine clades and genera. At the finest level, I compare disparity of the smallest juvenile amphibolurines with that of adults, to indicate the extent to which ontogeny may play a role in the skull shape of amphibolurines.

AIM 2: Investigate ontogenetic patterns

Because juvenile and adult skulls of the same species look dramatically different to one another, it is clear that ontogeny probably plays a major role in producing skull shape variation among amphibolurines. I characterise and compare ontogenetic patterns in skull morphology and tooth counts among amphibolurine species.

AIM 3: Characterise skull shape and identify what influences variation

I intend to quantitatively characterise the skull shapes observed in amphibolurine lizards, and investigate to what extent skull shape is dictated by phylogeny and adaptation. Since amphibolurines exhibit a broad range of body sizes, I also investigate the role of evolutionary allometry in facilitating diversity in skull shapes.

AIM 4: Obtain knowledge that will advance fossil interpretation

Since all chapters aim to improve our understanding of amphibolurine skull morphology, they collectively contribute towards an improved interpretation of amphibolurine cranial elements in the Australian fossil record. To supplement this improved knowledge, I suggest methods for advancing our ability to estimate body size and taxonomic affiliation of fossil jaw bones.

Over the next seven chapters, I address these aims, using a combination of morphological measurements and two-dimensional and three-dimensional geometric morphometrics. I assemble a large amount of morphological data, at several taxonomic levels, and use a suite of statistical techniques to characterise cranial morphology in the amphibolurine radiation of lizards and to identify the factors driving inter- and intraspecific variation.

Chapter outline

CHAPTER 2

Exceptional disparity in Australian agamid lizards is a possible result of arrival into vacant niche

I examine the major cranial proportions of 1144 iguanian specimens using 2D morphometrics to explicitly quantify the morphological disparity of Australian agamid lizards and compare it to the disparity of agamid, acrodont, and iguanian clades from other parts of the world.

CHAPTER 3

Patterns in tooth number among Australian agamid lizards

I examine tooth counts during growth in amphibolurine lizards, to detect allometric patterns within and among taxa and increase the capacity to understand their fossil record. I collect data from 578 specimens, representing 63 species and 14 genera.

CHAPTER 4

Changes in ontogenetic patterns facilitate diversification in skull shape of Australian agamid lizards

I use 2D geometric morphometric methods to characterise the ontogenetic patterns of variation in shape of the crania of 18 species of amphibolurine lizards and investigate the associations between postnatal growth patterns, life habit, and phylogeny.

CHAPTER 5

Evolution of cranial shape in a continental-scale evolutionary radiation of Australian lizards

I use 3D geometric morphometrics to characterise skull shapes in Australian agamids and their Asian agamid relatives (52 species in total), and identify associations between skull shape, and phylogeny and ecological life habit.

CHAPTER 6

Implications of using captive lizards in geometric morphometric analyses

I use 3D geometric morphometrics to observe the differences in cranial shape and ontogenetic patterns between samples of wild and captive jacky lizards, and examine how captive lizards may be interpreted in a broader data set containing multiple species.

CHAPTER 7

Using jaw bones to estimate Australian dragon body size

I use the maxilla and dentary bones of Australian agamid lizards to examine the relationship between tooth row length and snout-vent length, to provide a method for estimating agamid body sizes in fossil assemblages.

CHAPTER 8

Geometric morphometrics provides a more objective approach for interpreting the affinity of fossil lizard jaws

I evaluate the taxonomic affinity of a fossil maxilla from the Holocene deposits of Kelly Hill Caves (Kangaroo Island, South Australia) by comparing them to a sample of modern agamid lizards using computer models generated from X-ray computed tomography data and 3D geometric morphometrics.

CHAPTER 9

Summary and conclusions

Anatomical reference for the lizard cranium

To accompany this thesis, I have produced an anatomical reference, showing cranial elements that are discussed within it and that are referred to in definitions of landmarks used for geometric morphometrics. The specimen used as an example is an adult jacky lizard (*Amphibolurus muricatus*), which has a fairly "average" shaped cranium. It must be noted that although the braincase is made of several elements fused together to varying degrees (see below), the elements are shown in the same colour, for clarity in the overall cranium structure.

Table 1.1 – Key to abbreviations used to label elements and structures in anatomical reference. Based mostly on those defined and used (with some changes in capitalisation) in Evans, 2008 (p 2-4), unless otherwise indicated.

ac.tt	Acrodont teeth*	p.f	Parietal foramen
b.tb	Basal tubercle†	Pa	Palatine
Bo	Basioccipital†	pg	Squamosal ventral "peg"
bo.co	Basioccipital condyle†	pl.tt	Pleurodont teeth*
bpt.p	Basipterygoid process	Po	Postorbital
Ec	Ectopterygoid	pocc	Paroccipital process†
Ep	Epipterygoid	Prf	Prefrontal
f.pr	Facial process of maxilla	prf.p	Prefrontal process*
Fr	Frontal	Pro	Prootic†
io.f	Infraorbital fenestra*	Pt	Pterygoid
J	Jugal	pt.fl	Pterygoid flange
L	Lacrimal	Px	Premaxilla
l.f	Lacrimal foramen	Q	Quadrate
Mx	Maxilla	So	Supraoccipital†
mx.lp	Maxillary lappet	Sq	Squamosal
N	Nasal	St	Supratemporal
n.b	Narial basin*	Stp	Stapes
or	Orbital*	Sx	Septomaxilla
Ot	Otooccipital†	utf	Upper temporal fenestra
P	Parietal	V	Vomer

* Structures not in Evans, 2008, defined by the author.
† Braincase elements.

Figure 1.5 – Key for colours used to label bone elements in anatomical reference.

Figure 1.6 – Anatomical reference. Dorsal (A) and ventral (B) views of the cranium of *Amphibolurus muricatus* **(Australian Museum specimen R154972).**
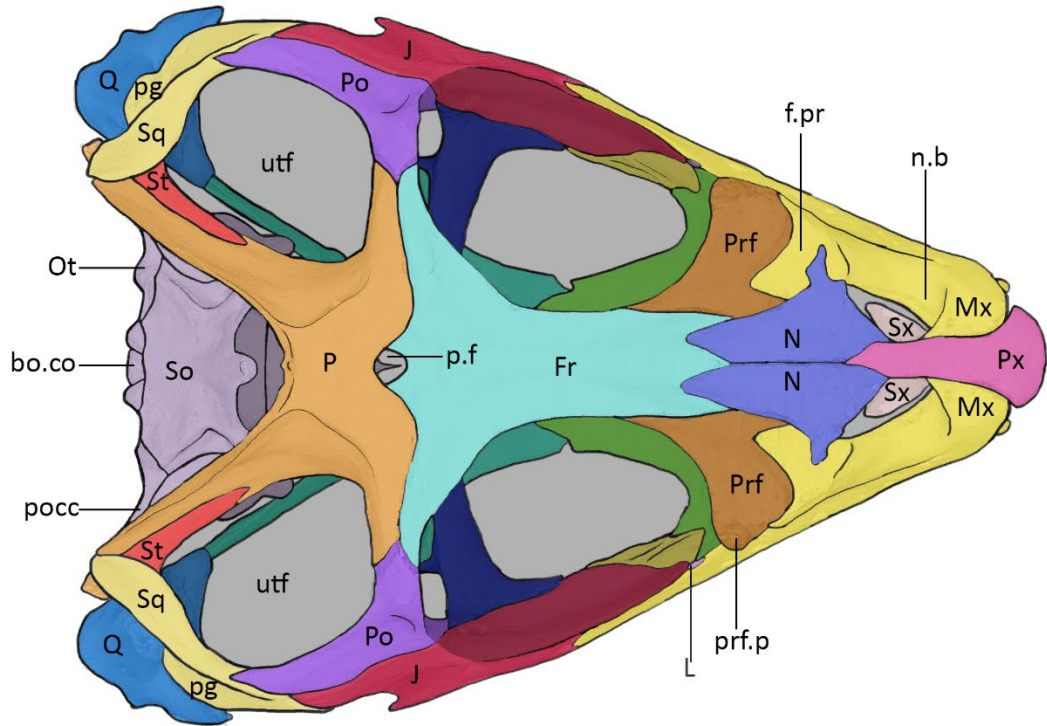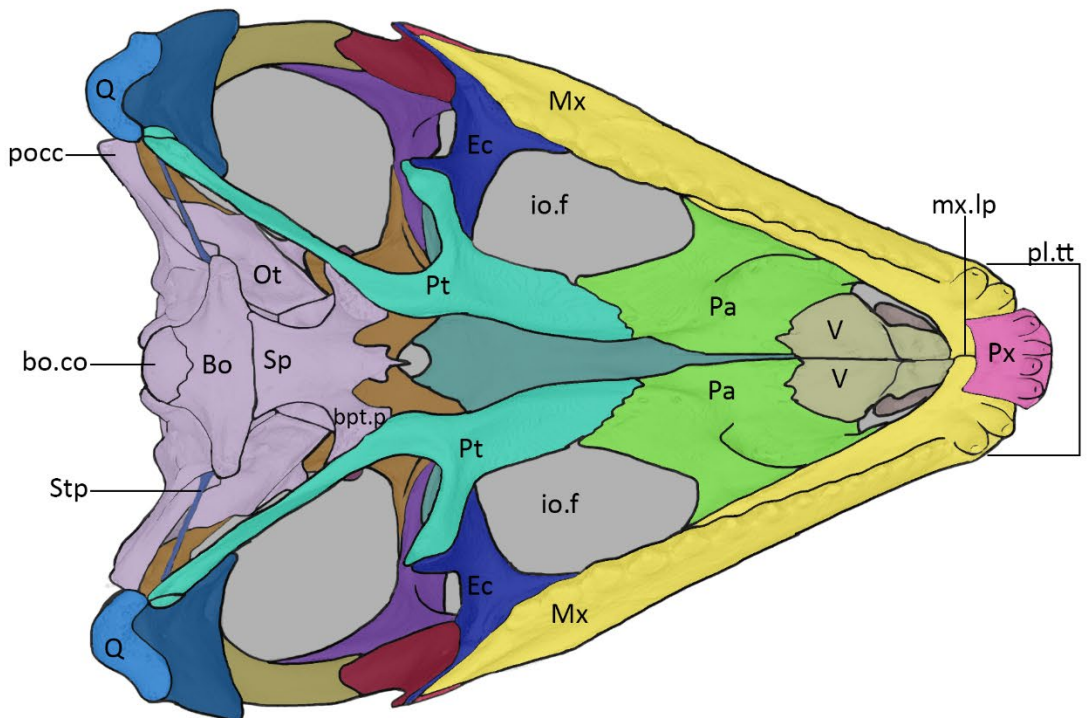
Figure 1.7 – Anatomical reference. Lateral (A), anterior (B), and posterior (D) views of the cranium of *Amphibolurus muricatus* (Australian Museum specimen R154972).
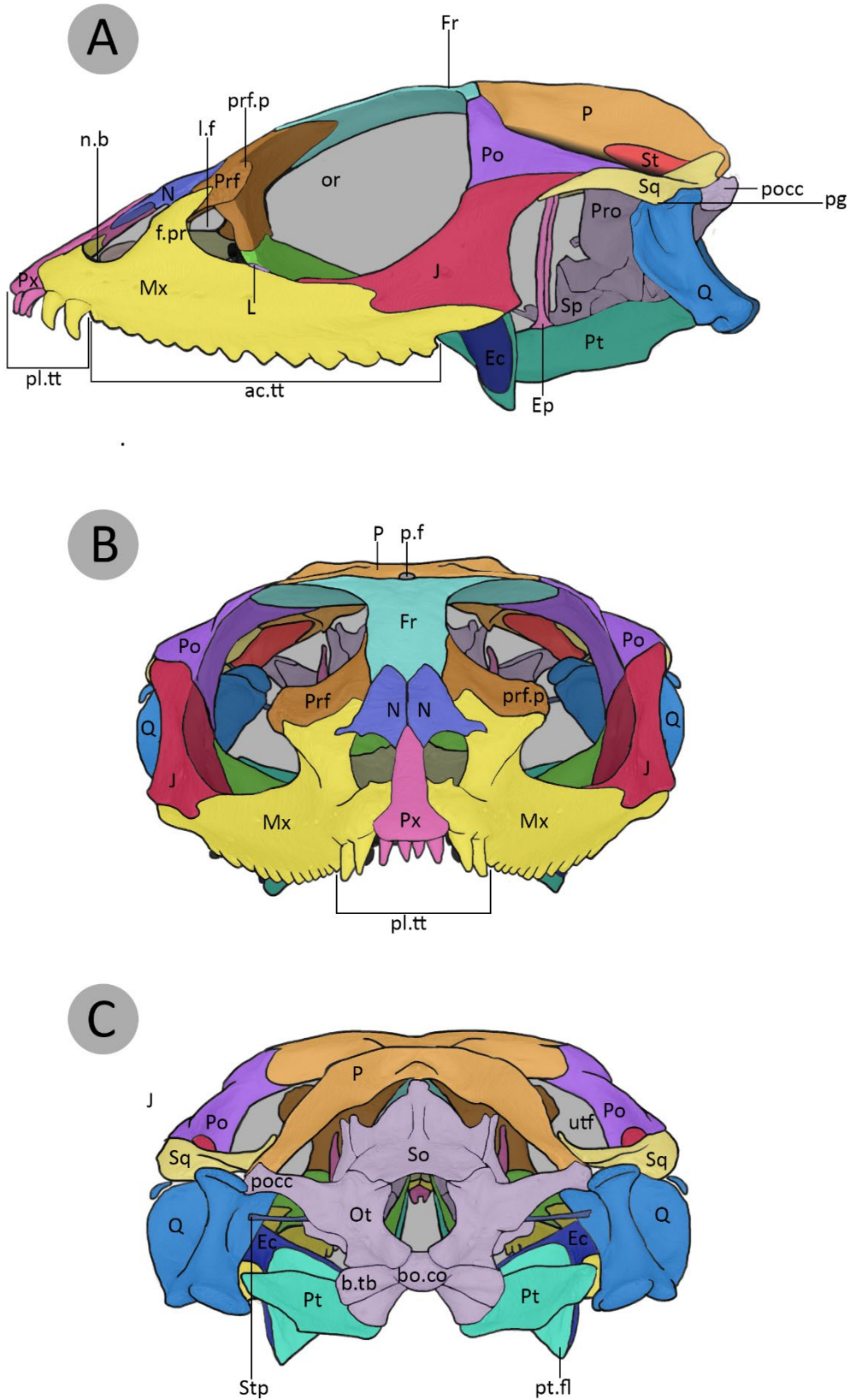
References

Adams DC. 1999. Methods for shape analysis of landmark data from articulated structures. Evol Ecol 1:959-970.

Adams DC. 2014. A generalized K statistic for estimating phylogenetic signal from shape and other high dimensional multivariate data. Syst Biol 63:685-697.

Adams DC, Collyer ML. 2009. A general framework for the analysis of phenotypic trajectories in evolutionary studies. Evolution 63:1143-1154.

Adams DC, Rohlf FJ, Slice DE. 2004. Geometric morphometrics: ten years of progress following the 'revolution'. Ital J Zool 71:5-16.

Archer M, Arena DA, Bassarova M, Beck RMD, Black K, Boles WE, Brewer P, Cooke BN, Crosby K, Gillespie A, Godthelp H, Hand SJ, Kear BP, Louys J, Morrell A, Muirhead J, Roberts KK, Scanlon JD, Travouillon KJ, Wroe S. 2006. Current status of species-level representation in faunas from selected fossil localities in the Riversleigh World Heritage Area, northwestern Queensland. Alcheringa 30:1-17.

Badham JA. 1976. The *Amphibolurus barbatus* species-group (Lacertilia: Agamidae). Aust J Zool 24:423-443.

Bell CJ, Mead JI, Swift SL. 2009. Cranial osteology of *Moloch horridus* (Reptilia: Squamata: Agamidae). Rec West Aust Mus 25:201-237.

Berkovitz BK. 2007. Tooth replacement patterns in non-mammalian vertabrates. In: Teaford MF, Smith MM, Ferguson MWJ, editors. Development, function and evolution of teeth. New York: Cambridge University Press.

Bookstein FL. 1989. Principal warps: thin-plate splines and the decomposition of deformations. IEEE Trans Pattern Anal Mach Intell 11:567-585.

Bookstein FL. 1991. Morphometric tools for landmark data: geometry and biology. Cambridge: Cambridge University Press.

Caldwell MW. 1999. Squamate phylogeny and the relationships of snakes and mosasauroids. Zool J Linnean Soc 125:115-147.

Camp CL. 1923. Classification of the lizards. Bull Amer Mus Nat Hist 48:289-481.

Cock AG. 1966. Genetical aspects of metrical growth and form in animals. Q Rev Biol 41:131-190.

Collyer ML, Sekora DJ, Adams DC. 2015. A method for analysis of phenotypic change for phenotypes described by high-dimensional data. Heredity 115:357-365.

Conrad JL. 2008. Phylogeny and systematics of Squamata (Reptilia) based on morphology. Bull Am Mus Nat Hist 310:1-82.

Cooper JS, Poole DFG. 1973. The dentition and dental tissues of the agamid lizard, *Uromastyx*. J Zool 169:85-100.

Cooper JS, Poole DFG, Lawson R. 1970. The dentition of agamid lizards with special reference to tooth replacement. J Zool 162:85-98.

Covacevich J, Couper P, Molnar RE, Witten G, Young W. 1990. Miocene dragons from Riversleigh: new data on the history of the family Agamidae (Reptilia: Squamata) in Australia. Mem Queensl Mus 29:339-360.

Dryden I, Mardia K. 1998. Statistical shape analysis. John Wiley & Sons.

El Toubi M. 1945. Notes on the cranial osteology of *Uromastix aegyptia* (Forskal). Bull Fac Sci Cairo Fouad I Univ 25:1-10.

Estes R, de Queiroz K, Gauthier J. 1988. Phylogenetic relationships within Squamata. In: Estes R, Pregill G, editors. Phylogenetic relationships of the lizard families. Stanford University Press. p 119-281.

Evans SE. 2008. The skull of lizards and tuatara. In: Gans C, Gaunt AS, Adler K, editors. Biology of the Reptilia 20, Morphology H, The skull of Lepidosauria. Ithaca, New York: Society for the Study of Amphibians and Reptiles. p 1-347.

Foote M. 1990. Nearest-neighbour analysis of trilobite morphospace. Syst Zool 39:371-382.

Foote M. 1991. Morphologic patterns of diversification: examples from trilobites. Palaeontology 34:461-485.

Foote M. 1993a. Contributions of individual taxa to overall disparity. Paleobiology 19:403-419.

Foote M. 1993b. Discordance and concordance between morphological and taxonomic diversity. Paleobiology 19:185-204.

Foote M. 1997. The evolution of morphological disparity. Annu Rev Ecol Syst 28:129-152.

Friedman M. 2010. Explosive morphological diversification of spiny-finned teleost fishes in the aftermath of the end-Cretaceous extinction. Proc R Soc B 277:1675-1683.

Frost DR, Etheridge R. 1989. A phylogenetic analysis and taxonomy of iguanian lizards. Pub Univ Kansas 81:1-65.

Frost DR, Etheridge R, Janies D, Titus TA. 2001. Total evidence, sequence alignment, evolution of polychrotid Lizards, and a reclassification of the Iguania (Squamata: Iguania). Am Mus Novit 3343:1-39.

Fujioka T, Chappell J. 2010. History of Australian aridity: chronology in the evolution of arid landscapes. Geol Soc, Special Publications 346:121-139.

Fujioka T, Chappell J, Honda M, Yatsevich I, Fifield LK, Fabel D. 2005. Global cooling initiated stony deserts in central Australia 2–4 Ma, dated by cosmogenic 21Ne-10Be. Geology 33:993-996.

Gauthier JA, Kearney M, Anderson Maisano J, Rieppel O, Behlke ADB. 2012. Assembling the squamate tree of life: perspectives from the phenotype and the fossil record. B Peabody Mus Nat Hi 53:3-308.

Gould SJ. 1966. Allometry and size in ontogeny and phylogeny. Biol Rev 41:587-640.

Gould SJ. 1989. A developmental constraint in *Cerion*, with comments on the definition and interpretation of constraint in evolution. Evolution 43:516-539.

Greer AE. 1989. Agamidae - dragon lizards. In: The biology and evolution of Australian lizards. Chipping Norton, Australia: Surrey Beatty & Sons Pty Ltd. p 9-50.

Griffiths AD, Christian KA. 1996. Diet and habitat use of frillneck lizards in a seasonal tropical environment. Oecologica 106:39-48.

Hanken J, Hall BK. 1993. Functional and evolutionary mechanisms. Chicago: University of Chicago Press.

Harris VA. 1963. The anatomy of the rainbow lizard, *Agama agama*. London: Hutchison.

Herrel A, Aerts P, Fret J, de Vree F. 1999. Morphology of the feeding system in agamid lizards: ecological correlates. Anat Rec 254:496-507.

Hocknull SA. 2000. The phylogeny and fossil record of Australopapuan dragon lizards (Squamata: Agamidae). Honours thesis: University of Queensland.

Hocknull SA. 2002. Comparative maxillary and dentary morphology of the Australian dragons (Agamidae: Squamata): a framework for fossil identification. Mem Queensl Mus 48:125-145.

Hocknull SA, Zhao J-x, Feng Y-x, Webb GE. 2007. Responses of Quaternary rainforest vertebrates to climate change in Australia. Earth Planet Sci Lett 264:317-331.

Honda M, Ota H, Kobayashi M, Nabhitabhata J, Yong H-S, Sengoku S, Hikida T. 2000. Phylogenetic relationships of the family Agamidae (Reptilia: Iguania) inferred from mitochondrial DNA sequences. Zool Sci 17:527-537.

Hugall AF, Foster R, Hutchinson M, Lee MSY. 2008. Phylogeny of Australian agamid lizards based on nuclear and mitchondrial genes: implications for morphological evolution and biogeography. Biol J Linnean Soc 93:343-358.

Huxley JS, Teissier G. 1936. Terminology of relative growth. Nature 114:895-896.

Jollie MT. 1960. The head skeleton of the lizard. Acta Zoologica 41:1-64.

Klingenberg CP. 1998. Heterochrony and allometry: the analysis of evolutionary change in ontogeny. Biol Rev 73:79-123.

Klingenberg CP. 2010. Evolution and development of shape: integrating quantitative approaches. Nat Rev Genet 11:623-635.

Klingenberg CP. 2016. Size, shape, and form: concepts of allometry in geometric morphometrics. Dev Genes Evol 226:1-25.

Klingenberg CP, Marugán-Lobón J. 2013. Evolutionary covariation in geometric morphometric data: analyzing integration, modularity, and allometry in a phylogenetic context. Syst Biol 62:591-610.

Macey JR, Schulte IIJA, Larson A, Ananjeva NB, Wang Y, Pethiyagoda R, Rastegar-Pouyani N, Papenfuss TJ. 2000. Evaluating trans-tethys migration: an example using acrodont lizard phylogenetics. Syst Biol 49:233-256.

Mackey BG, Berry SL, Brown T. 2008. Reconciling approaches to biogeographical regionalization: a systematic and generic framework examined with a case study of the Australian continent. J Biogeogr 35:213-229.

Manthey U, Denzer W. 2006. A revision of the Melanesian-Australian angle head lizards of the genus *Hypsilurus* (Sauria: Agamidae: Amphibolurinae), with description of four new species and one new subspecies. Hamadryad 30:1-40.

Martin HA. 2006. Cenozoic climatic change and the development of the arid vegetation in Australia. J Arid Env 66:533-563.

McGowran B, Holdgate GR, Li Q, Gallagher SJ. 2004. Cenozoic stratigraphic succession in southeastern Australia. Aust J Earth Sci 51:459-496.

Melville J, Harmon LJ, Losos JB. 2006. Intercontinental community convergence of ecology and morphology in desert lizards. Proc R Soc B 273:557-563.

Melville J, Schulte JA, Larson A. 2001. A molecular phylogenetic study of ecological diversification in the Australian lizard genus *Ctenophorus*. J Exp Zool 291:339-353.

Metzger KA, Herrel A. 2005. Correlations between lizard cranial shape and diet: a quantitative, phylogenetically informed analysis. Biol J Linnean Soc 86:433-466.

Mittroecker P, Bookstein F. 2011. Linear discrimination, ordination, and the visualisation of selection gradients in modern morphometrics. Evol Biol 38:100-114.

Moody SM. 1980. Phylogenetic and historical biogeographical relationships of the genera in the family Agamidae (Reptilia, Lacertilia). Doctoral Dissertation: University of Michigan.

Moriarty KC, McCulloch MT, Wells RT, McDowell MC. 2000. Mid-Pleistocene cave fills, megafaunal remains and climate change at Naracoorte, South Australia: towards a predictive model using U-Th dating of speleothems. Palaeogeogr Palaeoclimatol Palaeoecol 159:113-143.

Oliver PM, Hugall AF. 2017. Phylogenetic evidence for mid-Cenozoic turnover of a diverse continental biota. Nat Ecol Evol 1:1896.

Pethiyagoda R, Manamendra-Arachchi K. 1998. A revision of the endemic Sri Lankan agamid lizard genus *Ceratophora* Gray, 1835, with description of two new species. J South Asian Nat Hist 3:1-50.

Pianka ER. 1971. Ecology of the agamid lizard *Amphibolurus isolepis* in Western Australia. Copeia 1971:527-536.

Pianka ER. 2013a. Notes on the ecology and natural history of two uncommon arboreal agamid lizards *Diporiphora*. West Austral Nat 29:77-84.

Pianka ER. 2013b. Notes on the ecology and natural history of two uncommon terrestrial agamid lizards *Ctenophorus clayi* and *C. fordi* in the Great Victoria Desert of Western Australia. West Austral Nat 29:85-93.

Pianka ER. 2013c. Notes on the natural history of the rarely recorded agamid lizard *Caimanops amphiboluroides* in Western Australia. West Austral Nat 29:99-102.

Pianka ER. 2014a. Notes on a collection of lizards from the Eucla sand dunes in Western Australia. West Austral Nat 30:155-161.

Pianka ER. 2014b. Notes on the ecology and natural history of *Ctenophorus reticulatus* (Agamidae) in Western Australia. West Austral Nat 30:222-225.

Pianka ER, Goodyear SE. 2012. Lizard responses to wildfire in arid interior Australia: long-term experimental data and commonalities with other studies. Austral Ecol 37:1-11.

Pianka ER, Pianka HD. 1970. The ecology of *Moloch horridus* (Lacertilia: Agamidae) in Western Australia. Copeia 1970:90-103.

Radder RS, Warner D, Shine R. 2007. Compensating for a bad start: catch-up growth in juvenile lizards (*Amphibolurus muricatus*, Agamidae). J Exp Zool 307A:500-508.

Rieppel O. 1990. Ontogeny—a way forward for systematics, a way backward for phylogeny. Biol J Linnean Soc 39:177-191.

Robinson PM. 1976. How *Sphenodon* and *Uromastyx* grow their teeth and use them. Morphol Biol Reptiles 3:43-64.

Runnegar B. 1987. Rates and modes of evolution in the Mollusca. In: Rates of evolution. London: Allen and Unwin. p 39-60.

Schmidt-Nielsen K. 1984. Scaling: why is animal size so important? Cambridge University Press.

Schulte JA, Melville J, Larson A. 2003. Molecular phylogenetic evidence for ancient divergence of lizard taxa on either side of Wallace's Line. Proc R Soc Lond B 270:597-603.

Sereno PC. 1999. Definitions in phylogenetic taxonomy: critique and rationale. Syst Biol 48:329-351.

Siebenrock F. 1895. Das skelett der Agamidae. Sittzungsber Akad Wiss Wien 104.

Simões TR, Caldwell MW, Talanda M, Bernardi M, Palci A, Vernygora O, Bernardini F, Mancini L, Nydam RL. 2018. The origin of squamates revealed by a Middle Triassic lizard from the Italian Alps. Nature 557:706-709.

Smirina EM, Ananjeva NB. 2007. Growth layers in bones and acrodont teeth of the agamid lizard *Laudakia stoliczkana* (Blanford, 1875) (Agamidae, Sauria). Amphibia-Reptilia 28:193-204.

Smith K. 2011. On the phylogenetic affinity of the extinct acrodontan lizard *Tinosaurus*. In: Tropical vertebrates in a changing world. p 9-27.

Smith MJ. 1976. Small fossil vertebrates from Victoria Cave, Naracoorte, South Australia. Trans R Soc S Aust 100:39-51.

Stayton CT. 2005. Morphological evolution of the lizard skull: a geometric morphometrics survey. J Morphol 263:47-59.

Stayton CT. 2006. Testing hypotheses of convergence with multivariate data: morphological and functional convergence among herbivorous lizards. Evolution 60:824-841.

Stilson KT, Bell CJ, Mead JI. 2017. Patterns of variation in the cranial osteology of three species of endemic Australian lizards (*Ctenophorus*: Squamata: Agamidae): implications for the fossil record and morphological analyses made with limited sample sizes. J Herpetol 51:316-329.

Stuart-Smith J, Swain R, Welling A. 2005. Reproductive ecology of the mountain dragon, *Rankinia* (*Tympanocryptis*) *diemensis* (Reptilia: Squamata: Agamidae) in Tasmania. Pap Proc R Soc Tasmania 139:23-28.

Townsend TM, Mulcahy DG, Noonan BP, Sites JWJ, Kuczynski CA, Wiens JJ, Reeder TW. 2011. Phylogeny of iguanian lizards inferred from 29 nuclear loci, and a comparison of concatenated and species-tree approaches for an ancient, rapid radiation. Mol Phylogenet Evol 61:1363-1380.

Wilson S, Swan G. 2013. A complete guide to reptiles of Australia, 4th ed. Chatswood: New Holland Publishers.

Zaher H, Rieppel O. 1999. Tooth implantation and replacement in squamates, with special reference to mosasaur lizards and snakes. Am Mus Novit 10024:1-19.

STATEMENT OF AUTHORSHIP

Title of Paper	Exceptional disparity of Australian agamid lizards is a possible result of arrival into vacant niche.
Publication Status	☐ Published ☐ Accepted for Publication ☑ Submitted for Publication ☐ Unpublished and Unsubmitted work written in manuscript style
Publication Details	Submitted to The Anatomical record on 30.07.2018

Principal Author

Name of Principal Author (Candidate)	Jaimi Gray		
Contribution to the Paper	Designed research, data collection and analysis, wrote first version of manuscript, edited later versions of manuscript.		
Overall percentage (%)	85%		
Certification:	This paper reports on original research I conducted during the period of my Higher Degree by Research candidature and is not subject to any obligations or contractual agreements with a third party that would constrain its inclusion in this thesis. I am the primary author of this paper.		
Signature		Date	23.08.2018

Co-Author Contributions

By signing the Statement of Authorship, each author certifies that:

i.   the candidate's stated contribution to the publication is accurate (as detailed above);

ii.   permission is granted for the candidate in include the publication in the thesis; and

iii.   the sum of all co-author contributions is equal to 100% less the candidate's stated contribution.

Name of Co-Author	Mark N. Hutchinson		
Contribution to the Paper	Helped design research, and edited manuscript.		
Signature		Date	28/08/2018

Name of Co-Author	Marc E. H. Jones		
Contribution to the Paper	Helped design research, provided guidance for data analysis, and edited manuscript.		
Signature		Date	23rd August 2018

CHAPTER 2

Exceptional disparity in
Australian agamid lizards is
a possible result of arrival
into vacant niche
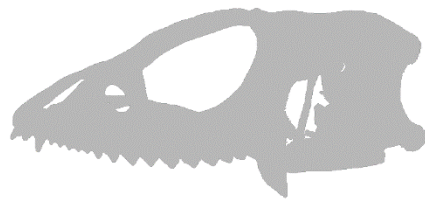
CHAPTER 2 – Exceptional disparity in Australian agamid lizards is a possible result of arrival into vacant niche

Jaimi A. Gray, Mark N. Hutchinson, Marc E. H. Jones

Abstract

Australia provides abundant examples of continental-scale evolutionary radiations. The initiation of the collision of the Asian and Australian tectonic plates, around 30 million years ago, facilitated an influx of squamates into Australia, and the subsequent squamate radiations resulted in high taxonomic diversity. The morphological disparity seen in these major squamate groups, however, remains underexplored. Here, we examine the major cranial proportions of 1144 specimens, representing 240 species, using 2D linear measurements, to explicitly quantify the morphological disparity of Australian agamid lizards (Amphibolurinae) and compare it to that of agamid, acrodont, and iguanian clades from other parts of the world. Our results indicate the Australian Amphibolurinae have a high degree of cranial disparity, that exceeds that of any other group examined, and we suggest that this is linked to the relaxed selective environment that greeted the founders of Amphibolurinae when they first arrived in Australia.

Key words: Agamidae, cranium, Iguania, morphological disparity, ternary diagram

Introduction

Evolutionary radiations (Losos and Mahler, 2010) are often linked to particular events, such as a clade invading a new geographic area (Nilsson et al., 2004), new environment (e.g. Slater et al., 2010) or following a major extinction event (e.g. Jarvis et al., 2014). In such cases factors such as new resources, freedom from competition, and an absence of predators and pathogens can lead to rapid speciation (diversity) which is often, but not always (Rundell and Price, 2009), accompanied by expansion into new ecological niches that drive a shift or expansion of morphospace (disparity). This phenomenon is particularly associated with island faunas, where examples of adaptive radiations are well known, e.g. Tahitian snails, (Murray et al., 1993), Hawaiian honeycreepers (Lovette et al., 2002), and Caribbean *Anolis* lizards (Yoder et al., 2010; Losos, 2011). The taxonomic diversity exhibited by such island radiations has been well documented, however phenotypic disparity has only recently come under more detailed scrutiny (Harmon et al., 2003). Moreover, continental-scale radiations remain poorly studied in general.

Australia is rich with examples of successful continental-scale evolutionary radiations. Around 30 million years ago (Ma), the northward-drifting margin of the Australian plate (Sahul shelf) collided with continental crust of Southeast Asia (Sunda shelf) in the New Guinea-Timor region, narrowing the ocean gap between the two landmasses and filling the intervening ocean with island arcs and terrain fragments that provided an archipelagic sweepstakes route for faunal exchange between tropical Asia and Australia (Hall, 2001). In this exchange, Australia (previously temperate-polar and apparently with poor taxonomic squamate diversity) appears to have received most of its current squamate taxonomic diversity, including agamids (Hugall et al., 2008; Chen et al., 2013), scincids (Skinner et al., 2011), varanids (Ast, 2001; Vidal et al., 2012), elapids (Keogh, 1998; Sanders et al., 2008), typhlopids (Vidal et al., 2010) and boids (Scanlon and Lee, 2011) from a small number of tropical Asian invaders (Oliver and Hugall, 2017). Most Australian clades appear to be monophyletic, implying single origins, and all of these Australian clades show the characteristics of adaptive radiations, with numerous species (over 1000 Australian squamate species) and highly varied body forms.

The taxonomic diversity associated with Australian squamates is immense (see Cogger, 2014), but their morphological disparity remains underexplored. One of the colonising groups, the agamid lizards, is represented today by the amphibolurine radiation (Hugall et al., 2008; Melville et al., 2011) which is taxonomically diverse (around 108 species) and varied in body size (adult mass from 2-3 g to 1000 g) and ecological niche (Pianka et al., 2017). They occupy almost every habitat on the Australian continent (Powney et al., 2010) and the adjacent islands of

Melanesia (Manthey and Denzer, 2006). Amphibolurinae provides a model group to investigate morphological disparity of an evolutionarily successful group. To date, discussion of the morphological disparity in this group has tended to be qualitative, highlighting extreme examples such as *Moloch* (Bell et al., 2009) or *Chlamydosaurus* (Shine, 1990), or if quantitative, limited to a few factors such as limb proportions (Melville et al., 2006; Collar et al., 2010) and locomotor performance (Thompson and Withers, 2005; Clemente et al., 2008). Broad patterns in the skull morphology in these lizards may be associated with functional or developmental constraints, and therefore represent an important element of the anatomy to examine in an adaptive context.

Today, two-dimensional and three-dimensional shape analysis is commonly used to assess morphological disparity, especially for sturdy structures such as the skull. These methods are robust, widely accepted, and provide a wealth of informative data. However, the thoroughness and time required for data collection means that it can often be difficult to acquire large sample sizes. For this study, we required a method that would allow us to include a remarkably large sample size, that didn't necessarily require direct access to specimens (i.e. able to take measurements from images or standard fossil reconstructions), and that would allow the inclusion of incomplete specimens (as long as a general shape is able to be discerned). We therefore use two-dimensional linear measurements of cranial proportions to provide an explicit quantitative measure of cranial disparity for Australian agamids and their relatives. We provide insights into macroevolutionary patterns in Australian agamids and include comparisons with other agamid, acrodont and iguanian clades.

Material and methods

We sampled 1144 iguanians from multiple collections (see Tables 2.1 and supplementary material: ES2.1) representing between 33% and 100% of the genera in each sampled family. As far as available material allowed, we assembled a comprehensive representation of the taxonomic diversity across the amphibolurines and several outgroup clades, and also endeavoured to include specimens that would represent the broadest range of cranial geometries. We included iguanian families from the Acrodonta clade (Chamaeleonidae and Agamidae), and from the Pleurodonta clade (all other iguanian families). The complete data set included skeletal specimens as well as images taken of surface reconstructions of X-ray computed tomography (CT) scans. We also included measurements from the reconstructed images of five fossils that are generally regarded as early members of Iguania, the priscagamids (Alifanov, 1996), *Ctenomastax parva* (Keqin and Norell, 2000) and *Saichangurvel davidsoni* (Conrad and Norell, 2007).

Head shape was assessed via two-dimensional linear measurments (cf. Marugán-Lobón and Buscalioni, 2003, see Fig. 2.1). This approach was used to allow a large and encompassing sample size including both images of specimens and images of reconstructed fossils. Use of 2D measurements enables this study to be more readily compared to previous studies, as well as any future additions to this data set. Crania were imaged in lateral view and aligned using the long axis of the maxillary tooth row (defined by the anterior end of the anteriormost tooth and posterior end of the posteriormost tooth, for agamids the acrodont tooth row was used due to dorsal curvature in the anterior set of pleurodont teeth in many species).
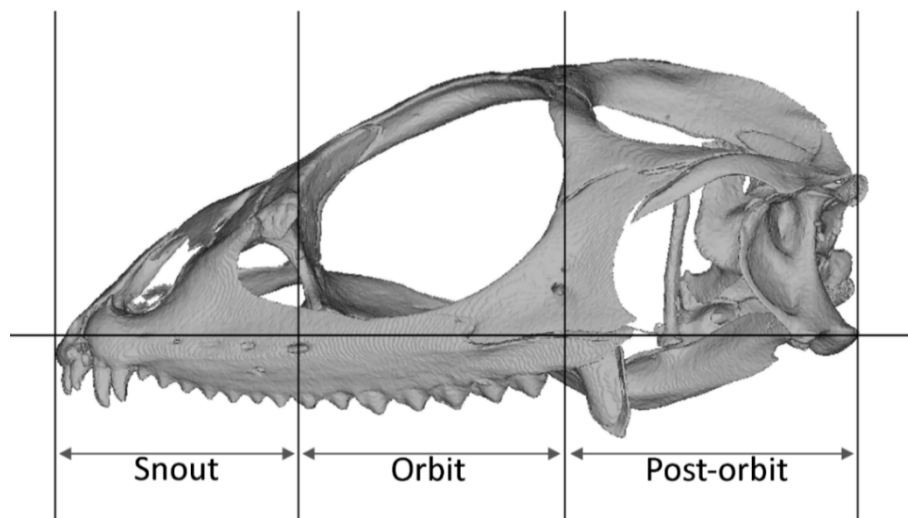
Figure 2.1 – Image of *Amphibolurus muricatus* **(Australian Museum specimen R154969) cranium in lateral view, with boundaries of proportional measurements used in this study.**

We subdivided the cranium into three units: snout, orbit, and post-orbit (Fig. 2.1). These units are comparable to those used in the Marugán-Lobón and Buscalioni (2003) study on Archosauria, with terminology and boundaries adjusted for consistency with squamate skull anatomy. The snout spans between the tip of the premaxilla and anterior-most boundary of the orbit whereas the post-orbit spans between the posterior-most boundary of the orbit and the posterior-most point of the parietal. For each specimen, we measured the length of each unit of the cranium using ImageJ v 1.52 (Schneider et al., 2012), and calculated proportions of units with respect to skull length.

All measurements were plotted on a morphospace represented by a ternary diagram using the R (v 3.4.0) package *ggtern* (Hamilton, 2018). The theoretical morphospace shows all theoretically possible combinations between percentages of the snout, orbit, and post-orbit (see Fig. 2.2). Each sub-triangle is equal to 1% of the theoretical morphospace. The empirical morphospace is the area of morphospace occupied by this data set. We calculated convex hulls and their areas (% of theoretical morphospace) to compare disparity of iguanians. To check for sample size bias, we plotted the disparity against log transformed sampled diversity for each group. The disparity of Iguania, and each major clade (e.g. Acrodonta), family (e.g. Agamidae), and subfamily (e.g. Agaminae) was regressed against species and generic diversity (number of taxa sampled) to measure the relationship between diversity and disparity and identify any exceptions.
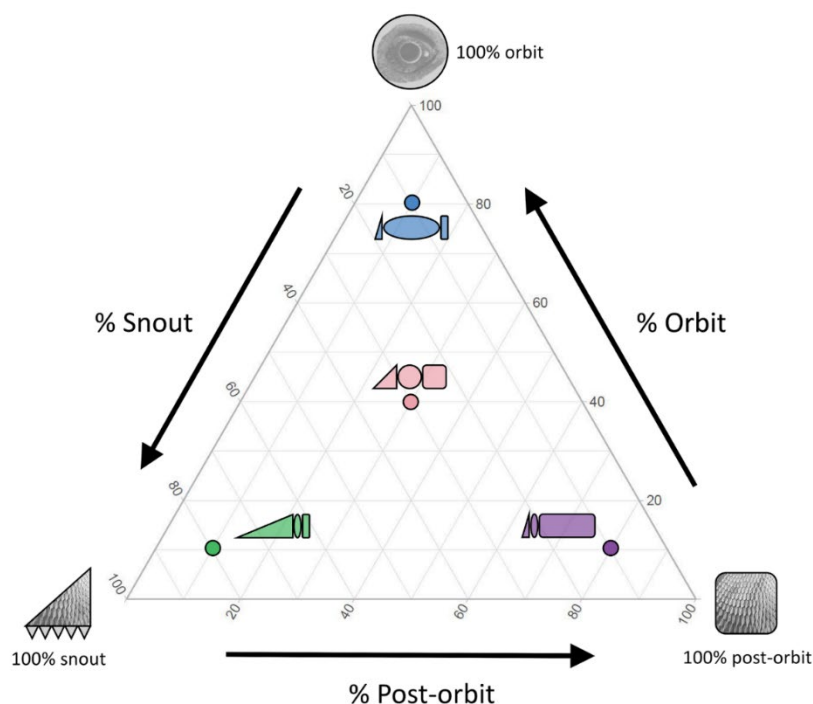
Figure 2.2 – Theoretical morphospace diagram showing examples of theoretical skull proportions (note that all theoretical skulls are the same height).

Results

Disparity of iguanian families

The total sample of iguanians (see Fig. 2.3) occupied 11.69% of the theoretical morphospace, a relatively tightly packed, rounded cluster of points. Of the iguanian families, Agamidae (10.29%) was the most disparate (see Fig. 2.3A and Table 2.1), followed by Phrynosomatidae (4.32%), Iguanidae (4.04%), and Chamaeleonidae (3.24%). The remaining families (e.g. Corytophanidae, Crotaphytidae, Dactyloidae, Polychrotidae, and Tropiduridae) each occupied less than 2% of the morphospace. The morphospace area occupied by pleurodont iguanians was almost entirely overlapped by the acrodontans, the only exceptions to this were Dactyloidae, and small peripheral areas of the morphospaces of Chamaeleonidae, Iguanidae and Phrynosomatidae. There were two areas of the morphospace occupied exclusively by Agamidae. These areas represented, firstly, a relatively long snout and short post-orbit, and secondly, a relatively large post-orbit and short snout.

Disparity of iguanian subclades

Morphospace areas identified as exclusively agamid seem to be associated almost entirely with disparity of Amphibolurinae (see Fig. 2.3B). The Amphibolurinae had the highest disparity of the agamid clades (10.15%), followed by Draconinae (4.30%). The remaining agamid clades each occupied 2% or less of the theoretical morphospace. While most of the disparity in the other groups is encompassed by that of Amphibolurinae, there is a marginal area where Draconinae extends past the amphibolurine morphospace. *Gowidon longirostris, Pogona vitticeps, Moloch horridus*, and *Ctenophorus reticulatus* are all examples (among others), of amphibolurines with extreme skull proportions. The fossil specimens fell mostly within morphospace areas that were shared by many of the iguanian families, with two of the priscagamids in the peripheral areas of amphibolurine morphospace (see Fig. 2.3A and B).

Diversity versus disparity

There is a positive relationship between disparity and log taxic diversity (Fig. 2.4, see also Table 2.1). The R^2 value for disparity versus diversity at the genus level is 0.93 (**$P = < 0.001$**), and the R^2 value for disparity versus diversity at the species level is 0.95 (**$P = < 0.001$**). Amphibolurinae is a clear outlier, with approximately twice the disparity than we might except for the sampled diversity. Of the larger and well sampled families, Phrynosomatidae had the lowest level of disparity at both the generic and species level. Chamaeleonidae, Draconinae, and Agaminae also had low disparity relative to their diversity.
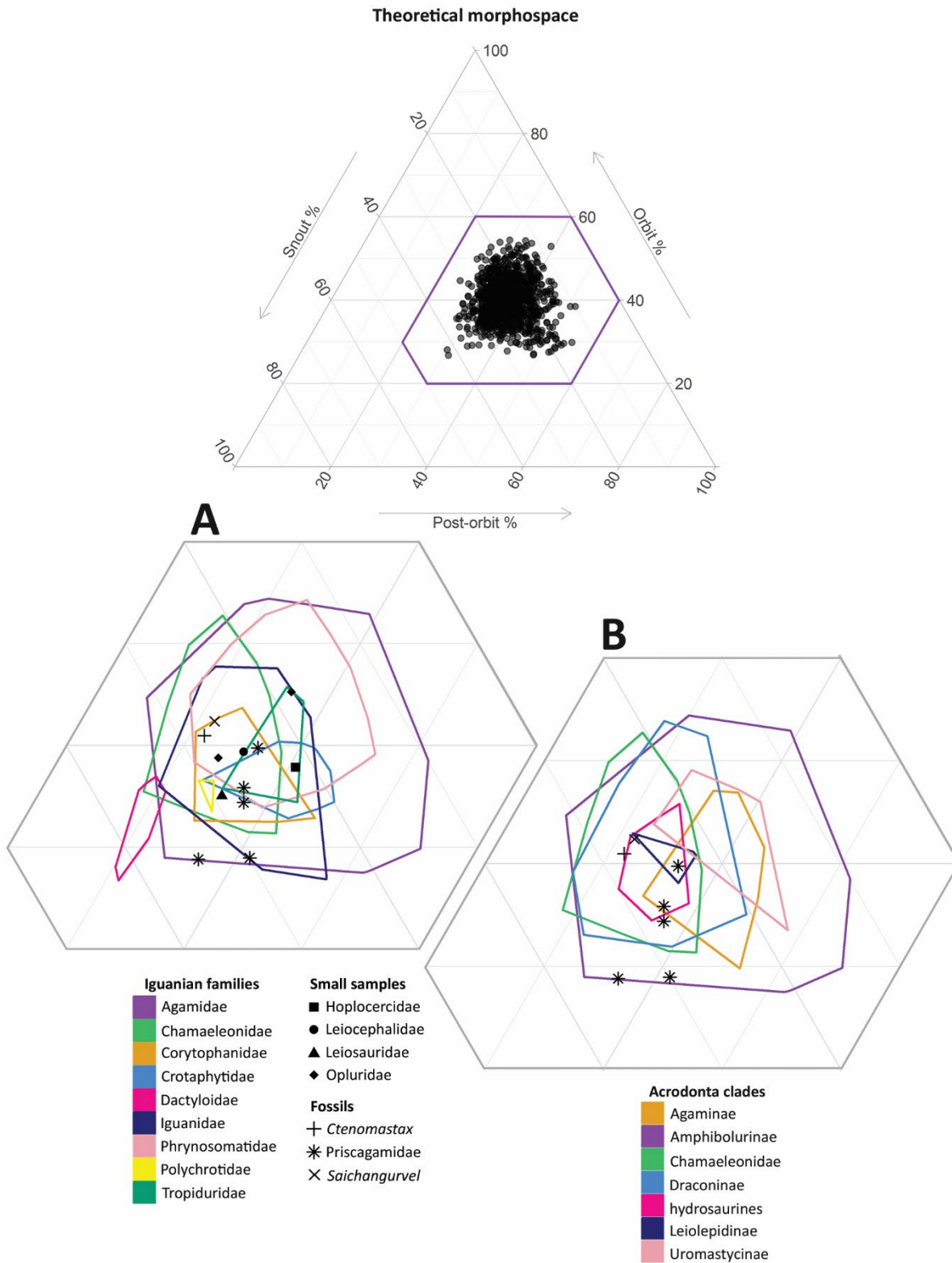
Figure 2.3 – Theoretical morphospace showing distribution of our entire sample, and comparison of morphospace occupation of different iguanian families (A), and acrodontan clades (B), with fossil specimens represented by stars and crosses.

Table 2.1 – Generic and specific diversity and disparity recorded and compared in this chapter.

Taxa	Described genera	Described species	Total specimens	Sampled genera	Sampled species	% described genera sampled	% described species sampled	% ternary plot
Iguania	119	1876	1144	81	240	68.07	12.79	11.69
Acrodonta	73	694	740	47	147	64.38	21.18	10.61
Pleurodonta	47	1183	397	34	93	72.34	7.86	8.58
Agamidae	60	488	674	37	123	61.67	25.20	10.29
Chamaeleonidae	12	206	61	9	21	75.00	10.19	3.24
Corytophanidae	3	9	27	3	6	100.00	66.67	1.49
Crotaphytidae	2	12	32	2	5	100.00	41.67	1.01
Dactyloidae	1	424	8	1	4	100.00	0.94	0.35
Hoplocercidae	3	19	1	1	1	33.33	5.26	NA
Iguanidae	9	44	69	9	10	100.00	22.73	4.04
Leiocephalidae	1	31	1	1	1	100.00	3.23	NA
Leiosauridae	6	33	2	2	2	33.33	6.06	NA
Phrynosomatidae	10	155	243	10	58	100.00	37.42	4.32
Polychrotidae	1	8	3	1	2	100.00	25.00	0.04
Tropiduridae	8	136	9	4	4	50.00	2.94	0.87
Agaminae	10	128	50	7	13	70.00	10.16	2.02
Amphibolurinae	15	108	522	14	67	93.33	62.04	10.15
Draconinae	29	220	71	11	29	37.93	13.18	4.30
hydrosaurines	2	4	14	2	3	100.00	75.00	0.88
Leiolepidinae	1	9	5	1	3	100.00	33.33	0.19
Uromastycinae	2	18	17	2	7	100.00	38.89	1.58
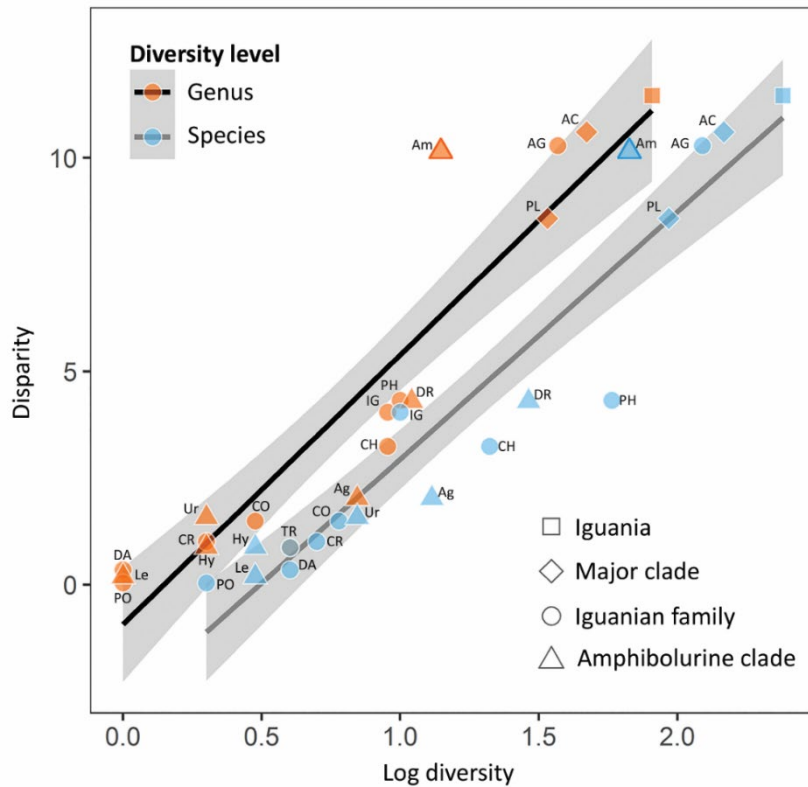
Figure 2.4 – Log diversity (sampled taxa), at both the genus and species level, versus disparity (% morphospace area occupied), with taxa of interest (Amphibolurinae) outlined, and 95% confidence intervals shown in grey. Abbreviations: AC= Acrodonta, PL= Pleurodonta, AG= Agamidae, CH= Chamaeleonidae, CO= Corytophanidae, CR= Crotaphytidae, DA= Dactyloidae, IG= Iguanidae, PH= Phrynosomatidae, PO= Polychrotidae, TR= Tropiduridae, Ag= Agaminae, Am= Amphibolurinae, Dr= Draconinae, Hy = hydrosaurines, Le = Leiolepidinae, Ur= Uromastycinae.

Discussion

All of the iguanian families plot as a single set within a relatively tight region of the theoretical morphospace. This is unlike similar morphospaces constructed for archosaur skulls, where discrete skull types can be discerned according to a broad but patchy distribution of taxa (Marugán-Lobón and Buscalioni, 2003). Against this background pattern, our data reveal that, not only is Agamidae more morphologically disparate than any of the sampled iguanian families, its Australian component, Amphibolurinae, contributes a substantial component of this disparity. The amphibolurines have expanded into new areas of the morphospace that currently remain unoccupied by other extant iguanian families.

50

Although our data set had a focus on Agamidae, and Amphibolurinae in particular, our results imply that amphibolurine disparity is higher than expected for its taxonomic diversity, at both the generic and specific levels. Draconinae is the sister clade to the Amphibolurinae, and the two clades have therefore had an equivalent evolutionary time frame in which to achieve their observed diversity. The taxonomic diversity of the draconines is markedly greater than that of the amphibolurines. We may therefore expect that draconine disparity to also be greater than that of amphibolurines, but we observe the reverse. However, care must be taken when comparing clades when uneven sampling is present. This difference could be due to less extensive sampling of draconines compared to that of amphibolurines. Future work to complete the draconine sampling would provide an interesting perspective on how time frames may limit the elaboration of disparity.

Phrynosomatidae were very well sampled and permit a less tentative comparison to Amphibolurinae. Phrynosomatidae show lower disparity despite being another species-rich continental radiation. One possible explanation for this might be clade age – if Phrynosomatidae was a younger clade and had less time to diversify. However, estimates for the origin of Phrynosomatidae are in excess of 40 Ma (Townsend et al., 2011), which is distinctly older than estimates of 25-30 Ma for Amphibolurinae (Chen et al., 2013). An alternative explanation is that competition has limited or enhanced evolutionary possibilities in the two clades. Phrynosomatidae evolved in sympatry with its close relatives (phylogenetically, behaviourally, and ontogenetically), the crotaphytids and iguanids, hence the iguanian morphospace may have been preoccupied (Pianka et al., 2017) throughout phrynosomatine evolution. In contrast, Amphibolurinae, diversifying in Australia (Hugall et al., 2008; Oliver and Hugall, 2017), were presented with vacant niches and reduced competition. The absence of other anatomically and ecologically similar squamate families may have allowed amphibolurines to expand into the morphospace of other iguanians, as well as novel morphospace. It may be worthwhile testing whether clades of Australian varanids and skinks, which diversified in parallel with Amphibolurinae since the late Oligocene (Blom et al., 2016; Oliver and Hugall, 2017), show a similar pattern of enhanced disparity compared to Asian counterparts.

The presence or absence of competing related clades may have had an additional role in respectively constraining or permitting diversification, in that extinction of some morphotypes may also have resulted from more intense competitive pressure. Thus some of the lower levels of disparity in clades such as phrynosomatids may stem from pruning via extinction (Rabosky and Lovette, 2008) in more selectively stringent continental areas compared with better survival of disparate clades in the less biotically rigorous Australian environment. Fossil acrodontan jaws

from the Eocene of India show a range of extinct dentition that suggest a range of extinct skull shapes (e.g. Rana et al., 2013), and this possibility would be worthwhile investigating further where fossil data are available.

The amphibolurines explore exclusive combinations of post-orbit and snout lengths that are more extreme than other agamids or iguanians. Variation in the iguanian skull shape space potentially relates morphological disparity to ecomorphological breadth (Collar et al., 2010; Pianka et al., 2017), representing differences in functional traits. The length of the post-orbit region may be related to the size of the jaw closing muscles, and snout length related to outlever and gape (Jones, 2008). The different sizes of these particular units could to be the result of trade-offs between greater bite force and enhanced prey capturing ability (Olson, 1961; Kohlsdorf et al., 2008). A greater bite-force does not necessarily relate to prey capture, and in some lizards it has been shown that to have head dimensions that produce a bite force in excess of that required for prey capture (Herrel et al., 1999; Lopez-Darias et al., 2014) It is likely that variation in cranial shape may also reflect other factors such as combat ability or male to male competition (Lappin and Husak, 2005; Husak et al., 2006). Many new studies of the evolution of shape are taking advantage of 3D morphometric methods and software, but we found that the relatively simple proportional measurements used in our 2D analysis allowed a larger and more encompassing sample size than is currently feasible with 3D landmarks. As 2D analysis has been more widely used to examine morphology, by using the same approach we have been able to readily compare our results to those of previous studies. It also allows the inclusion of fossil agamids with fewer assumptions. We have, however, also done 3D analyses on a smaller sample size of agamid skulls. This study showed different but complimentary results and has been submitted for publication elsewhere.

Due to the patchy nature of available data in natural history collections used in this study, we were unable to account for sexual dimorphism or ontogeny in our data collection. Future work should seek to assess the role of underlying factors such as functional traits, competition, sexual dimorphism, or ontogeny to gain an understanding of the drivers behind disparity in iguanian lizards.

Acknowledgements

Melbourne Museum, for access to specimens. We also thanks Ruth Williams and Amy Parker Watson from the University of Adelaide for their assistance with scanning.

Supplementary material

Electronic files

File ES2.1 – Iguanian specimen numbers and information with proportional measurements (CSV).

References

Alifanov VR. 1996. The Lizard Families Priscagamidae and Hoplocercidae (Sauria, Iguania): Phylogenetic Position and New Representatives from the Late Cretaceous of Mongolia. Paleontologicheskii Zhurnal 3:100-118.

Ast JC. 2001. Mitochondrial DNA evidence and evolution in Varanoidea (Squamata). Cladistics 17:211-226.

Bell CJ, Mead JI, Swift SL. 2009. Cranial osteology of *Moloch horridus* (Reptilia: Squamata: Agamidae). Rec West Aust Mus 25:201-237.

Blom MPK, Horner P, Moritz C. 2016. Convergence across a continent: adaptive diversification in a recent radiation of Australian lizards. Proc R Soc B 283:20160181.

Chen I-P, Symonds MRE, Melville J, Stuart-Fox D. 2013. Factors shaping the evolution of colour patterns in Australian agamid lizards (Agamidae): a comparative study. Biol J Linnean Soc 109:101-112.

Clemente CJ, Withers PC, Thompson G, Lloyd D. 2008. Why go bipedal? Locomotion and morphology in Australian agamid lizards. J Exp Biol 211:2058–2065.

Cogger H. 2014. Reptiles and amphibians of Australia, 7th ed. Collingwood: CSIRO Publishing.

Collar DC, Schulte JA, O'Meara BC, Losos JB. 2010. Habitat use affects morphological diversification in dragon lizards. J Evol Biol 23:1033-1049.

Conrad JL, Norell MA. 2007. A complete late Cretaceous iguanian (Squamata, Reptilia) from the Gobi and identification of a new iguanian clade. Am Mus Novit 6:1-47.

Hall R. 2001. Cenozoic reconstructions of SE Asia and the SW Pacific: changing patterns of land and sea. In: Metcalfe I, Smith JMB, Morwood M, Davidson I, editors. Faunal and Floral Migrations and Evolution in SE Asia-Australasia. Lisse: Swets & Zeitlinger. p 961-964.

Hamilton N. 2018. ggtern: an extension to 'ggplot2', for the creation of ternary diagrams. R package version 2.2.2. https://CRANR-projectorg/package=ggtern.

Harmon LJ, Schulte JA, Larson A, Losos JB. 2003. Tempo and mode of evolutionary radiation in iguanian lizards. Science 301:961-964.

Hugall AF, Foster R, Hutchinson M, Lee MSY. 2008. Phylogeny of Australian agamid lizards based on nuclear and mitchondrial genes: implications for morphological evolution and biogeography. Biol J Linnean Soc 93:343-358.

Husak JF, Lappin AK, Fox SF, Lemos-Espinal JA. 2006. Bite-force performance predicts dominance in male venerable collared lizards (*Crotaphytus antiquus*). Copeia 2006:301-306.

Herrel A, Spithoven L, Van Damme R, De Vree F. 1999. Sexual dimorphism of head size in *Gallotia galloti*: testing the niche divergence hypothesis by functional analyses. Func Ecol 13:289-297.

Jarvis ED, Mirarab S, Aberer AJ, Li B, Houde P, Li C, Ho SYW, Faircloth BC, Nabholz B, Howard JT, Suh A, Weber CC, da Fonseca RR, Li J, Zhang F, Li H, Zhou L, Narula N, Liu L, Ganapathy G, Boussau B,

Bayzid MS, Zavidovych V, Subramanian S, Gabaldón T, Capella-Gutiérrez S, Huerta-Cepas J, Rekepalli B, Munch K, Schierup M, Lindow B, Warren WC, Ray D, Green RE, Bruford MW, Zhan X, Dixon A, Li S, Li N, Huang Y, Derryberry EP, Bertelsen MF, Sheldon FH, Brumfield RT, Mello CV, Lovell PV, Wirthlin M, Schneider MPC, Prosdocimi F, Samaniego JA, Velazquez AMV, Alfaro-Núñez A, Campos PF, Petersen B, Sicheritz-Ponten T, Pas A, Bailey T, Scofield P, Bunce M, Lambert DM, Zhou Q, Perelman P, Driskell AC, Shapiro B, Xiong Z, Zeng Y, Liu S, Li Z, Liu B, Wu K, Xiao J, Yinqi X, Zheng Q, Zhang Y, Yang H, Wang J, Smeds L, Rheindt FE, Braun M, Fjeldsa J, Orlando L, Barker FK, Jønsson KA, Johnson W, Koepfli K-P, O'Brien S, Haussler D, Ryder OA, Rahbek C, Willerslev E, Graves GR, Glenn TC, McCormack J, Burt D, Ellegren H, Alström P, Edwards SV, Stamatakis A, Mindell DP, Cracraft J, Braun EL, Warnow T, Jun W, Gilbert MTP, Zhang G. 2014. Whole-genome analyses resolve early branches in the tree of life of modern birds. Science 346:1320-1331.

Jones MEH. 2008. Skull shape and feeding strategy in *Sphenodon* and other Rhynchocephalia. J Morphol 269:945-966.

Keogh JS. 1998. Molecular phylogeny of elapid snakes and a consideration of their biogeographic history. Biol J Linnean Soc 63:177-203.

Keqin G, Norell MA. 2000. Taxonomic composition and systematics of late Cretaceous lizard assemblages from Ukhaa Tolgod and adjacent localities, Mongolian Gobi Desert. Bull Am Mus Nat Hist 249:1-118.

Kohlsdorf T, Grizante MB, Navas CA, Herrel A. 2008. Head shape evolution in Tropidurinae lizards: does locomotion constrain diet? J Evol Biol 21:781-790.

Lappin AK, Husak JF. 2005. Weapon performance, not size, determines mating success and potential reproductive output in the collared lizard (*Crotaphytus collaris*). Am Nat 166:426-436.

Lopez-Darias M, Vanhooydonck B, Cornette R, Herrel A. 2015. Sex-specific differences in ecomorphological relationships in lizards of the genus *Gallotia*. Func Ecol 29:506-514.

Losos JB. 2011. Lizards in an evolutionary tree: ecology and adaptive radiation of anoles. Oakland, California: University of California Press.

Losos JB, Mahler DL. 2010. Adaptive radiation: the interaction of ecological opportunity, adaptation, and speciation. In: Bell MA, Futuyma DJ, Eanes WF, Levinton JS, editors. Evolution since Darwin: the first 150 years. Sunderland: Sinauer Association. p 381-420.

Lovette IJ, Bermingham E, Ricklefs RE. 2002. Clade-specific morphological diversification and adaptive radiation in Hawaiian songbirds. Proc R Soc B 269:37-42.

Manthey U, Denzer W. 2006. A revision of the Melanesian-Australian angle head lizards of the genus *Hypsilurus* (Sauria: Agamidae: Amphibolurinae), with description of four new species and one new subspecies. Hamadryad 30:1-40.

Marugán-Lobón J, Buscalioni ÁD. 2003. Disparity and geometry of the skull in Archosauria (Reptilia:

Melville J, Harmon LJ, Losos JB. 2006. Intercontinental community convergence of ecology and morphology in desert lizards. Proc R Soc B 273:557-563.

Melville J, Ritchie EG, Chapple SNJ, Glor RE, Schulte JA. 2011. Evolutionary origins and diversification of dragon lizards in Australia's tropical savannas. Mol Phylogenet Evol 58:257-270.

Murray J, Clark B, S JM. 1993. Adaptive radiation and community structure of *Partula* on Moorea. Proc R Soc B 254:205–211.

Nilsson MA, Arnason U, Spencer PBS, Janke A. 2004. Marsupial relationships and a timeline for marsupial radiation in South Gondwana. Gene 340:189-196.

Oliver PM, Hugall AF. 2017. Phylogenetic evidence for mid-Cenozoic turnover of a diverse continental biota. Nat Ecol Evol 1:1896.

Olson EC. 1961. Jaw mechanisms: rhipidistians, amphibians, reptiles. Amer Zool 1: 205-215.

Pianka ER, Vitt LJ, Pelegrin N, Fitzgerald DB, Winemille KO. 2017. Toward a periodic table of niches, or exploring the lizard niche hypervolume. Am Nat 190:601-616.

Powney GD, Grenyer R, Orne CDL, Owens IPF, Meiri S. 2010. Hot, dry and different: Australian lizard richness is unlike that of mammals, amphibians and birds. Glob Ecol Biogeogr 19:386-396.

Rabosky DL, Lovette IJ. 2008. Explosive evolutionary radiations: decreasing speciation or increasing extinction through time? Evolution 62:1866-1875.

Rana RS, Auge M, Folie A, Rose KD, Kumar K, Singh L, Sahni A, Smith T. 2013. High diversity of acrodontan lizards in the early Eocene Vastan Lignite Mine of India. Geologica Belgica 16:290-301.

Rundell RJ, Price TD. 2009. Adaptive radiation, nonadaptive radiation, ecological speciation and nonecological speciation. Trends Ecol Evol 24:394-399.

Sanders KL, Lee MSY, Leys R, Foster R, Keogh JS. 2008. Molecular phylogeny and divergence dates for Australasian elapids and sea snakes (Hydrophiinae): evidence from seven genes for rapid evolutionary radiations. J Evol Biol 21:682-695.

Scanlon JD, Lee MS. 2011. The major clades of living snakes: Morphological evolution, molecular phylogeny, and divergence dates. In: Sever D, Aldridge R, editors. Reproductive biology and phylogeny of snakes. Boca Raton: Science Publishers, Inc. p 55-95.

Schneider CA, Rasband WS, Elcieri KW. 2012. NIH Image to ImageJ: 25 years of image analysis. Nat Methods 9:671-675.

Shine R. 1990. Function and evolution of the frill of the frillneck lizard, *Chlamydosaurus kingii* (Sauria: Agamidae). Biol J Linnean Soc 40:11-20.

Skinner A, Hugall AF, Hutchinson MN. 2011. Lygosomine phylogeny and the origins of Australian scincid lizards. J Biogeogr 38:1044-1058.

Slater GJ, Price SA, Santini F, Alfaro ME. 2010. Diversity versus disparity and the radiation of modern cetaceans. Proc R Soc B 277:3097–3104.

Thompson G, Withers P. 2005. Size-free shape differences between male and female Western Australian dragon lizards (Agamidae). Amphibia-Reptilia 26:55-63.

Townsend TM, Mulcahy DG, Noonan BP, Sites JWJ, Kuczynski CA, Wiens JJ, Reeder TW. 2011. Phylogeny of iguanian lizards inferred from 29 nuclear loci, and a comparison of concatenated and species-tree approaches for an ancient, rapid radiation. Mol Phylogenet Evol 61:1363-1380.

Vidal N, Marin J, Morini M, Donnellan S, Branch WR, Thomas R, Vences M, Wynn A, Cruaud C, Blair Hedges S. 2010. Blindsnake evolutionary tree reveals long history on Gondwana. Biol Lett rsbl20100220.

Vidal N, Marin J, Sassi J, Battistuzzi FU, Donnellan S, Fitch AJ, Fry BG, Vonk FJ, Rodriguez de la Vega RC, Couloux A, Hedges SB. 2012. Molecular evidence for an Asian origin of monitor lizards followed by Tertiary dispersals to Africa and Australasia. Biol Letters rsbl20120460.

Yoder JB, Clancey E, Roches SD, Eastman JM, Gentry L, Godsoe W, Hagey TJ, Jochimsen D, Oswald BP, Robertson J, Sarver BAJ, Schenk JJ, Spear SF, Harmon LJ. 2010. Ecological opportunity and the origin of adaptive radiations. J Evol Biol 23:1581-1596.

STATEMENT OF AUTHORSHIP

Title of Paper	Patterns in tooth number among Australian agamids
Publication Status	☐ Published ☐ Accepted for Publication ☐ Submitted for Publication ☑ Unpublished and Unsubmitted work written in manuscript style
Publication Details	Prepared for submission to Journal of Anatomy

Principal Author

Name of Principal Author (Candidate)	Jaimi Gray		
Contribution to the Paper	Designed research, data collection and analysis, wrote first version of manuscript, edited later versions of manuscript.		
Overall percentage (%)	85%		
Certification:	This paper reports on original research I conducted during the period of my Higher Degree by Research candidature and is not subject to any obligations or contractual agreements with a third party that would constrain its inclusion in this thesis. I am the primary author of this paper.		
Signature		Date	23.08.2018

Co-Author Contributions

By signing the Statement of Authorship, each author certifies that:

  i.   the candidate's stated contribution to the publication is accurate (as detailed above);

 ii.   permission is granted for the candidate in include the publication in the thesis; and

iii.   the sum of all co-author contributions is equal to 100% less the candidate's stated contribution.

Name of Co-Author	Mark N. Hutchinson		
Contribution to the Paper	Helped design research, provided guidance for data analysis, and edited manuscript.		
Signature		Date	28/08/2018

Name of Co-Author	Marc E. H. Jones		
Contribution to the Paper	Helped design research, provided guidance for data analysis, and edited manuscript.		
Signature		Date	23rd August 2018

CHAPTER 3

Patterns in tooth number among Australian agamids

CHAPTER 3 – Patterns in tooth number among Australian agamids

Jaimi A. Gray, Mark N. Hutchinson, Marc E. H. Jones

Abstract

Teeth have great potential as tools for investigating many different biological patterns, thanks to their character rich nature, prevalence in the fossil record, and association with ecology. Data collected from teeth can reveal ontogenetic and phylogenetic variation, but quantitative studies on reptile teeth remain limited. Here we report on tooth counts in 578 specimens, representing 63 species and 14 genera of the Australian radiation of agamid lizards (Amphibolurinae), to examine patterns during growth. Amphibolurine agamids have the lowest recorded tooth counts among squamates of similar sizes. Within the Amphibolurinae, tooth counts consistently increase with size, and variation among taxonomic groups reflects phylogenetic relatedness. The patterns in tooth counts through growth will likely have consequences for how food may be orally processed (e.g. point loading, cutting surface area) and provide the beginnings of data that will help to retrieve species-level differences within amphibolurines.

Keywords: Agamidae, dentition, macroevolutionary patterns, Squamata, teeth,

Introduction

Teeth are an important tool for investigating ontogenetic, functional, phylogenetic and ecological patterns in extant and extinct animals, thanks to their character rich nature. Data concerning teeth, including shape, microanatomy, and tooth counts are commonly used to identify patterns in extant amniotes (Osborn, 1907; Gingerich, 1974; Massare, 1987; Farlow et al., 1991; Sues and Reisz, 1998; Reisz and Tsuji, 2006; Meloro and Jones, 2012; LeBlanc and Reisz, 2013; Brink and Reisz, 2014). Teeth can also provide insights that can help affiliate fossil specimens with taxonomic groups (Gingerich, 1974; Archer et al., 1989). There is a major data deficiency for squamates (lizards and snakes), even though they make up a crucial component of biodiversity in many past and present ecosystems (Powney et al., 2010; Jones et al., 2013). Although squamate fossil jaws are commonly recovered from fossil deposits (e.g. Covacevich et al., 1990; Lee et al., 2009; Longrich et al., 2012), a lack of basic knowledge of the dentition means that their interpretation is difficult. The confirmed value of dentition for interpreting other fossil taxa (e.g. mammals), highlights a potential for more informed taxonomic, phylogenetic, and ecological interpretations of fossil squamates (Worthy, 2016). A more thorough understanding of the patterns among extant squamate taxa is needed to fulfil this potential.

Tooth number is one aspect of dentition that can exhibit a great deal of phylogenetic and ontogenetic variation. It is also a meristic variable that is easy to systematically record in a reproducible way. Consequently, the number of teeth, or tooth positions, in tooth bearing bones has been commonly recorded and used in phylogenetic and taxonomic analyses of adult squamates (Kluge, 1962; Ray, 1965; Montanucci, 1968; Greer, 1991; Hutchinson, 1992; Hocknull, 2002; Gauthier et al., 2012). Some tooth development patterns during postnatal growth have been reported for particular squamate species, but there has been little investigation into the interspecific variation in these patterns that may occur among or within squamate families or clades. Reports using small sample sizes (i.e. one or two species) have shown that increasing the number of teeth during growth is a common pattern in many groups, as has been reported in Iguanidae (Ray, 1965; Montanucci, 1968; Kline and Cullum, 1984), Gekkonidae (Kluge, 1962; Thorpe, 1983), and Scincidae (Arnold, 1980; Greer, 1991). However, some squamate groups appear to maintain a consistent number of teeth during growth, as reported for Teiidae (Dessem, 1985), Serpentes (Rasmussen, 1996), and Varanidae (Brown et al., 2015). Moreover, decreasing tooth counts during growth have been reported in Anguidae (Cooper, 1966) and Lacertidae (Cooper, 1963). These varying patterns suggest that being able to predict patterns of tooth counts during growth is highly dependent on the taxonomic group of interest.

For the lizard family Agamidae, total tooth counts observed in adult animals have been reported for a few species, including several from the Australian clade (Hocknull, 2002). However, tooth count patterns during growth have been documented in only two species of agamids, *Agama agama* (Cooper et al., 1970) and *Uromastyx hardwickii* (Cooper and Poole, 1973). While patterns of tooth counts during growth in agamids seem to be distinctly different compared with other squamates (see Fig. 6 in Brown et al., 2015), more sampling is obviously needed and it is unknown how these patterns may vary among different agamid species.

With around 108 currently recognised species, the amphibolurine agamids of Australia are a continental-scale evolutionary radiation of lizards. Since their arrival to Australia from Southeast Asia around 30 million years ago (Ma) (Oliver and Hugall, 2017), they have successfully adapted to a range of different habitats across the entire continent, ranging from deserts in the arid zone to subtropical rainforest habitats (Powney et al., 2010). While their taxonomic diversity has long been recognised, morphological patterns that accompany this diversity remain to be quantitatively explored. This study aims to use tooth numbers of the maxillary and dentary bones of agamid lizards to test whether different patterns in tooth counts during growth can be detected at multiple taxonomic levels, and to examine the nature of these patterns.

Material and methods

Material

Measurements were taken from a combination of dry skeletal specimens (articulated and disarticulated) and three-dimensional (3D) reconstructions of X-ray micro computed tomography scans of amphibolurine lizards from South Australian Museum, Queensland Museum, Field Museum of Natural History, University of Texas at Austin, Melbourne Museum, and Western Australian Museum. In total, 578 specimens of amphibolurine skulls were measured. This sample included *Intellagama*, 31 species from the *Amphibolurus* group (of Hugall et al., 2008), 29 species of *Ctenophorus* (Table 1), and six species from the least nest monophyletic group (LN group).

Measurements

For dry skulls, number of visible tooth positions were counted for the maxilla (upper jaw bone) and dentary (lower jaw bone), on both the left and right sides. Teeth on the premaxilla were counted but tooth counts were erratic and displayed few discernible patterns. For very small specimens, a binocular light microscope was used to obtain tooth position counts. Digital callipers were used to measure tooth row length. For 3D models of skulls based on CT data, tooth positions were counted in Avizo v 9.0 (Visualization Sciences Group, 2013), and where necessary cross-sections were examined. The "measure 3D" tool in Avizo was used to measure tooth row length. For this study, tooth row length was considered a proxy for size and growth, as was confirmed by significant positive correlations between available snout-vent length data and measured tooth row lengths ($R^2 = 0.86$, see Chapter 7). All analyses were conducted using code written for the R v 3.5.0 statistical framework (R Core Development Team, 2018).

Monophyletic group	Genera	Species	Dentary	Maxilla
Amphibolurus group	8	31	239	262
Ctenophorus group	1	25	224	236
Intellagama	1	1	24	34
LN group	4	6	41	46
Total	**14**	**63**	**528**	**578**

Table 3.1 – Sample used to explore tooth counts during growth. LN = least nested.

Examining patterns in tooth counts during growth

To illustrate the range of tooth counts observed in particular species of amphibolurine lizards, we extracted data for all species from the data set for which we had a sample size of ten or more and used a dumbbell plot to represent the range of tooth counts observed in those species, for both the maxilla and dentary bones. To study the relationships between tooth count and tooth row length in amphibolurine lizards, we ran analysis of variance (ANOVA) models (using a type III sum of squares), using log transformed tooth row length (a proxy for size), taxonomic affiliation, and their interaction as model effects (count ~ log (row length) * taxa). If the interaction terms were significant, this indicated that the allometric patterns (increases in tooth count associated with increases in size) differed in either slope or elevation (or both), among taxa. Analyses were performed for both the maxilla and dentary, at the monophyletic group, genus, and species level. To minimise the effect of asymmetry due to missing or broken teeth, for each specimen, the parallel maximum was used in the analyses where either the left or right side was used (depending on which side had the most teeth). For ANOVAs at the broadest taxonomic level, we defined four groups, all of which represent monophyletic clades: the *Ctenophorus* group (all species in the *Ctenophorus* genus); the *Amphibolurus* group (eight genera: *Amphibolurus, Chlamydosaurus, Diporiphora, Gowidon, Lophognathus, Pogona, Rankinia*, and *Tympanocryptis*); *Intellagama* (which is the lone sister taxon to *Ctenophorus* and the *Amphibolurus* group); LN group (three genera: *Lophosaurus, Chelosania*, and *Moloch*); and *Intellagama*. We also performed separate ANOVAs for the generic level (12 genera), and species level (20 species). For analyses at the generic and species levels we excluded taxa with a sample size of less than 10. Taxa-specific allometric patterns were visualised using plots of tooth count, regressed on log transformed tooth row length.

When significant interaction terms were obtained, we performed pairwise tests to identify which taxa significantly differed in allometric slope from one each other in both elevation and slope, for the maxilla and dentary. All post hoc pairwise tests were carried out using the *smatr* package in R (Warton et al., 2012). First, we performed separate tests for differences in slope and elevation among allometric trajectories. This was done for the maxilla and dentary at the group, genus, and species levels. If the *P*-values for these tests were significant, this indicated that there were significant differences among taxa for either elevation or slope (depending which test was done). Secondly, we carried out pairwise comparisons that identified which taxa's elevations and slopes differed significantly from each other, at each taxonomic level. To assess differences, we examined pairwise *P*-values for differences between taxa for both slope and elevation, as well as correlation coefficients, slopes, and intercepts for dentary and maxilla of each taxon.

Results

Variation in observed tooth count ranges

For most species of amphibolurine lizard, the minimum and maximum tooth count observed for the dentary were higher than that of the maxilla (Fig. 3.1). This pattern was not unexpected as part of the upper tooth row is occupied by the premaxilla. Exceptions included *Chlamydosaurus kingii* and *Intellagama lesueurii*, where the observed maximum maxillary tooth count was higher than the observed maximum dentary tooth count, and also *Moloch horridus*, where the observed maximum and minimum tooth counts were the same for the maxilla and dentary. For species of *Diporiphora* and *Ctenophorus reticulatus*, the observed maximum counts examined for the dentary and maxilla were the same. The highest tooth count of any species was achieved by *Ch. kingii*, with a maximum observed count of 25 teeth for the maxilla. *Ch. Kingii* also showed the broadest range of tooth counts of any of the species included (8-25, for the maxilla). The narrowest range in tooth counts was observed in *D. winneckei* and *Ct. fionni* (8-14 and 11-17, respectively).

Allometric variation and pairwise comparisons
Differences among groups

There is a significant positive allometric relationship between tooth count and size for the maxilla and dentary in each group (Fig. 3.2A and B). R^2 values indicated that this relationship is very weak in the LN group, and individuals belonging to the LN group are spread out over the entire occupied range of the dentary and maxilla counts (see supplementary material: Fig. S3.1). For both the dentary and maxilla, the *Ctenophorus* group has the highest slope and therefore adds the most teeth for a given increase in size. The LN group has the lowest slope and therefore adds the fewest teeth for a given increase in size. For both jaw bones, the *Amphibolurus* group and *Intellagama* reach the greatest jaw lengths. Significant differences in slope indicated that, although they end up with the same number of teeth in the largest individuals, smaller dragons of a given size in the *Amphibolurus* group have more teeth than *Intellagama* of the same size. If we compare the *Ctenophorus* group with the *Amphibolurus* group, smaller individuals from both groups start out with similar numbers of teeth. While the *Ctenophorus* group and *Intellagama* were not significantly different from one another in terms of slope, they did have significantly different elevations. Even though the *Ctenophorus* group have more teeth than *Intellagama* of a given size, the two groups increase their tooth counts at a similar rate. All coefficients and pairwise *P*-values can be observed in supplementary material: Tables S3.1 and S3.2.
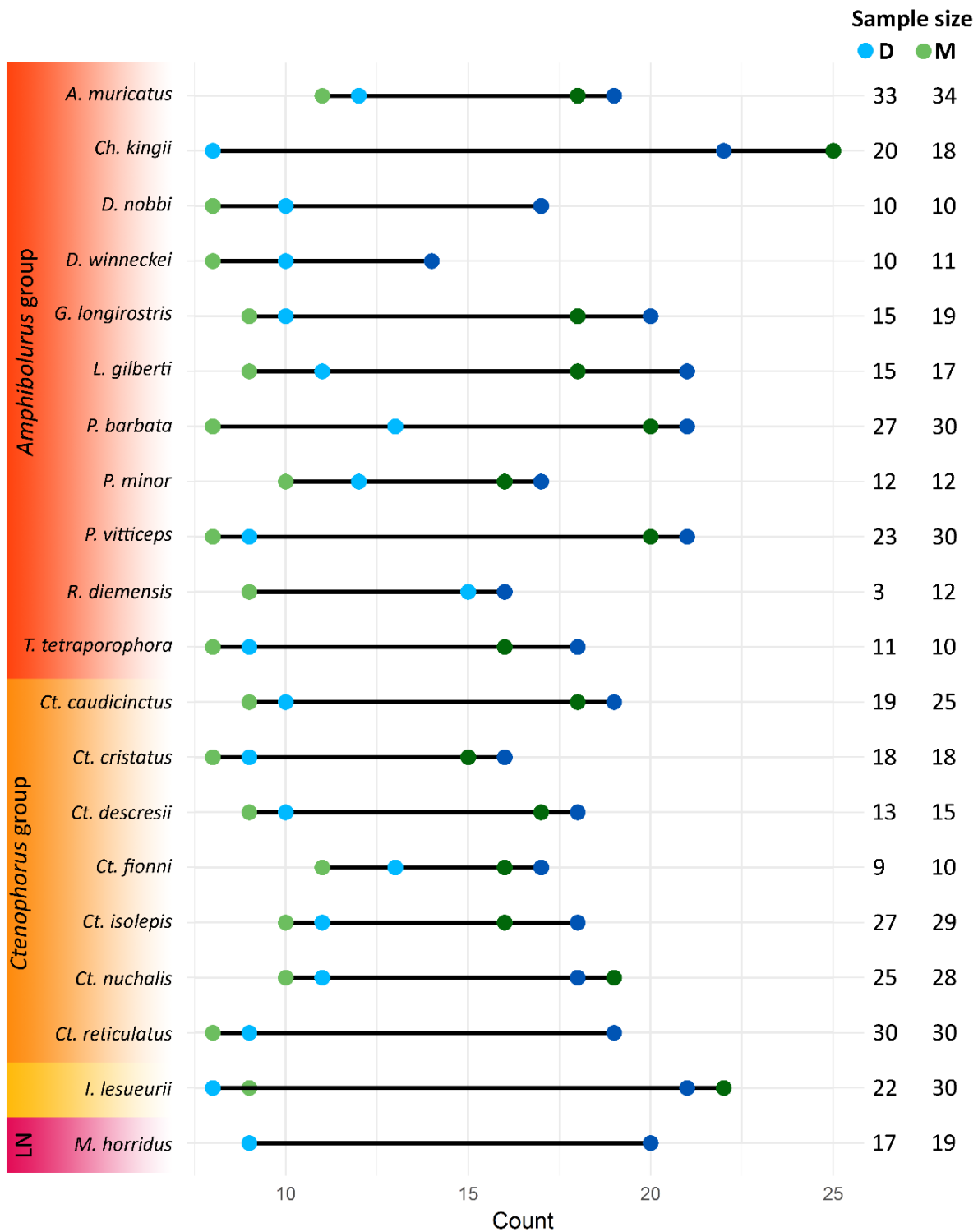
Figure 3.1 – Minimum and maximum observed tooth counts for 20 different species of amphibolurine lizards (samples of ≥ 10). Green points represent maxillary counts, and blue points represent dentary counts. Light colours represent the minimum observed values, and dark colours represent the maximum observed values. Sample sizes for each species and jaw bone can be found on the right side of the plot.

Table 3.2 – ANOVA results of maxilla and dentary tooth counts and tooth row length (log transformed), at different taxonomic levels (count ~ log (row length) * taxa). *P*-values < 0.05 in bold.

Dentary	SS	DF	F value	*P*-value
Monophyletic group				
Intercept	203.55	1	58.98	**<0.0001**
Log (row length)	943.34	1	273.35	**<0.0001**
Group	140.54	3	13.57	**<0.0001**
Log (row length : group)	147.83	3	14.28	**<0.0001**
Residuals	1701.37	493		
Genus				
Intercept	0.23	1	0.09	0.7680
Log (row length)	64.98	1	24.72	**<0.0001**
Group	80.94	11	2.80	**0.0015**
Log (row length : group)	64.34	11	2.22	**0.0124**
Residuals	1225.27	466		
Species				
Intercept	17.14	1	9.38	**0.0024**
Log (row length)	76.57	1	41.91	**<0.0001**
Group	87.59	19	2.52	**0.0005**
Log (row length : group)	97.14	19	2.80	**0.0001**
Residuals	582.77	319		
Maxilla	SS	DF	F value	*P*-value
Monophyletic group				
Intercept	78.65	1	28.03	**<0.0001**
Log (row length)	1481.96	1	528.16	**<0.0001**
Group	147.89	3	17.57	**<0.0001**
Log (row length : group)	144.07	3	17.12	**<0.0001**
Residuals	1562.88	557		
Genus				
Intercept	0.29	1	0.14	0.7060
Log (row length)	90.75	1	45.20	**<0.0001**
Group	85.06	11	3.85	**<0.0001**
Log (row length : group)	41.14	11	1.86	**0.0417**
Residuals	1058.15	527		
Species				
Intercept	18.54	1	14.77	**0.0001**
Log (row length)	212.03	1	168.84	**<0.0001**
Group	58.83	19	2.47	**0.0007**
Log (row length : group)	64.25	19	2.69	**0.0002**
Residuals	460.89	367		

Differences among genera

There was a significant positive allometric relationship between tooth count and size for the maxilla and dentary of each genus except *Lophosaurus* (see Fig. 3.2C and D). We also did not detect a significant result for *Rankinia* dentaries, but this was a product of small sample size due to the inclusion of museum specimens that lacked dentaries. While many pairwise differences in elevation were detected (43 for dentary and 47 for maxilla, out of a possible 66), very few pairwise differences were detected in slope (five for dentary and three for maxilla, out of a possible 66). *Moloch* has the steepest slope (for both maxilla and dentary), and therefore it adds the most teeth as size increases. The remaining genera all have similar slopes with no pairwise differences detected among them. Of these remaining genera, *Chlamydosaurus* exhibits the lowest elevation (for both maxilla and dentary), while *Amphibolurus* and *Tympanocryptis* have the highest elevations (for maxilla and dentary). *Ctenophorus*, *Diporiphora*, and *Rankinia* all tend toward the high range of values for observed elevations. The sporadic distribution of points observed in the LN group for the "among groups" comparison can be explained by the large difference between *Moloch* and *Lophosaurus* (both LN) identified by generic pairwise comparisons. All coefficients and pairwise *P*-values can be observed in supplementary material: Tables S3.3 and S3.4.

Differences among species

There was a significant positive allometric relationship between tooth count and size for the maxilla and dentary in each species (see Fig. 3.2E and F). Exceptions were dentaries of *P. minor*, which was due to a lack of smaller representative specimens, and also *Rankinia,* (issue identified above). While many pairwise differences in elevation were detected (108 for dentary and 112 for maxilla, out of a possible 190), very few pairwise differences were detected in slope (ten for dentary and nine for maxilla, out of a possible 190). Among the sufficiently sampled species, *Moloch* has the steepest slope, which was unsurprising given it is the sole member of its genus and also exhibits the steepest slope in the generic comparison. *Ct. reticulatus* has a relatively steep slope, (for maxilla and dentary, also reflected in the pairwise *P*-values), and therefore adds the most teeth (apart from *Moloch*) as size increases. Among the elevation differences between species, the most distinct character exhibited (by both maxilla and dentary) is the large tooth row lengths and considerably lower elevations achieved by *Chlamydosaurus, Intellagama, P. barbata,* and *P. vitticeps*. This indicates fewer teeth for a given size than other species in the sample, but they have an ability to achieve a similar (or greater) number of teeth by growing larger. Among remaining species, there are no distinct patterns that separate species belonging to particular groups or genera, but rather a continuum of different elevations among species. All coefficients and pairwise *P*-values can be observed in supplementary material: Tables S3.6 and S3.7.
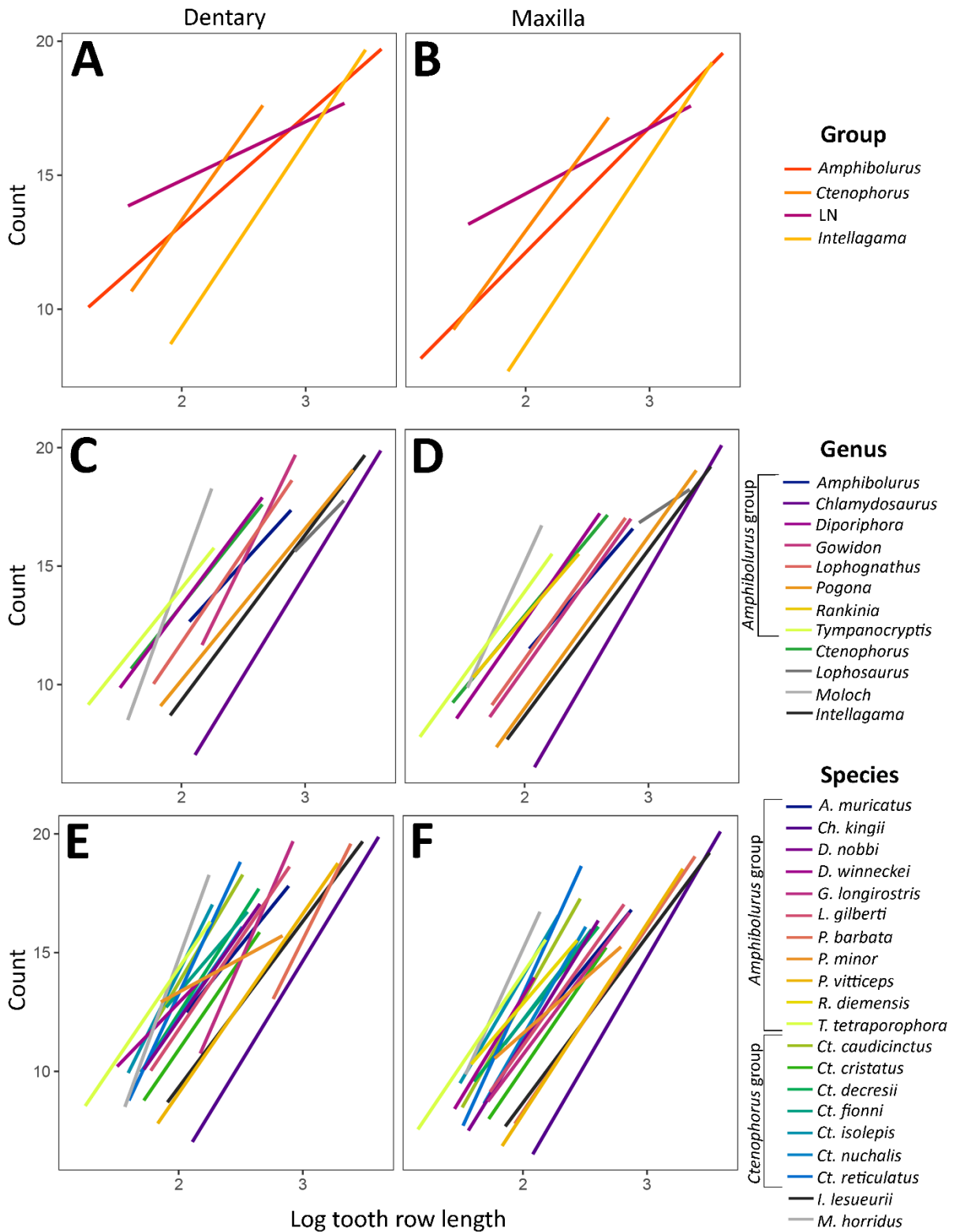
Figure 3.2 – Tooth count allometry showing the patterns detected by statistical testing, at the monophyletic group (A and B), genus (C and D), and species (E and F) levels, for both the maxilla (A, C, E) and dentary (B, D, F), See supplementary material: Figure S3.1 for distributions of individual data points.

Discussion

We confirm that all amphibolurine agamids increase tooth counts during growth, as suggested by the few existing reports on agamid postnatal tooth development (Cooper et al., 1970; Cooper and Poole, 1973). This was expected, since agamids add additional teeth to the posterior of the tooth row during growth, and don't lose or replace their existing acrodont teeth (Cooper et al., 1970). Different amphibolurine agamid taxa largely have a common slope of tooth counts during growth, as shown by the overwhelmingly small amount of pairwise differences among generic and specific slopes. By contrast, the very large amount of pairwise differences in elevation imply that differences in tooth number are already present among young dragons, and species then proceed to add teeth during growth at similar rates, maintaining differences in tooth counts among different dragon taxa of a given size. Interestingly, amphibolurines that have higher elevations (more teeth for a given tooth row length) also seem to be species with smaller adult sizes (e.g. *Ctenophorus*, *Tympanocryptis*). Indicating that smaller dragons have smaller teeth relative to their body size. Phylogenetic history is a contributing factor for tooth growth patterns, but unexplained variation in the data (see supplementary material: Fig. S3.1) indicates additional factors are introducing complexity to these patterns.

There are several known features of agamids that may contribute to the complexity in tooth count patterns during growth. Firstly, and perhaps most importantly, their dentition is typically made up of teeth with two markedly different tooth shapes and replacement patterns (Berkovitz and Shellis, 2017). Secondly, acrodont teeth generally increase in size at more posterior tooth row positions, with teeth at the posterior end of the tooth row markedly larger than teeth at the anterior end (Cooper et al., 1970). The distribution of teeth along the jaw is further complicated as posterior teeth tend to be rotated slightly about their vertical axis, producing overlap between them (Cooper et al., 1970). Thirdly, growth is accompanied by wear of the teeth and the hard tissues surrounding them, which in some cases is so severe that individual teeth are indistinguishable in older anterior dentition. Lastly, here we use a proxy for relative size, but it is not necessarily a proxy for age (Petermann et al., 2017), as the growth rates of agamids can vary through time (associated with resource availability, Radder et al., 2007). There are likely to be some complex underlying mechanisms that regulate tooth growth relative to overall growth in agamids, contributing to the variation we observe in allometric patterns (e.g. Handrigan and Richman, 2011; Jernvall and Thesleff, 2012). Since the variation introduced by these factors may vary among different taxa, finer level analyses that examine variation relating to these factors, in particular agamid clades, genera, and species are needed to solidify our knowledge of different growth patterns in agamid teeth.

Where dentition is concerned, just as *Uromastyx* is an outlier among agamids (Edmund, 1969; Robinson, 1976), so too is *Moloch* among amphibolurines. Because *Moloch* is such a distinctive species, it is one of the few that have received great attention in morphological descriptions, including dentition. The distinctive dentition of *Moloch* was reflected in our results, as departures from common amphibolurine patterns (i.e. differences in elevation rather than slope), almost exclusively involve *Moloch*. There are a number of reported characters that contribute to this distinctiveness. Not only is its tooth shape distinct, and markedly different between the maxilla and dentary, it also lacks caniniform pleurodont teeth (they are instead small, peg-like, and often completely eroded in adults), and a progression in tooth sizes along the jaw (Bell et al., 2009): characters that seem to be consistent in other amphibolurines (Hocknull, 2002; Bell et al., 2009; Berkovitz and Shellis, 2017). Although the functional significance of their dentition remains a mystery, our results are in concordance with the large body of evidence indicating that *Moloch* is a highly specialised lizard (Pianka and Pianka, 1970); Meyers and Herrel, 2005). This same level of understanding is yet to be achieved for other amphibolurine species, but would enhance our understanding of the patterns observed for other taxa in this study.

The relationship between tooth counts and size is known for very few other squamate taxa, as shown by the summary by Brown et al. (2015) of current knowledge of the patterns of tooth counts during growth for squamate groups. This review was constrained by very small sample sizes, with very large families represented by only one to four species (and only one species of agamid). Before now, there has been no comprehensive investigation into variation in tooth growth patterns among taxa within any squamate clade. The fact that we have been able to observe a relatively large amount of variation within just one subfamily of the much larger agamid family indicates a dire need for more data for the other agamid clades, and for other squamate families, if we are to consider the entirety of variation in any given clade.

Results from this study will be strengthened when expanded to include other jaw bone characters including tooth sizes and shape. We have shown that group membership of amphibolurine fossil jaw specimens can probably not be predicted using tooth counts and tooth row lengths alone. Although some taxonomic groups may be more readily distinguished with the consideration of these variables, it is essential to combine tooth data with other tooth and jaw characters (e.g. Hocknull, 2002) to devise a more holistic inference. Some observations made here may help refine the taxonomic possibilities. For example, only a few species reach the maximum tooth counts recorded, and observing such counts in a fossil specimen would narrow the pool of comparative taxa. Differences we observe here in tooth growth patterns, combined with tooth sizes, shapes, and other characters, may also have adaptive significance for food

processing (Lucas and Luke, 1984; Kraklau, 1991; Evans and Sanson, 1998; Freeman and Lemen, 2005; Jones, 2006; Jones, 2009). Investigation into the feeding mechanisms (cf. Moazen et al., 2009; Jones et al., 2012) of dragons of different sizes and taxonomic affinity may advance our understanding of the role of teeth in food processing and hence improve our understanding of growth patterns in teeth.

Acknowledgements

Supplementary material

Figures

Electronic files

File ES3.1 – Amphibolurine tooth counts and tooth row length data (CSV).

References

Archer M, Godthelp H, Hand SJ, Megirian D. 1989. Fossil mammals of Riversleigh, northwestern Queensland: preliminary overview of biostratigraphy, correlation and environmental change. Aust Zool 25:29-65.

Arnold E. 1980. Recently extinct reptile populations from Mauritius and Reunion, Indian Ocean. J Zool, Lond 191:33-47.

Bell CJ, Mead JI, Swift SL. 2009. Cranial osteology of *Moloch horridus* (Reptilia: Squamata: Agamidae). Rec West Aust Mus 25:201-237.

Berkovitz BK, Shellis P. 2017. Chapter 6 - Reptiles 1: Tuatara and lizards. In: The teeth of non-mammalian vertebrates. Academic Press.

Brink KS, Reisz RR. 2014. Hidden dental diversity in the oldest terrestrial apex predator *Dimetrodon*. Nat Commun 5:3269.

Brown CM, VanBuren CS, Larson DW, Brink KS, Campione NE, Vavrek MJ, Evans DC. 2015. Tooth counts through growth in diapsid reptiles: implications for interpreting individual and size related varition in the fossil record. J Anat 226:322-333.

Cooper JS. 1963. The dental anatomy of the genus *Lacerta*. Doctoral Dissertation: University of Bristol.

Cooper JS. 1966. Tooth replacement in the slow worm (*Anguis fragilis*). J Zool 150:235-248.

Cooper JS, Poole DFG. 1973. The dentition and dental tissues of the agamid lizard, *Uromastyx*. J Zool 169:85-100.

Cooper JS, Poole DFG, Lawson R. 1970. The dentition of agamid lizards with special reference to tooth replacement. J Zool 162:85-98.

Covacevich J, Couper P, Molnar RE, Witten G, Young W. 1990. Miocene dragons from Riversleigh: new data on the history of the family Agamidae (Reptilia: Squamata) in Australia. Mem Queensl Mus 29:339-360.

Dessem D. 1985. Ontogenetic changes in the dentition and diet of *Tupinambis* (Lacertilia: Teiidae). Copeia 1985:245-247.

Edmund. 1969. Dentition. Biology of the reptilia I. Morphology A. London & New York: Academic Press.

Evans AR, Sanson GD. 1998. The effect of tooth shape on the breakdown of insects. J Zool 246:391-400.

Farlow JO, Brinkman DL, Abler WL, Currie PJ. 1991. Size, shape, and serration density of theropod dinosaur lateral teeth. Mod Geol 16:161-198.

Freeman PW, Lemen C. 2005. Puncturing ability of idealized canine teeth: edged and non-edged shanks. J Zool 269:51-56.

Gauthier JA, Kearney M, Anderson Maisano J, Rieppel O, Behlke ADB. 2012. Assembling the squamate tree of life: perspectives from the phenotype and the fossil record. B Peabody Mus Nat Hi 53:3-308.

Gingerich PD. 1974. Size variability of the teeth in living mammals and the diagnosis of closely related sympatric fossil species. J Paleontol 48:895-903.

Greer AE. 1991. Tooth number in the scincid lizard genus *Ctenotus*. J Herpetol 25:473-477.

Handrigan GR, Richman JM. 2011. Unicuspid and bicuspid tooth crown formation in squamates. J Exp Zool (Mol Dev Evol) 316:598-608.

Hocknull SA. 2002. Comparative maxillary and dentary morphology of the Australian dragons (Agamidae: Squamata): a framework for fossil identification. Mem Queensl Mus 48:125-145.

Hugall AF, Foster R, Hutchinson M, Lee MSY. 2008. Phylogeny of Australian agamid lizards based on nuclear and mitchondrial genes: implications for morphological evolution and biogeography. Biol J Linnean Soc 93:343-358.

Hutchinson MN. 1992. Origins of the Australian scincid lizards: a preliminary report on the skinks of Riversleigh. The Beagle 9:61-70.

Jernvall J, Thesleff I. 2012. Tooth shape formation and tooth renewal: evolving with the same signals. Development 139:3487-3497.

Jones M. 2009. Dentary tooth shape in *Sphenodon* and its fossil relatives (Diapsida: Lepidosauria: Rhynchocephalia). Comp Dental Morphol 13:9-15.

Jones ME. 2006. Tooth diversity and function in the Rhynchocephalia (Diapsida: Lepidosauria). In: Ninth International Symposium on Mesozoic Terrestrial Ecosystems and Biota: Natural History Museum. p 163.

Jones MEH, Anderson CL, Hipsley CA, Muller J, Evans SE, Schoch RR. 2013. Integration of molecules and new fossils supports a Triassic origin for Lepidosauria (lizards, snakes, and tuatara). BMC Evol Biol 13:208.

Jones MEH, O'higgins P, Fagan MJ, Evans SE, Curtis N. 2012. Shearing mechanics and the influence of a flexible symphysis during oral food processing in *Sphenodon* (Lepidosauria: Rhynchocephalia). Anat Rec 295:1075-1091.

Kline L, Cullum D. 1984. A long term study of the tooth replacement phenomenon in the young green iguana, *Iguana iguana*. J Herpetol 18:176-185.

Kluge AG. 1962. Comparative osteology of the eublepharid lizard genus *Coleonyx* Gray. J Morphol 110:299-332.

Kraklau DM. 1991. Kinematics of prey capture and chewing in the lizard *Agama agama* (Squamata: Agamidae). J Morphol 210:195-212.

LeBlanc ARH, Reisz RR. 2013. Periodontal ligament, cementum, and alveolar bone in the oldest herbivorous tetrapods, and their evolutionary significance. PLOS ONE 8:e74697.

Lee MSY, Hutchinson MN, Worthy TH, Archer M, Tennyson AJD, Worthy JP, Scofield RP. 2009. Miocene skinks and geckos reveal long-term conservatism of New Zealand's lizard fauna. Biol Lett 5:833-837.

Longrich NR, Bhullar B-AS, Gauthier JA. 2012. Mass extinction of lizards and snakes at the Cretaceous-Paleogene boundary. PNAS 109:21396-21401.

Lucas PW, Luke DA. 1984. Chewing it over: basic principles of food breakdown. In: Chivers DK, Wood BA, Bilsborough A, editors. Food acquisition and processing in primates. New York: Plenum Press. p 283-301.

Massare JA. 1987. Tooth morphology and prey preference of Mesozoic marine reptiles. J Vert Paleontol 7:121-137.

Meloro C, Jones MEH. 2012. Tooth and cranial disparity in the fossil relatives of *Sphenodon* (Rhyncocephalia) dispute the persistent 'living fossil' label. J Evol biol 25:2194-2209.

Meyers JJ, Herrel A. 2005. Prey capture kinematics of ant-eating lizards. J Exp Biol 208:113-127

Moazen M, Curtis N, O'Higgins P, Jones MEH, Evans SE, Fagan MJ. 2009. Assessment of the role of sutures in a lizard skull: a computer modelling study. Proc R Soc B 276:39-46.

Montanucci RR. 1968. Comparative dentition in four iguanid lizards. Herpetologica 24:305-315.

Oliver PM, Hugall AF. 2017. Phylogenetic evidence for mid-Cenozoic turnover of a diverse continental biota. Nat Ecol Evol 1:1896.

Osborn HF. 1907. Evolution of mammalian molar teeth. Macmillan.

Petermann H, Mongiardino Koch N, Gauthier JA. 2017. Osteohistology and sequence of suture fusion reveal complex environmentally influenced growth in the teiid lizard *Aspidoscelis tigris* - implications for fossil squamates. Palaeogeogr Palaeoclimatol, Palaeoecol 475:12-22.

Pianka ER, Pianka HD. 1970. The ecology of *Moloch horridus* (Lacertilia: Agamidae) in Western Australia. Copeia 1:90-103.

Powney GD, Grenyer R, Orne CDL, Owens IPF, Meiri S. 2010. Hot, dry and different: Australian lizard richness is unlike that of mammals, amphibians and birds. Glob Ecol Biogeogr 19:386-396.

Radder RS, Warner D, Shine R. 2007. Compensating for a bad start: catch-up growth in juvenile lizards (*Amphibolurus muricatus*, Agamidae). J Exp Zool 307A:500-508.

Rasmussen J. 1996. Maxillary tooth number in the African tree-snakes genus *Dipsadoboa*. J Herpetol 30:297-300.

Ray CE. 1965. Variation in the number of marginal tooth positions in three species of iguanid lizards. Breviora 236:1-14.

Reisz RR, Tsuji LA. 2006. An articulated skeleton of *Varanops* with bite marks: the oldest known evidence of scavenging among terrestrial vertebrates. J Vert Paleontol 26:1021-1023.

Robinson PM. 1976. How *Sphenodon* and *Uromastyx* grow their teeth and use them. Morphol Biol Reptiles 3:43-64.

Sues HD, Reisz RR. 1998. Origins and early evolution of herbivory in tetrapods. TREE 13:141-145.

Thorpe R. 1983. A biometric study of the effects of growth on the analysis of geographic variation: tooth number in green geckos (Reptilia: *Phelsuma*). J Zool, Lond 201:13-26.

Visualization Sciences Group. 2013. Avizo. FEI Corporate Headquarters, Oregon.

Warton DI, Duursma RA, Falster DS, Taskinen S. 2012. smatr 3– an R package for estimation and inference about allometric lines. Methods Ecol Evol 3:257-259.

Worthy TH. 2016. A review of the fossil record of New Zealand lizards. In: New Zealand lizards. Springer. p 65-86.

STATEMENT OF AUTHORSHIP

Title of Paper	Changes in ontogenetic patterns facilitate diversification in skull shape of Australian agamid lizards
Publication Status	☐ Published ☐ Accepted for Publication ☑ Submitted for Publication ☐ Unpublished and Unsubmitted work written in manuscript style
Publication Details	Submitted to BMC Evolutionary Biology on 22.05.2018. Reviews received 08.08.2018, this chapter is a revised version ready for resubmission.

Principal Author

Name of Principal Author (Candidate)	Jaimi Gray		
Contribution to the Paper	Designed research, data collection and analysis, wrote first version of manuscript, edited later versions of manuscript.		
Overall percentage (%)	80%		
Certification:	This paper reports on original research I conducted during the period of my Higher Degree by Research candidature and is not subject to any obligations or contractual agreements with a third party that would constrain its inclusion in this thesis. I am the primary author of this paper.		
Signature		Date	23.08.2018

Co-Author Contributions

By signing the Statement of Authorship, each author certifies that:

i. the candidate's stated contribution to the publication is accurate (as detailed above);

ii. permission is granted for the candidate in include the publication in the thesis; and

iii. the sum of all co-author contributions is equal to 100% less the candidate's stated contribution.

Name of Co-Author	Emma Sherratt		
Contribution to the Paper	Provided guidance for data analysis, and edited manuscript.		
Signature		Date	24/08/2018

Name of Co-Author	Mark N. Hutchinson		
Contribution to the Paper	Helped design research, and edited manuscript.		
Signature		Date	28/08/2018

Name of Co-Author	Marc E. H. Jones		
Contribution to the Paper	Helped design research, provided guidance for data analysis, and edited manuscript.		
Signature		Date	23rd August 2018

CHAPTER 4

Changes in ontogenetic patterns facilitate diversification in skull shape of Australian agamid lizards
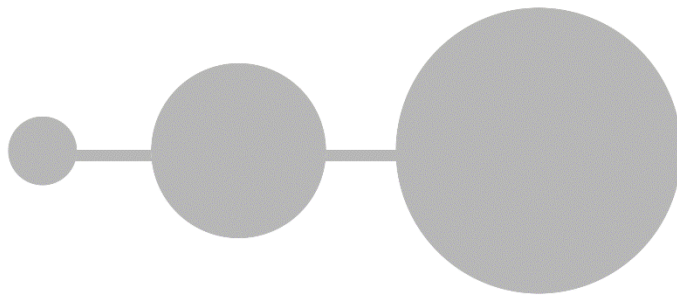
CHAPTER 4 – Changes in ontogenetic patterns facilitate diversification in skull shape of Australian agamid lizards

Jaimi A. Gray, Emma Sherratt, Mark N. Hutchinson, Marc E. H. Jones

Abstract

Morphological diversity among closely related animals can be the result of differing growth patterns. The Australian radiation of agamid lizards (Amphibolurinae) exhibits great ecological and morphological diversity, which they have achieved on a continent-wide scale, in a relatively short period of time (30 million years). Amphibolurines therefore make an ideal study group for examining ontogenetic allometry. We used two-dimensional landmark based geometric morphometric methods to characterise the postnatal growth patterns in cranial shape of 18 species of amphibolurine lizards and investigate the associations between cranial morphology, and life habit and phylogeny. For most amphibolurine species there is a similar juvenile cranial phenotype. By adulthood crania are more disparate in shape and occupy different sub-spaces of the total shape space. To achieve this disparity, cranial shapes do not follow a common growth pattern, and there are differences among species in both the direction of growth in morphospace, and the magnitude of growth. Our results show great variability in growth trajectories among species that results in a diversity of adult cranial shapes in the Australian agamids. We found that different growth patterns among the amphibolurines are significantly associated with different ecological life habits. The clade *Ctenophorus* includes species that undergo small magnitudes of shape change during growth. They have dorsoventrally deep, blunt-snouted skulls (associated with terrestrial lifestyles), and also dorsoventrally flat skulls (associated with saxicolous lifestyles). The sister clade to *Ctenophorus*, which includes the bearded dragon (*Pogona*), frill-neck lizard (*Chlamydosaurus*), and long-nosed dragon (*Gowidon*), includes shapes that involve differing snout lengths and broad and robust post-orbital regions, (both associated with scansorial lifestyles). Phylogenetic signal in cranial morphology appears to be largely overwritten by signals that reflect adaptive responses. This knowledge about growth patterns and skull shape diversity in agamid lizards will be valuable for placing phylogenetic, functional and ecological studies in a morphological context.

Keywords: Agamidae, evolutionary development, geometric morphometrics, lizards, ontogeny, skull

Introduction

A great deal of research has highlighted the role of natural selection in producing morphological variation, and subsequently researchers have proposed adaptive explanations for patterns of diversification (Losos, 2011; Tokita et al., 2017). The range of possible forms that natural selection can act upon is limited by the changes that can be produced by several processes, including growth and development (ontogeny) (Klingenberg, 1998, 2016). Throughout their development, organisms can undergo changes in shape, due to differences in relative growth of components, and alterations in timing of their growth, a concept defined as ontogenetic allometry (Klingenberg, 1998, 2016). Studies on ontogenetic allometry have been carried out since 1930, and considerable advances in methodology have allowed exploration of patterns in more refined detail (Huxley and Teissier, 1936; Gould, 1966; Gould, 1977; Nelson, 1985; Klingenberg, 1996; Klingenberg, 1998; Klingenberg and Marugán-Lobón, 2013). These studies have shown that changes in the attributes of ontogenetic patterns are important for facilitating evolutionary processes, (Cock, 1966; Gould, 1966; Klingenberg, 1998; Wilson and Sánchez-Villagra, 2010, 2011) and evolutionary flexibility of ontogenies has been reported in several recent works (e.g. Adams and Nistri, 2010; Klingenberg, 2010b; Hugi et al., 2012; Esquerré et al., 2017).

Due to allometry, there are two ways in which changes to an ancestral growth pathway can generate morphological diversity. Firstly, changes in adult shape can occur due to changes in adult size, without changes to the shape-size relationship. Modifications in timing or rate of the ancestral growth pathway (heterochrony) account for diversification of shape. Such heterochronic changes, "when a descendant retains the ancestral relationship between size and shape" (Klingenberg, 1998 p. 87), are referred to as the ontogenetic scaling hypothesis (Gould, 1977; Klingenberg, 1998). Secondly, changes in adult shape can occur due to departure from the ancestral growth pathway: changes to the relationship between size and shape (on a plot, changes in slope, intercept, or a combination of both). This instance may be inferred when ontogenetic variation among members of a group does not map onto a common ontogenetic trajectory. Generally it was thought that ontogenetic pathways are phylogenetically stable, and that the ontogenetic scaling hypothesis can explain most variation (West et al., 1997; Gould, 2002). However, growth pathways certainly can change. Closely related taxa can show varying patterns of heterochrony (Klingenberg and Zimmermann, 1992; Adams and Nistri, 2010; Hipsley and Müller, 2017), and ontogenetic divergence (Bastir and Rosas, 2004) and convergence (Piras et al., 2010). Variation in growth patterns among related taxa show that selection can rapidly modify

postnatal developmental pathways under some circumstances (e.g. (Adams and Nistri, 2010; Wilson and Sánchez-Villagra, 2010, 2011; Urošević et al., 2013)).

Differences in ontogenetic patterns have often been associated with differences in ecology, in an interplay between selective forces and developmental processes. Evolutionary radiations consisting of many closely related species provide opportunities to examine how changes to an ancestral growth pathway may have contributed to morphological diversification within a particular clade. The Australian radiation of dragon lizards, the Amphibolurinae (Agamidae), includes iconic species such as the frill-neck lizard, bearded dragon, and thorny devil. They constitute a diverse component of Australia's reptile fauna comprising around 108 species, and probably represent the descendants of a single continental colonisation from Southeast Asia approximately 30 million years ago (Ma) (Hugall et al., 2008; Melville et al., 2011; Oliver and Hugall, 2017). They diversified into a range of distinct morphotypes and ecological niches as the continent became increasingly arid (Melville et al., 2001; Fujioka and Chappell, 2010), and today they are particularly diverse in the arid zone (Melville et al., 2006; Powney et al., 2010). Among the most ecomorphologically relevant features of lizards is their head morphology (e.g. Kohlsdorf et al., 2008); its role in supporting sensory structures, in food gathering, for social signalling and as a weapon, mean that it must be responsive to multiple selective pressures. Amphibolurinae includes some markedly varied and specialised skull shapes (Siebenrock, 1895; Bell et al., 2009), but apart from one recent limited study (Stilson et al., 2017), there has been little examination of cranial growth patterns among different species.

This study aims to investigate whether the evolution of different cranial shapes among 18 species of the Amphibolurinae is achieved through heterochrony: without changes to the ancestral growth pathway (as predicted by the ontogenetic scaling hypothesis), or through modification of these pathways. We use two-dimensional landmark based geometric morphometrics to characterise cranial shape, and compare the direction and magnitude of postnatal growth trajectories using a phenotypic trajectory analysis (Collyer and Adams, 2013). We also test for associations between ontogenetic patterns and life habit (Collyer et al., 2015), and whether there is a phylogenetic signal in juvenile or adult skull shapes (Adams, 2014).

Material and methods

Study specimens

Material comprised 2D lateral view images of 361 specimens representing 18 different species of amphibolurine lizards (Table 4.1, see supplementary material: File ES4.1 for images). The species were chosen to optimise taxonomic breadth, skull shape diversity, and size, but limited to species where the sample size was 10 specimens or more and included both juveniles and adults. We collected data from skeletal specimens from several institutions including South Australian Museum, University of Texas at Austin, Western Australian Museum, Field Museum of Natural History, Queensland Museum, University of Adelaide, and Melbourne Museum. Institution and specimen catalogue numbers and images of specimens can be found in supplementary material: File ES4.2, and on the MorphoBank repository (http://morphobank.org/permalink/?P3110).

Table 4.1 – Species studied. Sample sizes were dependent on availability from collections. Average skull length is the mean of the basal skull length of the largest three individuals of each species. Life habit categories were based on records in Wilson and Swan (2013) and Cogger (2014).

Species	n	Average adult skull length (mm)	Life habit
Ctenophorus caudicinctus	26	22.43	Saxicolous
Ctenophorus cristatus	15	24.39	Terrestrial
Ctenophorus decresii	10	23.51	Saxicolous
Ctenophorus isolepis	30	17.72	Terrestrial
Ctenophorus nuchalis	21	29.07	Terrestrial
Ctenophorus reticulatus	29	26.05	Terrestrial
Amphibolurus muricatus	34	28.72	Semi-arboreal
Chlamydosaurus kingii	17	75.97	Semi-arboreal
Diporiphora nobbi	12	23.22	Semi-arboreal
Diporiphora winneckei	12	13.37	Semi-arboreal
Gowidon longirostris	20	32.65	Semi-arboreal
Lophognathus gilberti	16	31.80	Semi-arboreal
Pogona barbata	29	64.83	Semi-arboreal
Pogona vitticeps	29	60.46	Semi-arboreal
Rankinia diemensis	12	18.97	Terrestrial
Tympanocryptis tetraporophora	11	15.93	Terrestrial
Intellagama lesueurii	22	70.96	Semi-arboreal
Moloch horridus	15	16.31	Terrestrial

Imaging

The left side of the cranium was studied from 2D images. Each skeletal specimen was oriented using dry sand (black in colour for contrast) and photographed using an Olympus TG-4 camera mounted on a large flexible tripod, with a ruler set to the sagittal (midline) axis of the skull as a reference for scale. We also used 2D images of 3D rendered surface models generated from micro-Computed Tomography (CT) reconstructions of specimens in alcohol from South Australian Museum. These specimens had been micro CT scanned at either ~18 or ~9 μm resolution (depending on the size of the specimen) using a Skyscan 1076 (Bruker micro-CT) at Adelaide Microscopy. Each CT scan was reconstructed using the NRecon software interface (Skyscan, 2011). We used Avizo v 9.0 (Visualization Sciences Group, 2013) to digitally segment the cranium, threshold non-bone components from the scan, and render a surface model, which was then oriented laterally to capture a 2D image within Avizo, with a scale bar.

Landmarks and Shape Analysis

Lateral cranial shape was characterised using 2D landmark based geometric morphometrics. Landmarks were digitised on the images of the crania using tpsDig v. 2.21 (Rohlf, 2016). We set the scale for each specimen using scale bars present in the digital images, and digitised 16 single point landmarks (see Fig. 4.1), that represented equivalent points on bones at suture junctions, boundaries, and extremes of curvature on structures (see supplementary material: Table S4.1
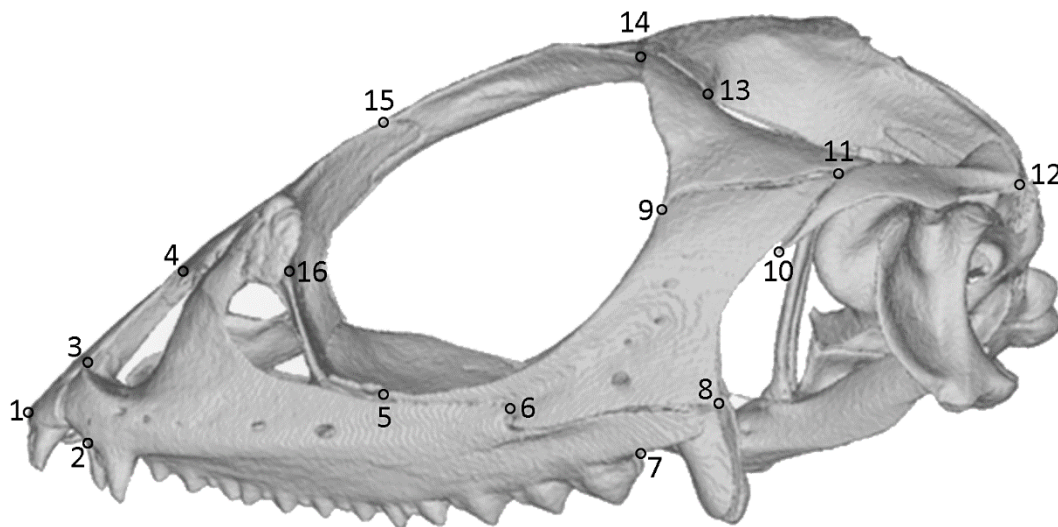
Figure 4.1 – Lateral image of *Amphibolurus muricatus* showing positions of 2D landmarks used to characterise shape. Number correspond to landmark definitions in supplementary material: Table S4.1.

for landmark definitions). All subsequent analyses were performed using a routine written for the R statistical framework v 3.4.0. The raw 2D landmark coordinates (which are in supplementary material: File ES4.3) were subjected to a generalised Procrustes alignment (GPA) using the R package *geomorph* (Adams et al., 2018). This effectively removed differences in size, position, and orientation, leaving only shape variation (Rohlf and Slice, 1990). The resulting Procrustes aligned shape coordinates were used as shape variables in subsequent analyses. Centroid size (the square root of the sum of the square distances of each landmark before GPA) was used as a proxy for body size. We were unable to use snout-vent length measurements because this data was not available for most of the skeletal specimens used.

Visualising shape variation

We performed a principal component analysis (PCA) on the Procrustes aligned shape coordinates to visualise the variation among sets of landmarks in the data set. To interpret the shape differences described by the major axes of variation identified by the PCA, we plotted a morphospace (PC1 versus PC2) with points identified by size and species. To visualise the shape variation associated with the major axes of variation, we used thin-plate spline deformation grids (Bookstein, 1991), produced using the "PlotRefToTarget" function in *geomorph*, and a wireframe representation of the skull, to represent shape differences between corresponding landmarks of the mean shape and minimum or maximum values for PC1 and PC2.

Examining allometry

To examine whether the morphological disparity in cranial shape among species differs between juveniles and adults, we quantified the disparity for two separate groups: the smallest three juveniles of each species (start of growth trajectory); and the largest three adults of each species (end of growth trajectory). We calculated morphological disparity using the "morphol.disparity" function in *geomorph*, which estimates Procrustes variance while accounting for group size, and uses absolute differences in variances to test for pairwise differences in morphological disparity between groups. The statistical significance between the juvenile and adult groups was assessed using a randomised residual permutation test with 1000 iterations.

We determined whether any species displayed isometric growth (no change in shape with a change in size), by fitting individual regression of log transformed size on shape for each species, using the "procD.lm" function from the R package *geomorph*, which assesses significance via distributions generated with resampling permutations (we used 1000 iterations). If the association between size and shape for a particular species was significant the null hypothesis of

isometry was rejected and revealed that there was an ontogenetic allometric pattern present for that particular species.

To test whether ontogenetic trajectories differ among species we conducted a phenotypic trajectory analysis (PTA) (Adams and Collyer, 2009) on the shape coordinates using the "trajectory.analysis" function in *geomorph*. This procedure quantifies different attributes of a shape change trajectory between two or more points, in this case we measure the attributes of shape change between two groups: juveniles and adults. To circumvent issues with estimating nearness to adulthood in a clade with such broad variation in adult body sizes, we were able to categorise each specimen as either a juvenile or adult based on the number of acrodont teeth they had. If a specimen had more than 80% of the maximum number of acrodont teeth observed for that species, they were categorised as an adult. This was a necessary shortcut in the absence of hard data in the literature. 80% seemed to be the point where growth levelled off and was therefore used as an estimate of a species approaching adulthood. In some cases we altered the categorisation if a specimen was missing enough teeth to hinder obtaining a count, and were able to categorise these as either juveniles or adults based on the centroid sizes observed for other specimens of that particular species. We used species as groups, and juveniles and adults as the trajectory points. This analysis involved pairwise comparisons of two different attributes: the magnitudes of the trajectories among species, and also directions of the trajectories among species. Attribute differences were evaluated from sampling distributions generated from 1000 random permutations (based on a null model that lacked coefficients for a species-transect interaction) (Collyer and Adams, 2013). To visualise the ontogenetic phenotypic trajectories, we plotted the first two PCs of shape variation with arrows representing vectors of shape change (where the start of the arrows represents mean juvenile shapes and the end of the arrows represents mean adult shapes) and used thin-plate spline deformation grids to visualise shape change.

We tested for differences in ontogenetic allometric patterns of skull shape among ecological life habit groups by running a multivariate analysis of covariance (MANCOVA) model using the *geomorph* function "procD.allometry", with log transformed centroid size, life habit, and their interaction as model effects. Life habit was split into three categories (see Table 1), based on information available in Wilson and Swan (Wilson and Swan, 2013) and Cogger (Cogger, 2014). Statistical significance was evaluated using Goodall's (Goodall, 1991) F-ratio and a randomised residual permutation procedure using 1000 iterations (Collyer et al., 2015). If the interaction terms were significant, this indicated that the allometric trajectories differed among life habit groups. We identified which life habits groups differed from each other, using the

"advanced.procD.lm" function in *geomorph*. These tests identified which life habit groups significantly differed in allometric slope from each other, via pairwise assessments of the similarity in slopes and intercepts through 1000 randomised residual permutations. To visualise ontogenetic allometric trajectories of species with different life habits, we plotted the predicted shape scores (from a multivariate regression of shape ~ log (size) * species), on log transformed centroid size, and identified points by life habit.

Phylogenetic signal

We inferred an evolutionary tree using Hugall et al., Melville et al., and Pyron et al. (Melville et al., 2001; Hugall et al., 2008; Pyron et al., 2013), and used this tree to estimate phylogenetic signal present in shape and size of the smallest juveniles and adults, relative to what is expected for the inferred phylogeny under a Brownian motion model of evolution (see supplementary material: File ES4.4 for nexus tree). We used the mean shape of the smallest three individuals (by centroid size) for each species to estimate phylogenetic signal in juvenile shapes, and the mean of the largest three individuals (by centroid size) of each species to estimate phylogenetic signal in adult shapes. To estimate phylogenetic signal we calculated K_{mult} (Adams, 2014), which is a generalisation of Blomberg's K-statistic appropriate for high-dimensional and multivariate data (Blomberg et al., 2003). We determined statistical significance of K_{mult} using phylogenetic permutation with 1000 iterations, which is calculated by permuting the multivariate shape data of the specimens among all tips of the phylogenetic tree. This was done using the "physignal" function in *geomorph*. To visualise how shape variation among species is associated with phylogeny we carried out separate PCAs on the landmark data for the mean shape of the three smallest juveniles and mean shape of the three largest adults, and used the phylomorphospace approach to project a phylogeny into the juvenile and adult PC biplots (with internal nodes estimated using maximum likelihood), implemented with the function "phylomorphospace" in the R package *phytools* (Revell, 2012).

Results

Variation in cranial shape

A principal component analysis (PCA) characterising cranial shape show that most of the smaller individuals have high PC1 values and low PC2 values (Fig. 4.2, see also supplementary material: Table S4.2 for PC summary), which characterises skulls with relatively larger orbits and relatively shorter, smaller, and more slender post-orbit elements (jugal, postorbital, squamosal, parietal), and short blunt snouts. The other three quadrants of the morphospace are each associated with one of three major adult morphotypes. *Gowidon longirostris* is one example of an extreme morphotype (low PC1 values and low PC2 values) which has a relatively long and pointed snout, long maxillary facial process, a wide postorbital bar (jugal), small orbit, and an overall dorsoventrally shallow skull.
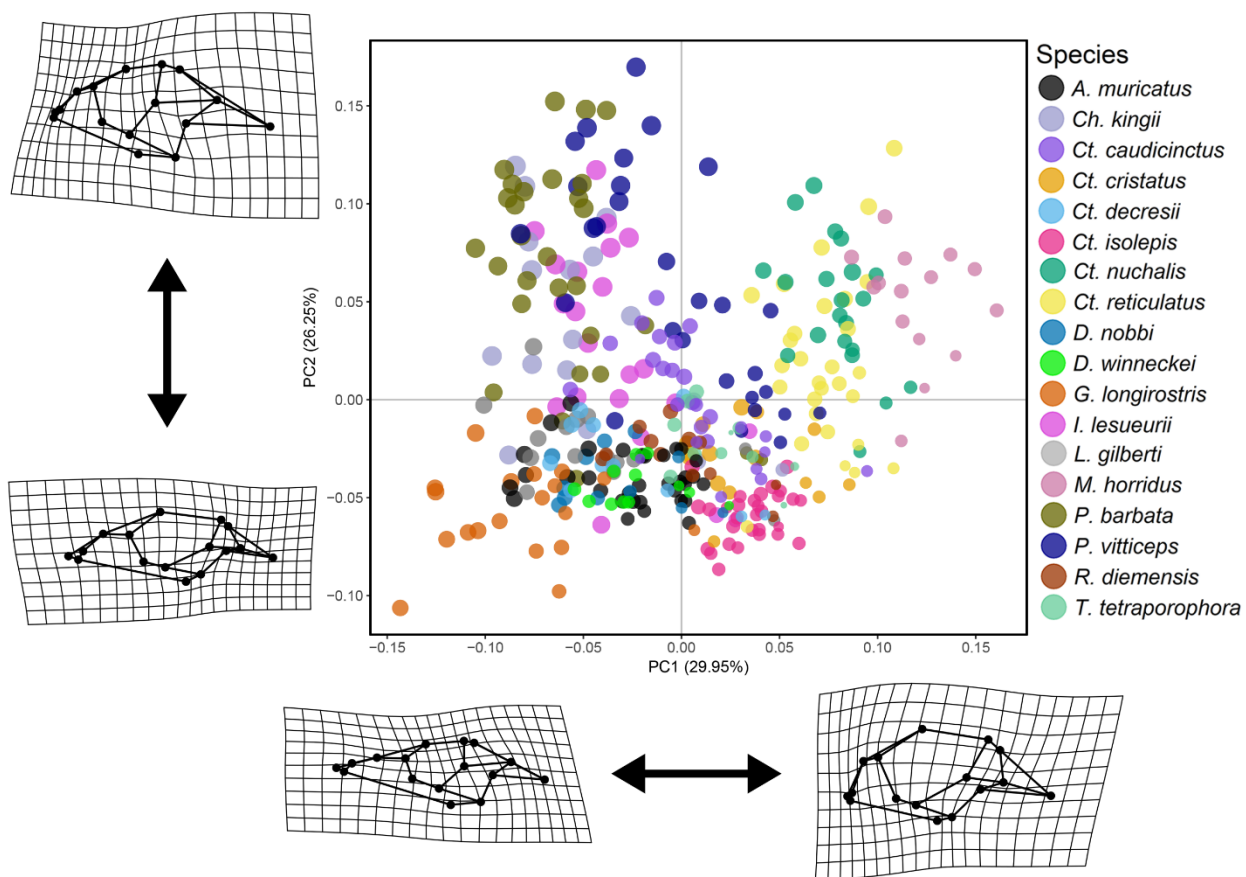
Figure 4.2 – Cranial morphospace representing the two main axes of shape variation from a PCA of the sets of Procrustes aligned landmark coordinates. Points are coloured according to species affiliation, and scaled according to centroid size. TPS deformation grids and wireframes represent shape differences between corresponding landmarks of the mean shape and minimum and maximum values for PC1 and PC2 of the geometric morphometric data.

Chlamydosaurus kingii, *Intellagama lesueurii*, *Pogona barbata* and *P. vitticeps* have relatively short snouts (compared to the most long snouted forms) and broad, robust post-orbit elements (low PC1 values and high PC2 values). Interestingly, these four species are also those with the largest adult size. *Ch. kingii* and both species of *Pogona* have relatively short but pointed snouts, whereas *I. lesueurii* has a more rounded snout. The third extreme form of shape variation has a short and blunt snout, robust post-orbit elements, and a dorsoventrally deep overall skull profile, e.g. *Ctenophorus nuchalis*, *Ct. reticulatus* and *Moloch horridus*. For any particular species, the intermediate and adult ontogenetic stages occupy morphospace between the large-orbit form associated with smaller individuals (high PC1 values and low PC2 values), and one of these three broad morphotypes.

Examining ontogenetic allometry

Morphological disparity (Procrustes variance) was significantly ($P = 0.001$) greater in the three largest adults of each species (Procrustes variance = 0.0148) than in the three smallest juveniles of each species (Procrustes variance = 0.0099). The disparity calculated for the smallest juvenile and largest adult representatives of each species show that different agamid species begin life with a similar cranial shape and later disperse towards more disparate adult forms.

Tests for isometry in growth patterns for each species indicated that all species have significant allometric growth (lack of isometry): changes in shape that are associated with changes in size. The variation detected in the shape data by a phenotypic trajectory analysis (PTA) revealed significant differences in growth trajectories: among directions (angles) of shape change, and also among magnitudes of shape change. Vectors representing ontogenetic trajectories of different species are shown in Figure 4.3a, where the start of an arrow represents the mean juvenile shape and the end of the arrow represents the mean adult shape. For PC1, most species trajectories move from high values as juveniles, to low values as adults. For PC2, most species trajectories move from low values as juveniles, to high values as adults.

The direction of ontogenetic shape change in different species in the sample are shown by the direction of the arrows in Figure 4.3a. Pairwise *P*-values for direction (angle) differences in the PTA are reported in supplementary material: Table S4.3. Out of 153 possible pairs of species, 74 shared a common slope, while the remaining 79 pairs had significantly different directions of ontogenetic shape change. The pairwise results show that there are several cases where members belonging to the same genus have different directions of ontogenetic shape change. *M. horridus* has a significantly different direction of shape change than all other sampled species. *I. lesueurii*,
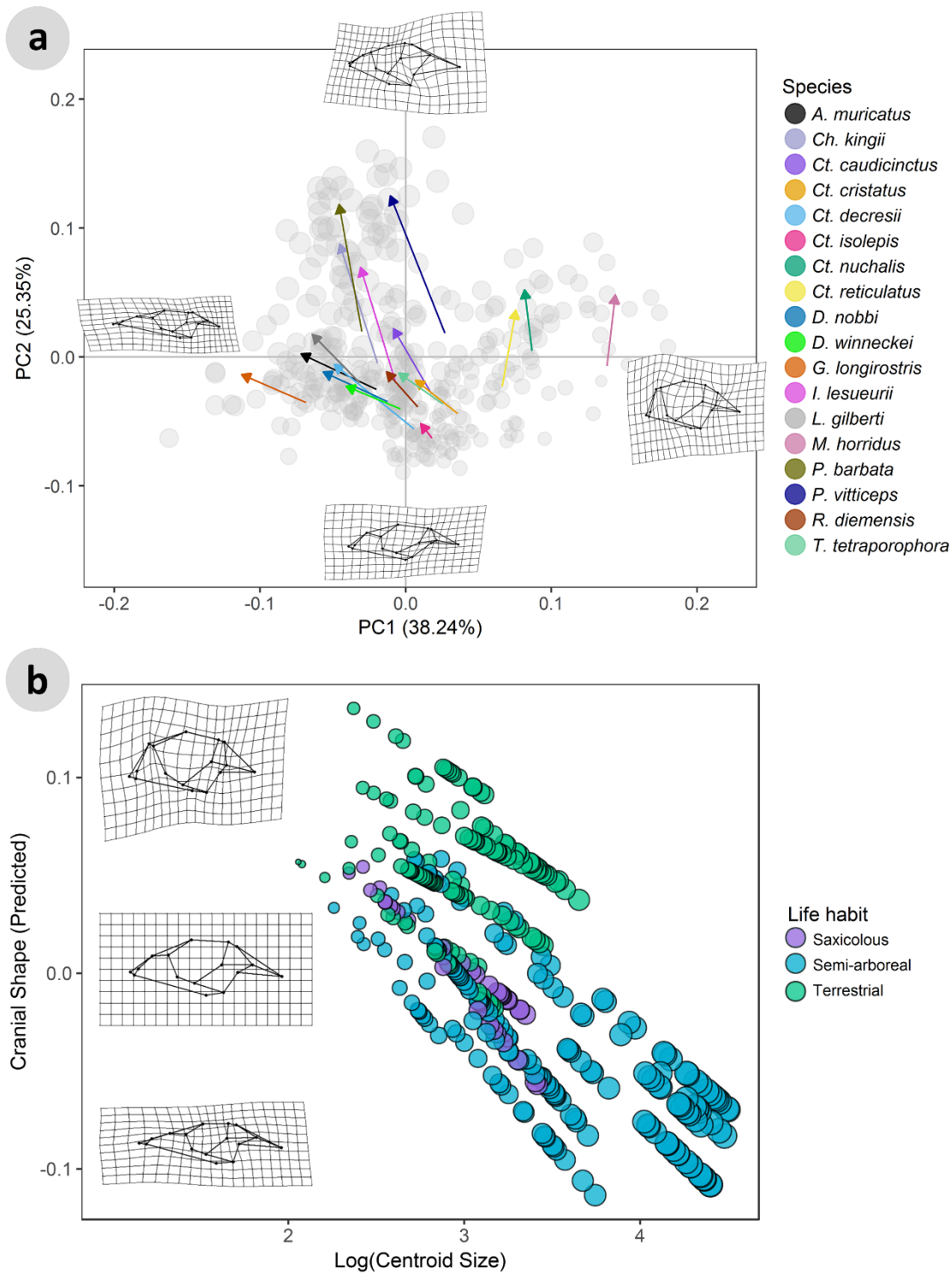
Figure 4.3 – Ontogenetic allometric trajectories derived from the phenotypic allometric trajectory analysis (a) and the species ontogenetic allometric patterns identified by life habit (b). For both plots, the size of points for each specimen is scaled to centroid size. In a, specimens are plotted on a morphospace represented by PCs 1 and 2 on the x and y axes respectively. The arrows represent predicted trajectories for each species. The arrows start at the mean juvenile shape and end at the mean adult shape. The grey points represent the total variation within the sample. TPS deformation grids represent the shape change from the mean shape of the data set to the shape at the minimum and maximum values on that axis. In b, the x-axis represents log-transformed centroid size, and the y-axis represents the first principal component of the predicted values of multivariate regression of shape on size (as identified by MANCOVA). TPS deformations grids represent the shape change from the mean shape of the data set to the shape of the smallest and largest specimens in the data set.

Ch. kingii, *P. barbata*, and *P. vitticeps* have the largest adult size, and all have similar directions of ontogenetic shape change. The species with the smallest adult sizes are *Ct. isolepis, Diporiphora winneckei, Rankinia diemensis, Tympanocryptis tetraporophora,* and *M. horridus,* and they also have mostly similar directions of ontogenetic shape change, apart from *M. horridus.*

Magnitudes of shape change for the different species in the sample can be observed by the length of the trajectory arrows in Figure 4.3a. Pairwise *P*-values for magnitude in the PTA are reported in supplementary material: Table S4.4. Out of 153 possible pairs of species, 90 had a similar magnitude of shape change, while the remaining 63 pairs had significantly different magnitudes of shape change. Species in this study with a larger adult size (*Ch. kingii, I. lesueurii, P. barbata, P. vitticeps*) have greater magnitudes of ontogenetic shape changes than other sampled agamids. *Ct. isolepis* shows the smallest magnitude of shape change compared with all other sampled species. *Ct. cristatus, Ct. decresii, Ct. nuchalis and Ct. reticulatus* all have relatively small magnitudes of shape change. In *Ctenophorus*, only three significant pairwise differences in magnitude were detected (both involving *Ct. isolepis*). Within the sister clade to *Ctenophorus* we detected 21 pairwise differences, mostly involving *Ch. kingii* and the species of *Pogona,* which show the largest magnitude of shape change of any species (Table S4.4).

Cranial shape is influenced by size, life habit and the interactions of the two (MANCOVA, size $F_{(1, 361)}$ = 128.35, ***P* = 0.001**; habit $F_{(3, 361)}$ = 39.83, ***P* = 0.001**; size*habit $F_{(3, 361)}$ = 5.24, ***P* = 0.001**). The MANCOVA results indicated that there is significant allometry in cranial shape, and that this allometry differs among life habit categories (see supplementary material: Table S4.5). The differences in ontogenetic allometric patterns (log transformed centroid size vs. predicted cranial shape) between species with different life habits is evident in a plot of size versus predicted shape (Fig. 4.3b). Pairwise comparisons revealed that all life habit groups have significantly different slopes (direction of shape change) from one another, except for the semi-arboreal and saxicolous groups. There were also significant pairwise differences in trajectory length (amount of shape change) detected in pairwise comparisons for all three life habit groups (see supplementary material: Table S4.6 for *P*-values for pairwise angle and length differences for life habit groups).
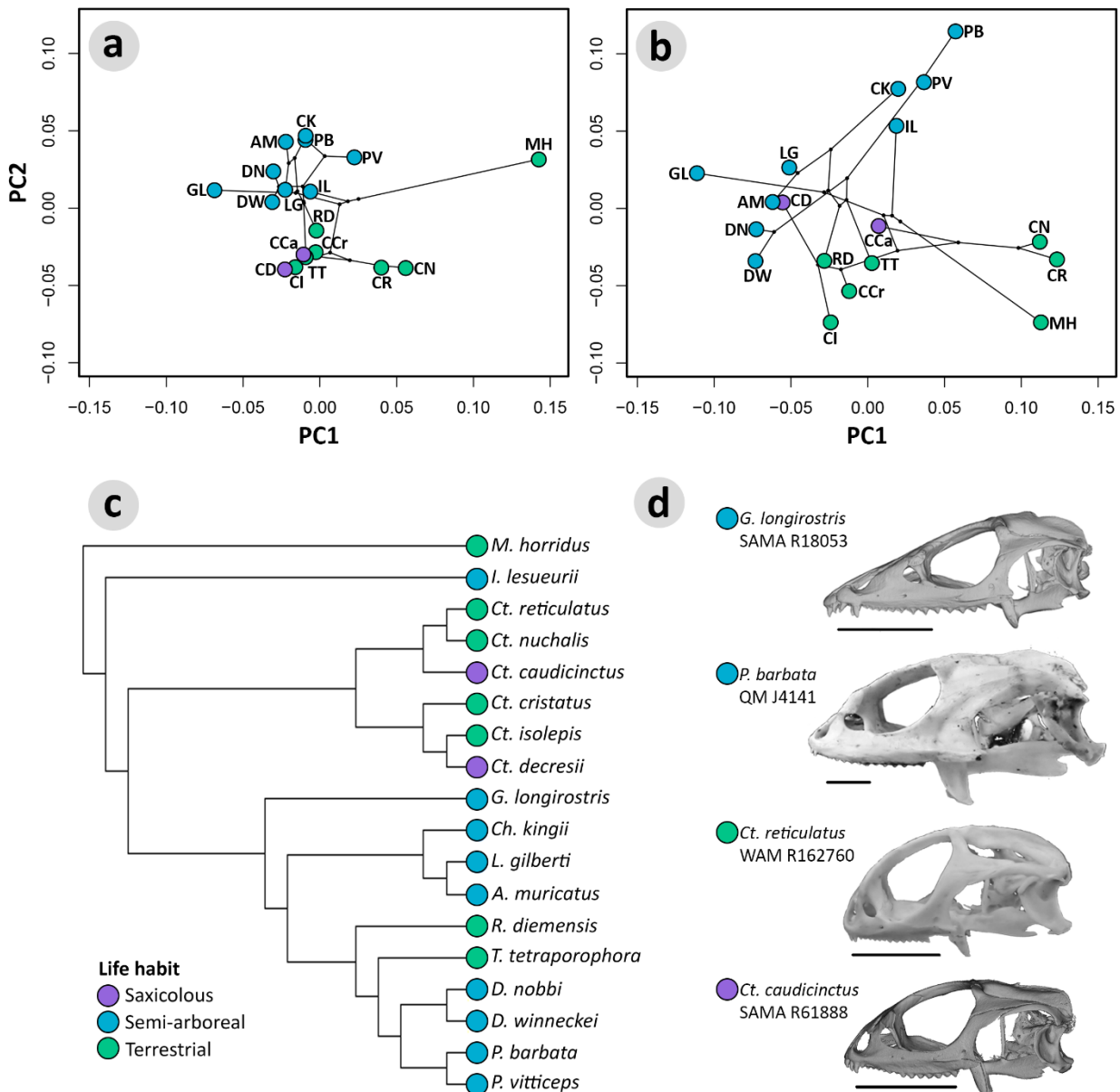
Figure 4.4 – Phylomorphospaces (of PC1 versus PC2) for smallest juvenile (a) and largest adult shapes (b). Abbreviations are as follows: AM = *A. muricatus*, CH = *Ch. kingii*, CCa = *Ct. caudicinctus*, CCr = *Ct. cristatus*, CD = *Ct. decresii*, CI = *Ct. isolepis*, CN = *Ct. nuchalis*, CR = *Ct. reticulatus*, DN = *D. nobbi*, DW = *D. winneckei*, GL = *G. longirostris*, IL = *I. lesueurii*, LG = *L. gilberti*, MH = *M. horridus*, PB = *P. barbata*, PV = *P. vitticeps*, RD = *R. diemensis*, TT = *T. tetraporophora*. c shows the inferred phylogenetic tree of relationships between agamids used in this study. All points are coloured according to life habit category. d shows examples of adult skulls that represent extreme variation in shape and different life habits. Scale bar = 10 mm.

Phylogenetic signal

Tests for phylogenetic signal (relative to what is expected under a Brownian motion model of evolution) in cranial shape of the smallest juveniles and the largest adults revealed that both juveniles and adults show significant phylogenetic signal in their shape (juvenile: K_{mult} = 0.44, **P = 0.001**; adult: K_{mult} = 0.44, **P = 0.001**). The amount of phylogenetic signal is moderate, and the same for both the juvenile and adult shape data. Even though the amount of phylogenetic signal in both sets of shape data is the same, the relative distribution of the species in the cranial morphospace is not the same for juveniles and adults. The phylomorphospaces (see Fig. 4.4) show distributions of the juvenile and adult shape data in morphospace relative to the phylogeny, and that many of the branches overlap with one another. The distribution of points in the juvenile and adult cranial morphospaces supports the detected disparity differences between juveniles and adults, with the juvenile skulls occupying a much more restricted area of the same cranial morphospace than the adult skulls. There was no significant phylogenetic signal detected in cranial size (juveniles: K = 0.31, P = 0.130; adults, K = 0.36, P = 0.063).

Discussion

The amphibolurine post-natal growth pathway is evolutionarily flexible and has played a major role in producing great morphological disparity in adult cranial shape. Different ontogenetic patterns are significantly associated with different life habits, suggesting that at least some of the variation in adult cranial shape is adaptive. Shape variation in both juveniles and adults had some phylogenetic signal, indicating that inheritance plays some role in structuring the morphological and ontogenetic variation we observe. Overall, it appears that an interaction between evolutionary history and environmental pressures influences ontogenetic patterns in skull shape of this radiation of lizards.

Most of the disparity in the adult cranial form of the sampled amphibolurines develops during post-hatching ontogeny. For just under half of the sampled species, we observe shape changes along a shared slope, with indicates paedomorphy is the particular heterochronic pattern in a number of species of *Ctenophorus*. This finding is consistent with the ontogenetic scaling hypothesis (changes in the time or rate of development along the growth pathway). However, heterochrony is insufficient to explain the entirety of morphological diversity of the amphibolurines. More often than not, we observe differences in both direction and magnitude of growth pathways between pairs of species, which suggests that ontogenetic divergence has been a major factor in the evolution of the disparity seen in adult amphibolurine lizards.

The extent to which ontogenies are conserved during evolution has been a continued topic of controversy that has influenced the development of phylogenetic methods (Gould, 1977; de Queiroz, 1985; Kluge and Strauss, 1985; Nelson, 1985), and this study adds to the growing amount of evidence that morphological ontogenies are as prone to selection and evolutionary change as other aspects of morphology. It has been suggested that changes in the direction of allometric slopes are rare, since they represent costly alterations to growth dynamics (Huxley and Teissier, 1936; Gould, 1966; Gould, 1977), but our study adds to the many others that have suggested that such changes occur frequently (Adams and Nistri, 2010; Klingenberg, 2010a; Wilson and Sánchez-Villagra, 2011). The importance of evolving ontogenies in generating morphological diversity in amphibolurines resembles what has been shown in other reptiles (Esquerré et al., 2017), other vertebrates (Weston, 2003; Wilson, 2018), and even in plants (Strelin et al., 2016). In some cases, developmental pathways do represent an evolutionary constraint, canalising the phenotypic variation of species into particular portions of morphospace, as has been reported in lacertid lizards (Piras et al., 2011). It seems that ontogenies are more flexible than previously thought, and can allow morphology to explore previously unoccupied areas of morphospace.

In both juvenile and adult skull shapes, phylogenetic affinity is less strongly supported than are correlations with ecological groups. This is in agreement with other studies on the skulls of reptiles (Claude et al., 2004; Hipsley and Müller, 2017), mammals (Wilson, 2010; Fuchs et al., 2015), and fish (Frédérich and Vandewalle, 2011), that have identified greater associations between morphology and diet (Wilson and Sánchez-Villagra, 2010; Fuchs et al., 2015), feeding habits (Herrel et al., 2006; Frédérich and Vandewalle, 2011), habitat (Urošević et al., 2013; Hipsley et al., 2016), and environmental factors (Frédérich and Vandewalle, 2011; Marcy et al., 2016), than with phylogeny. In contrast, some studies confirm a strong phylogenetic signal in morphological variation, such that ecological correlations are not evident (Hipsley et al., 2016; Dial et al., 2017; Doke et al., 2017), or seem to have minimal effect (Powder et al., 2015). While adaptive factors and phylogeny both undoubtedly play a role in shaping morphological diversity, the extent of this role evidently differs amongst clades and should be assessed on a case-by-case basis.

Our findings add to the growing body of evidence (Klingenberg, 1996; Wilson and Sánchez-Villagra, 2010; Collyer and Adams, 2013; Wilson et al., 2013; Collyer et al., 2015) that highlights the importance of using a rigorous quantitative framework to investigate the underlying basis of phenotypic variation. We have yet to investigate the influence of sexual dimorphism on amphibolurine lizards because of the lack of sex information for most of the museum specimens studied. Sexual size dimorphism has been recorded for at least one species in this study (see (Badham, 1976; Thompson and Withers, 2005)), and therefore we cannot discount the possibility that it has an influence on skull shape, considering the strong allometric effects observed in these lizards. Therefore, future studies are encouraged to investigate the effect of sexual dimorphism on morphological variation in this clade. Furthermore, the influence on growth of diet and feeding habits on skull shape are yet to be studied in this group but are required to fully understand the evolutionary patterns we have observed. Our study thus serves as foundation for further studies to examine hypotheses about these factors, and to that end we provide a morphological database (http://morphobank.org/permalink/?P3110).

Conclusions

Diversity in cranial shape of amphibolurine lizards seems to be the result of a combination of heterochrony and changes in growth patterns, which are related to phylogenetic affinity and adaptive evolution. The expectation of a conserved phylogenetic pattern, as predicted by the ontogenetic scaling hypothesis, does not fully explain the variation in skull shapes, and we have strong evidence that there is an adaptive basis for much of the variation in ontogenetic allometry

that we observe. Our study emphasises the power of growth pathways for facilitating the morphological variation that is characteristic of large and speciose evolutionary radiations. It also underlines the importance of using quantitative multivariate analyses to properly appreciate the role of developmental processes in shaping phenotypic diversity across species.

Acknowledgements

Supplementary material

Tables

Electronic files

File ES4.1 – Zipped file containing crania images used for 2D landmarking (ZIP).

File ES4.2 – Specimen numbers and information used to examine ontogenetic patterns (CSV).

File ES4.3 – 2D landmark coordinates used to characterise crania in this study (TPS).

File ES4.4 – Nexus tree of 18 agamid species, used to build phylomorphospaces (NEX).

References

Adams DC. 2014. A generalized K statistic for estimating phylogenetic signal from shape and other high dimensional multivariate data. Syst Biol 63:685-697.

Adams DC, Collyer ML. 2009. A general framework for the analysis of phenotypic trajectories in evolutionary studies. Evolution 63:1143-1154.

Adams DC, Collyer ML, Kaliontzopoulou. 2018. geomorph: software for geometric morphometric analyses. R package version 3.0.6. https://CRANR-projectorg/package=geomorph.

Adams DC, Nistri A. 2010. Ontogenetic convergence and evolution of foot morphology in European cave salamanders (Family: Plethodontidae). BMC Evol Biol 10:216.

Badham JA. 1976. The *Amphibolurus barbatus* species-group (Lacertilia: Agamidae). Aust J Zool 24:423-443.

Bastir M, Rosas A. 2004. Facial heights: Evolutionary relevance of postnatal ontogeny for facial orientation and skull morphology in humans and chimpanzees. J Hum Evol 47:359-381.

Bell CJ, Mead JI, Swift SL. 2009. Cranial osteology of *Moloch horridus* (Reptilia: Squamata: Agamidae). Rec West Aust Mus 25:201-237.

Blomberg SP, Garland TJ, Ives AR. 2003. Testing for phylogenetic signal in comparative data: behavioural traits are more labile. Evolution 57:717-745.

Bookstein FL. 1991. Morphometric tools for landmark data: geometry and biology. Cambridge: Cambridge University Press.

Claude J, Pritchard PCH, Tong H, Paradis E, Auffray J-C. 2004. Ecological correlates and evolutionary divergence in the skull of turtles: a geometric morphometric assessment. Syst Biol 53:933-948.

Cock AG. 1966. Genetical aspects of metrical growth and form in animals. Q Rev Biol 41:131-190.

Cogger H. 2014. Reptiles and amphibians of Australia, 7th ed. Collingwood: CSIRO Publishing.

Collyer ML, Adams DC. 2013. Phenotypic trajectory analysis: comparison of shape change patterns in evolution and ecology. Hystrix 24:75-83.

Collyer ML, Sekora DJ, Adams DC. 2015. A method for analysis of phenotypic change for phenotypes described by high-dimensional data. Heredity 115:357-365.

de Queiroz K. 1985. The ontogenetic method for determining character polarity and its relevance to phylogenetic systematics. Syst Zool 34:280-299.

Dial TR, Reznick DN, Brainerd EL. 2017. Heterochrony in the evolution of Trinidadian guppy offspring size: maturation along a uniform ontogenetic trajectory. Proc R Soc B 284.

Doke D, Morey R, Dahanukar N, Padhye SM, Paripatyadar SV. 2017. Ontogenetic trajectory and allometry of *Diplonychus rusticus* (Fabricius), an Oriental aquatic bug (Hemiptera: Belostomatidae) from the Western Ghats of India. Arthropod Struct Dev 46:297-303.

Esquerré D, Sherratt E, Keogh JS. 2017. Evolution of extreme ontogenetic allometric diversity and heterochrony in pythons, a clade of giant and dwarf snakes. Evolution 71:2829-2844.

Frédérich B, Vandewalle P. 2011. Bipartite life cycle of coral reef fishes promotes increasing shape disparity of the head skeleton during ontogeny: an example from damselfishes (Pomacentridae). BMC Evol Biol 11:82.

Fuchs M, Geiger M, Stange M, Sánchez-Villagra MR. 2015. Growth trajectories in the cave bear and its extant relatives: an examination of ontogenetic patterns in phylogeny. BMC Evol Biol 15:239.

Fujioka T, Chappell J. 2010. History of Australian aridity: chronology in the evolution of arid landscapes. Geol Soc, Special Publications 346:121-139.

Goodall C. 1991. Procrustes methods in the statistical analysis of shape. J Royal Stat Soc B 53:285-339.

Gould S. 1966. Allometry and size in ontogeny and phylogeny. Biol Rev 41:587-640.

Gould SJ. 1977. Ontogeny and Phylogeny. Cambridge: Harvard University Press.

Gould SJ. 2002. The structure of evolutionary theory. Cambridge: Harvard University Press.

Herrel A, Joachim R, Vanhooydonck B, Irschick DJ. 2006. Ecological consequences of ontogenetic changes in head shape and bite performance in the Jamaican lizard *Anolis lineatopus*. Biol J Linnean Soc 89:443-454.

Hipsley CA, Müller J. 2017. Developmental dynamics of ecomorphological convergence in a transcontinental lizard radiation. Evolution 71:936-948.

Hipsley CA, Rentinck M-N, Rödel M-O, Müller J. 2016. Ontogenetic allometry constrains cranial shape of the head-first burrowing worm lizard *Cynisca leucura* (Squamata: Amphisbaenidae). J Morphol 277:1159-1167.

Hugall AF, Foster R, Hutchinson M, Lee MSY. 2008. Phylogeny of Australian agamid lizards based on nuclear and mitchondrial genes: implications for morphological evolution and biogeography. Biol J Linnean Soc 93:343-358.

Hugi J, Hutchinson MN, Koyabu D, Sánchez-Villagra MR. 2012. Heterochronic shifts in the ossification sequences of surface- and subsurface-dwelling skinks are correlated with the degree of limb reduction. Zoology 115:188-198.

Huxley JS, Teissier G. 1936. Terminology of relative growth. Nature 114:895-896.

Klingenberg CP. 1996. Multivariate allometry. In: Marcus LF, Corti M, Loy A, Naylor GJP, Slice DE, editors. Advances in Morphometrics. Boston: Springer US. p 23-49.

Klingenberg CP. 1998. Heterochrony and allometry: the analysis of evolutionary change in ontogeny. Biol Rev 73:79-123.

Klingenberg CP. 2010a. Evolution and development of shape: integrating quantitative approaches. Nat Rev Genet 11:623-635.

Klingenberg CP. 2010b. There's something afoot in the evolution of ontogenies. BMC Evol Biol 10:221.

Klingenberg CP. 2016. Size, shape, and form: concepts of allometry in geometric morphometrics. Dev Genes Evol 226:1-25.

Klingenberg CP, Marugán-Lobón J. 2013. Evolutionary covariation in geometric morphometric data: analyzing integration, modularity, and allometry in a phylogenetic context. Syst Biol 62:591-610.

Klingenberg CP, Zimmermann M. 1992. Static, ontogenetic and evolutionary allometry: a multivariate comparison in nine species of water striders. Am Nat 140:601-620.

Kluge AG, Strauss RE. 1985. Ontogeny and systematics. Ann Rev Ecol Syst 16:247-268.

Kohlsdorf T, Grizante MB, Navas CA, Herrel A. 2008. Head shape evolution in Tropidurinae lizards: does locomotion constrain diet? J Evol Biol 21:781-790.

Losos JB. 2011. Lizards in an evolutionary tree: ecology and adaptive radiation of anoles. Oakland, California: University of California Press.

Marcy AE, Hadly EA, Sherratt E, Garland K, Weisbecker V. 2016. Getting a head in hard soils: Convergent skull evolution and divergent allometric patterns explain shape variation in a highly diverse genus of pocket gophers (*Thomomys*). BMC Evol Biol 16:207.

Melville J, Harmon LJ, Losos JB. 2006. Intercontinental community convergence of ecology and morphology in desert lizards. Proc R Soc B 273:557-563.

Melville J, Ritchie EG, Chapple SNJ, Glor RE, Schulte JA. 2011. Evolutionary origins and diversification of dragon lizards in Australia's tropical savannas. Mol Phylogenet Evol 58:257-270.

Melville J, Schulte JA, Larson A. 2001. A molecular phylogenetic study of ecological diversification in the Australian lizard genus *Ctenophorus*. J Exp Zool 291:339-353.

Nelson G. 1985. Outgroups and ontogeny. Cladistics 1:29-45.

Oliver PM, Hugall AF. 2017. Phylogenetic evidence for mid-Cenozoic turnover of a diverse continental biota. Nat Ecol Evol 1:1896.

Piras P, Colangelo P, Adams DC, Buscalioni A, Cubo J, Kotsakis T, Meloro C, Raia P. 2010. The *Gavialis–Tomistoma* debate: the contribution of skull ontogenetic allometry and growth trajectories to the study of crocodylian relationships. Evol Dev 12:568-579.

Piras P, Salvi D, Ferrara G, Maiorino L, Delfino M, Pedde L, Kotsakis T. 2011. The role of post-natal ontogeny in the evolution of phenotypic diversity in *Podarcis* lizards. J Evol Biol 24:2705-2720.

Powder KE, Milch K, Asselin G, Albertson RC. 2015. Constraint and diversification of developmental trajectories in cichlid facial morphologies. EvoDevo 6:25.

Powney GD, Grenyer R, Orne CDL, Owens IPF, Meiri S. 2010. Hot, dry and different: Australian lizard richness is unlike that of mammals, amphibians and birds. Glob Ecol Biogeogr 19:386-396.

Pyron RA, Burbrink FT, Wiens JJ. 2013. A phylogeny and revised classification of Squamata, including 4161 species of lizards and snakes. BMC Evol Biol 13:1-53.

Revell LJ. 2012. phytools: an R package for phylogenetic comparative biology (and other things). Methods Ecol Evol 3:217-223.

Rohlf FJ. 2016. tpsDig, digitize landmarks and outlines. Stony Brook, Department of Ecology and Evolution, State University of New York: http://life.bio.sunysb.edu/morph/

Rohlf FJ, Slice DE. 1990. Extensions of the Procrustes method for the optimal superimposition of landmarks. Syst Zool 39:40-59.

Siebenrock F. 1895. Das skelett der Agamidae. Sittzungsber Akad Wiss Wien 104.

Skyscan. 2011. NRecon. Aartselaar, Belgium.

Stilson KT, Bell CJ, Mead JI. 2017. Patterns of variation in the cranial osteology of three species of endemic Australian lizards (*Ctenophorus*: Squamata: Agamidae): implications for the fossil record and morphological analyses made with limited sample sizes. J Herpetol 51:316-329.

Strelin MM, Benitez-Vieyra S, Fornoni J, Klingenberg CP, Cocucci AA. 2016. Exploring the ontogenetic scaling hypothesis during the diversification of pollination syndromes in *Caiophora* (Loasaceae, subfam. Loasoideae). Ann Bot 117:937-947.

Thompson G, Withers P. 2005. Size-free shape differences between male and female Western Australian dragon lizards (Agamidae). Amphibia-Reptilia 26:55-63.

Tokita M, Yano W, James HF, Abzhanov A. 2017. Cranial shape evolution in adaptive radiations of birds: comparative morphometrics of Darwin's finches and Hawaiian honeycreepers. Phil Trans R Soc B 372:20150481.

Urošević A, Ljubisavljević K, Ivanović A. 2013. Patterns of cranial ontogeny in lacertid lizards: morphological and allometric disparity. J Evol Biol 26:399-415.

Visualization Sciences Group. 2013. Avizo. FEI Corporate Headquarters, Oregon.

West GB, Brown JH, Enquist BJ. 1997. A general model for the origin of allometric scaling laws in biology. Science 276:122-126.

Weston EM. 2003. Evolution of ontogeny in the hippopotamus skull: using allometry to dissect developmental change. Biol J Linnean Soc 80:625-638.

Wilson LAB. 2010. The evolution of morphological diversity in rodents : patterns of cranial ontogeny. Doctoral Dissertation: University of Zurich.

Wilson LAB. 2018. The evolution of ontogenetic allometries in mammalian domestication. Evolution IN PRESS:doi: 10.1111/evo.13464.

Wilson LAB, Sánchez-Villagra MR. 2010. Diversity trends and their ontogenetic basis: an exploration of allometric disparity in rodents. Proc R Soc B 277:1227-1234.

Wilson LAB, Sánchez-Villagra MR. 2011. Evolution and phylogenetic signal of growth trajectories: the case of chelid turtles. J Exp Zool (Mol Dev Evol) 316B:50-60.

Wilson LB, Furrer H, Stockar R, Sanchez-Villagra MR. 2013. A quantitative evaluation of evolutionary patterns in opercle bone shape in *Saurichthys* (Actinopterygii: Saurichthyidae). Palaeontology 56:901-915.

Wilson S, Swan G. 2013. A complete guide to reptiles of Australia, 4th ed. Chatswood: New Holland Publishers.

STATEMENT OF AUTHORSHIP

Title of Paper	Evolution of cranial shape in a continental-scale adaptive radiation of Australian lizards
Publication Status	☐ Published ☐ Accepted for Publication ☐ Submitted for Publication ☑ Unpublished and Unsubmitted w ork w ritten in manuscript style
Publication Details	Prepared for submission to Evolution

Principal Author

Name of Principal Author (Candidate)	Jaimi Gray		
Contribution to the Paper	Designed research, data collection and analysis, wrote first version of manuscript, edited later versions of manuscript.		
Overall percentage (%)	80%		
Certification:	This paper reports on original research I conducted during the period of my Higher Degree by Research candidature and is not subject to any obligations or contractual agreements with a third party that would constrain its inclusion in this thesis. I am the primary author of this paper.		
Signature		Date	23.08.2018

Co-Author Contributions

By signing the Statement of Authorship, each author certifies that:

i. the candidate's stated contribution to the publication is accurate (as detailed above);

ii. permission is granted for the candidate in include the publication in the thesis; and

iii. the sum of all co-author contributions is equal to 100% less the candidate's stated contribution.

Name of Co-Author	Emma Sherratt		
Contribution to the Paper	Provided guidance for data analysis, and edited manuscript.		
Signature		Date	24/08/2018

Name of Co-Author	Mark N. Hutchinson		
Contribution to the Paper	Helped design research, and edited manuscript.		
Signature		Date	28/08/2018

Name of Co-Author	Marc E. H. Jones		
Contribution to the Paper	Helped design research, provided guidance for data analysis, and edited manuscript.		
Signature		Date	23rd August 2018

CHAPTER 5

Evolution of cranial shape
in a continental-scale
evolutionary radiation of
Australian lizards
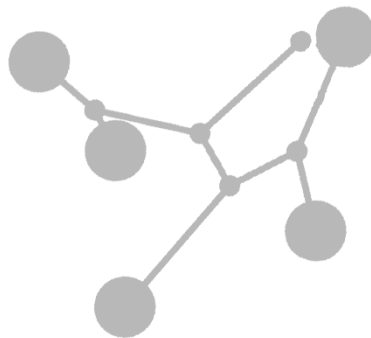
CHAPTER 5 – Evolution of cranial shape in a continental-scale evolutionary radiation of lizards

Jaimi A. Gray, Emma Sherratt, Mark N. Hutchinson, Marc E. H. Jones

Abstract

Morphological disparity can be generated during adaptive radiation in response to factors such as new resources, freedom from competition, and an absence of predators and pathogens. The oldest ancestor of the extant Australian radiation of agamid lizards (Amphibolurinae) arrived in Australia from Southeast Asia approximately 30 million years ago. Since then, Australian agamids have become a species-rich and ecologically diverse clade. Today, they are comprised of around 108 species distributed among every Australian habitat, and are particularly successful in arid environments. We have relatively sound knowledge of their taxonomic diversity and phylogenetic relationships, but their morphological diversity remains largely unexplored. Despite being such a taxonomically and ecologically diverse clade, their adaptive character has not been explicitly tested. Here, we use three-dimensional geometric morphometrics to characterise skull shape in Australian agamids and their Asian agamid relatives (Draconinae), and investigate the association between skull shape and ecological life habit. We find that in addition to phylogenetic affinity and evolutionary allometry, ecological factors play a major role in skull shape evolution of this clade, confirming their adaptive character. Through our evaluation of the cranial morphospace we find common themes of ecomorphology, where tree-dwelling species have long skulls and snouts, terrestrial species have short, blunt skulls, and saxicolous species have dorsoventrally flat skulls. These characteristics likely result from trade-offs to optimise functional capabilities, which often play a role in the evolution of skull shape.

Key words: adaptive, Agamidae, geometric morphometrics, lizards, phylomorphospace, skull

Introduction

A major aim of the discipline of evolutionary biology is to understand the processes underlying different patterns of morphological diversification, and one fascinating aspect of morphological diversity lies in adaptive radiation. The process of adaptive radiation involves "the rapid evolution of morphologically and ecologically diverse species from a single ancestor" (Osborn, 1902; Schluter, 2000). A fundamental concept in adaptive radiation is "ecological opportunity", where certain conditions allow rapid speciation through adaptation to different niches (Losos and Mahler, 2010). Rapid speciation can result from factors such as new resources, freedom from competition, and an absence of predators and pathogens. Consequently, adaptive radiations are often linked to particular events, such as a clade invading a new geographic area or environment (Lovette et al., 2002), or following a major extinction event (Jarvis et al., 2014). For adaptive radiations of animals, one of their defining characters is a diversity of morphological forms that are functionally associated with the use of different types of resources following the invasion of a range of vacant niches (Cooper et al., 2010; Monteiro and Nogueira, 2010; Dumont et al., 2011; Jønsson et al., 2012; Sanger et al., 2012; Wilson et al., 2012).

It has been hypothesised that island adaptive radiations represent a release from competition or a reduction in predation, and hence produce greater morphological and ecological diversity when compared to mainland radiations (Carlquist, 1974; Losos and Ricklefs, 2009). Australia is a unique case: although considered an island, because it is isolated and surrounded by sea, it is also a large continent. To explain the drivers behind Australian evolutionary radiations, it is important to consider the particular conditions that a clade's ancestor was presented with upon its arrival and subsequent diversification. There are two factors that highlight the potential for Australia to have presented an invading clade with ecological opportunity (Schluter, 2000). Firstly, up until 30 million years ago (Ma), Australia was likely deficient of almost all of the major squamate (lizards and snakes) clades (Oliver and Hugall, 2017), which potentially provided squamate invaders with a release from competition. Secondly, around 20 Ma, global climate change began (Fujioka et al., 2009; Fujioka and Chappell, 2010), which potentially opened up empty niches for invaders. These environmental circumstances suggest that Australia would have presented arriving ancestors of Australian radiations with the ecological opportunities that would facilitate adaptive radiation.

Dated molecular phylogenies show that the deepest divergences of Australian arid-adapted squamate taxa evolved from mesic-adapted ancestors around the same time that aridification began, and it is likely that these lineages were the result of oceanic dispersal from

proximal southern Asia (Oliver and Hugall, 2017). Inferred palaeoclimate trends suggest an extensive warm mesic environment in Australia at around 25-16 Ma, followed by fragmentation via aridification from around 15 Ma, and inland desertification since 7 Ma (Fujioka et al., 2005; Fujioka et al., 2009; Fujioka and Chappell, 2010). Rapid speciation within the arid zone is temporally consistent with the onset of aridification (Melville et al., 2001; Byrne et al., 2008; Shoo et al., 2008). Today, squamates make up the most taxonomically diverse constituent of the Australian vertebrate fauna and are distributed across the entire continent.

Amphibolurines (Agamidae) are a speciose (approximately 108 species) group of Australian lizards, with a relatively well-understood phylogeny (Hugall et al., 2008; Melville et al., 2011; Pyron et al., 2013). The group of taxa that are least nested (cf. Sereno, 1999), herein referred to as the "LN group", branched off outside the major furcation of the amphibolurine clade and includes a handful of rainforest adapted and semi-aquatic species, as well as the iconic thorny devil, *Moloch horridus* (Hugall et al., 2008). The second clade, comprises *Intellagama* plus a monophyletic grouping of the remaining amphibolurine species. This diverse clade is divided into two further clades that make up the core of the amphibolurine radiation: the *"Ctenophorus* group" and the "*Amphibolurus* group" (of Hugall et al., 2008). The *Ctenophorus* group is comprised of a single speciose genus (29 species), found throughout most of Australia and comprised of predominantly small, terrestrial dragons. The *Amphibolurus* group comprises ten genera comprised of different numbers of species, and, includes both semi-arboreal and terrestrial dragons. Generic diversity ranges from genera that contain a single species (e.g. *Rankinia*), to the much more speciose *Diporiphora* (22 species).

Amphibolurines are ecologically diverse and have adapted to life on and off the ground, inhabiting burrows, soil, grass, rocks, stumps, shrubs, and trees (Pianka and Pianka, 1970; Pianka, 1971; Collar et al., 2010; Pianka, 2013c, 2013b, 2013a, 2014). They have also developed many strategies for evading predators and catching prey, including speed (Cogger, 2014), crypsis (Shoo et al., 2008), defensive displays (Throckmorton et al., 1985; Shine, 1990), and spines (Pianka and Pianka, 1970). A detailed interspecific examination of variation in amphibolurine cranial morphology in an ecological context has yet to be attempted. Additionally, though considered to be an ecologically and evolutionarily successful group, their potential to be defined as an "adaptive radiation" has not yet been explicitly investigated.

The term "adaptive radiation" is given to clades that exhibit exceptional ecological and phenotypic disparity (Losos and Mahler, 2010). The main aim of this paper is to characterise the morphological diversity in the amphibolurines, and investigate whether it matches patterns

expected from the ecological process of adaptive radiation (Ricklefs, 2004; Gavrilets and Losos, 2009). We use three-dimensional geometric morphometrics to characterise cranial shape in a dataset of 52 species of agamid lizards, representing the broad range of phylogenetic and morphological diversity of Australian agamid lizards and their Asian sister clade (Draconinae). In an adaptive radiation, ecological factors play a key role in evolution, and therefore skull morphology should be significantly linked to adaptive ecology and ecological groups should be found in association in morphospace (Clabaut et al., 2007). We map the current phylogeny into the morphospace to infer aspects of the evolutionary history of cranial shape, using the phylomorphospace approach (sensu Sidlauskas, 2008). We perform statistical analyses that enable us to assess the adaptive character of this radiation of lizards, and consider the potential for particular skull shapes to be beneficial for adapting to different ecological zones.

Material and methods

Study samples

We sampled 52 individuals — both intact, alcohol preserved specimens and dry skeletal skull specimens — representing 52 species from the lizard family Agamidae: 44 from the Australian clade, Amphibolurinae, and eight from its Asian sister clade, Draconinae. Specimens were sampled primarily from the herpetology collection at South Australian Museum, Adelaide, and supplemented by loans from the Australian Museum in Sydney (see supplementary material: Table S5.1, for specimen information). Sampling included at least one representative from each currently recognised amphibolurine genus except *Cryptagama*. Draconinae species were sampled to represent the morphological variation observed in the group. All specimens were adults, as identified by a complete acrodont tooth row (Cooper et al., 1970).

Phylogeny

To infer the phylogenetic tree (Fig. 5.1) we used a combination of the most recent relevant phylogenetic studies (Melville et al., 2001; Hugall et al., 2008; Shoo et al., 2008; Melville et al., 2011; Pyron et al., 2013; Melville et al., 2014). We built a topological synthesis (i.e. without branch lengths) of well supported phylogenetic relationships using Mesquite v 3.51 (Maddison and Maddison, 2018). Branch lengths were subsequently estimated using the *ape* R package (Popescu et al., 2012) function "compute.brlen"*,* which uses the Grafen (1989) computation method. We defined and examined five major monophyletic clades in our data set: the Draconinae; the least nested (LN) group; *Intellagama*; the *Amphibolurus* group; and the *Ctenophorus* group.

Ecological categories

Life habit categorisations for species were based in information available in Wilson and Swan (2013), Cogger (2014), Grismer (2011), Kaiser et al. (2011), Somaweera and Somaweera (2009), and Jansen and Bopage (2011):

Arboreal: Primarily observed in trees and rarely on the ground.

Semi-arboreal: Observed spending considerable time on the ground and in trees or shrubs.

Terrestrial: Primarily observed on the ground, may use or dig burrows.

Saxicolous: Primarily confined to rocky ranges and outcrops.
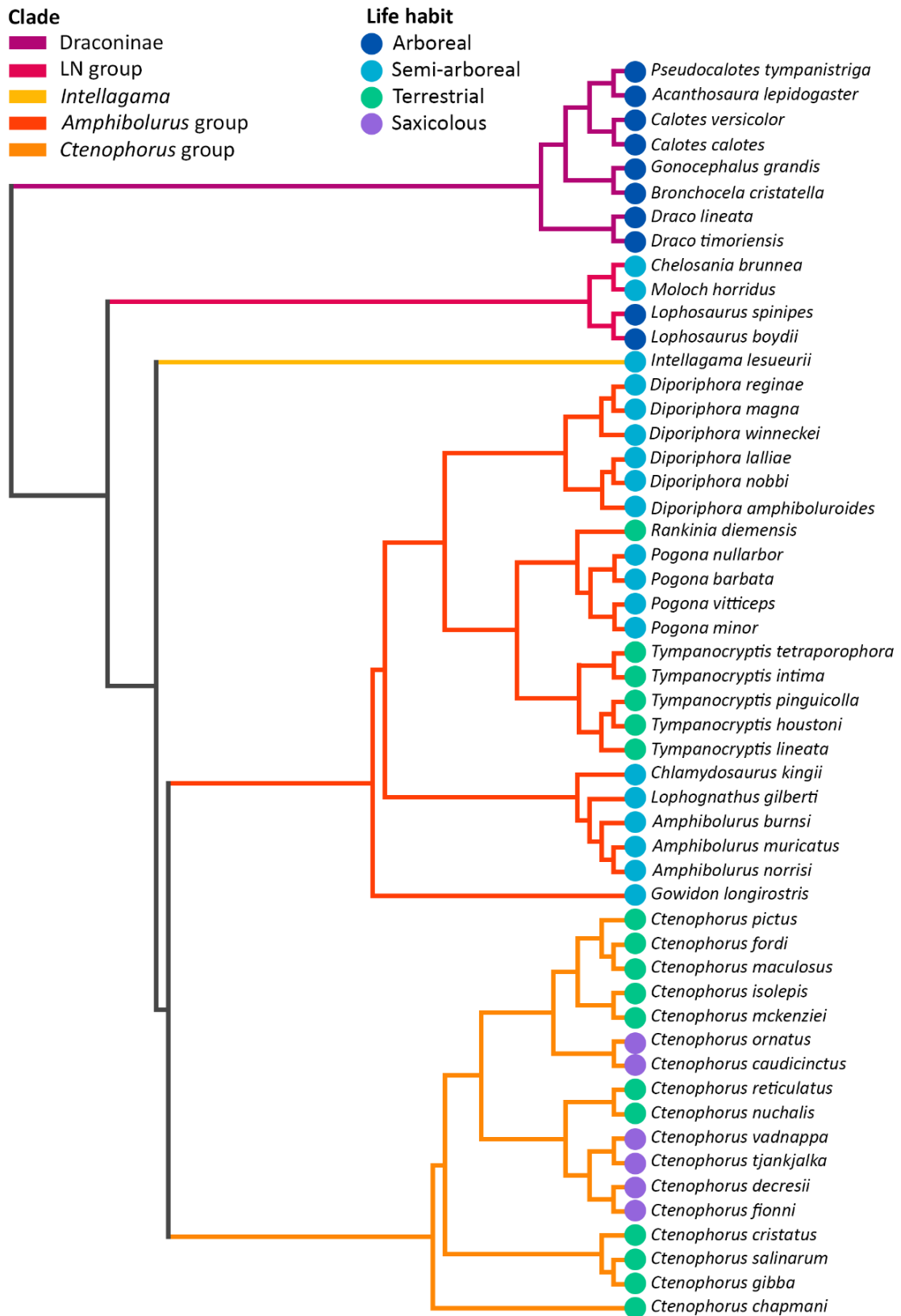
Figure 5.1 – Evolutionary tree of the agamid species studied here, inferred from multiple sources of recent phylogenetic studies, with coloured points to indicate life habits, and coloured tree branches to show the five major monophyletic clades. See "Phylogeny" section of "Materials and methods" for details.

X-ray computed tomography

To obtain digital reconstructions of skulls for measurement, we used high resolution X-ray micro computed tomography (CT) on the heads of whole specimens preserved in alcohol, and skeletal skull specimens. All CT scans were made with the Skyscan 1076 system at Adelaide Microscopy, at the University of Adelaide. Specimens were scanned with a voxel size of either 8 or 16 microns, dependent on the size of the specimen, with an appropriate range of X-ray settings including a current range of 100-250 µA, and a voltage range of 36-82 kV. An aluminium (0.5 mm) filter was used for all scans. CT scan data was reconstructed using Bruker Nrecon software v 6.6.9.4 (Skyscan, 2011). Crania were digitally segmented by applying a threshold for bone and extracted as 3D volumes using Avizo v 9.0 (Visualization Sciences Group, 2013). We digitally removed non-cranial bony elements (lower jaws, hyoids, scleral ossicles, and vertebrae), and cranial material was converted into a 3D surface model (a triangular mesh of approximately one million faces).

Landmarking and shape analysis

To characterise cranial shape, we used 3D landmark based geometric morphometric methods (Bookstein, 1996; Dryden and Mardia, 1998; Klingenberg, 2010). We digitised 102 landmarks in 3D over each cranium model (Fig 5.2, see also supplementary material: Table S5.2, for landmark definitions), which represented the cranial shape and were placed at equivalent points on bones at sutures, and extremes and boundaries of curvature of major structures, using Landmark Editor v 3.0.6 (Wiley et al., 2007). To confirm that our landmark set was sufficient to capture the shape variation in our sampled species, we used the "lasec" function in the R package *laMBDA* (Watanabe, 2018) (landmark sampling curve in supplementary material: Fig. S5.1). Landmark data were subjected to generalised Procrustes alignment (GPA) and projection into tangent space using the R package *geomorph* v 3.0.6 (Adams et al., 2018). The Procrustes fit corrected for object asymmetry, and we extracted coordinates for the symmetric component of shape (Klingenberg et al., 2002). These Procrustes-aligned coordinates were used in subsequent analyses.
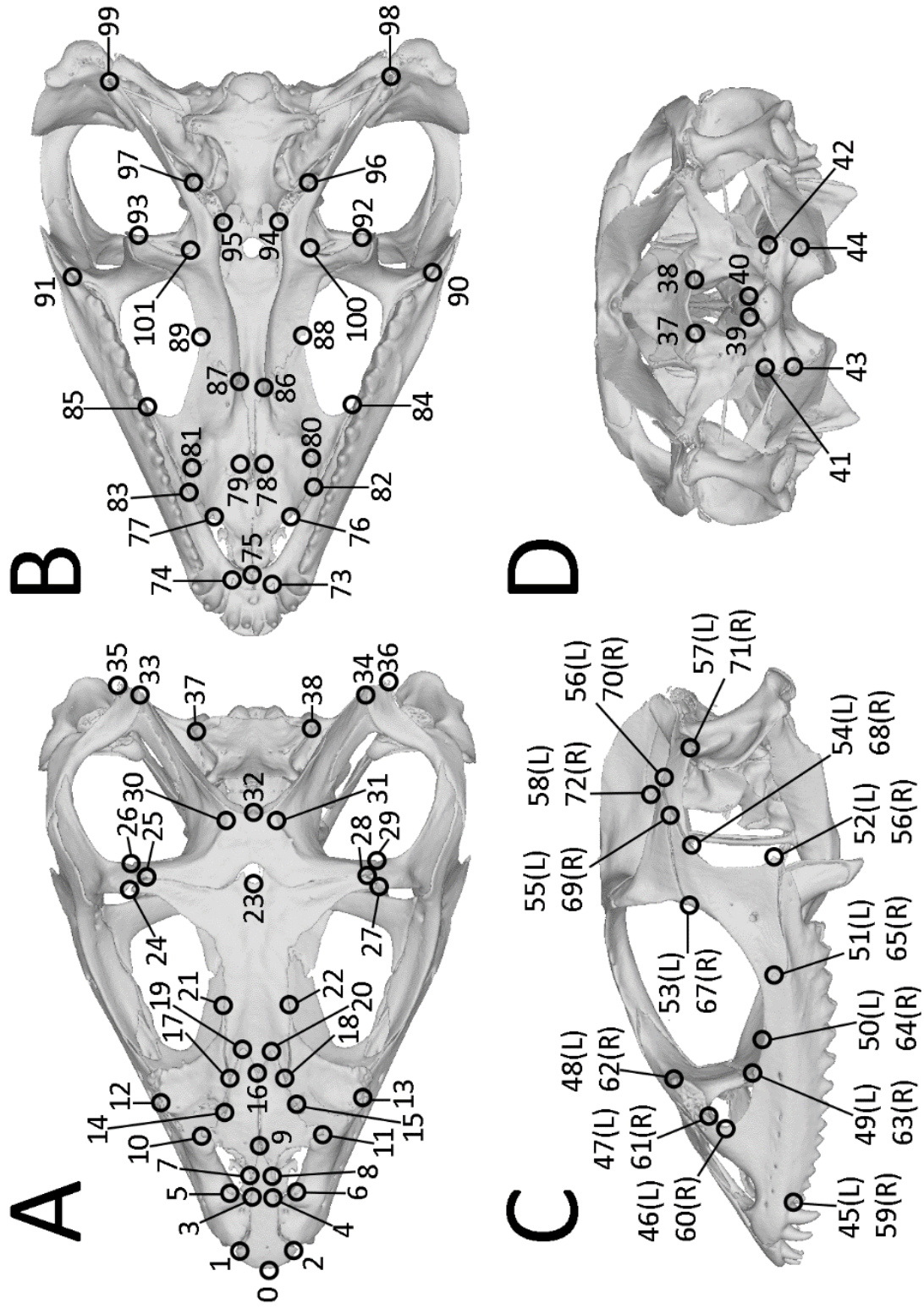
Figure 5.2 – Landmarks used to characterise cranial shape in 3D. Landmarks digitised on the cranium surface in dorsal view (A), palatal view (B) lateral view (C), and posterior view (D). Numbers are based on scheme used in IDAV Landmark Editor, and can be matched to definitions in supplementary material: Table S5.2.

Effect of phylogeny, evolutionary allometry, and life habit on skull shape

To recognise the degree to which variation in cranial shape among the sampled agamid species is evolutionarily associated with size variation (evolutionary allometry, see Klingenberg, 1996) and ecology, we performed a phylogenetic generalised least-squares (PGLS) analysis of shape on log transformed size and life habit while accounting for the phylogenetic relationships among agamid species, using the "procD.pgls" function in *geomorph*. The "procD.pgls" function performed 1000 permutations of shape data across the tips of the tree, and estimates were compared to observed values to assess significance (Adams and Collyer, 2018). Centroid size (a measure of size extracted from the landmarks) was used to represent head size (Dryden and Mardia, 1998). To visualise evolutionary allometry, we carried out a multivariate regression of shape on size using "procD.pgls" function, plotted the shape variation attributed to size as the regression score (Drake and Klingenberg, 2008), and identified the points by life habit and phylogenetic group. To illustrate the shape differences associated with the minimum and maximum skull sizes, we used to "plotRefToTarget" function in *geomorph* to warp a mesh representing the mean specimen to shapes representing the smallest and largest skulls in the data set.

We used the allometry corrected skull shape data for agamid specimens to examine the variation not associated with evolutionary allometry. To obtain allometry corrected shape data, we used a multivariate adaptation of phylogenetic size correction methods (Klingenberg, 2016). To obtain allometry corrected shape variables for each specimen, we performed a regression of shape on size using "procD.pgls", which computed the regression residuals for the cranial shape of each species, and these were added to the original shape variables. To examine phylogenetic structure in the cranial morphospace, we performed a principal component analysis (PCA) and generated a cranial morphospace by plotting the main axes of shape variation (see supplementary material: Fig. S5.2 for PCA before allometry correction). We projected the phylogeny into the cranial morphospace by calculating ancestral states of the internal nodes by maximum likelihood, using the "phylomorphospace" function in the R package *phytools* (Revell, 2012). To evaluate the degree of phylogenetic signal present in the shape and size variables relative to expectations under a Brownian motion model of evolution, we used the "physignal" function in geomorph, which uses K_{mult}, a mathematical generalisation of the K statistic (Blomberg et al., 2003) for highly multivariate data (Adams, 2014). Significance was tested for by 1000 permutations of data among the tips of the phylogenetic tree.

To examine the distribution of monophyletic clades in the cranial morphospace, we identified points in the cranial morphospace by their monophyletic clade (see Fig. 5.1). To assess whether the two most speciose clades of the Amphibolurinae, the *Ctenophorus* group and the *Amphibolurus* group (core of the Australian radiation), were different from one another in terms of their morphological disparity, we used the "morphol.disparity" function in geomorph, which calculates the Procrustes variance of each group, using residuals of a linear model fit (Zelditch et al., 2012). Significance was evaluated by 1000 permutations, where vectors of residuals were randomised among the two groups.

To observe and describe the shape differences associated with the main axes of variation in the allometry corrected shape variables, we used to "plotRefToTarget" function in *geomorph* to warp a mesh representing the mean shape to shapes representing the minimum and maximum values for the first four principal components (PCs).

Results

A PGLS model evaluating the influence of cranial size and ecology on cranial shape (see Table 5.1) revealed that 11% of the total variance of shape is significantly associated with size variation ($P = 0.001$), and 14% of the total variance of shape is significantly associated with life habit ($P = 0.001$). Life habit categories were partitioned along the allometric trajectory, which was represented by log transformed centroid size versus regression score (Fig. 5.3A). Relative to the mean shape, greater cranium size is associated with: a longer and dorsoventrally shallower snout; broader and more robust postorbitals and temporal bars (jugals, postorbits); larger and longer supratemporal fenestra; smaller orbits; dorsoventrally straighter tooth rows; a broader anterior end to the frontal; and a more anteriorly located braincase. Smaller cranium size is associated with: a shorter and more rounded snout; more slender and narrower postorbitals and temporal bars; smaller and shorter upper temporal fenestra; larger orbits; more dorsoventrally curved tooth rows; a narrower anterior end to the frontal; and a more posteriorly located braincase (see Fig. 5.3B).

The PCA of allometry corrected shape variables revealed that most of the shape variation among species is concentrated in four dimensions (out of 52, see supplementary material: Table S5.3 for summary of first six PCs) with subsequent PCs each contributing small amounts (<5%). The phylogenetic signal is very low in both cranial shape and size of the sampled agamid lizards (shape: $P = 0.001$, $K_{mult} = 0.112$; size: $P = 0.001$, $K_{mult} = 0.1786$), well below expectations of a Brownian motion model of evolution. These results, and the many crisscrossing branches in the phylomorphospace (see Fig. 5.4) show that there is substantial homoplasy in cranial shape of the sampled agamids. The four ecological life habit categories used in this study were associated with particular areas of the cranial morphospace (Fig. 5.4). Arboreal species occupy an almost exclusive area of morphospace representing negative PC1 values. Semi-arboreal species occupy a large area in the centre of the morphospace, and overlap with terrestrial and saxicolous species of dragons. Terrestrial species largely overlap with semi-arboreal species, but also extend into their own area of morphospace, associated with high values of PC1 and PC2. Saxicolous species overlap a little with semi-arboreal and terrestrial species, but mostly occupy their own area of the morphospace, associated with high PC1 values and low PC2 values.
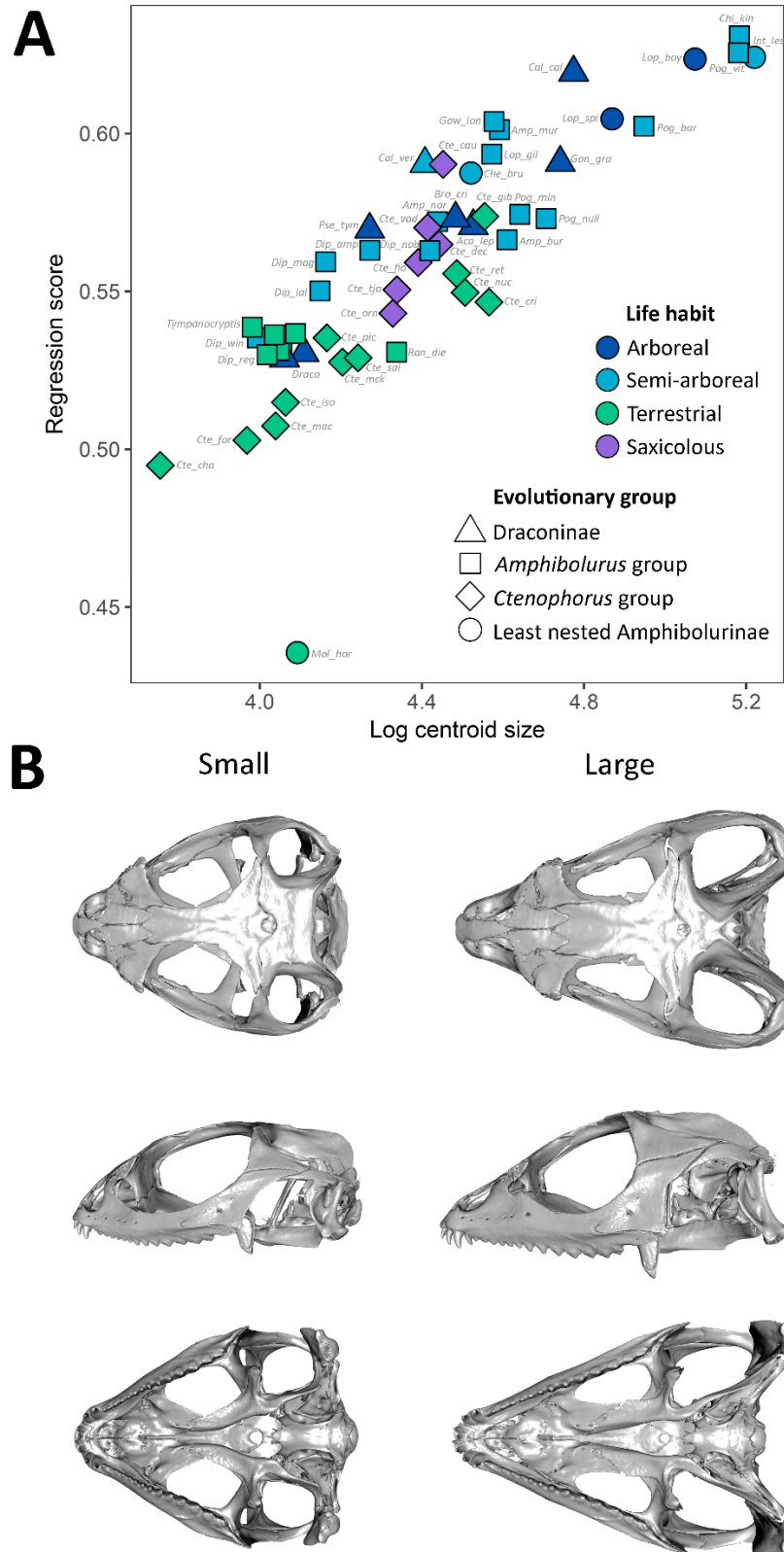
Figure 5.3 – Evolutionary allometry of the sampled agamid crania. In A, evolutionary allometry was examined by a multivariate regression of shape on log transformed centroid size. In B, warped surfaces represent shapes of the largest and smallest sampled crania.
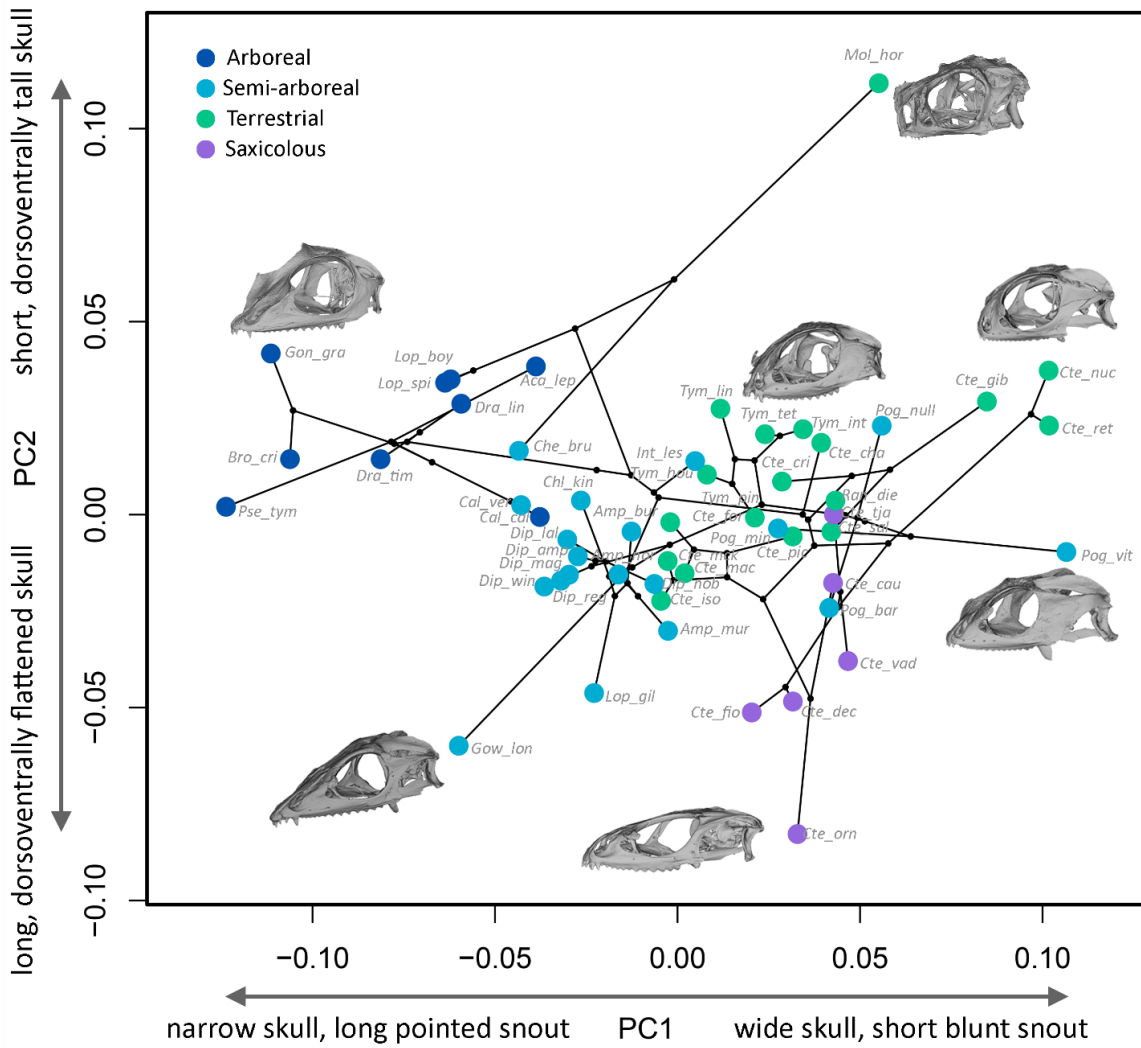
Figure 5.4 – Phylomorphospace illustrating the distribution of life habit groups in the allometry corrected cranial morphospace. Skull images are meshes of cranium specimens that represent extremes of shape variation.

Table 5.1 – Examining evolutionary allometry: results table for the PGLS model of cranial shape by size and life habit (shape ~ log (size) * life habit). The effect of centroid size and ecological life habit on cranial shapes within the 52 sampled species of agamid as evaluated by a phylogenetic least squares model (details in methods). Statistical significance was evaluated by permutation using 1000 iterations. Bold indicates *P*-values of less than 0.05.

	DF	SS	MS	R^2	F	Z	*P*-value
Log (size)	1	0.728	0.729	0.112	7.704	5.520	**0.001**
Habit	3	1.073	0.358	0.165	3.782	5.462	**0.001**
Log (size) : life habit	3	0.543	0.181	0.084	1.916	4.960	**0.001**
Residuals	44	4.160	0.095	0.640			
Total	51	6.505					
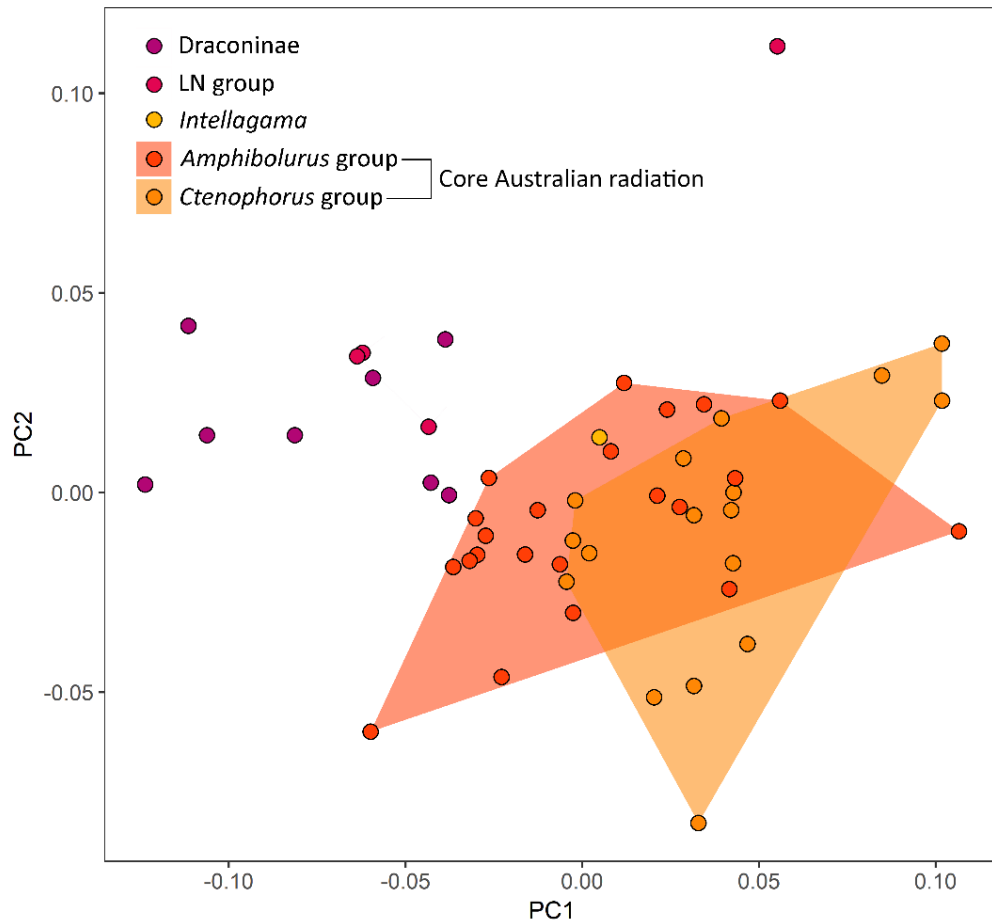
Figure 5.5 – Allometry corrected cranial morphospace illustrating the distribution of monophyletic clades, with convex hulls mapped on to represent the disparity of the two core lineages of the Amphibolurinae, the *Amphibolurus* **group and the** *Ctenophorus* **group.**

While there is no clear association between clade affiliation and evolutionary allometry (see Fig. 5.3A), the five clades seem to be associated with particular areas of the allometry corrected cranial morphospace. Draconines and the LN group mostly occupy the same corner of the morphospace (apart from *M. horridus*), at low PC1 values and high PC2 values, but are separate from each other within this area, with the LN group having lower PC1 values. The core of the amphibolurine radiation (*Ctenophorus* group and *Amphibolurus* group) occupy the opposite side of the morphospace, and the two groups overlap substantially with one another. The morphological disparity (Procrustes variance) of the *Amphibolurus* group and the *Ctenophorus* group are not significantly different from one another ($P = 0.856$), and they overlap considerably along the main axes of shape variation (see Fig. 5.5). Both groups also expand into their own exclusive areas of the cranial morphospace. PC1 describes major differences between draconines and amphibolurines. PC2 did not separate out particular taxonomic clades, but describes the major differences between *Moloch*, and the rest of the sample.

Shapes differences associated with the major PCs of the allometry corrected shape data can be observed in Figure 5.6. PC1 describes 33.33% of the total shape variation. Low PC1 scores represent a relatively long, narrow, and posteriorly rounded skull with a rounded orbit, whereas high PC1 scores represent a relatively short, wide, and posteriorly angular skull with a dorsoventrally compressed orbit. This axis also describes differences between a dorsoventrally straight tooth row (high values), and one that curves dorsally at its anterior end (low values). PC2 describes 11.66% of the total variation. Low PC2 scores represent a dorsoventrally shallow and elongate skull whereas high PC2 scores represent a short, dorsoventrally deep skull with an extremely blunt snout.
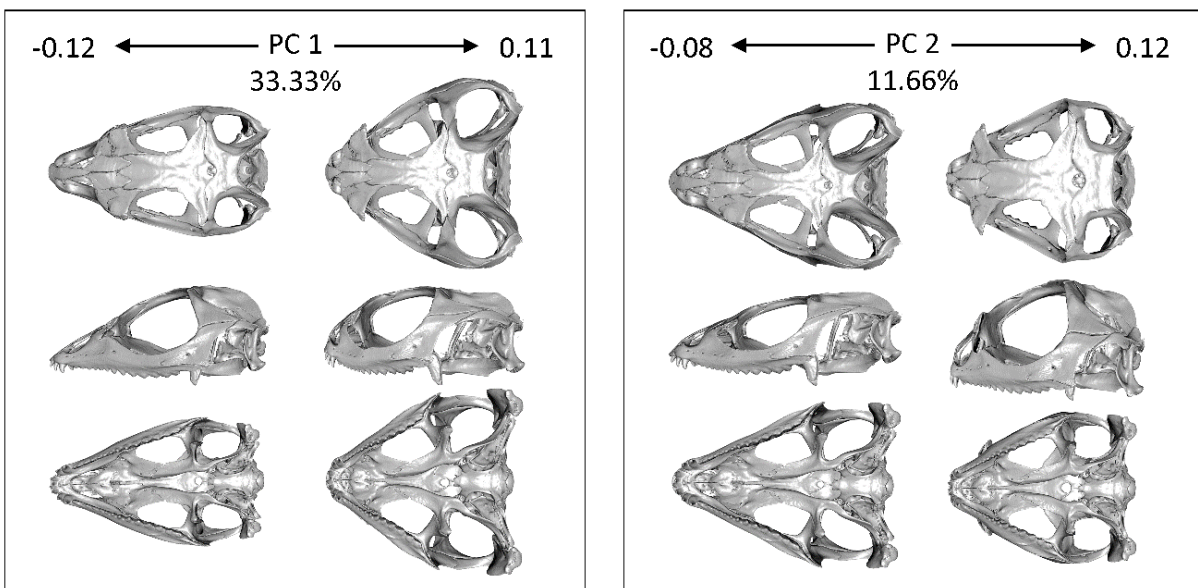
Figure 5.6 – The major axes of variation in cranial shape (from a PCA corrected for evolutionary allometry), shown as warped cranial surfaces. Cranial shape differences associated with the PCs are shown as shapes representing the positive and negative end of each axis.

Discussion

Australia, with its vast array of different habitats and biomes, is a fascinating place in which to explore the drivers of evolutionary radiation. We set out to do this using the Australian radiation of agamid lizards. Broadly, adaptive radiation can be defined as the evolution of ecological and phenotypic diversity in a rapidly multiplying lineage (Schluter, 2000). According to Schluter (2000), descendant species fit the "adaptive" criteria if there is an association between diverse phenotypes and their divergent environments. We explored the phenotypic variation in crania of Australian radiation of agamid lizards, and revealed that ancestral amphibolurines gave rise to new clades that today exhibit a morphologically diverse array of skull shapes. However, the pattern of morphological variation within the sampled agamid skulls is not closely tied to phylogenetic relatedness. Instead, species with the same life habits share morphological features and occur in association in the cranial morphospace, even when they are not each other's closest relatives. This emphasises the adaptive character of these lizards, and suggests they are strong contender to be considered an "adaptive radiation".

There is surprisingly little phylogenetic signal in skull shape among the sampled agamids. A lack of distinct phylogenetic structure is evident from the criss-crossing patterns of branches within amphibolurine genera, and extensive overlap of branches within the cranial morphospace. The range of potential skull shapes seems to be constrained to a particular region of morphospace, but within this space, evolution is relatively free and labile, which is similar to what has been seen in species of bird (Tokita et al., 2017), mammal (Goswami et al., 2014), and fish (Clabaut et al., 2007). To describe a similar pattern, Goswami et al. (2014) used the analogy of a fly trapped within a tube. We suggest evolution of the sampled agamid lizards is more analogous to a fly in a deflated balloon, as there seems to be some flexibility around the peripheral areas of the occupied morphospace. This flexibility allows the evolution of more extreme skull shapes for particular ecological groups, e.g. the very dorsoventrally flat skulls of rock dwellers, and the blunt-faced forms seen in some terrestrial species (that also happen to be burrowers: see Cogger, 2014). The patterns we observe in the cranial morphospace indicate that multiple cases of convergent and parallel evolution, and rapid morphological diversification exist in the Australian agamid lizard clade, and deserve further attention. This capacity to rapidly evolve a variety of different phenotypes appears to have led to a greater potential to exploit their respective environments (Vermeij, 1973).

If shared evolutionary history is not the main factor influencing similarities in the skull shapes among amphibolurine lizards, then the parallel and convergent evolution we observe in

this clade is probably the result of equivalent ecological conditions (Sturmbauer et al., 2003). Australian agamid skulls are distributed in the morphospace according to their life habit, and statistical tests confirmed that particular skull shapes are similar because of shared ecological characteristics. Our study adds to the growing body of literature showing that ecological role frequently overrides phylogenetic inheritance on a macroevolutionary scale (Clabaut et al., 2007; Pierce et al., 2008; Kimmel et al., 2009; Stayton, 2011; Sakamoto and Ruta, 2012; Casanovas-Vilar and van Dam, 2013; Klingenberg and Marugán-Lobón, 2013). It seems clear that ecological opportunity can be a powerful driver of morphological diversification, but it is also increasingly apparent that the morphological variation in any given clade is a consequence of the combination and interaction of several factors. Allometry, phylogeny, ecology, and development are all factors that determine morphological diversity, but which factors have the greatest influence over morphological variation, and to what extent, differs amongst clades.

The strong association between distribution of species in the cranial morphospace and ecological life habit indicates divergent selection for agamid lizards with different ecological life habits. Since selection acts, not directly on phenotypes, but on the functional capabilities of those phenotypes (Arnold, 1983; Garland and Losos, 1994) it is likely that homoplastic aspects of skull shape represent important functional aspects for life habit strategies. For example, the length of the snout has an effect on the length of the out-lever, and consequently, an effect on bite force (Olson, 1961). Although an elongate snout is therefore associated with a reduced bite force, there is also evidence that longer snouts can enhance capture efficiency of highly mobile prey (Kohlsdorf et al., 2008). Furthermore, having a taller head may indicate a further trade-off between greater bite forces (associated with taller heads), and faster climbing speeds (associated with flatter heads) (Herrel et al., 1999; Herrel et al., 2001). Our results indicate that ecological trade-offs have occurred in order to optimise function in different habitats, and this is likely to be a major factor that has shaped the evolution of skull shape in Australia's agamid lizard radiation.

Our study brings the adaptive character of amphibolurine lizards to light, even though specific interpretations are difficult, with various ecological parameters acting concurrently on the evolution of skull shape. In reality, life habit for these lizards may be considered a continuum, with various species displaying different extents of their assigned category. Our categories are a simplification of life history but this issue reflects the problem of characterising animals that live in complex environments for which field data remains lacking. This system would benefit from an in-depth ecological assessment akin to the perch height and diameter information of Caribbean lizard habitats (Losos, 1990). A more detailed examination of the

relationship between life history and skull shape may be possible in the future following further field research. There remains a lot to be gained from studying this system in more detail, including more in-depth ecological assessments, and exploratory investigation of the anatomy and function underlying the different skull shapes characterised here. Furthermore, similar work investigating the morphological diversification of other Australian squamate clades that are estimated to have arrived around a similar time would broaden our understanding of whether environmental change on the large, squamate-poor, island continent of Australia, may have facilitated adaptive radiation.

Conclusions

Our study uncovered the major patterns of morphological variation in amphibolurine lizards, and revealed that the constraint of phylogeny on the Australian radiation of agamid lizards is small. In contrast, the evolution of a broad array of different skull shapes has been notably impacted by ecological life habit, as can be expected for an "adaptive radiation" (Schluter, 2000). We suggest that a combination of evolutionary lability and ecological opportunity, presented to the ancestral agamid upon its arrival to Australia, and subsequent environmental changes, has culminated in a radiation of lizards that may indeed be considered "adaptive".

Supplementary material

Electronic files

File ES5.1 – Folder containing 3D ply models of cranial surfaces used for landmarking (file folder).

File ES5.2 – 3D landmark coordinates used in analyses (DTA).

File ES5.3 – Nexus tree used to plot phylomorphospace (NEX).

References

Adams DC. 2014. A generalized K statistic for estimating phylogenetic signal from shape and other high dimensional multivariate data. Syst Biol 63:685-697.

Adams DC, Collyer ML. 2018. Multivariate phylogenetic comparative methods: evaluations, comparisons, and recommendations. Syst Biol 67:14-31.

Adams DC, Collyer ML, Kaliontzopoulou. 2018. geomorph: software for geometric morphometric analyses. R package version 3.0.6. https://CRANR-projectorg/package=geomorph.

Arnold SJ. 1983. Morphology, performance and fitness. Amer Zool 23:347-361.

Blomberg SP, Garland TJ, Ives AR. 2003. Testing for phylogenetic signal in comparative data: behavioural traits are more labile. Evolution 57:717-745.

Bookstein FL. 1996. Biometrics, biomathematics and the morphometric synthesis. Bull Math Biol 58:313.

Byrne M, Yeates DK, Joseph L, Kearney M, Bowler J, Williams MAJ, Cooper S, Donnellan SC, Keogh JS, Leys R, Melville J, Murphy DJ, Porch N, Wyrwoll KH. 2008. Birth of a biome: insights into the assembly and maintenance of the Australian arid zone biota. Mol Ecol 17:4398-4417.

Carlquist S. 1974. Island biology. New York & London: Columbia University Press.

Casanovas-Vilar I, van Dam J. 2013. Conservatism and adaptability during squirrel radiation: what is mandible shape telling us? PLOS ONE 8:e61298.

Clabaut C, Bunje PME, Salzburger W, Meyer A. 2007. Geometric morphometric analyses provide evidence for the adaptive character of the tanganyikan cichlid fish radiations. Evolution 61:560-578.

Cogger H. 2014. Reptiles and amphibians of Australia, 7th ed. Collingwood: CSIRO Publishing.

Collar DC, Schulte JA, O'Meara BC, Losos JB. 2010. Habitat use affects morphological diversification in dragon lizards. J Evol Biol 23:1033-1049.

Cooper JS, Poole DFG, Lawson R. 1970. The dentition of agamid lizards with special reference to tooth replacement. J Zool 162:85-98.

Cooper WJ, Parsons K, McIntyre A, Kern B, McGee-Moore A, Albertson RC. 2010. Bentho-pelagic divergence of cichlid feeding architecture was prodigious and consistent during multiple adaptive radiations within African rift-lakes. PLOS ONE 5:e9551.

Drake AG, Klingenberg CP. 2008. The pace of morphological change: historical transformation of skull shape in St Bernard dogs. Proc R Soc B 275:71-76.

Dryden I, Mardia K. 1998. Statistical shape analysis. John Wiley & Sons.

Dumont ER, Dávalos LM, Goldberg A, Santana SE, Rex K, Voigt CC. 2011. Morphological innovation, diversification and invasion of a new adaptive zone. Proc R Soc B 279:1797-1805.

Fujioka T, Chappell J. 2010. History of Australian aridity: chronology in the evolution of arid landscapes. Geol Soc, Special Publications 346:121-139.

Fujioka T, Chappell J, Fifield LK, Rhodes EJ. 2009. Australian desert dune fields initiated with Pliocene–Pleistocene global climatic shift. Geology 37:51-54.

Fujioka T, Chappell J, Honda M, Yatsevich I, Fifield LK, Fabel D. 2005. Global cooling initiated stony deserts in central Australia 2–4 Ma, dated by cosmogenic 21Ne-10Be. Geology 33:993-996.

Garland TJ, Losos JB. 1994. Ecological morphology of locomotor performance in squamate reptiles. In: Wainwright PC, Reilly SM, editors. Ecological morphology: integrative organismal biology. Chicago & London: The University of Chicago Press. p 240-302.

Gavrilets S, Losos JB. 2009. Adaptive radiation: contrasting theory with data. Science 323:732-737.

Goswami A, Smaers JB, Soligo C, Polly PD. 2014. The macroevolutionary consequences of phenotypic integration: from development to deep time. Phil Trans R Soc B 369:20130254.

Grafen A. 1989. The phylogenetic regression. Phil Trans R Soc B 326:119-157.

Grismer LL. 2011. Lizards of Peninsular Malaysia, Singapore and their adjacent archipelagos. Germany: Edition Chaimera.

Herrel A, Aerts P, Fret J, de Vree F. 1999. Morphology of the feeding system in agamid lizards: ecological correlates. Anat Rec 254:496-507.

Herrel A, Damme RV, Vanhooydonck B, Vree FD. 2001. The implications of bite performance for diet in two species of lacertid lizards. Can J Zoology 79:662-670.

Hugall AF, Foster R, Hutchinson M, Lee MSY. 2008. Phylogeny of Australian agamid lizards based on nuclear and mitchondrial genes: implications for morphological evolution and biogeography. Biol J Linnean Soc 93:343-358.

Jansen P, Bopage M. 2011. The herpetofauna of a small and unprotected patch of tropical rainforest in Morningside, Sri Lanka. Amphib Reptile Conserv 5:1-13.

Jarvis ED, Mirarab S, Aberer AJ, Li B, Houde P, Li C, Ho SYW, Faircloth BC, Nabholz B, Howard JT, Suh A, Weber CC, da Fonseca RR, Li J, Zhang F, Li H, Zhou L, Narula N, Liu L, Ganapathy G, Boussau B, Bayzid MS, Zavidovych V, Subramanian S, Gabaldón T, Capella-Gutiérrez S, Huerta-Cepas J, Rekepalli B, Munch K, Schierup M, Lindow B, Warren WC, Ray D, Green RE, Bruford MW, Zhan X, Dixon A, Li S, Li N, Huang Y, Derryberry EP, Bertelsen MF, Sheldon FH, Brumfield RT, Mello CV, Lovell PV, Wirthlin M, Schneider MPC, Prosdocimi F, Samaniego JA, Velazquez AMV, Alfaro-Núñez A, Campos PF, Petersen B, Sicheritz-Ponten T, Pas A, Bailey T, Scofield P, Bunce M, Lambert DM, Zhou Q, Perelman P, Driskell AC, Shapiro B, Xiong Z, Zeng Y, Liu S, Li Z, Liu B, Wu K, Xiao J, Yinqi X, Zheng Q, Zhang Y, Yang H, Wang J, Smeds L, Rheindt FE, Braun M, Fjeldsa J, Orlando L, Barker FK, Jønsson KA, Johnson W, Koepfli K-P, O'Brien S, Haussler D, Ryder OA, Rahbek C, Willerslev E, Graves GR, Glenn TC, McCormack J, Burt D, Ellegren H, Alström P, Edwards SV, Stamatakis A, Mindell DP, Cracraft J, Braun EL, Warnow T, Jun W, Gilbert MTP, Zhang G. 2014. Whole-genome analyses resolve early branches in the tree of life of modern birds. Science 346:1320-1331.

Jønsson KA, Fabre PH, Fritz SA, Etienne RS, Ricklefs RE, Jørgensen TB, Fjeldså J, Rahbek C, Ericson PGP, Woog F, Pasquet E, Irestedt M. 2012. Ecological and evolutionary determinants for the adaptive radiation of the Madagascan vangas. PNAS 109:6620-6625.

Kaiser H, Carvalho VL, Ceballos J, Freed P, Heacox S, Lester B, Richards SJ, Trainor CR, Sanchez C, O'Shea M. 2011. The herpetofauna of Timor-Leste: a first report. ZooKeys 109:19-86.

Kimmel CB, Sidlauskas B, Clack JA. 2009. Linked morphological changes during palate evolution in early tetrapods. J Anat 215:91-109.

Klingenberg CP. 1996. Multivariate allometry. In: Marcus LF, Corti M, Loy A, Naylor GJP, Slice DE, editors. Advances in Morphometrics. Boston: Springer US. p 23-49.

Klingenberg CP. 2010. Evolution and development of shape: integrating quantitative approaches. Nat Rev Genet 11:623-635.

Klingenberg CP. 2016. Size, shape, and form: concepts of allometry in geometric morphometrics. Dev Genes Evol 226:1-25.

Klingenberg CP, Barluenga M, Meyer A. 2002. Shape analysis of symmetric structures: quantifying variation among individuals and asymmetry. Evolution 56:1909-1920.

Klingenberg CP, Marugán-Lobón J. 2013. Evolutionary covariation in geometric morphometric data: analyzing integration, modularity, and allometry in a phylogenetic context. Syst Biol 62:591-610.

Kohlsdorf T, Grizante MB, Navas CA, Herrel A. 2008. Head shape evolution in Tropidurinae lizards: does locomotion constrain diet? J Evol Biol 21:781-790.

Losos JB. 1990. Ecomorphology, performance capability, and scaling of west Indian *Anolis* lizards: an evolutionary analysis. Ecol Monogr 60:369-388.

Losos JB, Mahler DL. 2010. Adaptive radiation: the interaction of ecological opportunity, adaptation, and speciation. In: Bell MA, Futuyma DJ, Eanes WF, Levinton JS, editors. Evolution since Darwin: the first 150 years. Sunderland: Sinauer Association. p 381-420.

Losos JB, Ricklefs RE. 2009. Adaptation and diversification on islands. Nature 457:830-836.

Lovette IJ, Bermingham E, Ricklefs RE. 2002. Clade-specific morphological diversification and adaptive radiation in Hawaiian songbirds. Proc R Soc B 269:37-42.

Maddison WP, Maddison DR. 2018. Mesquite: a modular system for evolutionary analysis. http://mesquiteprojectorg.

Melville J, Ritchie EG, Chapple SNJ, Glor RE, Schulte JA. 2011. Evolutionary origins and diversification of dragon lizards in Australia's tropical savannas. Mol Phylogenet Evol 58:257-270.

Melville J, Schulte JA, Larson A. 2001. A molecular phylogenetic study of ecological diversification in the Australian lizard genus *Ctenophorus*. J Exp Zool 291:339-353.

Melville J, Smith K, Hobson R, Hunjan S, Shoo L. 2014. The role of integrative taxonomy in the conservation management of cryptic species: the taxonomic status of endangered earless dragons (Agamidae: *Tympanocryptis*) in the grasslands of Queensland, Australia. PLOS ONE 9:e101847.

Monteiro LR, Nogueira MR. 2010. Adaptive radiation, ecological specialisation, and the evolutionary integration of complex morphological structures. Evolution 64:724-744.

Oliver PM, Hugall AF. 2017. Phylogenetic evidence for mid-Cenozoic turnover of a diverse continental biota. Nat Ecol Evol 1:1896.

Olson EC. 1961. Jaw mechanisms: rhipidistians, amphibians, reptiles. Amer Zool 1:205-215.

Osborn HF. 1902. The law of adaptive radiation. Am Nat 36:353-363.

Pianka ER. 1971. Ecology of the agamid lizard *Amphibolurus isolepis* in Western Australia. Copeia 1971:527-536.

Pianka ER. 2013a. Notes on the ecology and natural history of two uncommon arboreal agamid lizards *Diporiphora*. West Austral Nat 29:77-84.

Pianka ER. 2013b. Notes on the ecology and natural history of two uncommon terrestrial agamid lizards *Ctenophorus clayi* and *C. fordi* in the Great Victoria Desert of Western Australia. West Austral Nat 29:85-93.

Pianka ER. 2013c. Notes on the natural history of the rarely recorded agamid lizard *Caimanops amphiboluroides* in Western Australia. West Austral Nat 29:99-102.

Pianka ER. 2014. Notes on a collection of lizards from the Eucla sand dunes in Western Australia. West Austral Nat 30:155-161.

Pianka ER, Pianka HD. 1970. The ecology of *Moloch horridus* (Lacertilia: Agamidae) in Western Australia. Copeia 1970:90-103.

Pierce SE, Angielczyk KD, Rayfield EJ. 2008. Patterns of morphospace occupation and mechanical performance in extant crocodilian skulls: a combined geometric morphometric and finite element modeling approach. J Morphol 269:840-864.

Popescu AA, Huber KT, Paradis E. 2012. ape 3.0: new tools for distance-based phylogenetics and evolutionary analysis in R. Bioinformatics 28:1536-1537.

Pyron RA, Burbrink FT, Wiens JJ. 2013. A phylogeny and revised classification of Squamata, including 4161 species of lizards and snakes. BMC Evol Biol 13:1-53.

Revell LJ. 2012. phytools: an R package for phylogenetic comparative biology (and other things). Methods Ecol Evol 3:217-223.

Ricklefs RE. 2004. Cladogenesis and morphological diversification in passerine birds. Nature 430:338.

Sakamoto M, Ruta M. 2012. Convergence and divergence in the evolution of cat skulls: temporal and spatial patterns of morphological diversity. PLOS ONE 7:e39752.

Sanger TJ, Mahler DL, Abzhanov A, Losos JB. 2012. Roles for modularity and constraint in the evolution of cranial diversity among *Anolis* lizards. Evolution 66:1525-1542.

Schluter D. 2000. The ecology of adaptive radiation. New York: Oxford University Press.

Sereno PC. 1999. Definitions in phylogenetic taxonomy: critique and rationale. Syst Biol 48:329-351.

Shine R. 1990. Function and evolution of the frill of the frillneck lizard, *Chlamydosaurus kingii* (Sauria: Agamidae). Biol J Linnean Soc 40:11-20.

Shoo L, Rose R, Doughty P, Austin JJ, Melville J. 2008. Diversification of pebble-mimic dragons are consistent with historical disruption of important corridors in arid Australia. Mol Phylogenetics Evol 48:528-542.

Sidlauskas B. 2008. Continuous and arrested morphological diversification in sister clades of characiform fishes: a phylomorphospace approach. Evolution 62:3135-3156.

Skyscan. 2011. NRecon. Aartselaar, Belgium.

Somaweera R, Somaweera N. 2009. Lizards of Sri Lanka: a colour guide with field keys. Andreas S. Brahm.

Stayton CT. 2011. Biomechanics on the half shell: functional performance influences patterns of morphological variation in the emydid turtle carapace. Zoology 114:213-223.

Sturmbauer C, Hainz U, Baric S, Verheyen E, Salzburger W. 2003. Evolution of the tribe Tropheini from Lake Tanganyika: synchronized explosive speciation producing multiple evolutionary parallelism. Hydrobiologia 500:51-64.

Throckmorton GS, Bavay JD, Chaffey W, Merrotsy B, Noske S, Noske R. 1985. The mechanism of frill erection in the bearded dragon *Amphibolurus barbatus* with comments on the jacky lizard *A. muricatus* (Agamidae). J Morphol 183:285-292.

Tokita M, Yano W, James HF, Abzhanov A. 2017. Cranial shape evolution in adaptive radiations of birds: comparative morphometrics of Darwin's finches and Hawaiian honeycreepers. Phil Trans R Soc B 372:20150481.

Vermeij GJ. 1973. Adaptation, versatility, and evolution. Syst Biol 22:466-477.

Visualization Sciences Group. 2013. Avizo.

Watanabe A. 2018. How many landmarks are enough to characterize shape and size variation? PLOS ONE 13:e0198341.

Wiley D, Amenta N, Alcantara D, Ghosh D, Kil Y, Delson E. 2007. Landmark Editor: Institute for Data Analysis and Visualization. University of California, Davis.

Wilson GP, Evans AR, Corfe IJ, Smits PD, Fortelius M, Jernvall J. 2012. Adaptive radiation of multituberculate mammals before the extinction of dinosaurs. Nature 483:457-460.

Wilson S, Swan G. 2013. A complete guide to reptiles of Australia, 4th ed. Chatswood: New Holland Publishers.

Zelditch ML, Swiderski DL, Sheets HD, Fink WL. 2012. Geometric morphometrics for biologists: a primer, 2nd ed. Academic Press.

STATEMENT OF AUTHORSHIP

Title of Paper	The implications of using captive-bred specimens in intra-specific morphological analyses.
Publication Status	☐ Published ☐ Accepted for Publication ☐ Submitted for Publication ☑ Unpublished and Unsubmitted w ork w ritten in manuscript style
Publication Details	Prepared for submission to Biodiversity and Conservation

Principal Author

Name of Principal Author (Candidate)	Jaimi Gray		
Contribution to the Paper	Designed research, data collection and analysis, wrote first version of manuscript, edited later versions of manuscript.		
Overall percentage (%)	90%		
Certification:	This paper reports on original research I conducted during the period of my Higher Degree by Research candidature and is not subject to any obligations or contractual agreements with a third party that would constrain its inclusion in this thesis. I am the primary author of this paper.		
Signature		Date	23.08.2018

Co-Author Contributions

By signing the Statement of Authorship, each author certifies that:

i. the candidate's stated contribution to the publication is accurate (as detailed above);

ii. permission is granted for the candidate in include the publication in the thesis; and

iii. the sum of all co-author contributions is equal to 100% less the candidate's stated contribution.

Name of Co-Author	Mark N. Hutchinson		
Contribution to the Paper	Provided feedback that facilitated this work, edited manuscript.		
Signature		Date	28/08/2018

Name of Co-Author	Marc E. H. Jones		
Contribution to the Paper	Provided feedback that facilitated this work, edited manuscript.		
Signature		Date	23rd August 2018

CHAPTER 6

Implications of using
captive lizards in geometric
morphometric analyses
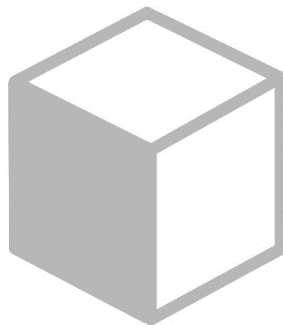
CHAPTER 6 – Implications of using captive lizards in morphological analyses

Jaimi A. Gray, Mark N. Hutchinson, Marc E. H. Jones

Abstract

It is inevitable that captive animal populations must be used in research and conservation efforts, but a suite of distinctive traits not present in wild predecessors is often observed in captive and domesticated populations. Although this issue has received much attention in mammals, the effects of captivity on reptiles are mostly unknown. Here, we use three-dimensional geometric morphometrics to detect differences in cranial shape between samples of wild and captive jacky lizards (*Amphibolurus muricatus*). We also place a selection of wild and captive lizards into a larger data set to explore how the inclusion of captive specimens might affect interspecific analyses and subsequent interpretation. Our results reveal that captive lizards have broader skulls and shorter faces than wild lizards, and the differences between captive and wild lizards are distinct, even in interspecific comparisons. The broad heads and short faces of captive jacky lizards are also characters associated with captivity in a broad range of other animal groups, suggesting uniformity in underlying mechanisms. Our research indicates that inferences made about wild populations from biological studies on captive reptiles should be made with caution. Although we have shed light on the effects of captivity in lizards, we are still far away from understanding the underlying causes and mechanisms. Since it is unavoidable that we must use captive populations for biological research, it is critical that further work is carried out to understand the underlying causes, as well the continuity of these traits among other reptiles.

Keywords: captivity, domestication, geometric morphometrics, lizards, reptiles, skull

Introduction

For over 150 years, dramatic biological differences between captive and wild animals have been observed and documented (Darwin, 1868). It is now well known that animals in captivity possess a collection of traits that are not seen in their wild counterparts. These reported differences have led to a perception that captive animals are biologically abnormal, and therefore should be used with caution in research (Hollister, 1917; Howell, 1925). Nevertheless, captive animals have played, and continue to play, a critical role in biological research and conservation efforts. This is particularly true when it is not possible to research extant species in their natural habitat, such is the case for endangered and rare species. Thus, data sets used for many different types of biological studies are often completely or partly made up of captive animal specimens (Bonnan et al., 2008). A well-rounded understanding of the effects of captivity still eludes biologists (particularly for non-mammal species), but is essential for ensuring optimal evolutionary success of captive populations, and also important in the interpretation of any biological data set that includes captive animals.

The propagation of captive animals can lead to a myriad of effects on the morphology and physiology of the resulting populations. Additionally, over multiple generations in captivity the magnitude of trait differences between wild and captive populations has been shown to increase (McPhee, 2004). Remarkably, some of the traits associated with captivity have been reported to occur in captive mammals, birds, reptiles, and fish, and this all-encompassing influence reflects intrinsic developmental links in the process of domestication (Moss, 1972; Crossley and del Mar Miguélez, 2001; Marchetti and Nevitt, 2003; Furrer et al., 2004; Connolly and Cree, 2008; Drake, 2011). Various reasons have been proposed to be the cause of the differences between captive and wild animals, including relaxed selective environments (Frankham et al., 1986), founder effects (McPhee, 2004), changes in the direction of selection (Endler, 1986), differences in diet compared to the natural state (Gore, 1993; Lieberman et al., 2004), and deficiencies in neural cells during development (Wilkins et al., 2014). Regardless of the reasons for the differences, they may ultimately render captive populations unsuitable as proxies for the wild state of a species, hindering research. Additionally, reintroductions to the wild after captive breeding have been seen to fail through poor foraging and lack of predator recognition (Frankham et al., 1986; Jolly et al., 2018), and in one case, a loss of ability for effective locomotion in their natural environment (Menzel and Beck, 2000; Wallece, 2000). For the benefit of captive populations and the research involving them, it is of critical importance

that we understand the effects of captivity over multiple generations and throughout development of individuals in the population.

Skeletons can be surprisingly phenotypically and evolutionarily plastic, and differences in cranial morphology attributable to being in captivity have been reported in a range of mammals and some reptiles (Groves, 1966; Groves, 1982; O'Regan, 2001; McPhee, 2004; Bello-Hellegouarch et al., 2013; Hartstone-Rose et al., 2014; Drumheller et al., 2016; Duong et al., 2017). Now that biologists have an extensive toolkit of geometric morphometric methods at their disposal to quantitatively characterise and compare the shapes of skeletal elements of animals (Bookstein, 1989; Bookstein, 1991; Bookstein, 1996; Klingenberg et al., 2002; Klingenberg, 2010; Zelditch et al., 2012), we can look at the way captivity affects morphology in more refined detail.

While we had been assembling data on cranial variation on Australian agamids, it become apparent that agamids from a captive colony were showing consistent differences in skull shape to wild lizards of the same species: *Amphibolurus muricatus*, also known as (and herein referred to as) the jacky lizard. We have taken advantage of these samples to present preliminary work. Here, we compare the cranial morphology of our samples of captive and wild jacky lizards of different body sizes, and also compare them to other Australian agamid species of different body sizes. Our objectives are to firstly, characterise the differences in cranial morphology between the sampled captive and wild lizards, secondly, determine whether differences between captive and wild jacky lizard skulls shapes were the result of heterochrony, and thirdly, examine how captivity may affect the interpretation of a broader taxonomic data set.

Materials and methods

Specimens

To compare cranial shape differences between a sample of captive and a sample of wild lizards, we used 26 alcohol preserved specimens of jacky lizards. Our sample included 18 captive specimens from the University of Canberra, which were a mixture of either one or two generation captive-reared animals. We also included seven wild specimens from the herpetology collection at South Australian Museum, Adelaide, and from the Australian Museum in Sydney (see supplementary material: Table S6.1 for specimen information). For a broader taxonomic dataset, representing a sample that might be used for interspecific comparisons, we included six other species of Australian agamids, comprised of a combination of alcohol preserved and dry skeletal specimens of different body sizes. Species included for comparison were *Ctenophorus isolepis, Diporiphora nobbi, Gowidon longirostris, Pogona barbata, Rankinia diemensis*, and *Tympanocryptis tetraporophora*. For each comparison species, four to six specimens of different sizes (representing different ontogenetic stages) were included (see supplementary material: Table S6.2 for specimen information).

X-ray computed tomography

To obtain skull data, we used high resolution X-ray micro computed tomography (CT). All CT scans were made with the Skyscan 1076 system at Adelaide Microscopy, at the University of Adelaide. Specimens were scanned at a resolution of either 8 or 16 microns, depending on the size of the specimen. Typically, an aluminium filter (0.5 mm) was used, with a voltage of 36-82 kV, and a current of 100-250 μA. CT scan data were segmented by applying a threshold to extract material of the same density as bone, then removing non-cranial bony elements (lower jaws, hyoids, scleral ossicles, and vertebrae). We rendered the crania as three-dimensional (3D) volumes using Avizo v 9.0 (Visualization Sciences Group, 2013). The resulting surfaces were used for landmarking (ply files can be found in supplementary material: File ES6.1).

Landmarking and shape analysis

Cranial shape was characterised using 3D landmark based geometric morphometric analysis (Bookstein, 1996; Dryden and Mardia, 1998; Klingenberg, 2010). We used IDAV Landmark Editor v 3.0.0.6 (Wiley et al., 2007) to digitise 102 landmarks in 3D over the cranium (the same landmarks that were used in Chapter 5, see Fig. 5.2 and supplementary material: Table S5.2), that represented the cranial shape and were placed at equivalent points on bones at sutures, and extremes and boundaries of curvature of major structures. Two landmark data sets were generated. One containing the 26 specimens of captive and wild jacky lizards (hereafter referred

to as data set A, see supplementary material: Table ES6.2 for landmark coordinates), and another containing all specimens of each comparison species, and eight jacky lizard specimens: four captive and four wild (hereafter referred to as data set B, see supplementary material: Table ES6.3 for comparison species landmark coordinates). The jacky lizards in data set B were chosen to represent the extremes of shape variation in the first two axes of a principal components analyses (PCA) of data set A, and also to represent the range of sizes of both captive and wild jacky lizards in data set A (see supplementary material: Table S6.2 for jacky lizards chosen).

For the data sets A and B, landmark data were subjected to a generalised Procrustes alignment (GPA) and projected into tangent space using the R package *geomorph* (Adams et al., 2018). The Procrustes fit for data set B corrected for asymmetry (Klingenberg et al., 2002). The Procrustes-aligned coordinates were used in subsequent analyses. We wanted to observe the shape variation in both data sets before and after allometric corrections, so we performed multivariate regressions of shape on size to calculate the degree of variation in cranial shape among specimens that was associated with variation in size (Klingenberg, 1996). Centroid size (a measure of size extracted from the landmarks) was used to represent head size (Dryden and Mardia, 1998).The specific procedures for each allometric correction are outlined in the following sections.

Cranial shape variation in captive and wild jacky lizards

To characterise the shape variation in data set A, we performed a PCA on the Procrustes aligned shape variables before any allometric corrections had been done (see supplementary material: File ES6.2 for coordinates). This analysis identified the main components of shape variation and illustrated the associated shape differences between the mean shape and the maximum and minimum of each PC. We visualised the shape differences identified by the PCA using vector diagrams representing the differences between landmark constellations of the mean shape and the minimum and maximum shape scores for PC1 and PC2, using the "plotRefToTarget" function in *geomorph*. We calculated the morphological disparity of the captive and wild samples and tested for a significant difference between them, using the "morphol.disparity" function in the R package *geomorph*. To investigate whether the differences between captive and wild skull shapes were the result of heterochrony, we estimated the allometric relationships between cranial shape and size by running a multivariate analysis of covariance (MANCOVA) model using log transformed centroid size, source (wild or captive), and their interaction as model effects (shape ~ log (size) * source). This was done using the "procD.allometry" function in *geomorph*. If the interaction terms were significant, this indicated that the allometric trajectories differed between

captive and wild samples, and that heterochronic changes along a single developmental pathway were not the reason for skull shape differences. To examine allometric patterns, we plotted regression scores on log transformed centroid size. To visualise the shape differences associated with size, we built wireframe diagrams representing the shape of the smallest and largest specimens, using the "plotRefToTarget" function in *geomorph* (see supplementary material: File ES6.4 for wireframe specifications). To obtain values of allometry corrected shape variables a regression of shape on size was performed using the "procD.lm" function in *geomorph*, and we obtained the regression coefficients. We used the coefficients to compute residual shape scores for the cranial shape of each specimen. To examine the non-allometric variation remaining in the data set, we performed a PCA on the shape variables after allometry correction. We calculated the morphological disparity (Procrustes variances) of the allometry corrected shape of captive and wild samples and tested for a significant difference between them, using the "morphol.disparity" function in the R package *geomorph*.

Using captive lizards in a broader taxonomic data set

To demonstrate the ways in which captive and wild jacky lizards would be interpreted in a larger data set, we characterised shape variation in the data set B, by performing a PCA on the shape variables (see supplementary material: File ES6.3 for coordinates). To obtain values of allometry-corrected shape variables a regression of shape on size was performed using the "procD.lm" function in *geomorph*, and we obtained the regression coefficients. We used the coefficients to compute residual shape scores for the cranial shape of each specimen. We carried out two versions of allometric correction for data set B, one without species as a factor (shape ~ log (size)), and one with species as a factor (shape ~ log (size) * species). We used the allometry corrected shape for each specimen to examine shape variation not attributable to allometry (Monteiro, 1999; Sidlauskas et al., 2011). To examine the distribution of specimens in morphospace, we performed three separate PCAs: one for shape variables before any allometry correction; after an allometry correction (shape ~ log (size)); and after an allometry correction with species as a factor (shape ~ log (size) * species). We calculated the morphological disparity (Procrustes variance) using "morphol.disparity", for each species and reported any clear differences between the jacky lizards and other species. We also plotted allometric trajectories (regression scores on log-transformed centroid size), to examine the distribution of wild and captive jacky lizards.

Results

Variation in cranial shape of wild and captive jacky lizards

The PCA of the 26 sampled jacky lizard specimens before allometric correction revealed that the first two principal component (PC) axes (see Fig. 6.1) account for 45% of the shape variation in the data set. The remaining PCs each explain less than 10% of the variation. PC1 almost completely divides the sampled wild and captive jacky lizards, and seems to be associated with size (the smallest specimens had the highest values while the largest specimens had the lowest values). PC2 seems to be associated with size (but is different for captive and wild samples), and the shape differences associated with this axis are more subtle (see Fig. 6.2). MANCOVA results (Table 6.2) showed that there is a significant difference in ontogenetic pattern between samples of captive and wild lizards. The MANCOVA results also indicate that size variation has a significant influence on skull shape for the entire jacky lizard data set. The captive and wild samples were not significantly different from one another in terms of their morphological disparity (Procrustes variances: captive = 0.00184; wild = 0.00258; P = 0.07).
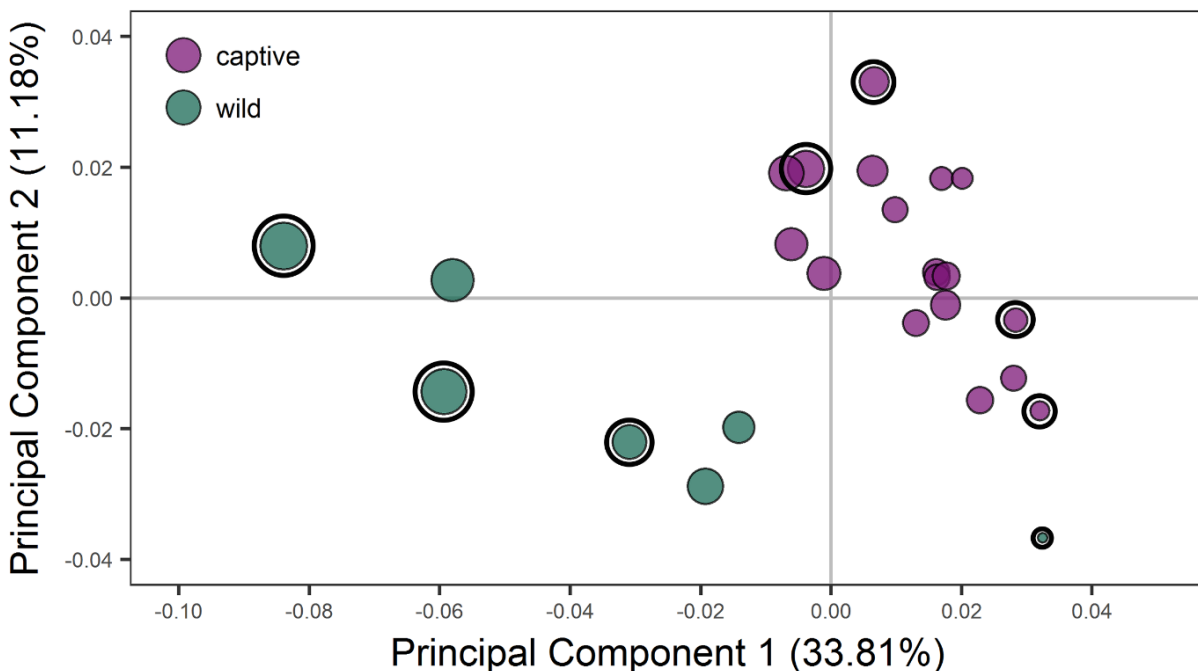
Figure 6.1 – Cranial morphospace (PC1 versus PC2) for data set A (all jacky lizard specimens), colour coded for source. Black rings indicate specimens selected for inclusion in data set B.
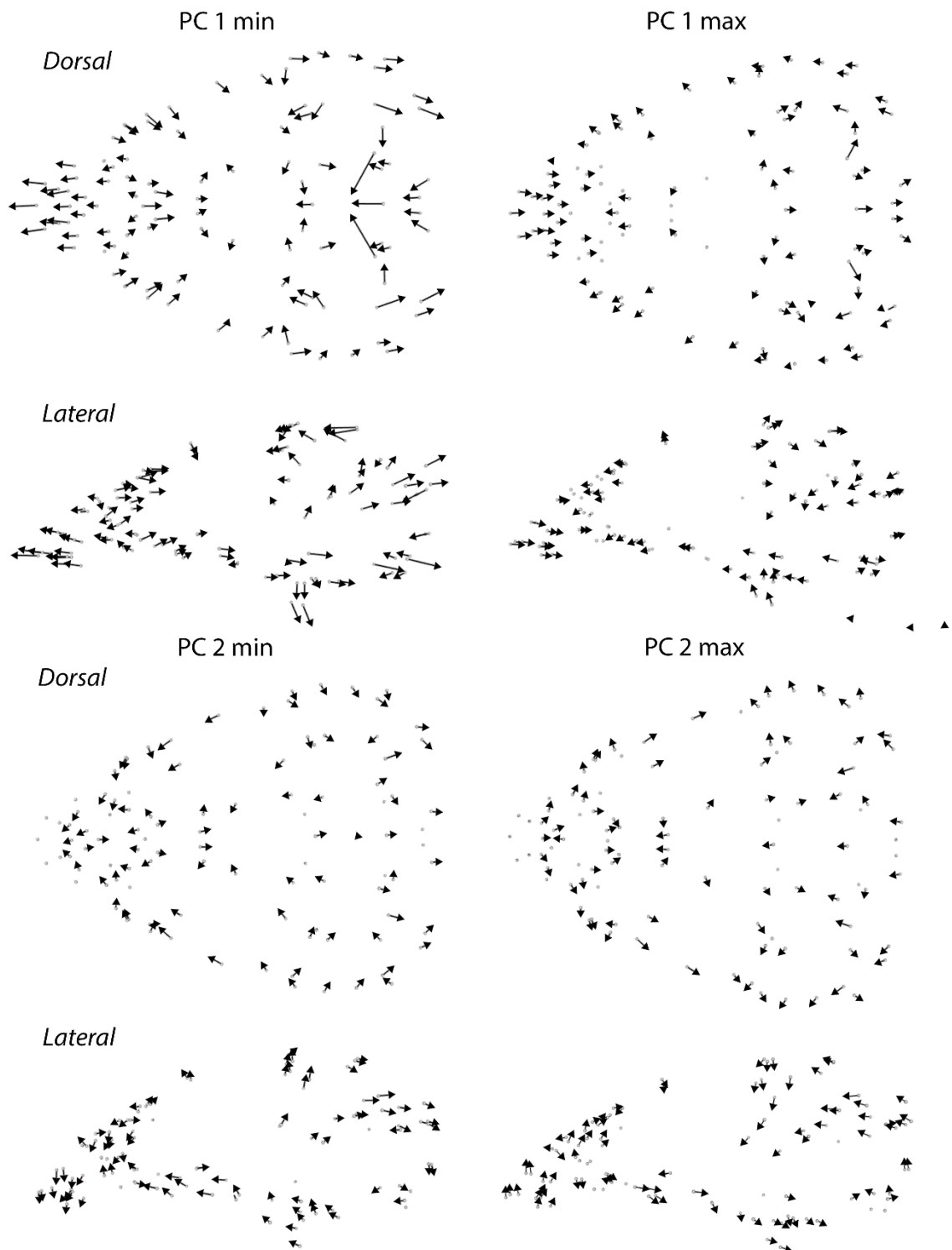
Figure 6.2 – Shape differences encompassed by the major axes of shape variation from a PCA of jacky lizards before allometry correction. Shape differences for landmarks are`1` represented by vectors that indicate direction and magnitude, and sets of landmarks are oriented with the anterior of the cranium to the left, and the posterior to the right.
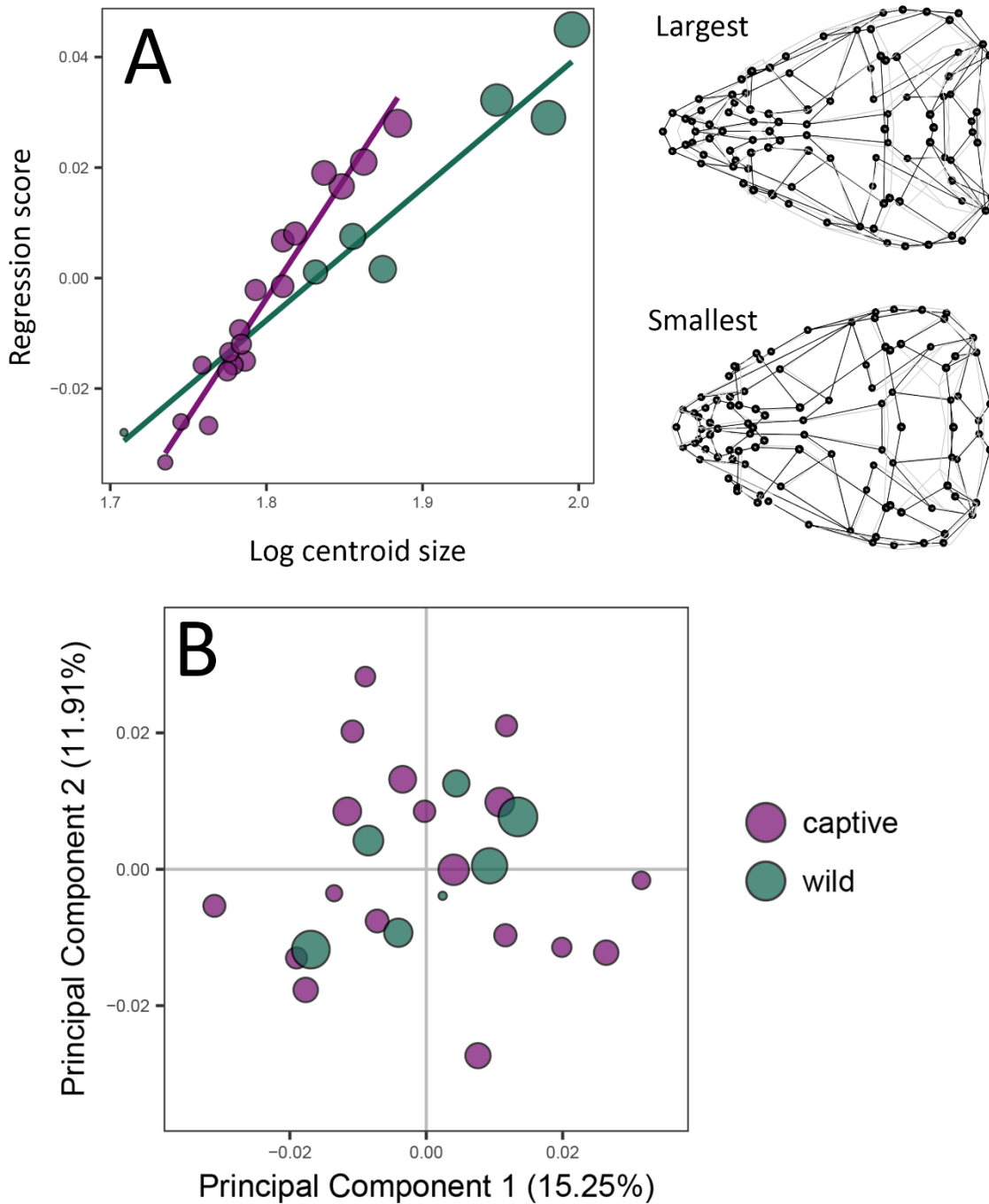
Figure 6.3 – Ontogenetic allometry of captive and wild jacky lizards. A shows allometric trajectories: regression scores on log transformed centroid size. B shows cranial morphospace after allometric correction. Point diagrams show the skull shapes associated with largest and smallest size, relative to the mean shape (shown in grey).

Table 6.1 – MANCOVA results for ontogenetic allometry of jacky lizard specimens (shape ~ log (size) * source).

	DF	SS	MS	Rsq	F	Z	*P*-value
*Data set A (shape ~ log (size) * source)*							
Log (size)	1	0.0201	0.0201	0.3100	11.84	6.01	**0.001**
Source	1	0.0062	0.0062	0.0957	3.65	6.43	**0.001**
Log (size) : source	1	0.0029	0.0029	0.0442	1.69	4.23	**0.001**
Residuals	21	0.0357	0.0017				
Total	24	0.0648					
*Data set B (shape ~ log (size) * species)*							
Log (size)	1	0.0990	0.0990	0.3408	43.44	7.07	**0.001**
Species	6	0.1149	0.0191	0.3956	8.40	11.50	**0.001**
Log (size) : species	6	0.0219	0.0036	0.0754	1.60	10.91	**0.001**
Residuals	24	0.0550	0.0023	0.1883			
Total	37	0.2904					

The plot of regression scores on log transformed centroid size (Fig. 6.2A) illustrates the difference in ontogenetic allometric patterns between wild and captive lizards. Collectively, the MANCOVA and the PCA results (before allometry correction) suggest that captive lizards appear to have a different cranial developmental pathway to that of wild caught lizards, and this has resulted in novel skull shapes. After allometric correction, the cranial morphospace no longer separates wild and captive jacky lizards (see Fig. 6.2B), highlighting the strong influence of ontogenetic allometry on shape in data set A. Notably, although they no longer occupied distinct areas of the cranial morphospace, captive jacky lizards exhibit a broader range of variation than wild lizards. This was confirmed by a significant difference in disparity between allometry corrected skull shapes in the captive and wild samples (Procrustes variances: captive = 0.00155; wild = 0.0011; $P = 0.024$).

135
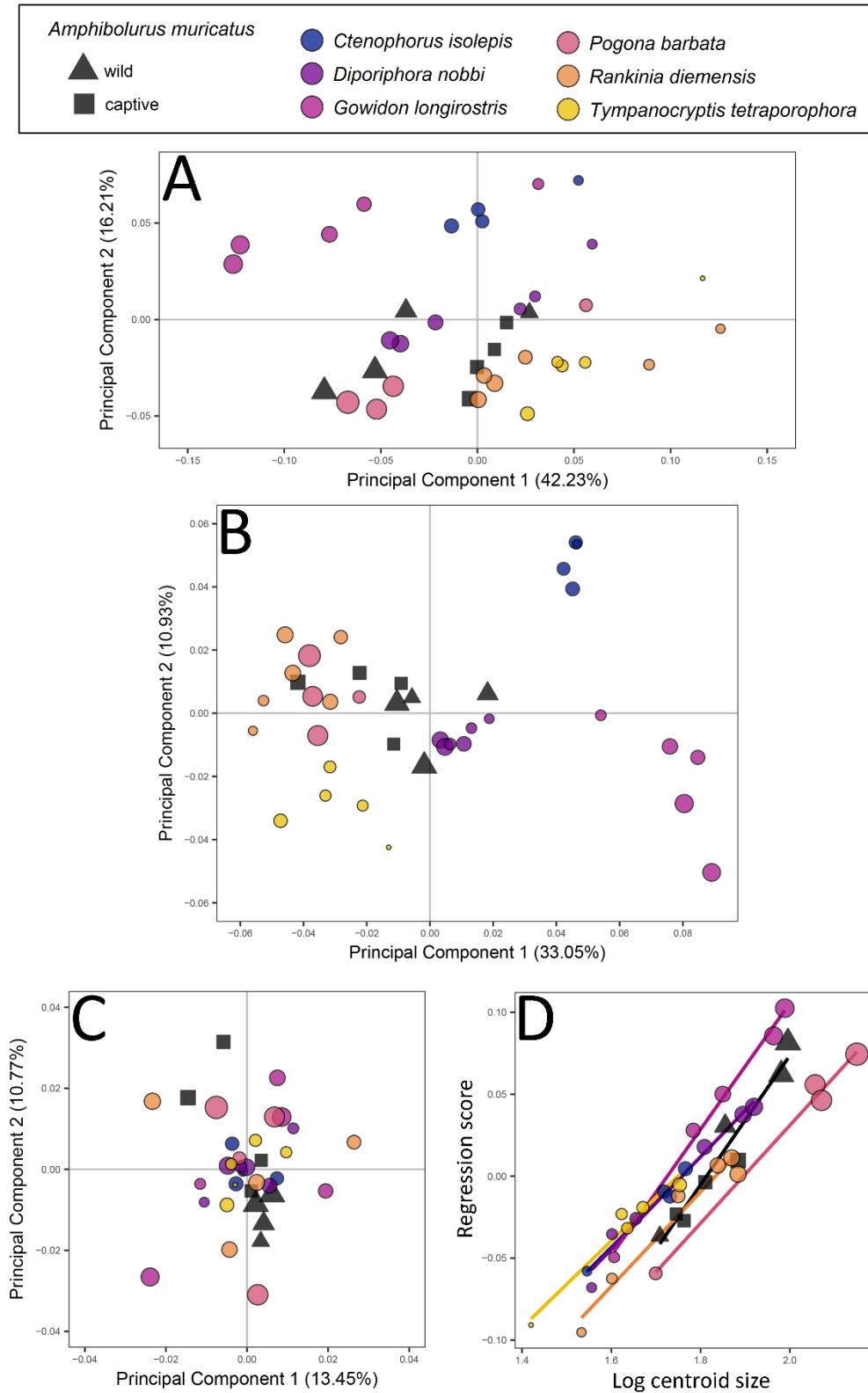
Figure 6.4 – Principal component (PC) 1 versus PC2 for different PCA results for data set B (A-C), coloured by species. A: before any allometry correction; B: After general allometry correction (shape ~ log (size)) C: after allometry correction with species as a factor (shape ~ log (size) * species); D: observing allometric patterns for different comparison species. All points are scaled to represent centroid size.

Comparison of captive specimens against a broader taxonomic sample

The shape space for data set B representing PC1 versus PC2 before allometric correction (Fig. 6.4A) accounts for 58.44% of the total shape variation in the data set. PC1 has a strong association with size: small lizards tend to have higher values and large lizards tend to have lower values. The captive and wild jacky lizards are almost completely separated by PC1 values, with the wild specimens mostly having lower PC1 values than captive specimens. The exception to this is the very smallest wild jacky lizard, which plotted similarly to the captive specimens. Once an allometric correction was performed, smaller and larger representatives of species plot closer to one another in the PC1 versus PC2 morphospace (Fig. 6.4B). The captive and wild jacky lizards still remain separate from each other. After a species specific allometry correction (see Fig. 6.4C), the PC1 versus PC2 morphospace no longer separates agamid species from one another, with most clustering haphazardly in the centre of the morphospace. Still, the captive and wild jacky lizards remain separate from each other. Combined, the captive and wild jacky lizards seem to display a larger amount of shape variation than the other species included for comparison, in each PCA example.

Multivariate regression (see Table 6.1) revealed that shape variation associated with size accounts for 34.08% of the total variation in the data set ($P = 0.001$), while species affiliation accounts for 39.56% of the total variation. The ontogenetic allometric trajectories (see Fig. 6.4D) reveal distinct patterns for some agamid species, while some are similar to others. Most importantly, the inclusion of captive specimens affects the jacky lizard ontogenetic allometric trajectory, as revealed by the distribution of specimens around the line of best fit: three out of four captives fall below the line, while three out of four wild specimens fall above the line.

Discussion

We found that cranial shape in our sample of captive jacky lizards was strikingly different to cranial shape in our sample of wild jacky lizards. Captive jacky lizards tended to have broader and shorter skulls than wild jacky lizards, a character that has also been associated with captivity in other animal groups that are distantly related to lizards (e.g. Cardini et al., 2015). Furthermore, we found that in the context of a broader data set including multiple different sized specimens of different species of agamid lizards, captive lizards consistently remain distinct from their wild counterparts.

Our results revealed the shape differences between captive and wild jacky lizards are not the result of simple heterochrony. Instead, captive jacky lizards have obtained a novel skull shape. Intriguingly, we can draw parallels here, between the captive jacky lizards and the case of domestic dogs. Early research suggested that domestic dogs evolved via heterochrony and were inferred to represent paedomorphic wolves (Wayne, 1986). However, this hypothesis was not upheld when the skulls were subjected to three-dimensional geometric morphometric analysis: like the jacky lizards, domestic dogs represent novel skull phenotypes, rather than paedomorphic forms of an ancestral phenotype (Drake, 2011). It is remarkable that such a pattern recurs in two very distantly related animal species, and suggests that there may be common underlying causes for differences in traits observed in skull shape of captive and wild animals.

A few prior studies on captive reptiles exist (Furrer et al., 2004; Connolly and Cree, 2008; Drumheller et al., 2016), and our results are consistent with previously demonstrated morphological distinctiveness of captive reptile populations (Connolly and Cree, 2008). The morphological distinctiveness of the sampled captive jacky lizards was apparent, even in the context of a larger data set designed to examine interspecific variation. Moreover, in some cases shape differences between captive and wild jacky lizards in the cranial morphospace were just as great as shape differences between different agamid species. Therefore, for studies that use data sets made up of either a combination of wild and captive lizards, or purely of captive lizards, intraspecific variation may be greater than we would otherwise expect. For species represented purely by captive individuals, their position in shape space may not be an accurate representation of the wild state of their morphology. The large amount of shape variation in the captive jacky lizards implies that perhaps relaxed selection for traits required to survive in the wild has allowed morphology to drift. An additional consideration is that the origin of the jacky lizards may have affected their morphology (the founder effect). If our results are corroborated by larger sample

sizes, biologists may need use more caution in the analysis and interpretation of data sets that include captive animals.

We have shown that differences in skull morphology between wild and captive lizards exist, but we are still a long way from understanding the underlying causes and mechanisms behind these differences. Often, captive populations provide the only viable opportunity to study the biology of a particular species. Therefore we need to understand the processes underlying the observed differences. The consistency between the traits observed in captive jacky lizards and those reported in other animals (i.e. broader and shorter faces) indicates that there may be common underlying causes for these characteristics (Trut, 1999; O'Regan and Kitchener, 2005; Drake, 2011; Hartstone-Rose et al., 2014). Non-mammal captive populations, including this one, would therefore benefit from an investigation into the underlying causes, for example, whether captive breeding in reptiles leads to similar neural crest cell deficiencies that have been suggested to be linked to the suite of traits observed in captive mammals (Wilkins et al., 2014; Sánchez-Villagra et al., 2016) to indicate whether causes are indeed recurrent in multiple, distantly related animal groups. These notions may also be strengthened by determining whether, along with the skull shape differences observed here, other traits associated with captivity that have been reported in other animals, also occur in lizards. Uniformity among the suite of traits associated with captivity, and the underlying causes, would provide a compelling case for a unified theory of the process of domestication.

Conclusions

This study documents the fact that, for our sample, there are pronounced morphological differences between captive and wild jacky lizards, a group that has not previously been examined at this level of detail. Although more work is required in order to understand the mechanisms behind these differences, our study highlights the need for caution when interpreting results from biological studies involving captive lizards. We show that traits associated with captivity, which have mostly been demonstrated in mammals, also occur in reptiles.

Acknowledgements

Supplementary material

Tables

Electronic files

File ES6.1 – Folder containing ply surface files used for landmarking (file folder).

File ES6.2 – 3D landmark coordinates used to characterise jacky lizard crania (DTA).

File ES6.3 – 3D landmark coordinates used to characterise comparison species crania (DTA).

File ES6.4 – Wireframe links used to build skull shape diagrams (CSV).

References

Adams DC, Collyer ML, Kaliontzopoulou. 2018. geomorph: software for geometric morphometric analyses. R package version 3.0.6. https://CRANR-projectorg/package=geomorph.

Bello-Hellegouarch G, Potau JM, Arias-Martorell J, Pastor JF, Pérez-Pérez A. 2013. Brief communication: morphological effects of captivity: a geometric morphometric analysis of the dorsal side of the scapula in captive-bred and wild-caught hominoidea. Am J Phy Anthropol 152:306-310.

Bonnan MF, Farlow JO, Masters SL. 2008. Using linear and geometric morphometrics to detect intraspecific variability and sexual dimorphism in femoral shape in *Alligator mississippiensis* and its implications for sexing fossil archosaurs. J Vert Palaeontol 28:422-431.

Bookstein FL. 1989. Principal warps: thin-plate splines and the decomposition of deformations. IEEE Trans Pattern Anal Mach Intell 11:567-585.

Bookstein FL. 1991. Morphometric tools for landmark data: geometry and biology. Cambridge: Cambridge University Press.

Bookstein FL. 1996. Biometrics, biomathematics and the morphometric synthesis. Bull Math Biol 58:313.

Cardini A, Polly D, Dawson R, Milne N. 2015. Why the long face? Kangaroos and wallabies follow the same 'rule' of cranial evolutionary allometry (CREA) as placentals. Evol Biol 42:169-176.

Connolly JD, Cree A. 2008. Risks of a late start to captive management for conservation: Phenotypic differences between wild and captive individuals of a viviparous endangered skink (*Oligosoma otagense*). Biol Cons 141:1283-1292.

Crossley DA, del Mar Miguélez M. 2001. Skull size and cheek-tooth length in wild-caught and captive-bred chinchillas. Arch Oral Biol 46:919-928.

Darwin C. 1868. The variation of animals and plants under domestication: O. Judd.

Drake AG. 2011. Dispelling dog dogma: an investigation of heterochrony in dogs using 3D geometric morphometric analysis of skull shape. Evol Dev 13:204-213.

Drumheller SK, Wilberg EW, Sadleir RW. 2016. The utility of captive animals in actualistic research: A geometric morphometric exploration of the tooth row of *Alligator mississippiensis* suggesting ecophenotypic influences and functional constraints. J Morphol 277:866-878.

Dryden I, Mardia K. 1998. Statistical shape analysis. John Wiley & Sons.

Duong T-Y, Nguyen T-T, Pham T-L. 2017. Morphological differentiation among cultured and wild *Clarias macrocephalus*, *C. macrocephalus* x *C. gariepinus* hybrids, and their parental species in the Mekong delta, Viet Nam. Int J Fish Aquat 5:233-240.

Endler JA. 1986. Natural selection in the wild, No 1. Princeton University Press.

Frankham R, Hemmer H, Ryder OA, Cothran EG, Soulé ME, Murray ND, Snyder M. 1986. Selection in captive populations. Zoo Biol 5:127-138.

Furrer SC, Hatt JM, Snell H, Marquez C, Honegger RE, Rübel A. 2004. Comparative study on the growth of juvenile Galapagos giant tortoises (*Geochelone nigra*) at the Charles Darwin Research Station (Galapagos Islands, Ecuador) and Zoo Zurich (Zurich, Switzerland). Zoo Biol 23:177-183.

Gore MA. 1993. A comparison of morphometry from captive and free-ranging *Macaca mulatta*. J Med Primatol 22:360-367.

Groves CP. 1966. Skull-changes due to captivity in certain Equidae. Zeitschrift fuer Saugietierkunde 31:44-46.

Groves CP. 1982. The skulls of Asian rhinoceroses: wild and captive. Zoo Biol 1:251-261.

Hartstone-Rose A, Selvey H, Villari JR, Atwell M, Schmidt T. 2014. The three-dimensional morphological effects of captivity. PLOS ONE 9:e113437.

Hollister N. 1917. Some effects of environment and habit on captive lions, Vol 53. US Government Printing Office.

Howell AB. 1925. Pathologic skulls of captive lions. J Mammal 6:163-168.

Jolly CJ, Webb JK, Phillips BL. 2018. The perils of paradise: an endangered species conserved on an island loses antipredator behaviours within 13 generations. Biol Lett 14:20180222.

Klingenberg CP. 1996. Multivariate allometry. In: Marcus LF, Corti M, Loy A, Naylor GJP, Slice DE, editors. Advances in morphometrics. Boston: Springer US. p 23-49.

Klingenberg CP. 2010. Evolution and development of shape: integrating quantitative approaches. Nat Rev Genet 11:623-635.

Klingenberg CP, Barluenga M, Meyer A. 2002. Shape analysis of symmetric structures: quantifying variation among individuals and asymmetry. Evolution 56:1909-1920.

Lieberman DE, Krovitz GE, Yates FW, Devlin M, St. Claire M. 2004. Effects of food processing on masticatory strain and craniofacial growth in a retrognathic face. J Hum Evol 46:655-677.

Marchetti MP, Nevitt GA. 2003. Effects of hatchery rearing on brain structures of rainbow trout, *Oncorhynchus mykiss*. Environ Biol Fishes 66:9-14.

McPhee ME. 2004. Morphological change in wild and captive oldfield mice *Peromyscus polionotus subgriseus*. J Mammal 85:1130-1137.

Menzel C, Beck B. 2000. Homing and detour behavior in golden lion tamarin social groups. In: On the move: how and why animals travel in groups. Chicago: University of Chicago Press. p 299-326.

Monteiro LR. 1999. Multivariate regression models and geometric morphometrics: the search for causal factors in the analysis of shape. Syst Biol 48:192-199.

Moss R. 1972. Effects of captivity on gut lengths in red grouse. J Wildl Manage 36:99-104.

O'Regan HJ. 2001. Morphological effects of captivity in big cat skulls. In: 3rd Annual Symposium on Zoo Research. Upton: The North of England Zoological Society. p 18-22.

O'Regan HJ, Kitchener AC. 2005. The effects of captivity on the morphology of captive, domesticated and feral mammals. Mammal Rev 35:215-230.

Sánchez-Villagra MR, Geiger M, Schneider RA. 2016. The taming of the neural crest: a developmental perspective on the origins of morphological covariation in domesticated mammals. Royal Soc Open Sci 3:160107.

Sidlauskas BL, Mol JH, Vari RP. 2011. Dealing with allometry in linear and geometric morphometrics: a taxonomic case study in the *Leporinus cylindriformis* group (Characiformes: Anostomidae) with description of a new species from Suriname. Zool J Linnean Soc 162:103-130.

Trut LN. 1999. Early canid domestication: the farm-fox experiment: foxes bred for tamability in a 40-year experiment exhibit remarkable transformations that suggest an interplay between behavioral genetics and development. Am Sci 87:160-169.

Visualization Sciences Group. 2013. Avizo. FEI Corporate Headquarters, Oregon.

Wallece M. 2000. Retaining natural behaviour in captivity for re-introduction programmes. Behav Cons:300-314.

Wayne RK. 1986. Cranial morphology of domestic and wild canids: the influence of development on morphological change. Evolution 40:243-261.

Wiley D, Amenta N, Alcantara D, Ghosh D, Kil Y, Delson E. 2007. Landmark Editor: Institute for Data Analysis and Visualization. University of California, Davis.

Wilkins AS, Wrangham RW, Fitch WT. 2014. The "domestication syndrome" in mammals: a unified explanation based on neural crest cell behavior and genetics. Genetics 197:795-808.

Zelditch ML, Swiderski DL, Sheets HD, Fink WL. 2012. Geometric morphometrics for biologists: a primer, 2nd ed. Academic Press.

STATEMENT OF AUTHORSHIP

Title of Paper	Using jaw bones to estimate dragon body size
Publication Status	☐ Published ☐ Accepted for Publication ☐ Submitted for Publication ☑ Unpublished and Unsubmitted work written in manuscript style
Publication Details	Prepared for submission to Journal of Vertebrate Paleontology

Principal Author

Name of Principal Author (Candidate)	Jaimi Gray		
Contribution to the Paper	Designed research, data collection and analysis, wrote first version of manuscript, edited later versions of manuscript.		
Overall percentage (%)	90%		
Certification:	This paper reports on original research I conducted during the period of my Higher Degree by Research candidature and is not subject to any obligations or contractual agreements with a third party that would constrain its inclusion in this thesis. I am the primary author of this paper.		
Signature		Date	23.08.2018

Co-Author Contributions

By signing the Statement of Authorship, each author certifies that:

  i.   the candidate's stated contribution to the publication is accurate (as detailed above);

  ii.   permission is granted for the candidate in include the publication in the thesis; and

  iii. the sum of all co-author contributions is equal to 100% less the candidate's stated contribution.

Name of Co-Author	Marc E. H. Jones		
Contribution to the Paper	Provided feedback that facilitated this work, edited manuscript.		
Signature		Date	23rd August 2018

Name of Co-Author	Mark N. Hutchinson		
Contribution to the Paper	Provided feedback that facilitated this work, edited manuscript.		
Signature		Date	28/08/2018

CHAPTER 7

Using jaw bones to
estimate Australian
dragon body size

CHAPTER 7 – Using jaw bones to estimate Australian dragon body size

Jaimi A. Gray, Marc E. H. Jones, Mark N. Hutchinson

Abstract

The body size of a fossil specimen can give palaeontologists an important indication of an animal's physiological capabilities and requirements, as well as its role in an ecosystem. Because material may be broken and incomplete, body length is often estimated using the dimensions of specific structures and relationships established with baseline data. This approach is frequently used for fossil mammal material but rarely used for fossil reptiles, even though reptile material can also be recovered in reasonable sample sizes. Here, we use the maxilla and dentary of Australian agamid lizards to examine the relationships between a quantitative linear measurement, tooth row length, and a body size proxy (snout-vent length). We find a positive linear relationship between tooth row length and snout-vent length (both log transformed) for the maxilla and dentary, which indicates that tooth row length of the jaw bones can be used effectively to estimate body size of Australian agamid lizards. We use a collection of maxillae from different South Australian cave deposits to demonstrate how snout-vent length can be estimated and how the results might be interpreted. Further work may involve expanding this data set to include other squamates, so fossil squamate material can make a greater contribution to palaeoecological reconstructions of specific localities and recent time (< 3 million years).

Key words: Agamidae, body size, cave deposits, dentary, fossil, jaw bone, maxilla

Introduction

Animal remains in fossil deposits can be used to determine presence, absence, abundance, and diversity of species through space and time, and are important for understanding the composition of past faunal communities. Comparisons of faunal assemblages over geological time scales have revealed that different species can have different responses to environmental change, and the structure and function of faunal assemblages can change markedly, even over relatively short time periods of several thousand years (Graham and Grimm, 1990; Lyons, 2005). An ability to compare faunal composition through time with palaeoenvironments, including climate change and geological processes, is essential for understanding the processes that shape biodiversity.

Understanding the evolution of body size is a common objective when modelling past ecosystems. Body sizes of fossil specimens are an important palaeontological factor that can give clues about an animal's adaptation to its environment and its place in an ecosystem (Wilson, 1975; Vézina, 1985; Gregory, 1986; Peters and Peters, 1986; Hurlburt, 1999; Woodward et al., 2005; Cooper and Stankowich, 2010). Even rough estimates of body size can be used to make inferences about individual fossil specimens, which also contribute to the overall interpretation of a fossil assemblage (e.g. Gregory, 1986; Finarelli and Flynn, 2006). Body size can provide an indication of many metabolic and physiological variables (Schmidt-Nielsen, 1984), and give an indication of an animal's ecological role and performance capacity (Huey and Hertz, 1982; Huey and Hertz, 1984; Garland, 1985), such home range, bite force, and limits on prey size. Body size of a particular individual can also affect what kind of refuges it can use to hide from predators, which microhabitats that species can occupy, and can inform ontogenetic and taxonomic interpretations. Obtaining body size information from fossils is therefore of great interest to palaeobiologists (Gingerich et al., 1982; Garland, 1985; Grabowski et al., 2015; Slavenko et al., 2016; Campione, 2017), but taphonomic processes render most fossil specimens incomplete (Behrensmeyer, 1984). Therefore, their overall linear dimensions can be difficult to estimate and palaeobiologists often use parts of the skeleton to extrapolate the size of an animal from bone fragments. Some skeletal data, such as tooth, skull or femur dimensions, have been shown to have a strong correlation with body size (Gingerich et al., 1982; Farlow et al., 2005; Young et al., 2011). However, most of this work has been done on mammals, and relatively little has been done on small non-mammalian vertebrate such as lizards and frogs (Esteban et al., 1995).

Squamate reptiles (lizards and snakes) in the fossil record are often represented by disarticulated cranial material that is often broken. Within squamates, lizards are most often

represented by the jaw bones (Worthy, 2016; Gray et al., 2017), the dentary (lower) and the maxilla (upper). The character rich nature of the jaw bones means they are readily assigned to major clades (e.g. families and major subgroups within families), but we generally lack the ability to affiliate them with more precise taxonomic groups (Bell and Mead, 2014). Even without precise taxonomic assignments, jaw bones can tell us about aspects of lizard biology, such as body size. In this study, we use the Australian agamid clade as an example and establish a method for estimating their body size from lizard jaw bones. Australian agamids arrived in Australia around 30 million years ago (Ma), and their current diversity is known to be around 108 species. Although their evolutionary success is apparent from their current ecological and taxonomic diversity, little exploration has been done into their evolutionary history since they first appeared in Australia (Hugall et al., 2008) and this is largely due to a poor understanding of their assemblages in the fossil record.

We assemble a data set of maxillary and dentary tooth row lengths for modern Australian agamids and test our approach using fossil maxilla from South Australian cave deposits (Kelly Hill Caves and Naracoorte Caves). We report on the usefulness of the maxilla and dentary bones as estimators of body size, with the overall aim of providing a method to predict body size in assemblages of fossil agamid lizards.

Methods

We used jaw bones from specimens of extant species with known snout-vent length (SVL). Specimens were from South Australian Museum, Queensland Museum, Western Australian Museum, Melbourne Museum, University of Texas at Austin, and the Field Museum of Natural History in Chicago. Although we collected baseline data from specimens of living species, we needed our data set to be applicable to fossil specimens. Therefore, we chose a parameter that would be frequently available despite the damage often evident in fossil material robust, given that fossil material is often damaged: tooth row length (see Fig. 7.1). We measured the tooth row length of 174 dentaries and 189 maxillae.

We estimated the linear dimension of body size: snout-vent length, rather than body mass (weight), because SVL measurements were more commonly available for the representative museum specimens used as comparative material. Also, SVL and body mass are closely related to one another in lizards (Meiri, 2010). To determine whether we could estimate SVL from tooth row length, from either the dentary or maxilla, we used ordinary least squares regression. Both tooth row lengths and SVL were log transformed for this analysis. Tooth row length was regressed against SVL, and correlation between these two variables was estimated using the correlation coefficient.

Figure 7.1 – Disarticulated maxilla (top) and dentary (bottom) of *Ctenophorus pictus* **(South Australian Museum specimen R07691), showing the boundaries used to measure tooth row length.**

We tested our approach by measuring the tooth row lengths of 17 fossil agamid maxillae specimens (registered at South Australian Museum) sorted from three South Australian cave deposits: Wet Cave and Blanche Cave at the Naracoorte Caves, and Kelly Hill Caves on Kangaroo Island (see Fig. 7.2). We used the fossil tooth row lengths and our calculated coefficients to estimate the SVL of the specimens, and provide an example of how the SVL may be used to make interpretations about fossil deposits.
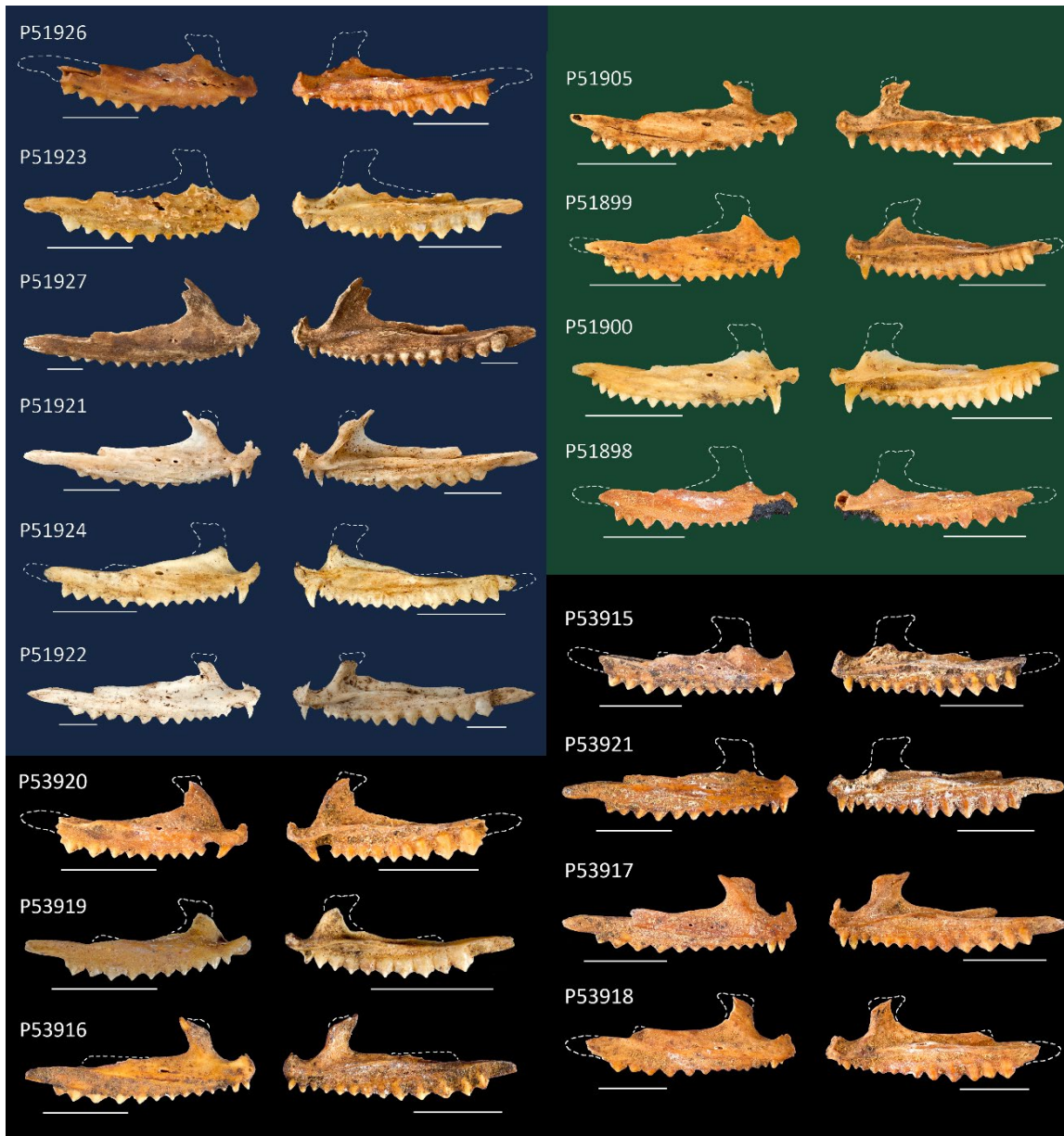
Figure 7.2 – Labial (left) and lingual (right) views of agamid fossil maxillae from Wet Cave (blue plate) and Blanche Cave (green plate) at Naracoorte Caves, and Kelly Hill Caves on Kangaroo Island (black plate), used to provide an example of estimating and interpreting snout-vent length. All specimens are registered at the South Australian Museum. Scale bars = 5 mm.

Results

Maxillary and dentary tooth row length are both significantly positively correlated with snout-vent length (SVL) (see Fig. 7.3). The correlation coefficients were relatively high for both the maxilla and dentary, and indicate that 86% (for the maxilla) and 87% (for the dentary) of the variation in tooth row length in our samples can be explained by SVL. All of the most distinct outliers above the upper 95% confidence interval for both the maxilla and dentary were *Moloch horridus*, which was expected due to its distinctive morphology. We used the coefficients resulting from the ordinary least squares regression (in Fig. 7.3) to estimate SVL for the fossil specimens in Figure 7.2.

In the Wet Cave deposits, estimated SVL values range from 76.07 mm to 198.65 mm (see Table 7.1). Several of these specimens tend towards the higher end of the range of observed SVL values for the extant Australian agamids, many of which cannot achieve such a large size during their lifetime. We may therefore use this information to tentatively infer that the largest fossil belonged to the largest local agamid genus (*Pogona*). For the Blanche Cave deposits, estimated SVL ranges from 67.59 mm to 73.85 mm. For the Kelly Hill Caves deposits, estimated SVL ranges from 51.83 mm to 89.74 mm. Most of the specimens in both the Blanche Cave and Kelly Hill Caves deposits tend towards the lower end of the SVL range of all sampled agamids, it is therefore likely that many of these specimens are either juvenile or smaller agamid species.
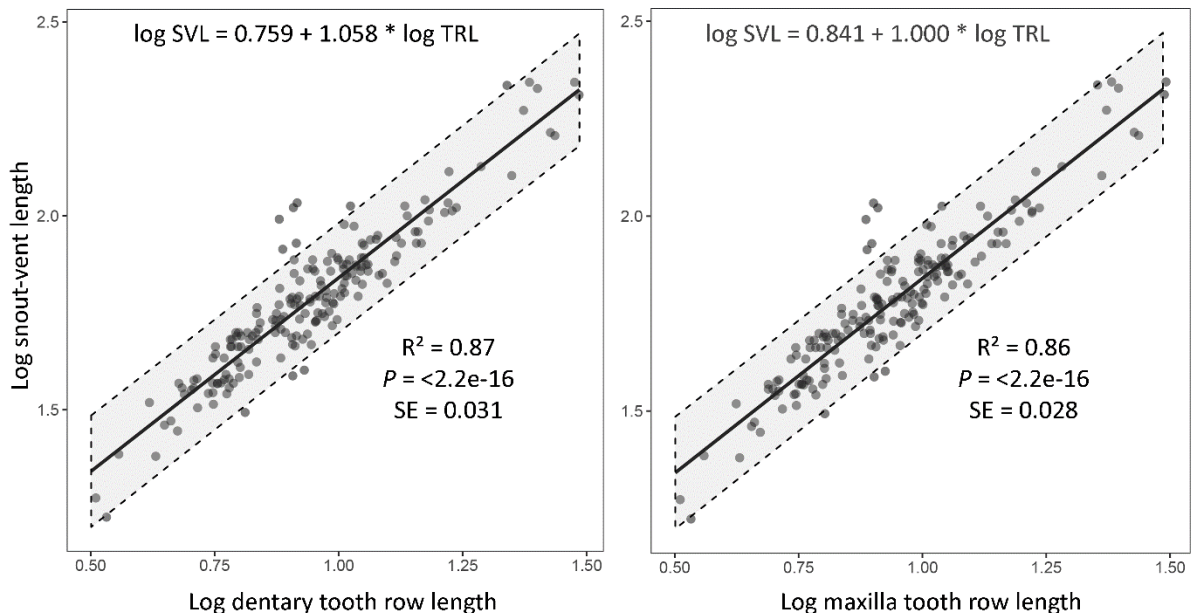
Figure 7.3 – Snout-vent length (SVL) versus tooth row length (TRL), both log transformed, for dentary (left) and maxilla (right), with 95% confidence interval. Includes coefficients and linear equations used to estimate SVL of fossil specimen.

Table 7.1 – List of fossil maxillae specimens from Australian cave deposits and snout-vent length (SVL) estimates (with 95% confidence interval) based on tooth row length. N = Naracoorte Caves; KI = Kangaroo Island. Specimens are all registered at South Australian Museum.

Specimen	Deposit	Tooth row length (mm)	SVL ± 3.73 (mm)
P51926	Wet Cave (N)	11.04	76.52
P51923	Wet Cave (N)	10.98	76.17
P51927	Wet Cave (N)	28.65	198.65
P51921	Wet Cave (N)	16.33	113.24
P51924	Wet Cave (N)	10.97	76.07
P51922	Wet Cave (N)	23.98	166.27
P51905	Blanche Cave (N)	9.75	67.59
P51899	Blanche Cave (N)	10.65	73.85
P51900	Blanche Cave (N)	10.16	70.43
P51898	Blanche Cave (N)	10.61	73.58
P53915	Kelly Hill Caves (KI)	10.64	73.79
P53921	Kelly Hill Caves (KI)	12.32	85.43
P53917	Kelly Hill Caves (KI)	11.78	81.69
P53918	Kelly Hill Caves (KI)	12.94	89.75
P53920	Kelly Hill Caves (KI)	9.19	63.73
P53919	Kelly Hill Caves (KI)	7.48	51.83
P53816	Kelly Hill Caves (KI)	11.48	79.63

Discussion

We present the first report of quantitative data for estimating the body size of Australian fossil agamids from jaw bones. We found that there was a positive linear relationship between snout-vent length (SVL) and tooth row length, for both the maxilla and dentary. Where comparative material is concerned, the SVL measurement is of particular interest, since it was common for many skeletal specimens in skeletal collections that we used, which are used as comparative material, to be accompanied by SVL data, but not body weight data. Standard guides for Australian reptiles such as Cogger (2014), and Wilson and Swan (2013), also report SVL in species descriptions. Although we estimated the linear dimension of body size, there is a strong correlation between SVL and body mass for the agamid family (Meiri, 2010). Therefore any estimation of SVL may also be used to make inferences about the approximate body mass of a particular individual.

Estimating body size in this way may allow inferences to be made about individual fossil specimens. For instance, if a particularly small body size is estimated for a fossil specimen, that is not consistent with the average observed size for any adult agamid, then it is possible that particular specimen is from a juvenile. Furthermore, there are only a certain few extant Australian agamids have an average adult SVL larger than 150 mm (Wilson and Swan, 2013), these include *Chlamydosaurus kingii* (258 mm), *Intellagama lesueurii* (245 mm), *Pogona barbata* (250 mm), and *Pogona vitticeps* (250 mm). Therefore, assuming that there has been no significant body size evolution, we can narrow down the possible comparative species pool for further analyses that use apomorphic characters (Bell et al., 2010; Stilson et al., 2017), or landmarks (Gray et al., 2017). The largest specimens from Wet Cave are most likely to be comparable to species of *Pogona*, since the historical and current distributions of *Chlamydosaurus* and *Intellagama* are both considerably more northern. At the other end of the scale, the smallest specimen (SVL estimate of 51.83 mm), from Kelly Hill Caves, is likely to be a juvenile, since there are relatively few agamids (but still some possibilities, e.g. *Ctenophorus chapmani*) with a recorded adult size this small. Even though some species are this small as adults, most of these have a different geographical distribution, such that the likelihood of them occurring in this deposit is low.

Identifying biases, such as the tendency towards smaller animals that we observe in the Blanche Cave and Kelly Hill Caves deposits, is important. The skulls of agamid lizards have been shown to vary dramatically through growth (see Chapter 4), such that a young dragon of a particular species may look more similar to a different dragon species that it does to its own adult counterpart. Current comparative skeletal data sets largely comprise adult representatives of

species, and therefore, if fossils are from juvenile animals, they may not be morphologically comparable. Any indication of body size bias may lead to further investigation into the way fossils are accumulated in their respective deposits. For example, animals that prey on lizards and transport them to caves may find smaller lizards easier to kill or carry, whether they are juveniles or smaller species (e.g. Leopole and Wolfe, 1970; Debus et al., 2004). A bias towards smaller lizards might also be indicated by observations of abundant juvenile lizards taking refuge in a particular cave (Reed, 2018) matched with an abundance of juveniles in the fossil assemblage in that cave (in less damaged specimens, juveniles can be identified by an underdeveloped tooth row). This kind of information about modes of accumulation can help palaeontologists make more informed interpretations of specific faunal assemblages.

There is a strong correlation between SVL and body mass in other squamate families that occur in the Australian fossil record, including Gekkonidae, Scincidae, and Varanidae (Meiri, 2010). Like agamids, their jaw bones are also commonly recovered from Australian fossil deposits (Hutchinson and Mackness, 2002; Archer et al., 2006; Reed and Bourne, 2009; Hollenshead et al., 2010). It is likely that tooth row lengths from other small reptile groups may be used in the same way to infer body size in the fossil record. Assembling an assortment of coefficients to estimate body size from jaw bones of other Australian reptiles would provide a useful resource for palaeontologists, and would allow inferences to be made about the accumulation and taphonomy processes in cave deposits, as well as contributing to palaeoenvironmental interpretations about reptile assemblages.

Supplementary material

Electronic files

File ES7.1 – Specimen numbers with tooth row length and snout-vent length data (CSV).

References

Archer M, Arena DA, Bassarova M, Beck RMD, Black K, Boles WE, Brewer P, Cooke BN, Crosby K, Gillespie A, Godthelp H, Hand SJ, Kear BP, Louys J, Morrell A, Muirhead J, Roberts KK, Scanlon JD, Travouillon KJ, Wroe S. 2006. Current status of species-level representation in faunas from selected fossil localities in the Riversleigh World Heritage Area, northwestern Queensland. Alcheringa 30:1-17.

Behrensmeyer AK. 1984. Taphonomy and the fossil record: the complex processes that preserve organic remains in rocks also leave their own traces, adding another dimension of information to fossil samples. Am Sci 72:558-566.

Bell CJ, Gauthier JA, Bever GS. 2010. Covert biases, circularity and apomorphies: a critical look at the North American Quaternary Herpetofaunal Stability Hypothesis. Quat Int 217:30-36.

Bell CJ, Mead JI. 2014. Not enough skeletons in the closet: collections-based anatomical research in an age of conservation conscience. Anat Rec 297:344-348.

Campione NE. 2017. Extrapolating body masses in large terrestrial vertebrates. Paleobiology 43:693-699.

Cogger H. 2014. Reptiles and amphibians of Australia, 7th ed. Collingwood: CSIRO Publishing.

Cooper JWE, Stankowich T. 2010. Prey or predator? Body size of an approaching animal affects decisions to attack or escape. Behav Ecol 21:1278-1284.

Debus S, Olsen J, Rose A. 2004. Diet of the barn owl *Tyto alba* near lake frome in arid South Australia. Corella 28:40-42.

Esteban M, Castanet J, Sanchiz B. 1995. Size inferences based on skeletal fragments of the common European frog *Rana temporaria*. Herpetol J 5:229-235.

Farlow JO, Hurlburt GR, Elsey RM, Britton ARC, Langston W. 2005. Femoral dimensions and body size of *Alligator mississippiensis*: estimating the size of extinct mesoeucrocodylians. J Vert Palaeontol 25:354-369.

Finarelli JA, Flynn JJ. 2006. Ancestral state reconstruction of body size in the Caniformia (Carnivora, Mammalia): the effects of incorporating data from the fossil record. Syst Biol 55:301-313.

Garland T. 1985. Ontogenetic and individual variation in size, shape and speed in the Australian agamid lizard *Amphibolurus nuchalis*. J Zool 207:425-439.

Gingerich PD, Smith BH, Rosenberg K. 1982. Allometric scaling in the dentition of primates and prediction of body weight from tooth size in fossils. Am J Phy Anthropol 58:81-100.

Grabowski M, Hatala KG, Jungers WL, Richmond BG. 2015. Body mass estimates of hominin fossils and the evolution of human body size. J Hum Evol 85:75-93.

Graham RW, Grimm EC. 1990. Effects of global climate change on the patterns of terrestrial biological communities. TREE 5:289-292.

Gray JA, McDowell MC, Hutchinson MN, Jones MEH. 2017. Geometric morphometrics provides an alternative approach for interpreting the affinity of fossil jaws. J Herpetol 51:375-382.

Gregory P. 1986. Body size of insular lizards: a pattern of Holocene dwarfism. Evolution 40:997-1008.

Hollenshead MG, Mead JI, Swift SL. 2010. Late Pleistocene *Egernia* group skinks (Squamata: Scincidae) from Devils Lair, Western Australia. Alcheringa 35:31-51.

Huey RB, Hertz PE. 1982. Effects of body size and slope on sprint speed of a lizard (*Stellio (Agama) stellio*). J Exp Biol 97:401-409.

Huey RB, Hertz PE. 1984. Effects of body size and slope on acceleration of a lizard (*Stellio Stellio*). J Exp Biol 110:113-123.

Hugall AF, Foster R, Hutchinson M, Lee MSY. 2008. Phylogeny of Australian agamid lizards based on nuclear and mitchondrial genes: implications for morphological evolution and biogeography. Biol J Linnean Soc 93:343-358.

Hurlburt G. 1999. Comparison of body mass estimation techniques, using recent reptiles and the pelycosaur *Edaphosaurus boanerges*. J Vert Palaeontol 19:338-350.

Hutchinson MN, Mackness BS. 2002. Fossil lizards from the Pliocene Chinchilla Local Fauna, Queensland, with a description of a new species. Rec Sth Aus Mus 35:169-184.

Leopole A, Wolfe T. 1970. Food habits of nesting wedge-tailed eagles, *Aquila audax,* in south-eastern Australia. CSIRO Wildl Res 15:1-17.

Lyons SK. 2005. A quantitative model for assessing community dynamics of Pleistocene mammals. Am Nat 165:E168-E185.

Meiri S. 2010. Length–weight allometries in lizards. J Zool 281:218-226.

Peters RH, Peters RH. 1986. The ecological implications of body size. Vol 2: Cambridge University Press.

Reed EH. 2018. Personal observation: juvenile dragons observed to commonly occur in caves at Naracoorte Caves, South Australia.

Reed EH, Bourne SJ. 2009. Pleistocene fossil vertebrate sites of the south east region of South Australia II. Trans R Soc S Aust 133:30-40.

Schmidt-Nielsen K. 1984. Scaling: why is animal size so important? Cambridge University Press.

Slavenko A, Tallowin OJ, Itescu Y, Raia P, Meiri S. 2016. Late Quaternary reptile extinctions: size matters, insularity dominates. Global Ecol Biogeogr 25:1308-1320.

Stilson KT, Bell CJ, Mead JI. 2017. Patterns of variation in the cranial osteology of three species of endemic Australian lizards (*Ctenophorus*: Squamata: Agamidae): implications for the fossil record and morphological analyses made with limited sample sizes. J Herpetol 51:316-329.

Vézina AF. 1985. Empirical relationships between predator and prey size among terrestrial vertebrate predators. Oecologia 67:555-565.

Wilson DS. 1975. The adequacy of body size as a niche difference. Am Nat 109:769-784.

Wilson S, Swan G. 2013. A complete guide to reptiles of Australia, 4th ed. Chatswood: New Holland Publishers.

Woodward G, Ebenman B, Emmerson M, Montoya JM, Olesen JM, Valido A, Warren PH. 2005. Body size in ecological networks. TREE 20:402-409.

Worthy TH. 2016. A review of the fossil record of New Zealand lizards. In: New Zealand lizards. Springer. p 65-86.

Young MT, Bell MA, De Andrade MB, Brusatte SL. 2011. Body size estimation and evolution in metriorhynchid crocodylomorphs: implications for species diversification and niche partitioning. Zool J Linnean Soc 163:1199-1216.

STATEMENT OF AUTHORSHIP

Title of Paper	Geometric morphometrics provides a more objective approach for interpreting the affinity of fossil lizard jaws
Publication Status	☑ Published ☐ Accepted for Publication ☐ Submitted for Publication ☐ Unpublished and Unsubmitted w ork w ritten in manuscript style
Publication Details	Published on 28.07.2017 in Journal of Herpetology, 51(3), pages 372-382.

Principal Author

Name of Principal Author (Candidate)	Jaimi Gray		
Contribution to the Paper	Designed research, data collection and analysis, wrote first version of manuscript, edited later versions of manuscript.		
Overall percentage (%)	80%		
Certification:	This paper reports on original research I conducted during the period of my Higher Degree by Research candidature and is not subject to any obligations or contractual agreements with a third party that would constrain its inclusion in this thesis. I am the primary author of this paper.		
Signature		Date	23.08.2018

Co-Author Contributions

By signing the Statement of Authorship, each author certifies that:

  i. the candidate's stated contribution to the publication is accurate (as detailed above);

  ii. permission is granted for the candidate in include the publication in the thesis; and

  iii. the sum of all co-author contributions is equal to 100% less the candidate's stated contribution.

Name of Co-Author	Matthew C. McDowell		
Contribution to the Paper	Excavated fossil specimen, and edited manuscript.		
Signature		Date	23-08-2018

Name of Co-Author	Mark N. Hutchinson		
Contribution to the Paper	Helped design research, and edited manuscript.		
Signature		Date	28/08/2018

Name of Co-Author	Marc E. H. Jones		
Contribution to the Paper	Helped design research, provided guidance for data analysis, and edited manuscript.		
Signature		Date	23rd August 2018

CHAPTER 8

Geometric morphometrics provides a more objective approach for interpreting the affinity of fossil jaws

CHAPTER 8 – Geometric morphometrics provides a more objective approach for interpreting the affinity of fossil lizard jaws

Jaimi A. Gray, Matthew C. McDowell, Mark N. Hutchinson, Marc E. H. Jones

Abstract

The jaws of lizards commonly occur in Quaternary fossil deposits and have the potential to inform our understanding of recent changes in climate and environment. However, interpretation of their taxonomic affinity is frequently difficult due to lack of morphological characters and identifications are sometimes no more than subjective visual comparisons. Here, we evaluate the taxonomic affinity of a maxilla from the Holocene of Kelly Hill Caves (Kangaroo Island, South Australia) by comparison to a sample of modern agamid lizards using computer models generated from X-ray computed tomography data and three-dimensional geometric morphometrics. To represent the shape of the maxilla we used 22 fixed landmarks and 30 semi-landmarks placed at equivalent points on the three-dimensional surface files of the maxillae. Procrustes distances show that with respect to overall shape difference, the fossil does not closely resemble *Ctenophorus decresii*, which is the only agamid currently present on Kangaroo Island. Preliminary comparisons to other candidate agamid taxa from southeastern Australia suggest instead that the fossil is most similar to *Amphibolurus muricatus* and *A. norrisi* and least similar to *Tympanocryptis lineata*. Geometric morphometrics shows promise as a more objective means of quantifying and characterising shape differences. However, reliable identifications require sufficient specimen collections that include ontogenetic and other sources of variation.

Keywords*: Agamidae, geometric morphometrics, Holocene, landmarks, maxilla, morphology, Squamata, taxonomy

Introduction

The study of fossils provides a unique window for research into the evolutionary history of taxa. The age, geographic origin, and palaeoenvironment of fossils provide important sources of evidence for the evolution of morphological characters, past distribution of taxa, and wider environmental changes. This is particularly true for recent fossils (< 500 ka) that may have close living relatives or even represent living species with ecological tolerances that are well understood. However, for such fossils to be of any use, it must first be possible to identify them to some taxonomic level with confidence. The reliability of the alpha taxonomy is of high importance because it is often used in broader studies to quantify past changes in diversity or constrain molecular divergence analyses (e.g. Bell et al., 2010; Parham et al., 2012; Mannion et al., 2015; Slavenko et al., 2016).

The Holocene-Pleistocene fossil reptile assemblages of Australia have not been well studied in comparison with their mammal counterparts (e.g. Travouillon et al., 2006). Members of reptile clades can be found in samples from many fossil localities, potentially representing most of the major components of an exceptionally diverse living squamate fauna. However, interpretation is inhibited by a poor understanding of reptile osteology at low taxonomic levels and an inability to make objective comparisons. Variation within and between species tends to involve subtle differences in the shapes of processes, and relative proportions which can be a challenge to compare holistically (Evans, 2008; Hollenshead et al., 2010; Sherratt et al., 2015). Specific characters can be defined and used as apomorphies (e.g. Hutchinson, 1997), but this requires some baseline knowledge of variation within the taxon being examined, and such data may not be available (Bell and Mead, 2014). Many skeletal collections lack adequate samples of lizards and the published descriptions and images can be of limited use because they are most often focused on the articulated cranium as a whole. The taxonomy of modern species tends to be derived from analysis of genetic data and external characters (e.g. scale number, proportions) and does not tend to provide any information on osteological characters (e.g. McLean et al., 2013). Authors documenting fossils tend to provide outline drawings or photographs of specimens (Covacevich et al., 1990; Hocknull et al., 2007; Prasad and Bajpai, 2008) which assist in broad comparisons but cannot convey the full three-dimensional aspect of the bones. Tooth positions can provide more objective comparisons (e.g. Hollenshead et al., 2010), but our understanding of the extent of associated variation in all taxa is poorly developed. Moreover, it may not be possible to count tooth positions in a fossil due to tooth wear or breakage.

Although it has yet to be widely applied to the isolated bones of Quaternary reptile fossils, geometric morphometrics provides an alternative and potentially more objective approach for characterising and comparing them (Adams et al., 2004). For comparing anatomical structures it generally involves the use of landmarks and outlines to quantify variation amongst specimens and analyses require multivariate statistics. Geometric morphometrics is considered superior to previous forms of biometrics (e.g. isolated linear measurements) because it records the geometric relationship between a cloud of landmarks, or set of curves, and thus provides a holistic measurement of overall shape in contrast to isolated linear measurements (Adams and Collyer, 2009). This facilitates standardisation between specimens of different size via Procrustes superimposition and permits visualisations that aid interpretation. Over the past decade geometric morphometrics has become an increasingly accessible approach for morphological analyses, and has been used to characterise and compare shape variation amongst two-dimensional images of reptile skulls (e.g. Stayton, 2005; Jones, 2008; Meloro and Jones, 2012; Sanger et al., 2013; Fabre et al., 2014; Openshaw et al., 2016), and it has also been applied to three-dimensional reptile anatomy using X-ray computed tomography (Parr et al., 2012; McCurry et al., 2015). In at least one case it has been used as an approach to associate fossils with modern taxa (Dollion et al., 2015).

Here we use three-dimensional (3D) geometric morphometrics (see Zelditch et al., 2012) to more objectively characterise the maxillae of modern agamid lizards from southern Australia to facilitate comparisons with a recent (< 20 ka) fossil specimen from Kangaroo Island. *Ctenophorus decresii* is the only agamid species present on Kangaroo Island today but fossil remains provide the opportunity to discover whether different taxa were present there in the past.

Material and methods

Fossil Material

We analysed an almost complete agamid fossil maxillae (South Australian Museum specimen P53917) from Kelly Hill Caves on Kangaroo Island. The specimen was recovered from sediments with an age range of 11,645–10,360 years before present (95% confidence interval), according to a chronological model developed by MCM using Bayesian analysis. The fossil assemblage was carefully excavated layer by layer and dated using U-Th dating of speleothems, AMS radiocarbon-dating of bone, and optically stimulated luminescence of quartz grains. Excavated sediment was wet-sieved using 1.5 mm mesh. The residues of small vertebrate remains were dried then sorted (picked) for taxonomically identifiable specimens. The specimen examined here is entirely removed from the matrix and has excellent surface preservation clearly showing the location of foramina and sutural facets (see Fig. 8.1). It is essentially complete except that the distal edges of the posterodorsal process may be rounded and a portion of the dorsal edge of the facial process is broken and missing.

Modern Material

We characterised ten modern species, each represented by a single specimen from South Australian Museum: *Amphibolurus muricatus* (R21375), *A. norrisi* (R60767), *Ctenophorus decresii* (R28618), *C. fordi* (R34489), *C. pictus* (R28608), *Pogona barbata* (R32503), *P. vitticeps* (R18545), *Tympanocryptis lineata* (R59721), and *Rankinia diemensis* (R269B). These taxa represent agamids living in South Australia today or that have been reported from South Australian fossil deposits (Reed and Bourne, 2009; Government of South Australia, 2013). Our set of specimens was intended to be a minimum sampling in order to assess the ease with which different species could be characterised, and used as a pilot data set for comparison of the modern fauna with recent fossils.

The fossil specimen was subjected to micro X-ray computed tomography (CT) at Adelaide Microscopy using a Bruker Skyscan 1076 at a resolution of 9 microns. CT scan reconstructions were obtained for each comparison species from the scanned specimen database at South Australian Museum. All CT scans used in this study were reconstructed using NRecon software provided by the scanner manufacturer (NRecon, version 1.6.9.4, Skyscan, Kontich, Belgium). The reconstructed scans were digitally segmented to extract the right maxilla from the cranium, and surface files were created using the "segmentation editor" in Avizo v 8.1 (Visualization Sciences Group, 2013) with minimal smoothing (Fig. 8.1, see also supplementary material: File ES8.1 for ply files).
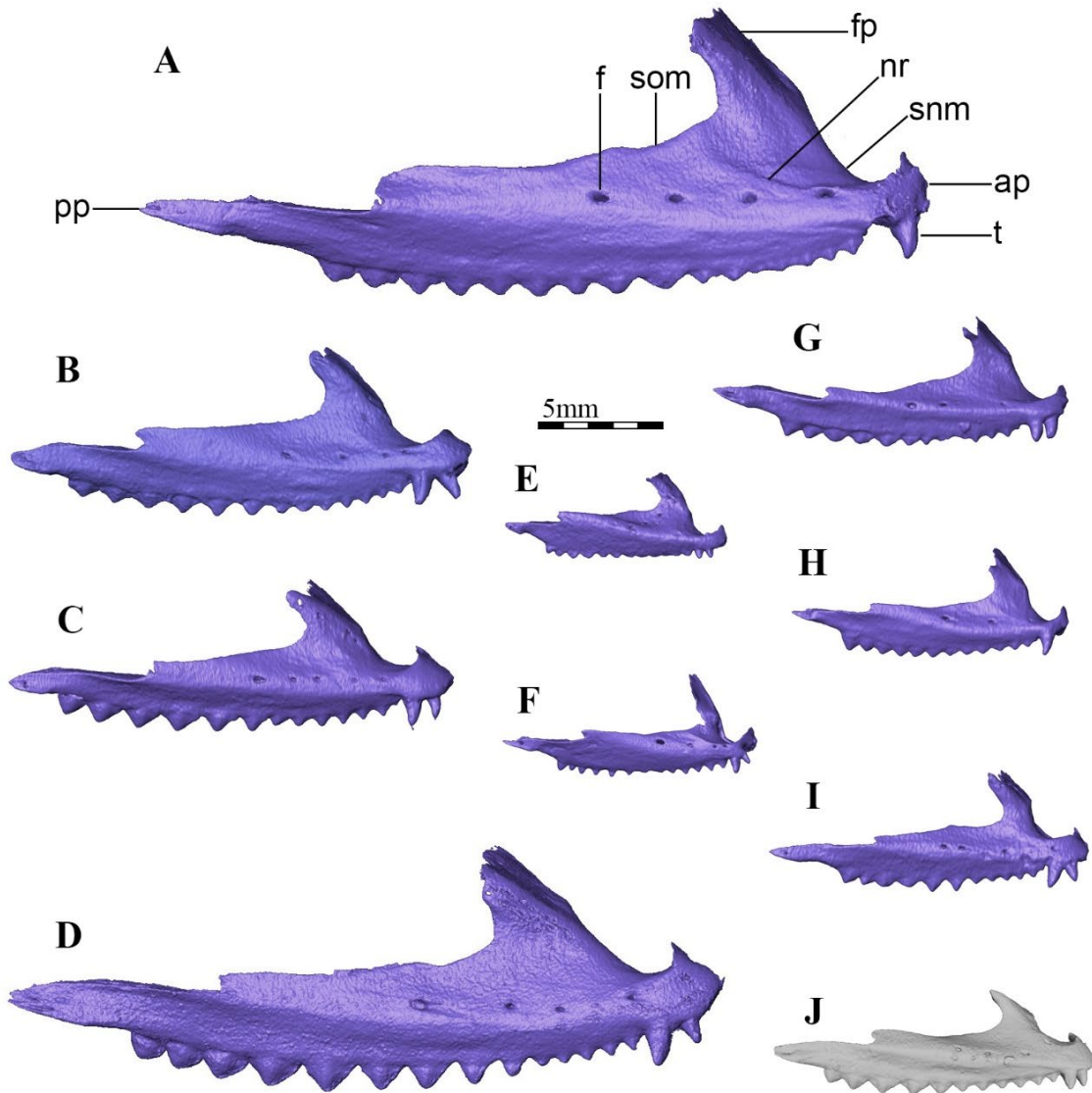
Figure 8.1 – Computer models of agamid maxillae surfaces in labial view. Specimens (all from South Australian Museum): A, *Pogona vitticeps* **(R18545); B,** *Amphibolurus muricatus* **(R34730); C,** *A. norrisi* **(R60767); D,** *P. barbata* **(R32503); E,** *Ctenophorus fordi* **(R34489); F,** *Tympanocryptis lineata* **(R59721); G,** *C. decresii* **(R28618); H,** *C. pictus* **(R28608); I,** *Rankinia diemensis* **(R269B); J, unnamed fossil (P53917). Abbreviations: ap, anterior process; f, foramen; fp, facial process; nr, narial ridge; pp, posterior process; snm, subnarial margin; som, suborbital margin; t, tooth. Scale bar is 5mm.**

Landmarking

Landmarks were placed on the surface files of the fossil and comparative maxillae using the software package "IDAV Landmark" (Institute for Data Analysis and Visualisation, 2005). Twenty-two fixed landmarks and 30 semi-landmarks were placed at equivalent points on the 3D surface files: at the most extreme points of particular features, and along the major curves (shown in Fig. 8.2, see also supplementary material: Table S8.1 for landmark definitions and Fig. S8.1 for nomenclature). Each fixed landmark consists of a single point on the surface of the bone with x, y, z coordinates, and each semi-landmark is part of a collection of ten evenly spaced points along a curve (see supplementary material: File ES8.2 for coordinates). For the fossil specimen, missing landmarks (2 and 7) were estimated using a multivariate regression method (where each landmark with missing values is regressed on all other landmarks for the set of complete specimens, and the missing landmark values are predicted by this linear regression model), using the "estimate.missing" function in the R package *geomorph* (Adams and Otárola-Castillo, 2013).
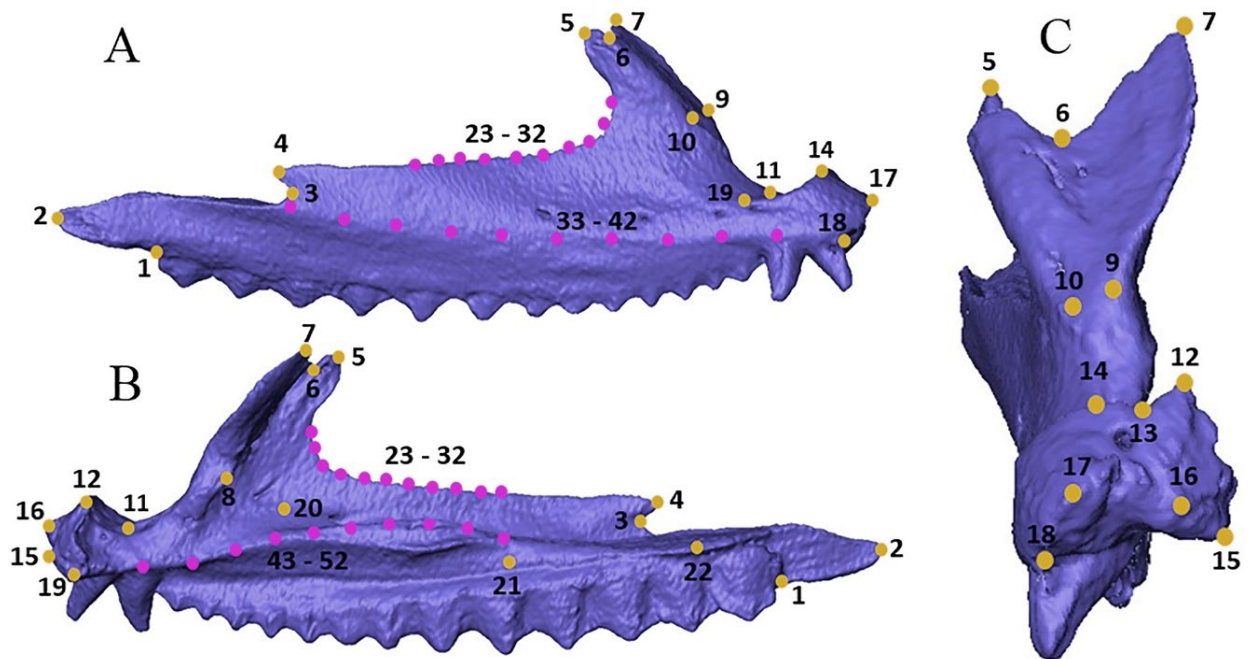
Figure 8.2 – Landmarks used in this study. Single point landmarks are shown in orange, semi-landmarks are shown in pink. Surface model of an example maxilla shown in labial view (A), lingual view (B), and anterior view (C). See supplementary material: Figure S8.1 for nomenclature used to describe landmarks, and Table S8.1 for corresponding landmark definitions.

Shape Analysis

We repeated the following analysis on two data sets: one data set contained all the extant comparison specimens, and the other contained all the extant comparison specimens and fossil specimen P53917. Both the Procrustes superimposition and principal component analysis (PCA) were carried out using the R package *geomorph*.

We performed a Procrustes superimposition to scale the sets of landmarks and fit the shapes to each other, to remove the shape differences related to absolute size (but not shape allometry) (Rohlf and Slice, 1990). This effectively fitted the landmark constellations around a mean constellation. Two distance matrices containing the Procrustes distances between each specimen for both data sets were calculated using *geomorph* in R, which provided an explicit and quantitative measure of overall shape similarity. Semi-landmark tangent sliding directions were specified using the "Procrustes distance criterion" (Bookstein, 1997). Next, we performed a PCA to find the linear combination of variables that represent maximum variance within the current specimen sample. A Mantel test (Mantel, 1967) was performed in R to evaluate the similarity of the Procrustes distances of the extant specimens resulting from analysis of both data sets.

We used the *geomorph* R package to first produce a mesh whose shape was defined by the mean shape of its landmark coordinates. We then warped this mesh into the shapes represented by the maximum and minimum values of PC1 and PC2. This provided a visualisation of the PCA results from which we could determine major shape differences for PC1 and PC2. All mesh warping was performed using the thin-plate spline method (Bookstein, 1989).

Results

Extant Specimens

The Procrustes distances (see top triangle of Table 8.1), indicate that the species pairs closest to one another in overall shape are *Amphibolurus muricatus - A. norrisi*, *A. muricatus - Ctenophorus pictus*, *A. norrisi - Pogona barbata*, and *C. pictus - P. vitticeps*. The two taxa most dissimilar to others are *C. fordi* and *Tympanocryptis lineata*, with quite large Procrustes distances between them and other specimens included in the analysis. The species-pairs most dissimilar to one another were *T. lineata - A. norrisi* and *T. lineata - C. fordi*. *Ctenophorus decresii* is most similar to *C. pictus*.

The PCA (Fig. 8.3) reveals that PC1 (34.9% of total shape variation) describes shape differences involving the anterior process, where it ranges from being relatively deep at negative values (e.g. *A. norrisi*), to relatively shallow at positive values (e.g. *T. lineata*). It also describes the shape of the facial process, from a swept back process that is relatively broad at its base at more negative values (e.g. *P. vitticeps*), to an upright process that is narrow at its base, at more positive values (e.g. *T. lineata*). The overall shape also contrasts between a dorsoventrally deep maxilla at more negative values, to a more dorsoventrally shallow maxilla at more positive values. Maxillary shape associated with minimum and maximum values of PC1 are shown in Figure 8.4.

PC2 (21.0% of variance) describes differences in shape of the suborbital margin, which is quite smooth at more positive values (see *A. norrisi*), and more irregular at more negative values (see *C. fordi*). The subnarial margin also contrasts considerably in shape, from being small and having an upright anterior margin at negative values, to being large with a sloped anterior margin at more positive values. The anterior process graduates from having a subtle bifurcation at negative values, to having a pronounced bifurcation at positive values. The shape of the maxillae for this PC differs from being curved along the long axis at negative values, to being relatively straight at positive values. Maxillary shape associated with minimum and maximum values of PC2 are shown in Figure 8.4. PC1 mainly recognises the difference between *T. lineata* and other agamids whereas PC2 mainly recognises the difference between species of *Ctenophorus*. *Amphibolurus muricatus* and *A. norrisi* have similar scores for PC1 and PC2. This is also true for *P. barbata* and *P. vitticeps*. The three species of *Ctenophorus* have similar scores for PC1. As indicated by the Procrustes distances, *T. lineata* and *C. fordi* are particularly different to everything else in the sample, plotting at extremes of PC1 and 2 respectively. PC3 (17.0%) mainly recognises the difference between *P. vitticeps* and *P. barbata* whereas PC4 (9.7%) recognises the differences between *Rankinia diemensis* and all other agamids.

Table 8.1 – **Pairwise Procrustes distances. Top triangle: all the extant comparison specimens included in the analysis. Bottom triangle: all the extant comparison specimens included in the analysis, after the inclusion of a not yet identified fossil specimen. Colours: closer pairwise distances in darker shades of green. Abbreviations: AM,** *A. muricatus*; **AN,** *A. norrisi*; **CD,** *C. decresii*; **CF,** *C. fordi*; **CP,** C. pictus; **PB,** *P. barbata*; **PV,** *P. vitticeps*; **RD,** *R. diemensis*; **TL,** *T. lineata*; **FS, fossil specimen.**

	AM	AN	CD	CF	CP	PB	PV	RD	TL
AM		0.083	0.119	0.156	0.095	0.115	0.107	0.107	0.202
AN	0.083		0.128	0.167	0.115	0.096	0.14	0.116	0.211
CD	0.118	0.127		0.133	0.104	0.113	0.148	0.126	0.172
CF	0.155	0.166	0.132		0.141	0.165	0.173	0.153	0.209
CP	0.094	0.114	0.103	0.14		0.119	0.097	0.112	0.158
PB	0.114	0.096	0.112	0.164	0.118		0.154	0.133	0.192
PV	0.106	0.139	0.147	0.172	0.096	0.152		0.136	0.205
RD	0.107	0.115	0.125	0.151	0.112	0.132	0.135		0.194
TL	0.199	0.208	0.169	0.206	0.155	0.189	0.202	0.191	
FS	0.112	0.117	0.138	0.162	0.123	0.14	0.127	0.121	0.209
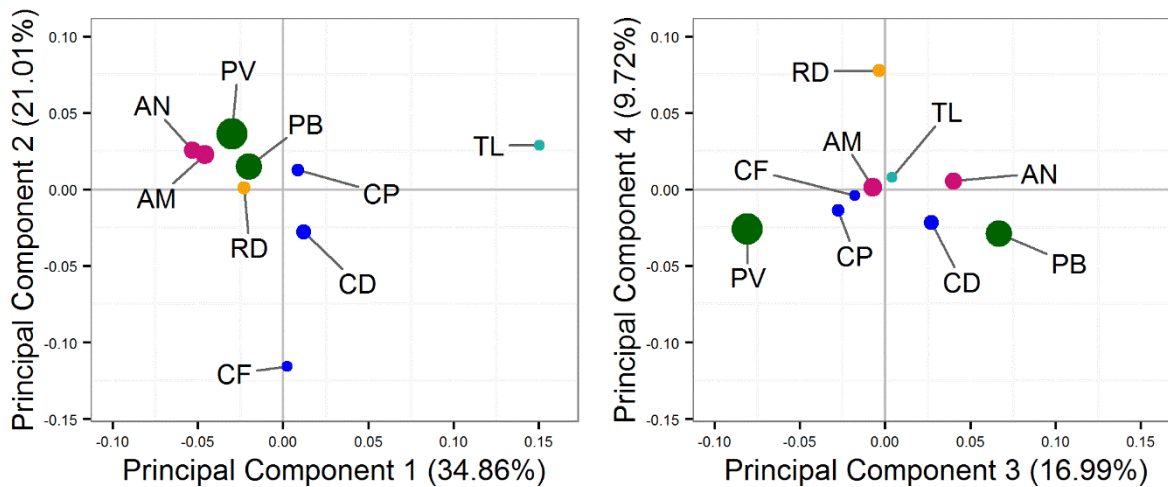
Figure 8.3 – **Principal component analysis results showing the major axes of variation amongst a sample of maxillae from extant agamid lizards. Left: PC1 vs. PC2. Right: PC3 vs. PC4. Points scaled according to centroid size. Abbreviations; AM,** *A. muricatus*; **AN,** *A. norrisi*; **CD,** *C. decresii*; **CF,** *C. fordi*; **CP,** *C. pictus*; **PB,** *P. barbata*; **PV,** *P. vitticeps*; **RD,** *R. diemensis*; **TL,** *T. lineata*.
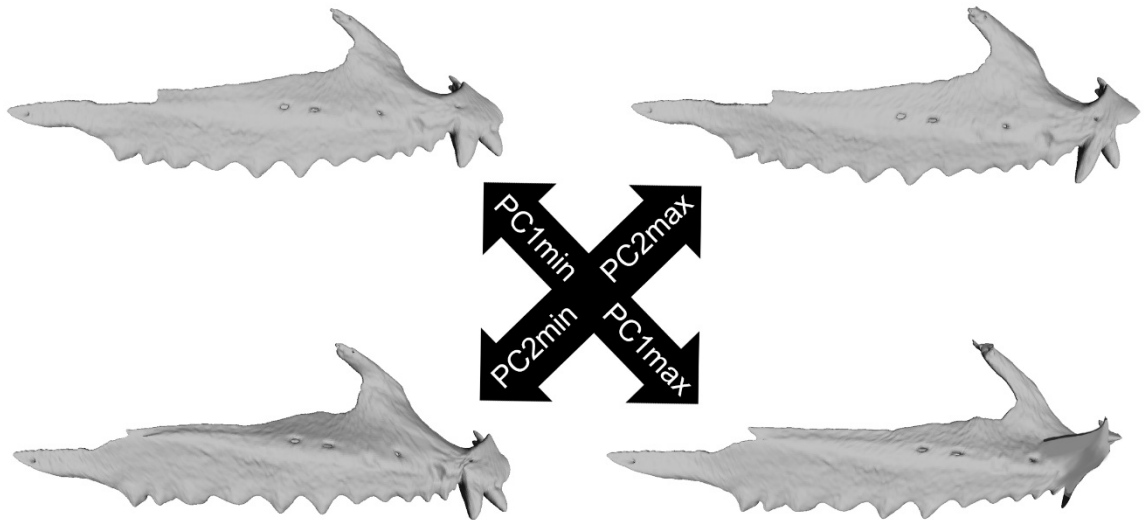
Figure 8.4 – Warped surface meshes (produced using the thin-plate spline method), in labial view, that represent the shape of the maxillae at the minimum and maximum values of PC1 and PC2.

Fossil Specimen

The Procrustes distances of the fossil specimen (see bottom triangle of Table 8.1) show that it is most similar in shape to *A. muricatus*, and least similar to *T. lineata*. The fossil is also quite dissimilar to *C. decresii.* A Mantel test comparing the Procrustes distances between extant specimens for both data sets produced an observed correlation coefficient of 0.999, and a *P*-value of 0.001 (at 999 permutations). These results indicate that the inclusion of the fossil specimen does not greatly alter the distances between the modern specimens. The pairs which are most similar (*A. muricatus-A. norrisi*) or dissimilar (*T. lineata-A. norrisi*) amongst the extant samples remain the same.

The fossil has scores for both PC1 and PC2 (together 51.6 % of total shape variation, see Fig. 8.5) that are similar to those of the two species of *Amphibolurus* having a relatively deep anterior process, swept back facial process that is wider ventrally, and deeper in shape dorso-ventrally. With respect to PC3 (15.6%), the fossil has similar scores to *C. pictus* and *C. fordi* and for PC4 (9.6%) it has similar scores to *R. diemensis*. Inclusion of the fossil in the PCA has little effect on the shape differences described by the main axes of shape variation (PCs 1–4) or the distribution of the extant species on those PCs. The fossil does not plot near *C. decresii* on any of the four main axes of variation (76.8%).
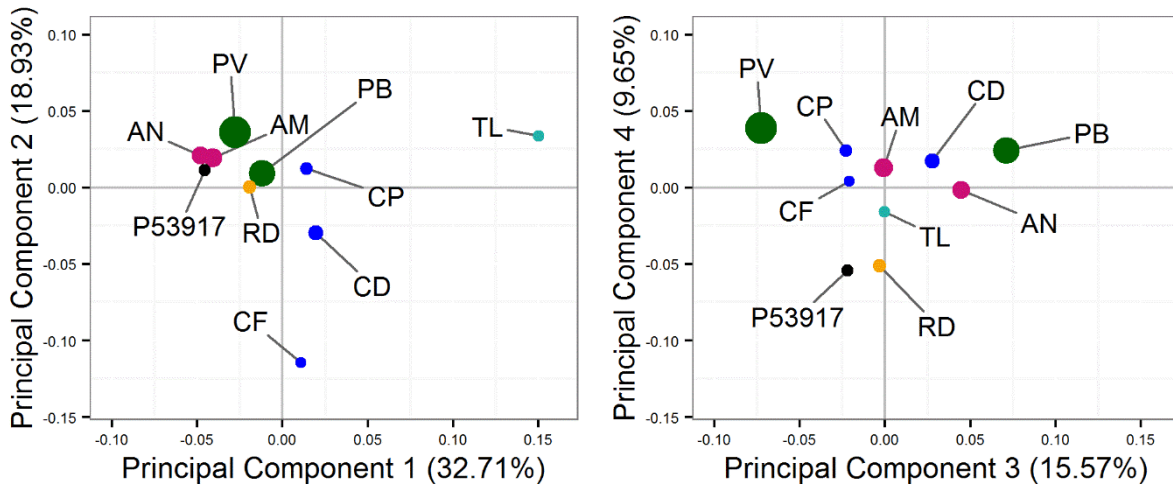
Figure 8.5 – Principal component analysis results showing the major axes of variation amongst a sample of maxillae from extant agamid lizards after inclusion of a not yet identified fossil specimen, P53917. Left: PC1 vs. PC2. Right: PC3 vs. PC4. Points scaled according to centroid size. Abbreviations; AM, *A. muricatus***; AN,** *A. norrisi***; CD,** *C. decresii***; CF,** *C. fordi***; CP,** *C. pictus***; PB,** *P. barbata***; PV,** *P. vitticeps***; RD,** *R. diemensis***; TL,** *T. lineata.*

Discussion

The fossil maxilla does not have a shape consistent with that of *C. decresii,* the only agamid currently present on Kangaroo Island. Instead, it most closely resembles the maxilla of species of *Amphibolurus*. One species, *A. norrisi,* currently occurs on two mainland areas immediately adjacent to Kangaroo Island (southern Yorke and Eyre Peninsulas), suggesting a good habitat match for this species with Kangaroo Island. If this was the species present, its loss from the island could be explicable by the isolation of the island at 9 ka (Adams et al., 2015), possibly due to the cooling effect of the surrounding ocean, or as a consequence of the island area effect (MacArthur and Wilson, 2001). Confident allocation of the fossil specimen will require greater sampling of the living candidate species, (*A. norrisi* and *A. muricatus*), both to ensure that these two can be distinguished from each other and to demonstrate to a higher degree of probability that the fossil falls within their range of variation. However it is notable that even single individuals of the candidate species appear to provide a useful framework for comparing the shape of the fossil and evaluating its likely identity. Our results provide the first evidence that in the past 20,000 years Kangaroo Island supported a different and possibly more diverse reptile fauna.

Geometric morphometric analysis of 3D scans provides a very promising approach for more objective comparisons of microvertebrate fossils. Previous geometric morphometric analyses of reptiles were carried out on the complete cranial structure, but we show here that a similar approach may be used for the analyses of the isolated elements often recovered in fossil deposits. Although the sample size in our pilot study limits our interpretations, we are still able to provide a repeatable, explicit, and quantitative index of the overall shape differences between specimens and can examine the relative distribution of the specimens in an empirical shape space. A larger sample size could be expected to allow much greater discrimination power (Close and Rayfield, 2012; Wilson et al., 2013). This approach would be a potentially powerful tool for analysis of new fossils and evaluation of previous identifications (e.g. Holman and Case, 1988; Hsio et al., 2016).

The method remains somewhat subjective with respect to landmark choice and sample used, but, once established, it allows explicit comparisons in terms of similarities and differences in shape. We chose landmarks with the aim of providing the best and most balanced representation of the bone shape and also so that they may be placed unambiguously on every specimen under the same definition (see supplementary material: Figure S8.1 and Table S8.1). Although we made our best effort to get the most likely species for comparison, it remains

possible that the deposits contain taxa that we did not include in our data set. Nevertheless the extreme unlikelihood of some matches may still be indicated. Although we acknowledge that a simple equivalence between a fossil and a similarly shaped living species risks over-interpretation (Bell et al., 2010), nevertheless it seems likely that the most successful comparisons will be with the younger sites where it is increasingly probable that the number of extinct species is lower. Geometric morphometrics thus adds another tool to reduce the subjectivity and "covert biases" noted by Bell et al. (2010).

The ability to estimate missing landmarks removes a long standing restriction of geometric morphometrics (Arbour and Brown, 2014). Before that development, missing landmarks needed to be removed from all specimens in the analysis, effectively excluding much of the shape information captured by the respective landmarks. This approach maximises the morphometry of all specimens, increasing the power to discriminate between species despite within species variance.

Acknowledgements

Supplementary material

Figures

Tables

Electronic files

File ES8.1 – Folder containing ply surface models of all specimens used in the analyses (file folder).

File ES8.2 – Folder containing separate DTA files of 3D landmark coordinates from maxillae models (file folder).

References

Adams DC, Collyer ML. 2009. A general framework for the analysis of phenotypic trajectories in evolutionary studies. Evolution 63:1143-1154.

Adams DC, Otárola-Castillo E. 2013. geomorph: an R package for the collection and analysis of geometric morphometric shape data. Methods Ecol Evol 4:393-399.

Adams DC, Rohlf FJ, Slice DE. 2004. Geometric morphometrics: ten years of progress following the 'revolution'. Ital J Zool 71:5-16.

Adams SJ, McDowell MC, Prideaux GJ. 2015. Understanding accumulation bias in the ecological interpretation of archaelogical and paleontological sites on Kangaroo Island, South Australia. J Archaeol Sci Rep 7:715-729.

Arbour JH, Brown CM. 2014. Incomplete specimens in geometric morphometric analyses. Methods Ecol Evol 5:16-26.

Bell CJ, Gauthier JA, Bever GS. 2010. Covert biases, circularity and apomorphies: a critical look at the North American Quaternary Herpetofaunal Stability Hypothesis. Quat Int 217:30-36.

Bell CJ, Mead JI. 2014. Not enough skeletons in the closet: collections-based anatomical research in an age of conservation conscience. Anat Rec 297:344-348.

Bookstein FL. 1989. Principal warps: thin-plate splines and the decomposition of deformations. IEEE Trans Pattern Anal Mach Intell 11:567-585.

Bookstein FL. 1997. Landmark methods for forms without landmarks: morphometrics of group differences in outline shape. Med Image Anal 1:225-243.

Close RA, Rayfield EJ. 2012. Functional morphometric analysis of the furcula in Mesozoic birds. PLOS ONE 7:e36664.

Covacevich J, Couper P, Molnar RE, Witten G, Young W. 1990. Miocene dragons from Riversleigh: new data on the history of the family Agamidae (Reptilia: Squamata) in Australia. Mem Queensl Mus 29:339-360.

Dollion AY, Cornette R, Tolley KA, Boistel R, Euriat A, Boller E, Fernandez V, Stynder D, Herrel A. 2015. Morphometric analysis of chameleon fossil fragments from the Early Pliocene of South Africa: a new piece of the chamaeleonid history. Sci Nat 102:2.

Evans SE. 2008. The skull of lizards and tuatara. In: Gans C, Gaunt AS, Adler K, editors. Biology of the Reptilia 20, Morphology H, The skull of Lepidosauria. Ithaca: Society for the Study of Amphibians and Reptiles. p 1-347.

Fabre A-C, Cornette R, Huyghe K, Andrade DV, Herrel A. 2014. Linear versus geometric morphometric approaches for the analysis of head shape dimorphism in lizards. J Morphol 275:1016-1026.

Government of South Australia. 2013. Census of South Australian vertebrates, 4th Edition. Department of Environment, Water and Natural Resources.

Hocknull SA, Zhao J, Feng Y, Webb GE. 2007. Responses of Quaternary rainforest vertebrates to climate change in Australia. Earth Planet Sci Lett 264:317-331.

Hollenshead MG, Mead JI, Swift SL. 2010. Late Pleistocene *Egernia* group skinks (Squamata: Scincidae) from Devils Lair, Western Australia. Alcheringa 35:31-51.

Holman AJ, Case GR. 1988. Reptiles from the Eocene Talahatta Formation of Alabama. J Vert Paleontol 8:328-333.

Hsio AS, Schubert BW, Winck GR, Onary-Alves SY, Avilla LS. 2016. New Quaternary teiid (Lepidosauria, Squamata) lizard remains from Gruta Do Urso, Tocantins, Brazil. Rev Bras Paleontol 19:233-242.

Hutchinson MN. 1997. The first fossil pygopod (Squamata: Gekkota) and a review of mandibular variation in living species. Mem Queensl Mus 41:355-366.

Institute for Data Analysis and Visualisation. 2005. Landmark editor.

Jones MEH. 2008. Skull shape and feeding strategy in *Sphenodon* and other Rhynchocephalia. J Morphol 269:945-966.

MacArthur RH, Wilson EO. 2001. The theory of island biogeography: Princeton University Press.

Mannion PD, Benson RBJ, Carrano MT, Tennant JP, Judd J, Butler RJ. 2015. Climate constrains the evolutionary history and biodiversity of crocodylians. Nat Comm 6:8438.

Mantel N. 1967. The detection of disease clustering and a generalized regression approach. Cancer Res 27:209-220.

McCurry MR, Mahony M, Clausen PD, Quayle MR, Walmsley CW, Jessop TS, Wroe S, Richards H, Mchenry CR. 2015. The relationship between cranial structure, biomechanical performance and ecological diversity in varanoid lizards. PLOS ONE 10:e0130625.

McLean CA, Moussalli A, Sass S, Stuart-Fox D. 2013. Taxonomic assessment of the *Ctenophorus decresii* complex (Reptilia: Agamidae) reveals a new species of dragon lizard from western New South Wales. Rec Aust Mus 65:51-63.

Meloro C, Jones MEH. 2012. Tooth and cranial disparity in the fossil relatives of *Sphenodon* (Rhyncocephalia) dispute the persistent 'living fossil' label. J Evol biol 25:2194-2209.

Openshaw G, D'Amore DC, Vidal-Garcia M, Keogh JS. 2016. Combining geometric morphometric analyses of multiple 2D observation views improves interpretation of evolutionary allometry and shape diversification in monitor lizard (*Varanus*) crania. Biol J Linnean Soc 120:539-552.

Parham JF, Donoghue PCJ, Bell CJ, Calway TD, Head JJ, Holroyd PA, Inoue JG, Irmis RB, Joyce WG, Ksepka DT, Patané JSL, Smith ND, Tarver JE, van Tuinen M, Yang Z, Angielczyk KD, Greenwood JM, Hipsley CA, Jacobs L, Makovicky PJ, Müller J, Smith KT, Theodor JM, Warnock RCM, Benton MJ. 2012. Best practices for justifying fossil calibrations. Syst Biol 61:346-359.

Parr WCH, Wroe S, Chamoli U, Richards HS, McCurry MR, Clausen PD, McHenry C. 2012. Toward integration of geometric morphometrics and computational biomechanics: new methods for 3D virtual reconstruction and quantitative analysis of Finite Element Models. J Theor Biol 301.

Prasad GVR, Bajpai S. 2008. Agamid lizards from the early Ecocene of western India: oldest Cenozoic lizards from South Asia. Palaeontol Electron 11:4A-19p.

Reed EH, Bourne SJ. 2009. Pleistocene fossil vertebrate sites of the south east region of South Australia II. Trans R Soc S Aust 133:30-40.

Rohlf FJ, Slice DE. 1990. Extensions of the Procrustes method for the optimal superimposition of landmarks. Syst Zool 39:40-59.

Sanger TJ, Sherratt E, McGlothlin JW, Brodie EDI, Losos JB, Abzhanov A. 2013. Convergent evolution of sexual dimorphism in skull shape using distinct developmental strategies. Evolution 67:2180-2193.

Sherratt E, del Rosario Castañeda M, Garwood RJ, Mahler DL, Sanger TJ, Herrel A, de Queiroz K, Losos JB. 2015. Amber fossils demonstrate deep-time stability of Caribbean lizard communities. PNAS 112:9961-9966.

Slavenko A, Tallowin OJ, Itescu Y, Raia P, Meiri S. 2016. Late Quaternary reptile extinctions: size matters, insularity dominates. Global Ecol Biogeogr 25:1308-1320.

Stayton CT. 2005. Morphological evolution of the lizard skull: a geometric morphometrics survey. J Morphol 263:47-59.

Travouillon KJ, Archer M, Hand SJ, Godthelp H. 2006. Multivariate analyses of Cenozoic mammalian faunas from Riversleigh, northwestern Queensland. Alcheringa 30:323-349.

Visualization Sciences Group. 2013. Avizo. FEI Corporate Headquarters, Oregon.

Wilson LB, Furrer H, Stockar R, Sanchez-Villagra MR. 2013. A quantitative evaluation of evolutionary patterns in opercle bone shape in *Saurichthys* (Actinopterygii: Saurichthyidae). Palaeontology 56:901-915.

Zelditch ML, Swiderski DL, Sheets HD, Fink WL. 2012. Geometric morphometrics for biologists: a primer, 2nd ed. Academic Press.

CHAPTER 9

Summary and conclusions

CHAPTER 9 – Summary and conclusions

Addressing the primary aims

Collectively, the chapters of this thesis present the first in-depth quantitative exploration of variation in skull morphology within and among species of Australian dragon lizards. I have gathered a large amount of quantitative morphological data, at various taxonomic levels, characterised the variety of skull shapes seen in Australia's dragon lizards, and placed them in an ecological and evolutionary context. Since the arrival of their ancestor to Australia 30 million years ago (Ma), skulls of amphibolurine lizards have undergone a great deal of morphological change. I was able to significantly link these changes with several factors, including phylogeny, allometry, and ecology. Undoubtedly, these aspects all closely interact and entwine with one another to contribute to the evolution of amphibolurine skull shape in a complex manner. I have endeavoured to disentangle them from one another and provide a thorough understanding of evolution of the amphibolurine skull. To achieve this end, I addressed the four "main aims" outlined in the first chapter.

AIM 1 – Explore disparity

Amphibolurines are a highly disparate clade that explores novel areas of morphospace

Two-dimensional measurements of skull proportions revealed that of all the iguanian families sampled, the Agamidae have the highest level of disparity. Not only is disparity of the amphibolurine clade considerably higher than we might expect for a clade of its taxonomic diversity, they also occupy almost the entirety of the Agamidae cranial morphospace. Furthermore, amphibolurines occupy exclusive areas of the morphospace, unexplored by any other sampled taxa, thereby represent much of the total disparity observed in Agamidae. My characterisations of three-dimensional skull shapes revealed that the two clades that make up the core of the amphibolurine radiation, the *Ctenophorus* group and the *Amphibolurus* group, did not have significantly different amounts of disparity. Some members of both groups occupied similar morphospace, but members of both groups also explored areas of exclusive morphospace. These novel skull shapes were associated with specialised ecological life habits. Lizards with exclusive skull shapes included burrowers (with short, flat faces), and rock dwellers (with dorsoventrally flattened heads), and it seems that specialisation for different environments is a major factor contributing to departures from the mean shape. In Chapter 4, I used two-dimensional

geometric morphometrics to quantify and compare the disparity between juvenile and adult skulls of amphibolurine species. The significant difference in disparity between juvenile and adult skull shapes indicated that ontogeny was playing a vital role in the evolution of the array of different skull shapes in amphibolurine lizards, and this finding facilitated the exploration of my second aim.

<div align="center">

AIM 2 — Investigate ontogenetic patterns

</div>

Variation in ontogenetic patterns plays a major role in evolution of skull morphology

For young dragon lizards, the journey to adulthood is accompanied by dramatic and varied increases in size, suggesting that ontogenetic patterns play an important role in their skull shape evolution. My exploration of skull shapes in different species of amphibolurines at different ontogenetic stages revealed that different species have relatively similar skull shapes as juveniles. During growth, they become more disparate in their shape, and by adulthood, different species exhibit a spectrum of different skull shapes. To achieve this disparity, amphibolurine species do not follow a common ontogenetic pattern. Although some different skull shapes are produced through variation of a common trajectory (implying heterochrony), there are several departures from this, and consequently, a range of different ontogenetic trajectories among amphibolurine lizards. In contrast, an investigation into tooth counts during growth in amphibolurines in showed minimal departures from the common ontogenetic pattern, indicating that each amphibolurine species grows additional teeth at a similar rate, even though different species may have different tooth counts at a given size. Moreover, for a given species, different elements of anatomy do not necessarily share common postnatal developmental patterns. Therefore, to gain a thorough understanding of these patterns, ontogenetic variation must be addressed on a case-by-case basis for particular anatomical elements.

<div align="center">

AIM 3 — Characterise skull shape and identify what influences variation

</div>

Amphibolurine skull shape has been influenced by size, phylogeny, and ecology

I detected significant associations between skull shape and three major factors: size, phylogeny, and ecological life habit. A significant phylogenetic signal was detected for the distribution of amphibolurine species in the cranial morphospaces in Chapters 4 and 5, and the distribution of points in both morphospaces seemed to reflect this at the broader taxonomic levels. However, at generic and species levels this signal was not particularly strong or distinctive. Even though heredity was playing an important role in skull shape, there was more to the story. I discovered

that evolutionary allometry accounts for a large amount of skull shape in adult amphibolurines, demonstrating that different skull shapes can be achieved through differences in size. The most striking result was the significant and prominent association between ecological life habit and skull shape. In Chapter 5, life habit was more closely associated with skull shape than evolutionary allometry or taxonomic affiliation, and this gave convincing evidence for the adaptive character of amphibolurines.

Contributions to the interpretation of agamids in the Australian fossil record

My findings advance our understanding of skull morphology of amphibolurine agamids, and consequently, we now have an improved level of baseline knowledge for interpreting agamids in the Australian fossil record, including a method for estimating the body size of agamids from jaw bones. Furthermore, the striking association between ecological life habit and skull shape points towards a potential for using fossil cranial elements to make inferences about the way an extinct animal may have interacted with its environment. I also explored the possibility of using geometric morphometric methods to make taxonomic inferences about fossil specimens. It seems there is promising potential for this method, if the sample of comparative material can be expanded to encompass more species and ontogenetic stages.

Advances in knowledge about agamid skulls

These chapters have built on the work of Siebenrock (1895), Moody (1980), and Evans (2008), whose important studies remain the only summaries of osteology of the skull as a whole in the agamid family. They also expand on the only work so far that has documented, in detail, patterns of variation in cranial elements among members of the Australian radiation of agamids, by Hocknull (2002), and Stilson et al. (2017). These works provided crucial first steps towards building a framework of qualitative osteological characters. Moreover, they identified the need for a rigorous evaluation of morphological differences within and among taxa to gain a more adequate understanding of variation and its drivers. Throughout the chapters of this thesis, I have provided an important advancement of this important work by exploring the quantitative patterns of variation in members of the Australian radiation of agamid lizards (see Fig. 9.1).

Within the agamids, Siebenrock (1895) recognised two basic skull types. Small and laterally compressed skulls, observed in mostly arboreal agamids like *Calotes, Draco, Gonocephalus*, and *Japalura,* and wide and flattened skulls, observed mostly in what he described as "terrestrial" agamids such as *Agama, Pogona, Leiolepis*, and *Uromastyx*. We know now that skull shapes in agamids cannot be neatly categorised in this manner. While my results are broadly in line with this generalisation (at least for adult representatives of species), it is apparent that amphibolurines collectively exhibit a continuum of different skull shapes. By conducting these analyses, I have not only provided abundant information regarding size-free, independent shape variables, but I have also created a database of images and three-dimensional models as a morphological record, upon which other sets of landmarks or morphological features may be measured and analysed. Furthermore, as the research on the ecology and evolution of the Australian dragons continues, I hope that my findings may be a used as a framework with which to test new hypotheses about the evolution of this ecologically diverse clade of lizards.

Evolutionary history of Australian dragons: another piece of the puzzle

The evolution of different skull shapes in multiple lineages in the core of the Australian agamid radiation adds to other lines of evidence suggesting that agamid lizards made the most of the fragmenting habitats during the aridification of Australia. Many phylogenetic studies have contributed to the story of how Australian agamids evolved into the morphologically and ecologically diverse group they are today. My results are broadly in line with phylogenetic work of Collar et al. (2010), and Melville et al. (2006) who found that habitat use in dragon lizards contributes to convergence in body form. Interestingly, Collar et al. (2010) found that semi-

arboreal animals and terrestrial animals evolve at faster rates than arboreal and saxicolous animals, and this is somewhat reflected in the morphospace occupation of the core amphibolurine radiation, as these semi-arboreal and terrestrial species collectively occupied a less restricted area of the cranial morphospace. This may also indicate that terrestrial and semi-arboreal life habit categories are broad, and encompass a wider variety of lifestyles than arboreal and saxicolous categories. The evolutionary success of the core of the Australian amphibolurine radiation in the desert and woodland habitats of Australia has been documented in broader studies on lizard diversity (Byrne et al., 2008; Powney et al., 2010), and in phylogenetic studies (Melville et al., 2001; Melville et al., 2006; Shoo et al., 2008; Edwards and Melville, 2010; Melville et al., 2011). Their skull shape seems to be evolutionarily flexible, and this evolutionary flexibility would have been advantageous for their adaptation to the fragmenting Australian environment over the last 20 million years. A substantial amount of intraspecific variation is indicative of phenotypic plasticity, and this was particularly apparent in the sampled captive lizards, suggesting a rapid and likely epigenetic effect of the surrounding environment on phenotype.

How amphibolurines fit into the bigger evolutionary picture

The overarching themes in this thesis ring true for other groups of organisms, not just reptiles, but also other vertebrates, and even plants. I explored evolutionary and ontogenetic allometry in amphibolurine lizard skulls, and outcomes were consistent with many other studies that have explored both types of allometric variation. Ontogenetic and evolutionary allometry are closely connected in Australian agamid skull morphology. Ontogenetic allometry has previously been considered a phenotypic constraint (Klingenberg, 2010), and there are studies that show considerable phenotypic variation can be achieved even with a constrained developmental pathway (e.g. Piras et al., 2011; Bhullar, 2012). This seems to be the case for tooth development patterns in Australian agamids. However, the universality of a conserved ontogenetic pattern (heterochrony) is not supported by postnatal growth patterns in skull morphology. My findings are consistent with previous research reporting that ontogenetic patterns can represent a continuum of developmental flexibility that is sensitive to adaptation, and they play in important role in shaping macroevolutionary patterns of diversification (Weston, 2003; Wilson, 2010; Frédérich and Vandewalle, 2011; Wilson and Sánchez-Villagra, 2011; Strelin et al., 2016; Esquerré et al., 2017; Hipsley and Müller, 2017). Collectively, my results and those of others show that ontogenetic patterns may vary depending on the organism or anatomical component of interest.

In the evolution of Australian agamid skulls, ontogenetic allometry is tightly interweaved with evolutionary allometry. Like the many researchers that came before me, I have demonstrated the important role that body size plays in the evolution of morphological disparity, revealing that like many other animal groups, Australian dragons can achieve different skull shapes simply by growing larger, or smaller. My findings that larger adult dragons tend to have longer faces, something that is also true for juvenile versus adult dragons (a hint at the close connection with ontogenetic allometry), is intriguingly similar to the cranial evolutionary allometry (CREA) "rule" demonstrated for multiple mammal lineages (Cardini and Polly, 2013; Cardini et al., 2015). This aspect of evolutionary allometry, where longer faces are associated with larger adult sizes, is conserved among multiple mammalian clades, but my results demonstrate that this "rule" may also hold true for Australian dragons, and has been observed in some other lizards (e.g. Hipsley and Müller, 2017), and also birds (e.g. Tokita et al., 2017). Perhaps even more intriguingly, it seems that this does not hold true for all herpetological fauna (e.g. Claude et al., 2004; Jones, 2008; Sherratt et al., 2014; Palci et al., 2016; Esquerré et al., 2017). My thesis emphasises the power of using different kinds of allometry as a quantitative framework for investigating the morphological variation that is characteristic of ecologically diverse radiations. I have also demonstrated that perhaps, concepts in evolutionary allometry that have been explored among closely related vertebrate species, warrant further investigation and comparisons at broader taxonomic levels.

I have found distinct patterns between ecology and skull shape. This is no surprise. Since Darwin's pivotal work on natural selection, scores of researchers have documented close ties between the ecology of organisms and their phenotype. My findings align with many other modern studies that have used multivariate methods to find an association between phenotype and ecology (Harmon et al., 2005; Fuchs et al., 2015; McCurry et al., 2015; Manzano et al., 2017; Meloro et al., 2017). I have also added to the large body of evidence that skull shape is evolutionarily labile and can reflect the functional demands placed on an animal (Sanger et al., 2012; McCurry et al., 2015; Meloro et al., 2017), and that skull shape reflects functional trade-offs there are made in response to these demands (e.g. Verwaijen et al., 2002; Kohlsdorf et al., 2008; Edwards et al., 2016). Studies concerning diets, foraging strategies, feeding styles, and sexual display (e.g. Perry and Garland, 2002; Vitt et al., 2003; Pianka and Goodyear, 2012), will all be improved by this greater understanding of the morphological variation that accompanies such adaptations.
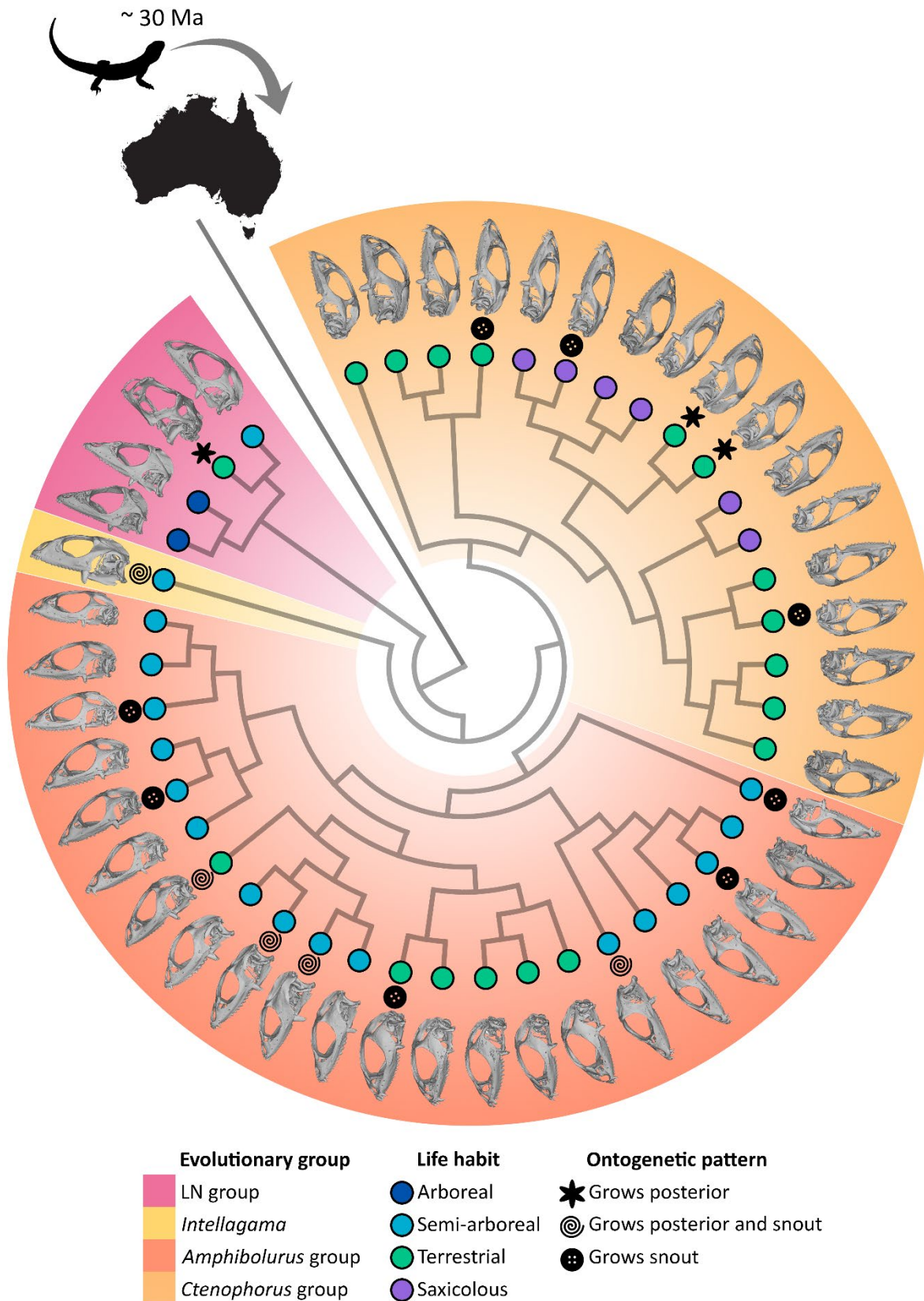
Figure 9.1 – Evolutionary tree of Australian dragon lizards used in this thesis, mapped with lateral images of their skulls, common ontogenetic patterns (which part of the skull grows relatively more than others), and life habits.

Future directions

The future of fossil identification

A substantial amount of agamid fossil material has been recovered from Australian deposits, and it has the potential to inform studies of palaeoenvironmental patterns through time. However, little information has been available for taxonomic comparisons or affiliations with extant Australian agamid taxa. It seems that some attributes of animals (e.g. body size) may be inferred from simple linear measurements from fossil jaw bones, and coupling this with future advances in our ability to make taxonomic affiliations may allow interpretations about ancestors of Australian agamids, leading to a more complete understanding of amphibolurine evolutionary history. It appears that geometric morphometric methods could be used for identification in Australian agamid fossils, but my work should be expanded upon to account for intraspecific and ontogenetic variation.

Implications for captive lizard populations

While I was able to detect significant differences in shape and ontogenetic patterns between sampled wild and captive jacky dragons in Chapter 7, including a more complete sampling of captive and wild lizards, would allow more robust conclusions to be made about the effect of captivity on lizard skull shape. Since captive reptile populations are important for research and conservation, further work may involve performing similar analyses for other species of agamids, and also other reptiles. We know that, in mammals, a whole suite of traits can be associated with captivity (Wilkins et al., 2014; Sánchez-Villagra et al., 2016), but very little work has been done to determine if this is also the case for other animal groups. Since the morphological characters we observe in captive jacky lizards are similar to some of those seen in mammals, the logical next step is to examine whether they possess other characteristics associated with captivity in other animals.

Variation at species and population levels

While I have examined a great deal of Australian agamid species in this thesis, the taxonomic breadth of my samples was subject to time constraints and availability. I have included a representative cross-section of Australian agamid species in my analyses, it would be advantageous to expand this sample to encompass all recognised species. Furthermore, the degree of intraspecific variation indicates that there is some skull shape variation that is not accounted for by allometry, phylogeny, or ecology, and it is feasible that there may be shape differences among different populations of the same species. Therefore, expanding the sample to

explore the variation that may be present among different populations of the same species would be an interesting avenue to go down.

Sexual dimorphism

Due to gaps in body size and sex data for some museum specimens, we were unable to investigate the influence of sexual dimorphism on Australian dragon lizards. Sexual dimorphism in size has been recorded for at least one species of amphibolurine (Badham, 1976), and therefore we cannot discount the possibility that it has an influence on skull shape, considering the strong allometric effects observed in these lizards. Hence, future directions would seek to include data on the sex of specimens used in analyses.

Association of skull shape with feeding

Many studies have shown that the morphology and mechanics of the skull are related to feeding (Metzger and Herrel, 2005). Agamids have generally been observed to be opportunist omnivores (Pough, 1973; Cooper and vitt, 2002), and categorising them in terms of diet is a difficult feat. A lack of available data concerning diet meant that, although we were able to discuss possible implications of diet and feeding on morphology, we were not able to explicitly test for associations between these factors and skull shape. In considering diet and feeding, we must account for not only what an animal eats, but also the size of the food, hardness of it, what the food is made of, and how the animal forages for this food (Evans and Sanson, 2005). We could expand our understanding of skull evolution in this group by systematically collected data concerning feeding to the morphological data in this thesis and testing for associations with skull shape. This data may also reveal details about the interplay between skull shape, life habit, and aspects of feeding.

Skull shape and soft tissues

How differences in skull shape are related to other parts of the head anatomy such as the jaw muscles, eyes, and brain could be examined using contrast-enhanced (stained) soft tissue scanning (see Gignac and Kley, 2014; Gignac and Kley, 2018), or MRI (Hoops et al., 2018). This approach could provide important insights into the development and function of specific structures. It could also inform computer based biomechanical modelling analyses such as. Multibody Dynamics and Finite Element Analysis (Moazen et al., 2009; Jones et al., 2012; Jones et al., 2017), and examination of in vivo bite force performance (Lappin and Jones, 2014)

Other avenues of research

Factors at the genetic and cellular level, such as epigenetics (Schlichting and Wund, 2014) and microbiomes (Colston and Jackson, 2016), probably have an important effect on form and

function, and may be another avenue of exploration that would help us achieve a comprehensive understanding of evolution and ecology of the Australian dragon lizards.

References

Badham JA. 1976. The *Amphibolurus barbatus s*pecies-group (Lacertilia: Agamidae). Aust J Zool 24:423-443.

Bhullar B-AS. 2012. A phylogenetic approach to ontogeny and heterochrony in the fossil record: cranial evolution and development in anguimorphan lizards (Reptilia: Squamata). J Exp Zool (Mol Dev Evol) 318:521-530.

Byrne M, Yeates DK, Joseph L, Kearney M, Bowler J, Williams MAJ, Cooper S, Donnellan SC, Keogh JS, Leys R, Melville J, Murphy DJ, Porch N, Wyrwoll KH. 2008. Birth of a biome: insights into the assembly and maintenance of the Australian arid zone biota. Mol Ecol 17:4398-4417.

Cardini A, Polly D, Dawson R, Milne N. 2015. Why the long face? Kangaroos and wallabies follow the same 'rule' of cranial evolutionary allometry (CREA) as placentals. Evol Biol 42:169-176.

Cardini A, Polly PD. 2013. Larger mammals have longer faces because of size-related constraints on skull form. Nat Comm 4:3458.

Claude J, Pritchard PCH, Tong H, Paradis E, Auffray J-C. 2004. Ecological correlates and evolutionary divergence in the skull of turtles: a geometric morphometric assessment. Syst Biol 53:933-948.

Collar DC, Schulte JA, O'Meara BC, Losos JB. 2010. Habitat use affects morphological diversification in dragon lizards. J Evol Biol 23:1033-1049.

Colston TJ, Jackson CR. 2016. Microbiome evolution along divergent branches of the vertebrate tree of life: what is known and unknown. Mol Ecol 25:3776-3800.

Cooper WEJ, vitt LJ. 2002. Distribution, extent, and evolution of plant consumption by lizards. Journal of Zoological Society of London 257:487-517.

Edwards DL, Melville J. 2010. Phylogeographic analysis detects congruent biogeographic patterns between a woodland agamid and Australian wet tropics taxa despite disparate evolutionary trajectories. J Biogeogr 37:1543-1556.

Edwards S, Herrel A, Vanhooydonck B, Measey GJ, Tolley KA. 2016. Diving in head first: trade-offs between phenotypic traits and sand-diving predator escape strategy in Meroles desert lizards. Biol J Linnean Soc 119:919-931.

Esquerré D, Sherratt E, Keogh JS. 2017. Evolution of extreme ontogenetic allometric diversity and heterochrony in pythons, a clade of giant and dwarf snakes. Evolution 71:2829-2844.

Evans AR, Sanson GD. 2005. Biomechanical properties of insects in relation to insectivory: cuticle thickness as an indicator of insect hardness and intractability. Aust J Zool 53:9-19.

Evans SE. 2008. The skull of lizards and tuatara. In: Gans C, Gaunt AS, Adler K, editors. Biology of the Reptilia 20, Morphology H, The skull of Lepidosauria. Ithaca, New York: Society for the Study of Amphibians and Reptiles. p 1-347.

Frédérich B, Vandewalle P. 2011. Bipartite life cycle of coral reef fishes promotes increasing shape disparity of the head skeleton during ontogeny: an example from damselfishes (Pomacentridae). BMC Evol Biol 11:82.

Fuchs M, Geiger M, Stange M, Sánchez-Villagra MR. 2015. Growth trajectories in the cave bear and its extant relatives: an examination of ontogenetic patterns in phylogeny. BMC Evol Biol 15:239.

Gignac PM, Kley NJ. 2014. Iodine-enhanced micro-CT imaging: methodological refinements for the study of the soft-tissue anatomy of post-embryonic vertebrates. J Exp Zool (Mol Dev Evol) 322:166-176.

Gignac PM, Kley NJ. 2018. The utility of DiceCT imaging for high-throughput comparative neuroanatomical stdies. Brain Behav Evol 91:180-190.

Harmon LJ, Kolbe JJ, Cheverud JM, Losos JB, Wainwright P. 2005. Convergence and the multidimensional niche. Evolution 59:409-421.

Hipsley CA, Müller J. 2017. Developmental dynamics of ecomorphological convergence in a transcontinental lizard radiation. Evolution 71:936-948.

Hocknull SA. 2002. Comparative maxillary and dentary morphology of the Australian dragons (Agamidae: Squamata): a framework for fossil identification. Mem Queensl Mus 48:125-145.

Hoops D, Desfilis E, Ullmann JFP, Janke AL, Stait-Gardner T, Devenyi GA, Price WS, Medina L, Whiting MJ, Keogh JS. 2018. A 3D MRI-based atlas of a lizard brain. J Comp Neurol Accepted for publication.

Jones MEH. 2008. Skull shape and feeding strategy in *Sphenodon* and other Rhynchocephalia. J Morphol 269:945-966.

Jones MEH, Gröning F, Dutel H, Sharp A, Fagan MJ, Evans SE. 2017. The biomechanical role of the chondrocranium and sutures in a lizard cranium. J R Soc Interface 14.

Jones MEH, O'higgins P, Fagan MJ, Evans SE, Curtis N. 2012. Shearing mechanics and the influence of a flexible symphysis during oral food processing in *Sphenodon* (Lepidosauria: Rhynchocephalia). Anat Rec 295:1075-1091.

Klingenberg CP. 2010. Evolution and development of shape: integrating quantitative approaches. Nat Rev Genet 11:623-635.

Kohlsdorf T, Grizante MB, Navas CA, Herrel A. 2008. Head shape evolution in Tropidurinae lizards: does locomotion constrain diet? J Evol Biol 21:781-790.

Lappin AK, Jones MEH. 2014. Reliable quantification of bite-force performance requires use of appropriate biting substrate and standardization of bite out-lever. J Exp Biol 217:4303-4312.

Manzano AS, Herrel A, Fabre AC, Abdala V. 2017. Variation in brain anatomy in frogs and its possible bearing on their locomotor ecology. J Anat 231:38-58.

McCurry MR, Mahony M, Clausen PD, Quayle MR, Walmsley CW, Jessop TS, Wroe S, Richards H, Mchenry CR. 2015. The relationship between cranial structure, biomechanical performance and ecological diversity in varanoid lizards. PLOS ONE 10:e0130625.

Meloro C, Hunter J, Tomsett L, Portela MR, Prevosti FJ, Brown RP. 2017. Evolutionary ecomorphology of the Falkland Islands wolf *Dusicyon australis*. Mammal Rev 47:159-163.

Melville J, Harmon LJ, Losos JB. 2006. Intercontinental community convergence of ecology and morphology in desert lizards. Proc R Soc B 273:557-563.

Melville J, Ritchie EG, Chapple SNJ, Glor RE, Schulte JA. 2011. Evolutionary origins and diversification of dragon lizards in Australia's tropical savannas. Mol Phylogenet Evol 58:257-270.

Melville J, Schulte JA, Larson A. 2001. A molecular phylogenetic study of ecological diversification in the Australian lizard genus *Ctenophorus*. J Exp Zool 291:339-353.

Metzger KA, Herrel A. 2005. Correlations between lizard cranial shape and diet: a quantitative, phylogenetically informed analysis. Biol J Linnean Soc 86:433-466.

Moazen M, Curtis N, O'Higgins P, Jones MEH, Evans SE, Fagan MJ. 2009. Assessment of the role of sutures in a lizard skull: a computer modelling study. Proc R Soc B 276:39-46.

Moody SM. 1980. Phylogenetic and historical biogeographical relationships of the genera in the family Agamidae (Reptilia, Lacertilia). Doctoral Dissertation: University of Michigan.

Palci A, Lee MSY, Hutchinson MN. 2016. Patterns of postnatal ontogeny of the skull and lower jaw of snakes as revealed by micro-CT scan data and three-dimensional geometric morphometrics. J Anat 229:723-754.

Perry G, Garland TJ. 2002. Lizard home ranges revisited: effects of sex, body size, diet, habitat, and phylogeny. Ecology 83:1870-1885.

Pianka ER, Goodyear SE. 2012. Lizard responses to wildfire in arid interior Australia: long-term experimental data and commonalities with other studies. Austral Ecol 37:1-11.

Piras P, Salvi D, Ferrara G, Maiorino L, Delfino M, Pedde L, Kotsakis T. 2011. The role of post-natal ontogeny in the evolution of phenotypic diversity in *Podarcis* lizards. J Evol Biol 24:2705-2720.

Pough FH. 1973. Lizard Energetics and Diet. Ecology 54:837-844.

Powney GD, Grenyer R, Orne CDL, Owens IPF, Meiri S. 2010. Hot, dry and different: Australian lizard richness is unlike that of mammals, amphibians and birds. Glob Ecol Biogeogr 19:386-396.

Sánchez-Villagra MR, Geiger M, Schneider RA. 2016. The taming of the neural crest: a developmental perspective on the origins of morphological covariation in domesticated mammals. Royal Soc Open Sci 3:160107.

Sanger TJ, Mahler DL, Abzhanov A, Losos JB. 2012. Roles for modularity and constraint in the evolution of cranial diversity among *Anolis* lizards. Evolution 66:1525-1542.

Schlichting CD, Wund MA. 2014. Phenotypic plasticity and epigenetic marking: an assessment of evidence for genetic accommodation. Evolution 68:656-672.

Sherratt E, Gower DJ, Klingenberg CP, Wilkinson M. 2014. Evolution of cranial shape in caecilians (Amphibia: Gymnophiona). Evol Biol 41:528-545.

Shoo L, Rose R, Doughty P, Austin JJ, Melville J. 2008. Diversification of pebble-mimic dragons are consistent with historical disruption of important corridors in arid Australia. Mol Phylogenetics Evol 48:528-542.

Siebenrock F. 1895. Das skelett der Agamidae. Sittzungsber Akad Wiss Wien 104.

Stilson KT, Bell CJ, Mead JI. 2017. Patterns of variation in the cranial osteology of three species of endemic Australian lizards (*Ctenophorus*: Squamata: Agamidae): implications for the fossil record and morphological analyses made with limited sample sizes. J Herpetol 51:316-329.

Strelin MM, Benitez-Vieyra S, Fornoni J, Klingenberg CP, Cocucci AA. 2016. Exploring the ontogenetic scaling hypothesis during the diversification of pollination syndromes in *Caiophora* (Loasaceae, subfam. Loasoideae). Ann Bot 117:937-947.

Tokita M, Yano W, James HF, Abzhanov A. 2017. Cranial shape evolution in adaptive radiations of birds: comparative morphometrics of Darwin's finches and Hawaiian honeycreepers. Phil Trans R Soc B 372:20150481.

Verwaijen D, Van Damme R, Herrel A. 2002. Relationships between head size, bite force, prey handling efficiency and diet in two sympatric lacertid lizards. Funct Ecol 16:842-850.

Vitt LJ, Pianka ER, Cooper WEJ, Schwenk K. 2003. History and the global ecology of squamate reptiles. Am Nat 162:44-60.

Weston EM. 2003. Evolution of ontogeny in the hippopotamus skull: using allometry to dissect developmental change. Biol J Linnean Soc 80:625-638.

Wilkins AS, Wrangham RW, Fitch WT. 2014. The "domestication syndrome" in mammals: a unified explanation based on neural crest cell behavior and genetics. Genetics 197:795-808.

Wilson LAB. 2010. The evolution of morphological diversity in rodents : patterns of cranial ontogeny. Doctoral Dissertation: University of Zurich.

Wilson LAB, Sánchez-Villagra MR. 2011. Evolution and phylogenetic signal of growth trajectories: the case of chelid turtles. J Exp Zool (Mol Dev Evol) 316B:50-60.

Supplementary material

Supplementary material for Chapter 3
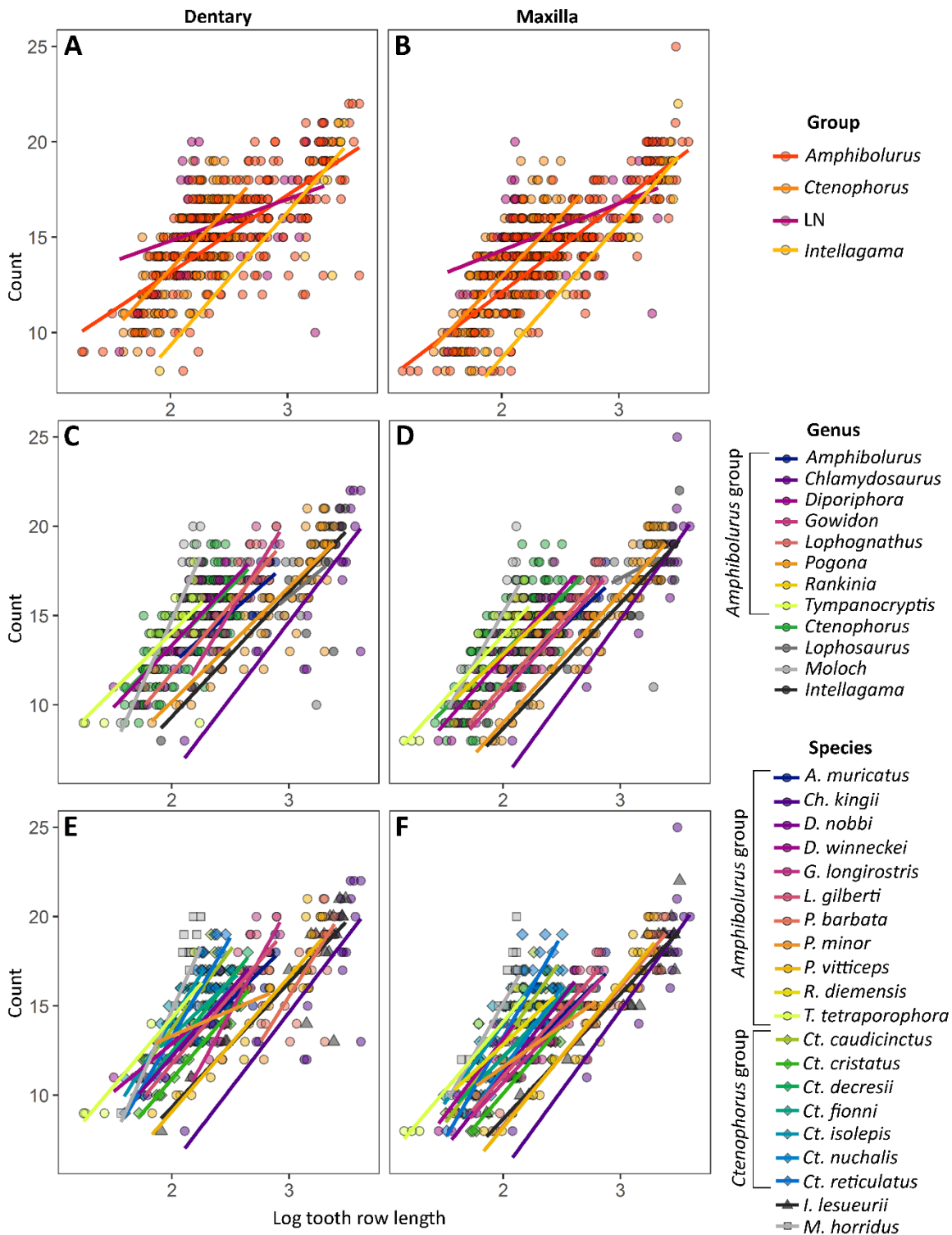
Figure S3.1 – Tooth count allometry with raw data points at the evolutionary group (A and B, LN=least nested group), genus (C and D) and species (E and F) levels, for both the maxilla (A, C, E) and dentary (B, D, F), showing the allometric patterns detected by statistical testing.

Table S3.1 – Linear coefficients for dentary and maxillary tooth counts regressed on log tooth row length, for each amphibolurine monophyletic clade (LN = least nested). Bold values indicate $P < 0.05$.

	DENTARY					MAXILLA				
Group	n	Elevation	Slope	R²	*P*-value	n	Elevation	Slope	R²	*P*-value
Amphibolurus	229	0.93	5.64	0.52	**<0.001**	257	0.17	5.71	0.67	**<0.001**
Ctenophorus	210	-4.54	8.74	0.56	**<0.001**	233	-4.03	8.37	0.57	**<0.001**
Intellagama	22	-7.66	7.95	0.77	**<0.001**	30	-6.62	7.42	0.89	**<0.001**
LN	40	1.03	5.85	0.14	**0.017**	45	3.50	4.78	0.26	**<0.001**

Table S3.2 – Pairwise ANOVA comparisons for dentary and maxillary tooth counts during growth, among amphibolurine monophyletic clades (LN = least nested). Top triangles are *P*-values for slope differences, bottom triangles are *P*-values for elevation differences. Bold values indicate $P < 0.05$.

	DENTARY				MAXILLA			
Group	*Amphibolurus*	*Ctenophorus*	*Intellagama*	LN	*Amphibolurus*	*Ctenophorus*	*Intellagama*	LN
Amphibolurus	-	**0.000**	**0.036**	1.000	-	**0.000**	**0.004**	0.733
Ctenophorus	**0.000**	-	0.964	0.072	**0.000**	-	0.528	**0.001**
Intellagama	**0.002**	**0.000**	-	0.473	**0.000**	**0.000**	-	**0.019**
LN	0.807	0.064	**0.001**	-	0.142	0.114	**0.000**	-

Table S3.3 – Linear coefficients for dentary and maxillary tooth counts regressed on log tooth row length, for each amphibolurine genus with n ≥ 10. Bold values indicate *P* < 0.05.

Genus	MAXILLA					DENTARY				
	n	Elevation	Slope	R²	*P*-value	n	Elevation	Slope	R²	*P*-value
Amphibolurus	39	-2.544	7.083	0.653	**<0.001**	40	-2.725	6.841	0.784	**<0.001**
Chlamydosaurus	20	-18.471	10.818	0.626	**<0.001**	18	-16.192	10.212	0.774	**<0.001**
Ctenophorus	210	-4.538	8.743	0.560	**<0.001**	233	-4.034	8.371	0.571	**<0.001**
Diporiphora	42	-3.492	8.289	0.710	**<0.001**	46	-4.577	8.563	0.762	**<0.001**
Gowidon	19	-15.547	12.237	0.755	**<0.001**	23	-5.680	8.025	0.834	**<0.001**
Intellagama	22	-7.657	7.954	0.771	**<0.001**	30	-6.621	7.419	0.890	**<0.001**
Lophognathus	15	-7.489	9.215	0.695	**<0.001**	17	-5.652	8.165	0.803	**<0.001**
Lophosaurus	12	-50.759	21.681	0.063	**<0.001**	12	-37.759	17.604	0.038	0.545
Moloch	17	-20.686	17.622	0.668	**<0.001**	19	-12.295	13.754	0.687	**<0.001**
Pogona	66	-6.517	7.725	0.689	**<0.001**	78	-6.775	7.690	0.885	**<0.001**
Rankinia	3	28.786	-5.966	0.255	0.663	12	-3.060	7.848	0.604	**0.003**
Tympanocryptis	25	-3.441	8.770	0.551	**<0.001**	23	-2.042	8.008	0.816	**<0.001**

Table S3.4 – Pairwise ANOVA comparisons for dentary and maxillary tooth counts during growth, among amphibolurine genera with n ≥ 10. Top triangles are *P*-values for slope differences, bottom triangles are *P*-values for elevation differences. Bold values indicate *P* < 0.05.

DENTARY	Amphibolurus	Chlamydosaurus	Ctenophorus	Diporiphora	Gowidon	Intellagama	Lophognathus	Lophosaurus	Moloch	Pogona	Rankinia	Tympanocryptis
Amphibolurus	-	0.728	0.974	1.000	0.065	1.000	1.000	0.105	**0.001**	1.000	1.000	1.000
Chlamydosaurus	**0.000**	-	1.000	1.000	1.000	0.999	1.000	0.968	0.807	0.948	1.000	1.000
Ctenophorus	**0.000**	**0.000**	-	1.000	0.630	1.000	1.000	0.387	**0.011**	1.000	1.000	1.000
Diporiphora	**0.000**	**0.000**	1.000	-	0.550	1.000	1.000	0.310	**0.009**	1.000	1.000	1.000
Gowidon	1.000	**0.000**	**0.000**	**0.000**	-	0.522	1.000	0.999	0.990	0.144	1.000	0.995
Intellagama	**0.000**	0.886	**0.000**	**0.000**	**0.000**	-	1.000	0.263	**0.009**	1.000	1.000	1.000
Lophognathus	1.000	**0.000**	**0.008**	0.053	1.000	**0.000**	-	0.716	0.278	1.000	1.000	1.000
Lophosaurus	0.055	1.000	**0.000**	**0.000**	**0.000**	1.000	**0.003**	-	1.000	0.179	1.000	0.545
Moloch	**0.000**	**0.000**	**0.009**	**0.020**	**0.000**	**0.000**	**0.000**	**0.000**	-	**0.002**	1.000	0.092
Pogona	**0.000**	0.159	**0.000**	**0.000**	**0.000**	1.000	**0.000**	1.000	**0.000**	-	1.000	1.000
Rankinia	0.930	**0.000**	1.000	1.000	0.765	**0.004**	0.999	0.246	0.949	**0.001**	-	1.000
Tympanocryptis	**0.000**	**0.000**	0.210	0.700	**0.000**	**0.000**	0.005	**0.000**	1.000	**0.000**	1.000	-
MAXILLA												
Amphibolurus	-	0.406	0.785	0.912	1.000	1.000	1.000	0.353	**0.006**	1.000	1.000	1.000
Chlamydosaurus	**0.000**	-	1.000	1.000	1.000	0.812	1.000	1.000	1.000	0.895	1.000	1.000
Ctenophorus	**0.000**	**0.000**	-	1.000	1.000	1.000	1.000	0.832	0.114	1.000	1.000	1.000
Diporiphora	**0.000**	**0.000**	1.000	-	1.000	1.000	1.000	0.895	0.254	1.000	1.000	1.000
Gowidon	1.000	**0.000**	**0.000**	**0.000**	-	1.000	1.000	0.780	0.134	1.000	1.000	1.000
Intellagama	**0.000**	1.000	**0.000**	**0.000**	**0.000**	-	1.000	0.539	**0.019**	1.000	1.000	1.000
Lophognathus	1.000	**0.000**	**0.000**	**0.000**	1.000	**0.000**	-	0.854	0.328	1.000	1.000	1.000
Lophosaurus	0.999	0.991	**0.000**	**0.000**	0.670	1.000	0.363	-	1.000	0.615	0.920	0.782
Moloch	**0.000**	**0.000**	**0.000**	**0.000**	**0.000**	**0.000**	**0.000**	**0.000**	-	**0.025**	0.867	0.146
Pogona	**0.000**	0.627	**0.000**	**0.000**	**0.000**	0.327	**0.000**	1.000	**0.000**	-	1.000	1.000
Rankinia	**0.002**	**0.000**	1.000	1.000	**0.001**	**0.000**	0.090	0.123	**0.002**	**0.000**	-	1.000
Tympanocryptis	**0.000**	**0.000**	**0.000**	**0.000**	**0.000**	**0.000**	**0.000**	**0.000**	0.855	**0.000**	0.327	-

Table S3.5 – Linear coefficients for dentary and maxillary tooth counts regressed on log tooth row length for amphibolurine species with n ≥ 10. Bold values indicate *P* < 0.05.

	DENTARY					MAXILLA				
Species	n	Elevation	Slope	R²	*P*-value	n	Elevation	Slope	R²	*P*-value
A. muricatus	33	-2.979	7.331	0.778	**<0.001**	34	-3.416	7.174	0.789	**<0.001**
Ch. kingii	20	-18.471	10.818	0.626	**<0.001**	18	-16.192	10.212	0.774	**<0.001**
Ct. caudicinctus	19	-5.547	9.564	0.852	**<0.001**	25	-6.790	9.870	0.876	**<0.001**
Ct. cristatus	18	-4.487	7.686	0.977	**<0.001**	18	-5.673	7.860	0.944	**<0.001**
Ct. decresii	13	-4.778	8.542	0.906	**<0.001**	15	-3.437	7.627	0.725	**<0.001**
Ct. fionni	9	-3.649	8.104	0.571	**0.019**	10	-3.703	7.776	0.786	**0.001**
Ct. isolepis	27	-8.747	11.466	0.830	**<0.001**	29	-6.888	10.525	0.715	**<0.001**
Ct. nuchalis	25	-5.658	8.776	0.727	**<0.001**	28	-9.016	10.116	0.806	**<0.001**
Ct. reticulatus	30	-11.923	12.459	0.806	**<0.001**	30	-12.940	12.986	0.780	**<0.001**
D. nobbi	10	-3.572	7.818	0.909	**<0.001**	10	-6.238	8.699	0.943	**<0.001**
D. winneckei	10	-0.124	6.569	0.678	**0.003**	11	-5.905	9.611	0.801	**<0.001**
G. longirostris	15	-18.166	13.075	0.835	**<0.001**	19	-4.824	7.611	0.836	**<0.001**
I. lesueurii	22	-7.657	7.954	0.771	**<0.001**	30	-6.621	7.419	0.890	**<0.001**
L. gilberti	15	-7.489	9.215	0.695	**<0.001**	17	-5.652	8.165	0.803	**<0.001**
M. horridus	17	-20.686	17.622	0.668	**<0.001**	19	-12.295	13.754	0.687	**<0.001**
P. barbata	27	-28.929	14.559	0.515	**<0.001**	30	-8.854	8.281	0.876	**<0.001**
P. minor	12	-1.200	6.186	0.211	0.133	12	0.859	5.197	0.788	**<0.001**
P. vitticeps	23	-7.465	8.062	0.877	**<0.001**	30	-8.520	8.264	0.940	**<0.001**
R. diemensis	3	28.786	-5.966	0.255	0.663	12	-3.060	7.848	0.604	**0.003**
T. tetraporophora	11	-1.948	8.180	0.885	**<0.001**	10	-1.994	8.097	0.917	**<0.001**

Table S3.6 – Pairwise ANOVA comparisons for dentary and maxillary tooth counts during growth, among amphibolurine species with n ≥ 10. Top triangles are P-values for slope differences, bottom triangles are P-values for elevation difference. Bold values indicate $P < 0.05$.

DENTARY	A. mur	Ch. kin	Ct. cau	Ct. cri	Ct. dec	Ct. fio	Ct. iso	Ct. nuc	Ct. ret	D. nob	D. win	G. lon	I. les	L. gil	M. hor	P. bar	P. min	P. vit	R. die	T. tet
A. muricatus	-	0.993	1.000	1.000	1.000	1.000	0.066	1.000	**0.006**	1.000	1.000	0.066	1.000	1.000	**0.004**	**0.018**	1.000	1.000	1.000	1.000
Ch. kingii	**0.000**	-	1.000	0.997	1.000	1.000	1.000	1.000	1.000	1.000	1.000	1.000	1.000	1.000	0.991	1.000	1.000	1.000	1.000	1.000
Ct. caudicinctus	**0.000**	**0.000**	-	1.000	1.000	1.000	1.000	1.000	1.000	1.000	1.000	1.000	1.000	1.000	0.267	0.951	1.000	1.000	1.000	1.000
Ct. cristatus	**0.034**	**0.000**	**0.000**	-	1.000	1.000	**0.017**	1.000	**0.001**	1.000	1.000	0.064	1.000	1.000	**0.004**	**0.013**	1.000	1.000	1.000	1.000
Ct. decresii	**0.023**	**0.000**	**0.001**	**0.000**	-	1.000	0.993	1.000	0.653	1.000	1.000	0.772	1.000	1.000	0.056	0.403	1.000	1.000	1.000	1.000
Ct. fionni	0.653	**0.000**	0.471	**0.002**	1.000	-	1.000	1.000	1.000	1.000	1.000	1.000	1.000	1.000	0.967	1.000	1.000	1.000	1.000	1.000
Ct. isolepis	**0.000**	**0.000**	0.831	**0.000**	**0.000**	**0.003**	-	1.000	1.000	0.902	0.991	1.000	0.852	1.000	0.967	1.000	1.000	0.440	1.000	0.995
Ct. nuchalis	0.776	**0.000**	**0.000**	**0.000**	1.000	1.000	**0.000**	-	0.931	1.000	1.000	0.955	1.000	1.000	0.112	0.680	1.000	1.000	1.000	1.000
Ct. reticulatus	**0.000**	**0.000**	1.000	**0.000**	**0.003**	0.268	0.077	**0.000**	-	0.501	0.897	1.000	0.308	1.000	1.000	1.000	0.994	0.062	1.000	0.788
D. nobbi	1.000	**0.000**	**0.000**	**0.006**	1.000	1.000	**0.000**	1.000	**0.018**	-	1.000	0.503	1.000	1.000	**0.028**	0.222	1.000	1.000	1.000	1.000
D. winneckei	0.400	**0.001**	1.000	**0.000**	1.000	1.000	1.000	0.968	1.000	1.000	-	0.846	1.000	1.000	0.177	0.590	1.000	1.000	1.000	1.000
G. longirostris	1.000	**0.000**	**0.000**	1.000	**0.018**	0.141	**0.000**	**0.039**	**0.000**	0.870	**0.002**	-	0.460	1.000	1.000	1.000	0.985	0.273	1.000	0.790
I. lesueurii	**0.000**	0.998	**0.000**	**0.000**	**0.000**	**0.000**	**0.000**	**0.000**	**0.000**	**0.000**	**0.002**	**0.000**	-	1.000	**0.025**	0.194	1.000	1.000	1.000	1.000
L. gilberti	1.000	**0.000**	**0.000**	1.000	1.000	1.000	**0.000**	1.000	**0.000**	1.000	1.000	1.000	**0.000**	-	0.609	0.999	1.000	1.000	1.000	1.000
M. horridus	**0.000**	**0.000**	0.636	**0.000**	**0.000**	**0.003**	1.000	**0.000**	0.076	**0.000**	1.000	**0.000**	**0.000**	**0.000**	-	1.000	0.413	**0.014**	1.000	0.063
P. barbata	**0.000**	0.997	**0.000**	**0.000**	**0.000**	**0.000**	**0.000**	**0.000**	**0.000**	**0.000**	**0.000**	**0.000**	1.000	**0.000**	**0.000**	-	0.885	0.092	1.000	0.438
P. minor	1.000	0.104	**0.000**	1.000	0.068	0.367	**0.000**	0.406	**0.000**	0.819	1.000	1.000	0.999	0.999	**0.000**	0.125	-	1.000	1.000	1.000
P. vitticeps	**0.000**	0.321	**0.000**	**0.000**	**0.000**	**0.000**	**0.000**	**0.000**	**0.000**	**0.000**	**0.000**	**0.000**	1.000	**0.000**	**0.000**	0.998	1.000	-	1.000	1.000
R. diemensis	1.000	**0.001**	1.000	0.789	1.000	1.000	1.000	1.000	1.000	1.000	1.000	0.734	**0.013**	1.000	1.000	**0.000**	0.996	**0.003**	-	1.000
T. tetraporophora	**0.000**	**0.000**	1.000	**0.000**	**0.007**	0.754	1.000	**0.000**	0.944	**0.001**	0.771	**0.000**	**0.000**	**0.007**	1.000	**0.000**	**0.002**	**0.000**	1.000	-
MAXILLA																				
A. muricatus	-	0.978	0.628	1.000	1.000	1.000	0.610	0.640	**0.001**	1.000	1.000	1.000	1.000	1.000	**0.046**	1.000	1.000	1.000	1.000	1.000
Ch. kingii	**0.000**	-	1.000	1.000	1.000	1.000	1.000	1.000	1.000	1.000	1.000	1.000	0.992	1.000	1.000	1.000	0.276	1.000	1.000	1.000
Ct. caudicinctus	**0.000**	**0.000**	-	0.982	1.000	1.000	1.000	1.000	0.983	1.000	1.000	1.000	0.605	1.000	1.000	1.000	0.215	1.000	1.000	1.000
Ct. cristatus	0.276	**0.000**	**0.000**	-	1.000	1.000	0.968	0.981	**0.004**	1.000	1.000	1.000	1.000	1.000	0.140	1.000	0.978	1.000	1.000	1.000
Ct. decresii	0.582	**0.000**	0.061	**0.001**	-	1.000	1.000	1.000	0.581	1.000	1.000	1.000	1.000	1.000	0.672	1.000	1.000	1.000	1.000	1.000
Ct. fionni	**0.007**	**0.000**	**0.002**	**0.000**	1.000	-	1.000	1.000	0.957	1.000	1.000	1.000	1.000	1.000	0.948	1.000	1.000	1.000	1.000	1.000
Ct. isolepis	**0.000**	**0.000**	**0.018**	**0.000**	**0.000**	**0.000**	-	1.000	1.000	1.000	1.000	0.995	0.650	1.000	1.000	1.000	0.146	0.999	1.000	1.000
Ct. nuchalis	**0.000**	**0.000**	**0.000**	**0.000**	1.000	1.000	**0.000**	-	1.000	1.000	1.000	0.999	0.651	1.000	1.000	1.000	0.187	1.000	1.000	1.000
Ct. reticulatus	**0.000**	**0.000**	1.000	**0.000**	**0.004**	**0.000**	0.549	**0.000**	-	0.496	1.000	**0.044**	**0.001**	0.448	1.000	**0.029**	**0.010**	**0.008**	0.999	0.423
D. nobbi	0.997	**0.000**	**0.000**	**0.004**	1.000	1.000	**0.000**	1.000	**0.000**	-	1.000	1.000	1.000	1.000	0.783	1.000	0.766	1.000	1.000	1.000
D. winneckei	**0.000**	**0.000**	1.000	**0.000**	0.811	0.795	1.000	**0.001**	1.000	**0.002**	-	1.000	1.000	1.000	1.000	1.000	0.794	1.000	1.000	1.000
G. longirostris	1.000	**0.000**	**0.000**	1.000	0.118	**0.001**	**0.000**	**0.000**	**0.000**	0.308	**0.000**	-	1.000	1.000	0.204	1.000	1.000	1.000	1.000	1.000
I. lesueurii	**0.000**	1.000	**0.000**	**0.000**	**0.000**	**0.000**	**0.000**	**0.000**	**0.000**	**0.000**	**0.000**	**0.000**	-	1.000	0.054	1.000	1.000	1.000	1.000	1.000
L. gilberti	1.000	**0.000**	**0.000**	0.999	1.000	0.924	**0.000**	0.371	**0.000**	1.000	**0.007**	1.000	**0.000**	-	0.682	1.000	0.991	1.000	1.000	1.000
M. horridus	**0.000**	**0.000**	**0.000**	**0.000**	**0.000**	**0.000**	0.999	**0.000**	**0.002**	**0.000**	0.559	**0.000**	**0.000**	**0.000**	-	0.346	**0.011**	0.254	0.997	0.570
P. barbata	**0.000**	0.999	**0.000**	**0.000**	**0.000**	**0.000**	**0.000**	**0.000**	**0.000**	**0.000**	**0.000**	**0.000**	1.000	**0.000**	**0.000**	-	0.875	1.000	1.000	1.000
P. minor	0.989	0.226	**0.000**	1.000	0.099	**0.001**	**0.000**	**0.000**	**0.000**	0.114	0.066	1.000	**0.039**	0.975	**0.000**	0.317	-	0.836	1.000	0.990
P. vitticeps	**0.000**	0.794	**0.000**	**0.000**	**0.000**	**0.000**	**0.000**	**0.000**	**0.000**	**0.000**	**0.000**	**0.000**	0.997	**0.000**	**0.000**	1.000	0.129	-	1.000	1.000
R. diemensis	**0.008**	**0.000**	1.000	**0.000**	1.000	1.000	0.318	0.999	1.000	0.793	1.000	**0.002**	**0.000**	0.239	**0.006**	**0.000**	0.053	**0.000**	-	1.000
T. tetraporophora	**0.000**	**0.000**	0.299	**0.000**	**0.006**	**0.005**	1.000	**0.000**	0.978	**0.000**	0.829	**0.000**	**0.000**	**0.000**	1.000	**0.000**	**0.000**	**0.000**	0.741	-

Supplementary material for Chapter 4

Table S4.1 – Landmark definitions used to characterise cranial shape in 2D (see Figs. 1.6, 1.7, and Evans 2008 for nomenclature of skeletal elements).

Number	Description
1	Anterior limit of the snout
2	Anterior limit of the base of the most anterior maxillary tooth
3	Most dorsal point of the anterior process of the maxilla
4	Dorsal limit of the nasal opening
5	Anterior limit of the jugal
6	Posterior limit of the maxillary posterior dorsal process
7	Posterior limit of the base of the most posterior acrodont tooth
8	Most posteroventral point of the jugal
9	Most anteroventral point of the postorbital
10	Anterior limit of the squamosal
11	Posterior limit of the jugal
12	Posterior limit of the squamosal
13	Most posterior point of the postorbital-parietal suture
14	Most anterior point of the postorbital-parietal suture
15	Most dorsal point of the prefrontal-frontal suture
16	Anterior limit of the orbital opening

Table S4.2 – Principal components summary resulting from principal component analysis of landmark data, showing proportion of variance and cumulative proportion of variance for the first six PCs.

	PC 1	PC 2	PC 3	PC 4	PC 5	PC 6
Proportion of variance	0.300	0.263	0.101	0.064	0.042	0.033
Cumulative proportion	0.300	0.562	0.663	0.727	0.769	0.802

Table S4.3 – Pairwise results for angles in phenotypic trajectory analysis. Top triangle shows pairwise *P*-values, while bottom triangle shows pairwise angle differences (bold values indicate *P* < 0.05). Abbreviations: first three letters of genus name, followed by the first three letters of species name.

	amp_mur	chl_kin	cte_cau	cte_cri	cte_dec	cte_iso	cte_nuc	cte_ret	dip_nob	dip_win	gow_lon	int_les	lop_gil	mol_hor	pog_bar	pog_vit	ran_die	tym_tet
amp_mur	-	**0.01**	0.09	0.11	0.63	**0.00**	**0.00**	**0.00**	0.40	0.52	0.45	**0.01**	0.27	**0.00**	**0.00**	**0.00**	0.06	0.06
chl_kin	56.39	-	0.45	**0.02**	0.31	**0.02**	0.51	0.13	0.09	**0.01**	**0.00**	0.85	0.27	**0.04**	0.68	0.72	0.21	**0.04**
cte_cau	38.29	33.44	-	**0.05**	0.56	**0.00**	0.26	**0.02**	0.14	0.10	**0.04**	0.72	0.44	**0.00**	0.13	0.41	0.28	**0.03**
cte_cri	43.20	59.55	48.11	-	0.37	**0.04**	**0.00**	**0.00**	0.23	0.08	0.07	**0.02**	0.20	**0.01**	**0.00**	**0.01**	**0.03**	0.05
cte_dec	33.77	45.78	35.32	43.77	-	**0.04**	0.08	**0.02**	0.51	0.42	0.39	0.21	0.57	**0.03**	0.13	0.20	0.39	0.49
cte_iso	52.96	54.96	51.82	48.09	59.15	-	**0.00**	**0.00**	**0.03**	**0.03**	**0.00**	**0.00**	0.18	**0.00**	**0.00**	**0.00**	**0.01**	**0.01**
cte_nuc	61.99	33.22	34.35	65.07	54.83	67.07	-	0.84	**0.01**	**0.01**	**0.00**	0.96	0.07	**0.01**	0.86	0.98	0.06	**0.00**
cte_ret	73.98	40.35	42.50	71.38	65.19	69.97	22.51	-	**0.00**	**0.00**	**0.00**	0.56	**0.01**	**0.01**	0.53	0.24	**0.01**	**0.00**
dip_nob	36.49	53.87	46.02	47.43	41.04	58.90	71.56	77.89	-	0.47	0.31	**0.03**	0.12	**0.01**	**0.01**	**0.02**	0.26	0.68
dip_win	35.64	67.62	52.76	56.49	45.88	58.70	73.14	86.09	42.58	-	0.43	**0.01**	0.23	**0.00**	**0.00**	**0.02**	0.30	0.20
gow_lon	30.12	62.80	44.24	47.47	40.97	65.02	61.62	75.07	41.37	39.02	-	**0.00**	0.19	**0.00**	**0.00**	**0.00**	0.27	**0.02**
int_les	53.13	26.34	25.85	54.87	46.63	55.73	20.97	27.85	59.19	67.15	56.03	-	0.32	**0.01**	0.81	0.99	0.11	**0.01**
lop_gil	35.90	40.84	32.55	43.34	38.02	38.24	46.86	58.37	50.96	48.61	40.91	37.28	-	**0.00**	**0.02**	0.28	0.24	**0.02**
mol_hor	77.57	58.01	65.33	71.09	66.60	76.14	63.24	59.48	77.50	87.23	84.98	62.07	77.10	-	**0.00**	**0.00**	**0.01**	**0.03**
pog_bar	63.84	28.48	35.95	68.94	50.12	72.31	22.95	26.99	64.11	74.94	64.89	24.24	52.04	62.85	-	0.70	**0.03**	**0.01**
pog_vit	53.75	27.46	29.17	55.77	44.09	59.36	18.47	31.11	61.57	66.19	53.26	15.54	35.83	66.09	24.12	-	0.12	**0.01**
ran_die	51.84	47.17	39.94	61.71	44.94	61.45	52.45	61.24	47.41	47.31	41.45	48.19	44.56	70.76	54.87	46.20	-	0.08
tym_tet	50.94	58.27	54.49	58.10	41.85	63.01	75.33	79.49	36.03	51.91	59.30	66.34	62.84	63.79	66.93	69.19	55.99	-

Table S4.4 – Pairwise results for magnitude in phenotypic trajectory analysis. Top triangle shows pairwise *P*-values, while bottom triangle shows pairwise magnitude differences (bold values indicate *P* < 0.05). Abbreviations: first three letters of genus name, followed by the first three letters of species name.

	amp_mur	chl_kin	cte_cau	cte_cri	cte_dec	cte_iso	cte_nuc	cte_ret	dip_nob	dip_win	gow_lon	int_les	lop_gil	mol_hor	pog_bar	pog_vit	ran_die	tym_tet
amp_mur	-	**0.02**	0.75	0.44	0.38	**0.01**	0.33	0.76	0.62	0.41	0.43	**0.01**	0.61	0.08	**0.00**	**0.00**	0.19	0.50
chl_kin	0.04	-	**0.01**	**0.00**	0.26	**0.00**	**0.00**	**0.04**	**0.01**	**0.01**	**0.00**	0.83	**0.01**	0.53	0.57	0.19	**0.00**	**0.01**
cte_cau	0.00	0.05	-	0.64	0.27	**0.01**	0.56	0.53	0.83	0.57	0.64	**0.01**	0.85	0.06	**0.00**	**0.00**	0.29	0.70
cte_cri	0.01	0.05	0.01	-	0.14	0.09	0.92	0.29	0.83	0.88	0.95	**0.00**	0.80	**0.03**	**0.00**	**0.00**	0.55	0.97
cte_dec	0.02	0.02	0.02	0.03	-	**0.01**	0.11	0.53	0.20	0.16	0.16	0.32	0.23	0.53	0.12	**0.04**	0.05	0.17
cte_iso	0.04	0.08	0.04	0.03	0.06	-	0.06	**0.00**	0.09	0.19	**0.04**	**0.00**	**0.03**	**0.00**	**0.00**	**0.00**	0.35	0.09
cte_nuc	0.01	0.05	0.01	0.00	0.03	0.03	-	0.21	0.75	0.95	0.87	**0.00**	0.69	**0.02**	**0.00**	**0.00**	0.59	0.90
cte_ret	0.00	0.04	0.01	0.02	0.01	0.05	0.02	-	0.46	0.29	0.25	**0.03**	0.44	0.15	**0.00**	**0.00**	0.12	0.36
dip_nob	0.01	0.05	0.00	0.00	0.03	0.03	0.01	0.01	-	0.74	0.89	**0.02**	0.97	0.06	**0.01**	**0.00**	0.46	0.88
dip_win	0.02	0.06	0.01	0.00	0.03	0.03	0.00	0.02	0.01	-	0.82	**0.01**	0.70	**0.03**	**0.00**	**0.00**	0.68	0.85
gow_lon	0.01	0.05	0.01	0.00	0.03	0.03	0.00	0.02	0.00	0.00	-	**0.00**	0.82	**0.03**	**0.00**	**0.00**	0.48	0.99
int_les	0.04	0.00	0.04	0.05	0.02	0.08	0.05	0.03	0.05	0.05	0.05	-	**0.01**	0.68	0.42	0.09	**0.01**	**0.01**
lop_gil	0.01	0.05	0.00	0.00	0.02	0.03	0.01	0.01	0.00	0.01	0.00	0.04	-	**0.04**	**0.00**	**0.00**	0.39	0.83
mol_hor	0.03	0.01	0.03	0.04	0.01	0.07	0.04	0.03	0.04	0.05	0.04	0.01	0.04	-	0.30	0.08	**0.01**	**0.04**
pog_bar	0.05	0.01	0.05	0.06	0.03	0.09	0.06	0.05	0.06	0.06	0.06	0.01	0.06	0.02	-	0.38	**0.00**	**0.00**
pog_vit	0.06	0.02	0.07	0.07	0.04	0.10	0.08	0.06	0.07	0.08	0.07	0.02	0.07	0.03	0.01	-	**0.00**	**0.00**
ran_die	0.02	0.06	0.02	0.01	0.04	0.02	0.01	0.03	0.02	0.01	0.01	0.06	0.02	0.05	0.07	0.09	-	0.54
tym_tet	0.01	0.05	0.01	0.00	0.03	0.03	0.00	0.02	0.00	0.00	0.00	0.05	0.00	0.04	0.06	0.07	0.01	-

Table S4.5 – Examining allometry: MANCOVA results of cranial shape by size and life habit (shape ~ size * habit). Bold values indicate $P < 0.05$.

	Df	SS	MS	R²	F	Z	*P*-value
Log (size)	1	0.9360	0.93502	0.224809	128.3495	8.6221	**0.001**
Habit	2	0.5809	0.29044	0.139513	39.8258	9.7491	**0.001**
Log (size) : habit	2	0.0578	0.02890	0.013883	3.9631	5.2379	**0.001**
Residuals	355	2.5889	0.00729				
Total	360	4.1636					

Table S4.6 – Examining allometry of life habit groups: pairwise angle and length differences. Top triangles = *P*-values (values < 0.05 in bold); bottom triangles = angles.

	Saxicolous	Semi-arboreal	Terrestrial
Angle			
Saxicolous	-	0.114	**0.005**
Semi-arboreal	34.07	-	**0.001**
Terrestrial	53.58	36.16	-
Length			
Saxicolous	-	**0.013**	**0.001**
Semi-arboreal	0.013405	-	**0.015**
Terrestrial	0.001075	0.01448	-

Supplementary material for Chapter 5

Figure S5.1 – Landmark sampling curve produced for landmark data in Chapter 5 using the *lambda* R package.
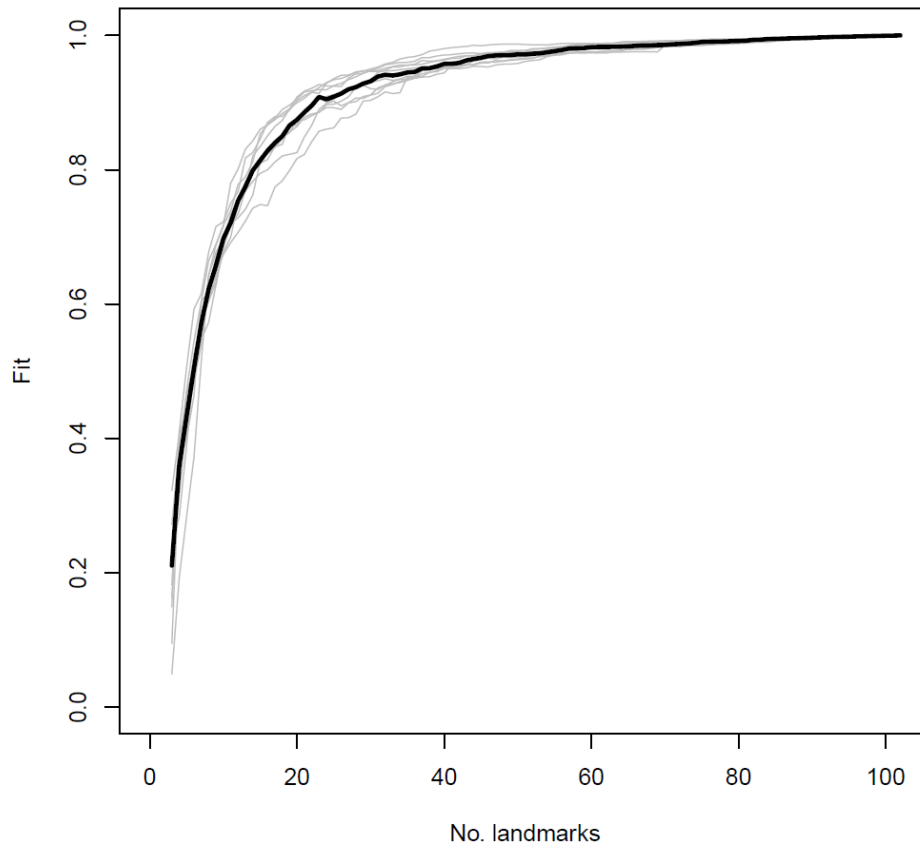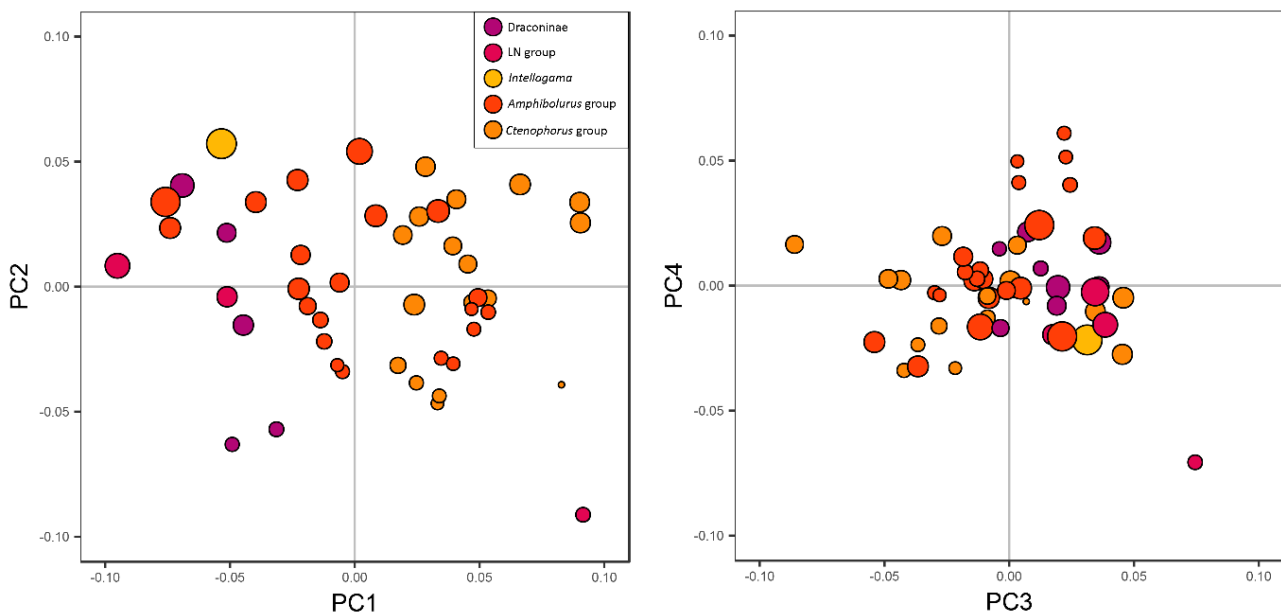

Figure S5.2 – PCA results before allometry correction.

Table S5.1 – Specimens used in shape analyses and relevant information. SAMA = South Australian Museum; AMS = Australian Museum. LN = Least nested group.

Genus	Species	Evolutionary Group	Reg. number	Specimen	Life habit
Acanthosaura	*lepidogaster*	Draconinae	SAMA R64182	Head	Arboreal
Amphibolurus	*burnsi*	*Amphibolurus*	SAMA R30986	Head	Semi-arboreal
Amphibolurus	*muricatus*	*Amphibolurus*	AMS R154972	Head	Semi-arboreal
Amphibolurus	*norrisi*	*Amphibolurus*	SAMA R60767	Head	Semi-arboreal
Bronchocela	*cristatella*	Draconinae	SAMA R22477	Skull	Arboreal
Calotes	*calotes*	Draconinae	SAMA R47735	Skull	Arboreal
Calotes	*versicolor*	Draconinae	SAMA R66808	Skull	Semi-arboreal
Chelosania	*brunnea*	LN	SAMA R140288	Head	Semi-arboreal
Chlamydosaurus	*kingii*	*Amphibolurus*	SAMA R21373	Skull	Semi-arboreal
Ctenophorus	*caudicinctus*	*Ctenophorus*	SAMA R61888	Head	Saxicolous
Ctenophorus	*chapmani*	*Ctenophorus*	SAMA R59616	Head	Terrestrial
Ctenophorus	*cristatus*	*Ctenophorus*	SAMA R59493	Head	Terrestrial
Ctenophorus	*decresii*	*Ctenophorus*	SAMA R53234	Skull	Saxicolous
Ctenophorus	*fionni*	*Ctenophorus*	SAMA R68126	Head	Saxicolous
Ctenophorus	*fordi*	*Ctenophorus*	SAMA R34489	Head	Terrestrial
Ctenophorus	*gibba*	*Ctenophorus*	SAMA R43604	Head	Terrestrial
Ctenophorus	*isolepis*	*Ctenophorus*	SAMA R59391	Head	Terrestrial
Ctenophorus	*maculatus*	*Ctenophorus*	SAMA R59600	Head	Terrestrial
Ctenophorus	*mckenziei*	*Ctenophorus*	SAMA R26160	Head	Terrestrial
Ctenophorus	*nuchalis*	*Ctenophorus*	SAMA R7296	Skull	Terrestrial
Ctenophorus	*ornatus*	*Ctenophorus*	SAMA R56064	Head	Saxicolous
Ctenophorus	*pictus*	*Ctenophorus*	SAMA R28608	Head	Terrestrial
Ctenophorus	*reticulatus*	*Ctenophorus*	SAMA R46987	Head	Terrestrial
Ctenophorus	*salinarum*	*Ctenophorus*	SAMA R59079	Head	Terrestrial
Ctenophorus	*tjankjalka*	*Ctenophorus*	SAMA R53804	head	Saxicolous
Ctenophorus	*vadnappa*	*Ctenophorus*	SAMA R45802	Head	Saxicolous
Diporiphora	*amphiboluroides*	*Amphibolurus*	SAMA R4838C	Head	Semi-arboreal
Diporiphora	*lalliae*	*Amphibolurus*	SAMA R65868	Head	Semi-arboreal
Diporiphora	*magna*	*Amphibolurus*	SAMA R58365	Head	Semi-arboreal
Diporiphora	*nobbi*	*Amphibolurus*	SAMA R21511	Head	Semi-arboreal
Diporiphora	*reginae*	*Amphibolurus*	SAMA R63999	Head	Semi-arboreal
Diporiphora	*winneckei*	*Amphibolurus*	SAMA R66514	Head	Semi-arboreal
Draco	*lineatus*	Draconinae	AMS R57460	Head	Arboreal
Draco	*timoriensis*	Draconinae	SAMA R13860B	Head	Arboreal
Gonocephalus	*grandis*	Draconinae	SAMA R66697	Skull	Arboreal
Gowidon	*longirostris*	*Amphibolurus*	SAMA R18053	Skull	Semi-arboreal
Intellagama	*lesueurii*	LN	SAMA R27305	Skull	Semi-arboreal
Lophosaurus	*boydii*	LN	AMS R68782	Head	Arboreal
Lophognathus	*gilberti*	*Amphibolurus*	SAMA R38793	Head	Semi-arboreal
Lophosaurus	*spinipes*	LN	SAMA R40742	Head	Arboreal
Moloch	*horridus*	LN	SAMA R17325	Head	Terrestrial
Pogona	*barbata*	*Amphibolurus*	SAMA R32503	Head	Semi-arboreal
Pogona	*minor*	*Amphibolurus*	SAMA R36706	Skull	Semi-arboreal
Pogona	*nullarbor*	*Amphibolurus*	SAMA R18581	Skull	Semi-arboreal
Pogona	*vitticeps*	*Amphibolurus*	SAMA R18545	Skull	Semi-arboreal
Pseudocalotes	*tympanistriga*	Draconinae	SAMA R35730	Head	Arboreal
Rankinia	*diemensis*	*Amphibolurus*	SAMA R1457B	Head	Terrestrial
Tympanocryptis	*houstoni*	*Amphibolurus*	SAMA R63157	Head	Terrestrial
Tympanocryptis	*intima*	*Amphibolurus*	SAMA R51044	Head	Terrestrial
Tympanocryptis	*lineata*	*Amphibolurus*	SAMA R59721	Head	Terrestrial
Tympanocryptis	*pinguicolla*	*Amphibolurus*	SAMA R44672	Head	Terrestrial
Tympanocryptis	*tetraporophora*	*Amphibolurus*	SAMA R67710	Head	Terrestrial

Table S5.2 – Landmark definitions for landmarks used to characterise 3D cranial shape in Chapters 5 and 6. Numbers correspond to format used in IDAV Landmark Editor (starting at 0). See Evans 2008 and anatomical reference in Chapter 1 for nomenclature of structures. *Table split over 3 pages.*

Number	Bone	Description
0	Premaxilla	Most anterior tip of the premaxilla (snout)
1	Premaxilla	Most right lateral external point
2	Premaxilla	Most left lateral external point
3	Maxilla (R)	Most dorsal external point of lateral anterior maxillary process
4	Maxilla (L)	Most dorsal external point of lateral anterior maxillary process
5	Maxilla (R)	Just anterior of right narial basin foramen
6	Maxilla (L)	Just anterior of left narial basin foramen
7	Nasal (R)	Most anterior external point
8	Nasal (L)	Most anterior external point
9	Premaxilla	Most posterior tip (external)
10	Nasal (R)	Most anterior point of right external nasal-maxilla suture
11	Nasal (L)	Most anterior point of left external nasal-maxilla suture
12	Maxilla (R)	Most posterior point of lateral maxillary facial process
13	Maxilla (L)	Most posterior point of lateral maxillary facial process
14	Prefrontal (R)	Most anterior external point of prefrontal-nasal process
15	Prefrontal (L)	Most anterior external point of prefrontal-nasal process
16	Frontal	Most anterior external point (central)
17	Frontal	Most anterior point of right external nasal-maxillary suture
18	Frontal	Most anterior point of left external nasal-maxillary suture
19	Nasal (R)	Most posterior point
20	Nasal (L)	Most posterior point
21	Frontal	Most posterior point of right external Prefrontal-frontal suture (part of the orbit)
22	Frontal	Most posterior point of left external Prefrontal-frontal suture (part of the orbit)
23	Frontal	Posteromedial point of frontal (anterior of parietal foramen)
24	Frontal	Most right lateral point
25	Postorbital (R)	Most dorsal external point
26	Parietal	Most lateral point of right postorbital-parietal suture
27	Frontal	Most left lateral point
28	Postorbital (L)	Most dorsal external point
29	Parietal	Most lateral point of left postorbital-parietal suture
30	Parietal	Most medial point of the right side of the parietal platform (or centre of the most medial point where it is long)
31	Parietal	Most medial point of the left side of the parietal platform (or centre of the most medial point where it is long)
32	Parietal	Most posterior point of the parietal platform (middle)
33	Squamosal (R)	Most posterodorsal point
34	Squamosal (L)	Most posterodorsal point
35	Supratemporal (R)	Most posterior point
36	Supratemporal (L)	Most posterior point
37	Supraoccipital	Most posterior point of the right external supraoccipital-otooccipital suture

Number	Bone	Description
38	Supraoccipital	Most posterior point of the left external supraoccipital-otooccipital suture
39	Otooccipital (L)	Most medial point
40	Otooccipital (R)	Most medial point
41	Basioccipital	Most dorsal point of the left side of the basal tubercle
42	Basioccipital	Most dorsal point of the right side of the basal tubercle
43	Basioccipital	Most ventral point of the left side of the basal tubercle
44	Basioccipital	Most ventral point of the right side of the basal tubercle
45	Maxilla (L)	Most posterior point of the most posterior pleurodont tooth attachment
46	Maxilla (L)	Most anterior point of the orbital boundary
47	Prefrontal (L)	Most posterior point of the lateral enlargement (meets with maxilla)
48	Prefrontal (L)	Medial limit of the prefrontal lateral enlargement
49	Maxilla (L)	Point of orbital opening level with prefrontal/palatal join to orbital
50	Maxilla (L)	Point of orbital opening level with most anterior external part of jugal
51	Maxilla (L)	Most posterior point of the posterodorsal process
52	Jugal(L)	Most posteroventral point
53	Postorbital (L)	Most anteroventral external point
54	Squamosal (L)	Most posterior external point
55	Jugal (L)	Most posterior external point
56	Postorbital (L)	Most posterior point
57	Squamosal (L)	Most posterior/broadest point of the "ventral peg" (see Evans 2008)
58	Supratemporal (L)	Most anterior point
59	Maxilla (R)	Most posterior point of the most posterior pleurodont tooth attachment
60	Maxilla (R)	Most anterior point of the orbital opening
61	Prefrontal (R)	Most posterior point of the lateral enlargement (meets with maxilla)
62	Prefrontal (R)	Medial limit of the prefrontal lateral enlargement
63	Maxilla (R)	Point of orbital opening level with prefrontal/palatal join to orbital
64	Maxilla (R)	Point of orbital opening level with most anterior external part of jugal
65	Maxilla (R)	Most posterior point of the posterodorsal process
66	Jugal(R)	Most posteroventral point
67	Postorbital (R)	Most anteroventral external point
68	Squamosal (R)	Most posterior external point
69	Jugal (R)	Most posterior external point
70	Postorbital (R)	Most posterior point
71	Squamosal (R)	Most posterior/broadest point of the "ventral peg" (see Evans 2008)
72	Supratemporal (R)	Most anterior point
73	Premaxilla	Most posteroventral point (right)
74	Premaxilla	Most posteroventral point (left)
75	Maxilla (B)	Most posterior point of the join in the maxillary lappet (see Evans 2008)
76	Vomer (R)	Most lateral point
77	Vomer (L)	Most lateral point
78	Vomer (R)	Most posterior point
79	Vomer (L)	Most posterior point
80	Palatine (R)	Most anterolateral point
81	Palatine (L)	Most anterolateral point
82	Palatine (R)	Most anterior point of the maxillary-palatine suture

Number	Bone	Description
83	Palatine (L)	Most anterior point of the maxillary-palatine suture
84	Palatine (R)	Most posterior point of the maxillary-palatine suture
85	Palatine (L)	Most posterior point of the maxillary-palatine suture
86	Palatine (R)	Most anterior point of palatine-pterygoid suture (ventral)
87	Palatine (L)	Most anterior point of palatine-pterygoid suture (ventral)
88	Pterygoid (R)	Most posterior point of palatine-pterygoid suture (ventral)
89	Pterygoid (L)	Most posterior point of palatine-pterygoid suture (ventral)
90	Maxilla (R)	Posterior limit of tooth row (level with jugal "enlargement")
91	Maxilla (L)	Posterior limit of tooth row (level with jugal "enlargement")
92	Pterygoid (R)	Most ventral point of pterygoid process
93	Pterygoid (L)	Most ventral point of pterygoid process
94	Basipterygoid	Most anterior point of right basipterygoid process
95	Basipterygoid	Most anterior point of left basipterygoid process
96	Basipterygoid	Most posterior point of right basipterygoid process
97	Basipterygoid	Most posterior point of left basipterygoid process
98	Pterygoid (R)	Most posteroventral point
99	Pterygoid (L)	Most posteroventral point
100	Pterygoid (R)	Most medial point of lateral edge (medial to pterygoid flange)
101	Pterygoid (L)	Most medial point of lateral edge (medial to pterygoid flange)

Table S5.3 – Summary for first six principal components, for principal components analysis of allometry corrected shape variables in Chapter 5.

	PC 1	PC 2	PC 3	PC 4	PC 5	PC 6
Proportion of variance	0.333	0.117	0.072	0.056	0.048	0.044
Cumulative proportion	0.333	0.450	0.051	0.578	0.625	0.669

Supplementary material for Chapter 6

Table S6.1 – Jacky lizard (*Amphibolurus muricatus*) specimens used in the captive versus wild comparison, and relevant information. UC = University of Canberra; AMS= Australian Museum; SAMA= South Australian Museum. Specimens included in the interspecific comparison are indicated by an X in the "data set B" column. SVL = snout-vent length.

Institution	Reg. number	Source	Data set B	SVL (mm)	Centroid size
UC	AA66262	Captive		68	70.50
UC	AA66263	Captive		65	68.69
UC	AA66268	Captive	X	75	76.57
UC	AA66274	Captive		56	61.15
UC	AA66276	Captive		54	60.09
UC	AA66278	Captive		52	59.74
UC	AA66280	Captive	X	47	57.94
UC	AA66282	Captive	X	62	64.64
UC	AA66284	Captive		63	65.83
UC	AA66286	Captive		70	72.83
UC	AA66292	Captive		53	62.10
UC	AA66294	Captive		49	54.35
UC	AA66296	Captive		56	60.65
UC	AA66300	Captive		54	57.39
UC	AA66302	Captive	X	48	55.63
UC	AA66304	Captive		56	60.80
UC	AA66308	Captive		60	64.62
UC	AA66312	Captive		53	59.56
AMS	R152446	Wild	X	43	51.14
AMS	R152464	Wild		78	74.90
AMS	R154969	Wild		72	88.63
AMS	R154972	Wild	X	102	99.01
AMS	R171161	Wild	X	72	71.66
AMS	R52459	Wild		62	67.83
SAMA	R34730	Wild	X	97	95.64

Table S6.2 – Specimens used for data set B in Chapter 6, and relevant information. UC = University of Canberra; AMS= Australian Museum; SAMA= South Australian Museum.

Species	Institution	Reg. number	Specimen type	Centroid size
Amphibolurus muricatus	UC	AA66268	Head	76.57
Amphibolurus muricatus	UC	AA66280	Head	57.94
Amphibolurus muricatus	UC	AA66282	Head	64.64
Amphibolurus muricatus	UC	AA66302	Head	55.63
Amphibolurus muricatus	AMS	R152446	Head	51.14
Amphibolurus muricatus	AMS	R154972	Head	99.01
Amphibolurus muricatus	AMS	R171161	Head	71.66
Amphibolurus muricatus	SAMA	R34730	Head	95.64
Ctenophorus isolepis	SAMA	R32154	Head	52.26
Ctenophorus isolepis	SAMA	R35553	Skull	53.88
Ctenophorus isolepis	SAMA	R59391	Head	58.35
Ctenophorus isolepis	SAMA	R60403	Head	35.13
Diporiphora nobbi	SAMA	R32501	Head	78.60
Diporiphora nobbi	SAMA	R21511	Head	83.13
Diporiphora nobbi	SAMA	R29709	Head	39.98
Diporiphora nobbi	SAMA	R35064	Head	64.40
Diporiphora nobbi	SAMA	R36319	Head	35.98
Diporiphora nobbi	SAMA	R3712	Head	45.20
Gowidon longirostris	SAMA	R18053	Skull	97.42
Gowidon longirostris	SAMA	R29290	Head	91.95
Gowidon longirostris	SAMA	R47292	Head	60.77
Gowidon longirostris	SAMA	R51542	Head	70.76
Gowidon longirostris	SAMA	R60498	Head	40.40
Pogona barbata	SAMA	R32503	Head	141.30
Pogona barbata	SAMA	R49512	Head	50.06
Pogona barbata	SAMA	R59743	Head	113.93
Pogona barbata	SAMA	R61274	Head	117.78
Rankinia diemensis	SAMA	R1457B	Head	76.57
Rankinia diemensis	SAMA	R269B	Head	68.97
Rankinia diemensis	SAMA	R3190	Head	34.14
Rankinia diemensis	SAMA	R3294	Head	39.96
Rankinia diemensis	SAMA	R3349	Head	56.23
Rankinia diemensis	SAMA	R269A	Head	74.07
Tympanocryptis tetraporophora	SAMA	R49733	Head	26.32
Tympanocryptis tetraporophora	SAMA	R58097	Head	43.25
Tympanocryptis tetraporophora	SAMA	R58194	Head	46.89
Tympanocryptis tetraporophora	SAMA	R64581	Head	42.01
Tympanocryptis tetraporophora	SAMA	R67710	Head	56.63

Table S6.3 – Summaries of first six principal components from PCAs in Chapter 6.

	PC 1	PC 2	PC 3	PC 4	PC5	PC 6
Jacky lizards before allometry correction						
Prop. of variance	0.3381	0.1118	0.0729	0.0646	0.0532	0.0412
Cumulative	0.3381	0.4499	0.5229	0.5875	0.6407	0.6819
Jacky lizards after allometry correction						
Prop. of variance	0.1525	0.1191	0.0943	0.0805	0.0691	0.609
Cumulative	0.1525	0.2715	0.3658	0.4463	0.5154	0.5762
Comparison species before allometry correction						
Prop. of variance	0.4223	0.1621	0.0665	0.619	0.0356	0.0344
Cumulative	0.4223	0.5844	0.6509	0.7127	0.7483	0.7827
Comparison species after allometry correction						
Prop. of variance	0.3305	0.1093	0.0940	0.0745	0.0538	0.0438
Cumulative	0.3305	0.4398	0.5338	0.6083	0.6621	0.7058
Comparison species after allometry correction with species as factor						
Prop. of variance	0.1345	0.1077	0.0980	0.0788	0.0735	0.06139
Cumulative	0.1345	0.2422	0.3400	0.4188	0.4942	0.5555

Supplementary material for Chapter 8

Figure S8.1 – Surface model of an example maxilla shown in labial view (A), lingual view (B), anterior view (C), to show nomenclature of components included in landmark definitions.
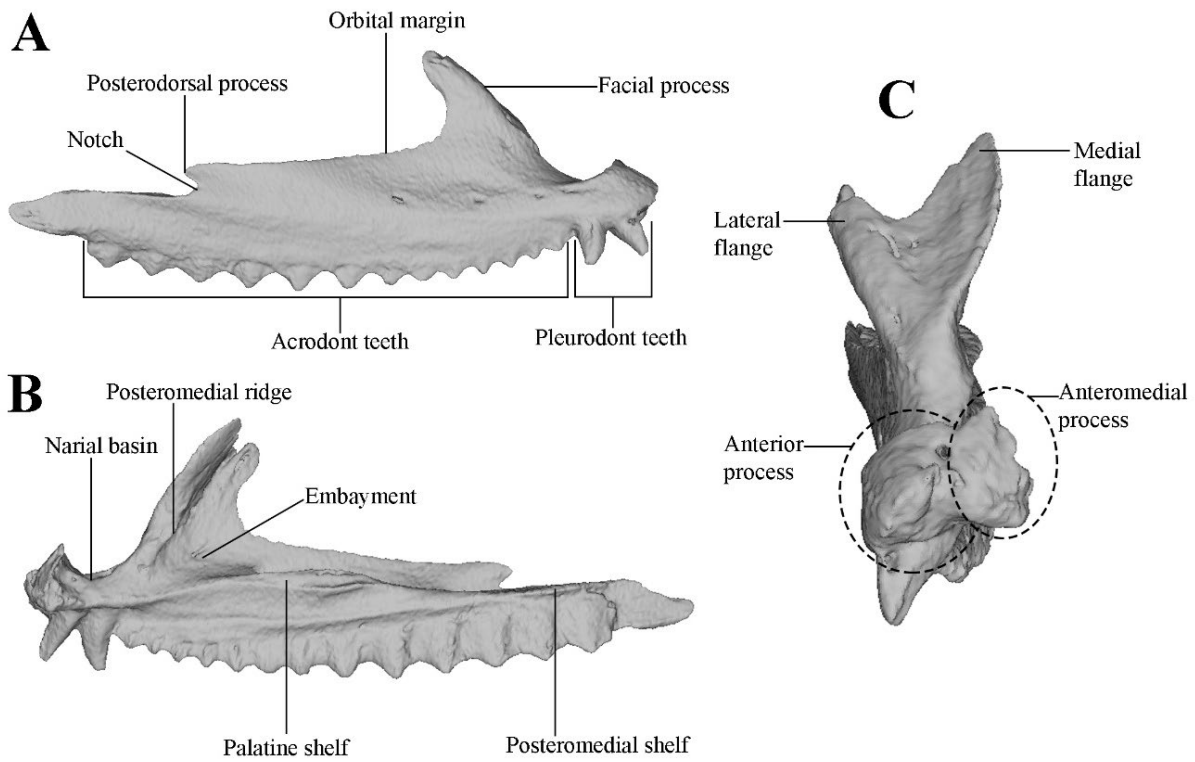
Table S8.1 – Table containing the definitions of all landmarks used to characterise the maxilla in 3D.

Landmarks	Description
1	Posterior end of the tooth row, directly posterior to the last acrodont tooth
2	Most posterior point of the maxilla
3	Most anterior point of the notch ventral to the apex of the posterodorsal process
4	Apex of the posterodorsal process.
5	Most dorsal point of the lateral flange on the facial process
6	Most ventral point between the lateral and medial flanges on the dorsal margin of the facial process
7	Most dorsal point of the medial flange of the facial process
8	Apex of the thickened posteromedial ridge on the internal margin of the facial process
9	The divergence point of the medial margin of the medial flange facial process
10	The divergence point of the lateral margin of the lateral flange of the facial process
11	Most ventral point of the narial basin (in the centre)
12	Most dorsal point (apex) of the anteromedial process
13	The dorsal point of the notch that separates the anterior and anteromedial processes (between 12 and 14)
14	Most dorsomedial point of the anterior process
15	Most ventromedial point of the anteromedial process
16	Most anterior point of the anteromedial process
17	Most anterior point of the anterior process
18	Anterior of the base of the most anterior pleurodont tooth
19	Most posterior visible point of the naris ridge
20	Most concave part of the embayment at the base of the facial process visible in medial view
21	Posterior end of the palatine shelf
22	Most posterior point of the posteromedial shelf
Semi-landmarks	
Curve 1 (23-32)	From the posterior end of the orbital margin (usually approximates the posterior end of the palatine shelf) to the most anterior point of the orbital margin.
Curve 2 (33-42)	Along the ridge on the lateral face of the maxilla, from a point level with the ventral, most point of the narial basin (11), to a point level with the most anterior point of the notch ventral to the apex of the posterodorsal (3)
Curve 3 (43-52)	From the anterior end of the palatine shelf, to the posterior end of the palatine shelf.